



PROGRESS REPORT ON RESEARCH ACTIVITIES

2015

HUNGARIAN
ACADEMY OF
SCIENCES
CENTRE FOR ENERGY
RESEARCH



HUNGARIAN ACADEMY OF SCIENCES
CENTRE FOR ENERGY RESEARCH

29-33 KONKOLY THEGE MIKLÓS ÚT
1121 BUDAPEST, HUNGARY

PROGRESS REPORT
ON RESEARCH ACTIVITIES
IN 2015

DEAR READER,

Welcome to the 2015 yearbook published by the MTA Centre for Energy Research (MTA EK), summarizing the scientific results and highlights in 2015. This booklet also provides a brief introduction to the departments and research groups working in the Centre. The capacities of MTA EK were enlarged in 2015 by its merger with the Institute of Technical Physics and Materials Science (MFA). The competences of MFA extend the capabilities of the Centre toward the research of complex functional materials and nanometer-scale structures.

Research in nuclear safety is supported by the National Nuclear Research Project within the frame of the Hungarian Sustainable Nuclear Technology Platform. The research topics in the Project, formulated by five member institutions of the Platform, were grouped in three main chapters: i) multiphysics modeling of phenomena in nuclear reactors, ii) experimental research, iii) management of spent fuel and radioactive waste, and research on Generation Four reactors. The long term planners of nuclear research in Hungary initiated a report about the future of the small research and educational reactors operated by MTA EK and the Budapest Technical University. The report summarizes the contributions of the small reactors to the nuclear safety culture and their role in the transfer of knowledge.

The finalization of the National Program for the Management of the Spent Fuel and Radioactive Water is a major milestone in the country. There is a new strategic direction in the National Program covering the research of the closure of the fuel cycle. The management of the spent fuel will not be an urgent question for the next few decades, but in order to formulate the national position, the launch of a research program is a prerequisite.

The supply of fresh fuel for the power reactors and the management of the spent fuel are key questions in the sustainability of nuclear power. We believe that the deployment of fast breeder reactors in the future is a key element to achieve the goals. The ALLEGRO project, aimed at building a new gas cooled fast reactor in the Central European region, started in 2010 with the strong technical support of the French CEA. The partners from the V4 countries each have their own national support for their contributions and the work is organized by the V4G4 Centre of Excellence. The activities were partly financed by the EU ALLIANCE and the VINCO projects as well. The project management formulated a new research and development roadmap in 2015.

In the year 2015, MTA EK became a member of the NERIS Platform (European Platform on preparedness for nuclear and radiological emergency response and recovery), and of the ETSON (European Technical Support Organization Network) and signed a collaboration agreement in the field of renewable energy technologies with the Karlsruhe Institute of Technology (Germany).

Ákos Horváth
Director General
horvath.akos@energia.mta.hu

CONTENTS

| | |
|--|-----------|
| Dear Reader, | 2 |
| Contents | 3 |
| Mission Statement of MTA Centre for Energy Research..... | 7 |
| Scientific Advisory Board of the MTA Centre for Energy Research..... | 7 |
| Organization Structure of the MTA Centre for Energy Research | 8 |
| Quality Management..... | 9 |
| Budapest Research Reactor..... | 10 |
| Environmental Protection Service | 12 |
| PROGRESS REPORT BY DEPARTMENTS | 13 |
| Institute for Atomic Energy Research..... | 14 |
| Reactor Analysis Department | 15 |
| Thermohydraulics Department | 15 |
| Fuel and Reactor Materials Department..... | 16 |
| Radiation Protection Department..... | 16 |
| Nuclear Security Department | 17 |
| Reactor Monitoring and Simulator Department | 18 |
| Institute for Energy Security and Environmental Safety | 19 |
| Surface Chemistry and Catalysis Department..... | 20 |
| Radiation Chemistry Department | 21 |
| Environmental Physics Department | 21 |
| Nuclear Analysis and Radiography Department..... | 23 |
| Institute of Technical Physics and Materials Science..... | 24 |
| Photonics Department..... | 25 |
| Complex System Department | 25 |
| Microtechnology Department | 26 |
| Nanostructures Department..... | 27 |
| Thin Film Physics Laboratory | 27 |
| Nanobiosensorics Group | 28 |
| I. RESEARCH RELATED TO NPP'S | 29 |
| Hungarian Nuclear Research Rrogram - Sustainable Nuclear Energy Technology PLATFORM | 30 |
| Ageing of Concrete Structure's Materials..... | 31 |
| Release of the FUROM-2.1 version. Verification and Introduction of an Extended Diffusion FGR Model | 32 |
| Safety Analysis of Advanced Fuel Rods During 15 Months Cycles | 33 |
| CODEX LOCA Tests with E110 and E110G Alloys..... | 34 |
| Mechanical Properties and Anisotropy of E110G Alloy | 35 |
| Numerical Simulation of Telescope Sipping Examination of a Leaking Fuel Assembly | 36 |
| Transport of Leaking Fuel Assemblies to Dry Storage Facility | 37 |
| Calculation of Leaking Fuel Characteristics..... | 38 |
| Investigation of Fuel Cladding Embrittlement With a Segmented Tool | 39 |
| Effect of High Temperature Treatment on the Ultimate Tensile Strength of Fuel Claddings..... | 40 |
| Re-evaluation of Surveillance Specimens of NPP Paks | 41 |
| Handbook of Reactor Materials | 42 |
| Validation of the New TRANSURANUS Code Version Against Ballooning-and-Burst Experiments..... | 43 |
| Simulation of Halden LOCA test IFA-650.10 | 44 |
| Simulation of the HATAC Radioactive Fission Gas Release Experiment | 45 |
| Simulation of the Halden Creep Test IFA-699 for VVER Cladding | 46 |
| Effect of Pre-oxidation on the Air Oxidation of Zirconium | 47 |
| Secondary Defects of Nuclear Fuels – Modelling of Hydrogen Formation Inside the Leaking Fuel..... | 48 |
| Validation of the KARATE Code System Against the Latest Operational Data and Startup Measurements | 49 |
| Uncertainties of Burnup Dependent Cell Calculations and of Active Core Calculations with Thermal-Hydraulics Feedback for VVER Reactors | 50 |
| Elaboration of New Versions of the Guides “Fuel Design” and “Active Core” for New NPP Units | 51 |
| Multi-physics Approach of the Safety Analysis Hot Channel Calculations; Development and Testing of a General Software Framework Tool | 52 |
| Supplementing the KARATE Code System with the Resonance Self Shielding Capability for the Plutonium Isotopes | 53 |

| | |
|---|------------|
| Development and testing of Statistical Version of the KARATE Code System | 54 |
| Using HZP States of Paks NPP for the Validation of Burnup Credit Calculations, Elaboration of a Detailed Full Core MCNP Model | 55 |
| Implementation and Validation of the New Rod Control and Reactor Power Contol System of Paks NPP Using the Full Scope Simulator..... | 56 |
| VERONA 7.0 the New Core Monitoring Systems of Paks NPP | 57 |
| Improvement of the Resistance of the Environmental and Radiation Monitoring System of Paks NPP Against Earthquakes and Station Black Out..... | 58 |
| Pilot Project for the Reconstruction of Two Neutron Monitoring Systems at Paks NPP..... | 59 |
| Reactor Noise Diagnostics Measurements and Maintenance of the PAZAR Measurement System at Paks NPP | 60 |
| Analysis of Propagating Temperature Perturbations in the Primary Circuit of PWRs | 61 |
| Development of Interaction Techniques for a Virtual Control Room | 62 |
| Safeguards Measurements at Paks NPP | 63 |
| Analysis of Corrosion Particles Originated from the Primary and Secondary Cooling System of Paks NPP.... | 64 |
| Measurement of Spent Fuel Assemblies from the Paks Nuclear Power Plant | 65 |
| Assessment of the Sources of Meteorological Data for the Paks NPP Site | 66 |
| Experimental Investigation of the Efficiency of External Cooling in the CERES Facility | 67 |
| Silver Measurement in Primary Water, Chemicals and Structural Materials | 68 |
| Kinetic Mesurement of ContaminaNts Accumulation on Stainless Steel Surface at High Temperature | 69 |
| In-Situ Gamma-Spectrometry at Block 2 of Paks NPP | 70 |
| II. GENERATION IV REACTORS | 71 |
| The ALLEGRO Project | 72 |
| Improving the Physical Model of the Fuel Cycle Simulation Code SITON | 73 |
| The ALLIANCE Project---Preparation for ALLEGRO - Implementing Advanced Nuclear in Central Europe | 74 |
| Development of Methodology and Computer Codes for Fast Spectrum Reactor Calculations | 75 |
| III. HEALTH PHYSICS, SPACE DOSIMETRY | 76 |
| The Pille Thermoluminescent Dosimeter System on Board the International Space Station..... | 77 |
| Dust, Plasma and Magnetic Field Measurements on Comet 67P/Churyumov-Gerasimenko | 78 |
| Monitoring the Effects of Radioactive Releases in Hungary | 80 |
| Acceptance Criteria for Safety Analyses: Application of Atmospheric Release Criteria | 80 |
| Further Development of the SINAC Program | 81 |
| A Comprehensive Dose Assessment for Normal Operation and Accidental Situations | 81 |
| Dose Consequences of a Severe Accident..... | 82 |
| Cosmic Ray Research Using Sounding Rockets | 83 |
| Tritel Silicon Detector Telescope Developement for the ESEO Satelite..... | 84 |
| Dose Mapping Inside The ISS | 85 |
| Numerical Modelling of the Biophysical Effects of Low Dose Ionising Radiation and Inhaled Aerosols | 86 |
| Modelling of Aerosol Drug Deposition in the Airways | 87 |
| Development of Laboratory Microscopic X-ray Fluorescence System for Metal Uptake Studies on Argillaceous Rocks..... | 88 |
| IV. NUCLEAR SECURITY, NON PROLIFERATION..... | 91 |
| Characterising of New, Unknown Uranium Samples | 92 |
| Effective Container Inspection at Border Control Points | 93 |
| Development of a Fast, Selective, More Sensitive Sample Preparation Method for In-Field Libs Measurements for Safeguards Purposes | 94 |
| Establishment of a Nuclear Forensic Database for Spent Nuclear Fuel | 95 |
| Development of National Nuclear Forensics Library | 96 |
| V. RENEWABLE AND FOSSIL ENERGY PRODUCTION | 97 |
| Decomposition of Hydrogen Sulfide Over HDS Catalysts | 98 |
| Water Oxidation – Initial Steps..... | 99 |
| Self-Assembly of Catalytic Surfaces | 100 |
| Visible Light Promoted Aerobic Benzyl Alcohol Oxidation on Alumina Supported Au-Cu Catalysts | 101 |
| Au-Containing Bimetallic Catalysts in Highly Selective Aerobic Oxidation Reactions | 102 |
| Correlation Between Activity and Coke Formation on Nickel-Based Dry Reforming Catalysts | 103 |
| Supporting the Integration of Residential Solar Photovoltaics with the Use of Hybrid Energy Storage | 104 |
| Surveying Methods for Development of Renewable Energy Potential..... | 105 |
| VI. ENERGY SAVING AND ENVIRONMENT STUDIES..... | 106 |
| Development of Highly Energy-Efficient Data Centre Infrastructure | 107 |

| | |
|---|------------|
| Hydroxyl Radical Reaction With Monuron | 108 |
| Vitrification - Development of Glass Matrices for High-Level Radioactive Wastes..... | 109 |
| Preparation, Structural Studies and Optimization of Oxide Glasses for High Level Waste Storage Applications | 110 |
| Rapid Method for Separation of ^{241}Am and Other Actinides on DGA Resin by Extraction Chromatography | 111 |
| VII. RESEARCH REACTOR | 112 |
| Budapest Neutron Centre - Scientific Utilization of the Budapest Research Reactor | 113 |
| Applications of Prompt Gamma Activation Analysis | 114 |
| Provenance Study of Lithic Raw Materials of Stone Tools Found in the Carpathian Basin..... | 116 |
| Non-Destructive Analysis of Metallic Samples Using PGAA and Complementary Methods | 118 |
| Radiography and Tomography at Channel No. 2 of BRR | 119 |
| Selected Applications of Mössbauer Spectroscopy | 120 |
| Progress in Separation-Method Development of Lanthanides and Minor-Actinides..... | 121 |
| VIII. MISCELLANEOUS | 122 |
| Evaluation of Fracture Tests Using Advanced Models | 123 |
| Age-Dating of Uranium Samples | 124 |
| Digital Geometry..... | 125 |
| Phase Equilibrium; Metastable and Supercritical Systems | 126 |
| Preliminary Neutron Activation Study for ESS | 127 |
| Development of Nuclear Analytical and Imaging Techniques, Nuclear Data Measurements and Related Training Activities | 128 |
| Progress at the Neutron Activation Analysis Laboratory | 130 |
| Analytical Approaches to the OH Radical Induced Degradation of Sulfonamide Antibiotics in Dilute Aqueous Solutions..... | 131 |
| Synthesis of Cellulose-Based Superabsorbent Hydrogels by High-Energy Irradiation in the Presence of Crosslinking Agent..... | 132 |
| One Electron Reduction of Penicillins in Relation to the Oxidative Stress Phenomenon..... | 133 |
| IX. INTERNATIONAL ACTIVITIES | 134 |
| Participation in the OECD SCIP III Project | 135 |
| Participation in the ESNII Plus EU Project | 135 |
| Participation in the SAFEST EU Project..... | 136 |
| Radiation Resistance of ITER Bolometers..... | 137 |
| Ageing of Reactor Structural Materials - Participation in the AGE-60 EU Project | 138 |
| DEMO Material Properties Handbook | 139 |
| Joint Hungarian-Korean Laboratory Program for Advancement of Nuclear Thermal-Hydraulics Safety..... | 140 |
| European Joint Programme for the Integration of Radiation Protection Research - CONCERT | 141 |
| Activities in the FP7 EURATOM CHANDA project | 142 |
| X. RESEARCH RELATED TO THE INSTITUTE OF TECHNICAL PHYSICS AND MATERIAL SCIENCES ... | 143 |
| Wafer-Scale Integration of Piezoelectric Nanowires..... | 144 |
| Nanoparticle Assemblies | 145 |
| Exfoliation of Large-Area Transition Metal Chalcogenide Single Layers..... | 147 |
| Structure and Properties of Graphene on Gold Nanoparticles | 148 |
| Electronic Properties of MoS ₂ Flakes Grown on Graphite | 149 |
| Atomic and Electronic Structure of Native Point Defects in MoS ₂ Single Layers Revealed by Scanning Tunneling Microscopy | 150 |
| Modulation of Physical Properties by Stacking of 2D Materials..... | 151 |
| Variability of Structural Coloration in Blue Butterfly Wings | 152 |
| Makyooh Topography | 153 |
| Radioecological Investigation of Butterflies..... | 154 |
| Nondestructive Indication of Fatigue Damage in Ferromagnetic Construction Materials | 155 |
| Determination of Migration of Ion-Implanted Ar and Zn in Silica by Backscattering Spectrometry | 156 |
| Effect of Heat Treatments on the Properties of Hydrogenated Amorphous Silicon for PV and PVT Applications..... | 156 |
| Verification of the Effective Medium Approximation for Surface Roughness by Finite Element Method | 157 |
| Plasmon-Enhanced Two-Channel Kretschmann Ellipsometry | 157 |
| Protein Adsorption, Cell Adhesion and Polyelectrolyte Deposition on Titania Nanoparticle Coatings Studied by Two-Channel Kretschmann Ellipsometry | 158 |
| Development of Optical Metrology Tool for In-line Qualification of Thin Films on Large Area..... | 159 |
| Modeling and Simulation @ MEMS Lab..... | 159 |

| | |
|---|-----|
| Preparation of Compact Nanoparticle Clusters from Polyethylene Glycol-coated Gold Nanoparticles by Fine-tuning Colloidal Interactions | 160 |
| Introducing Nanoscaled Surface Morphology and Percolation Barrier Network Into Mesoporous Silica Coatings | 161 |
| Fine-tuning of Gas Sensitivity by Modification of Nano-Crystalline WO_3 Layer Morphology..... | 162 |
| Wavelength Conversion in $\text{GaInAsP}/\text{InP}$ Near Infrared Surface Emitting Diodes | 163 |
| 3D Force Sensors for Minimal Invasive Surgery Applications | 164 |
| 3D Interpolated Potential for MD | 165 |
| Nanosize Effect on the Evolution of Magnetism on Curved Surfaces..... | 166 |
| Microfluidic System for Separation of Circulating Tumor Cells (CTC) | 167 |
| Finite Element Modeling (FEM) and Characterization of Cell and Molecular Advection in Continuous Microfluidic Systems | 168 |
| Autonomous Microfluidic Sample Transport Systems | 169 |
| Cell and Particle Sorting in Microfluidic Systems | 170 |
| Polymer Microecogs Optimized for in Vivo Pharmacological Investigations | 170 |
| Double Markers for Direct Contact Formation on Ultra-Low Dimension Objects | 171 |
| Silicon Probes Designed for Infrared Neural Stimulation..... | 172 |
| Iontophoretic Injection Microsystem Delivering Pathway Tracer Molecules in the Living Tissue..... | 172 |
| In Vitro Studies Revealing the Immune Response of the Living Tissue to Nanostructured Implant Surfaces | 173 |
| New Approaches in the Development of Hypoallergenic Implant Material in Orthopedics: Steps to Personalised Medicine | 173 |
| Homogeneous Transparent Conductive $\text{ZnO}: \text{Ga}$ by ALD for Large LED Wafers | 174 |
| Characterization of Biocompatible Ceramic $\text{TiC} / \text{Amorphous C}$ Thin Films Prepared by DC Magnetron Sputtering..... | 175 |
| Graphene-Ceramic Composites for Tribological Application in Aqueous Environments..... | 176 |
| Characterization of Defect Structure in Electrodeposited Nanocrystalline Ni Films..... | 176 |
| Microscopy of High Quality Cubic SiC Grown on Si | 177 |
| Low Cycle Thermomechanical Fatigue of a Reactor Steel: Microstructural Investigations | 178 |
| Characterization of the Topography of the Graphene Moiré Superlattice on $\text{Au}(111)$ and $\text{Cu}(111)$ Supports | 179 |
| Metal (Ni) Induced Crystallization in Amorphous Si Thin Films..... | 180 |
| Universal Nanopatterning Technique Using RF Plasma Etching Through Templates of Langmuir-Blodgett Films | 181 |
| CoPt/TiN Thin Films of Enhanced Perpendicular Coercivity by N_2 Incorporation During Deposition | 182 |
| A Device for Micro-Combinatorial TEM Studies | 183 |
| Grain Boundary Characterization Based on Diffraction Data | 184 |
| Hydrogel Film Fabrication for Biosensing | 185 |
| The Dynamics of Living Cell Adhesion on Nanostructured Genetically Engineered Molecular Layers Revealed by Label-Free Optical Biosensors | 185 |
| Label-Free Profiling of Cell Adhesion: Determination of the Dissociation Constant for Native Cell Membrane Adhesion Receptor-Ligand Interaction..... | 186 |
| Incubator Proof Miniaturized Holomonitor to In Situ Monitor Cancer Cells Exposed to Green Tea Polyphenol and Preosteoblast Cells Adhering on Nanostructured Titanate Surfaces: Validity of the Measured Parameters and Their Corrections..... | 187 |
| Biophysical Characteristics of Proteins and Living Cells Exposed to the Green Tea Polyphenol Epigallocatechin-3-Gallate (EGCg): Review of Recent Advances from Molecular Mechanisms to Nanomedicine and Clinical Trials | 188 |
| Automated Single Cell Isolation from Suspension with Computer Vision | 189 |
| Monitoring of Cellular Toxicity Assessment of Agrochemicals by Using Label-Free Optical Biosensor Technique | 190 |
| Eurasian mtDNA Analysis with a New Iterative Rank-Correlation Method..... | 190 |
| Does Knowing the Opponent's Strategy Guarantee Optimal Play? | 191 |
| Griffiths Phases and Localization in Hierarchical Modular Networks | 192 |
| ABBREVIATIONS..... | 193 |

MISSION STATEMENT OF MTA CENTRE FOR ENERGY RESEARCH

- Research and development in the field of nuclear science and technology for facilitating the adoption and the safe use of nuclear technology in Hungary.
- To participate in international research effort aiming at the establishing a new generation of nuclear power plants and closing the fuel cycle.
- Maintaining and improving competence in nuclear science and technology, especially in the field of nuclear safety, security, health physics, nuclear and isotope chemistry.
- To guarantee the safe operation of Budapest Research Reactor (BRR), and to ensure the accessibility of the research facilities around the reactor.
- Research activities to improve nuclear analytical and imaging methods and their applications for energy and materials science.
- Perform studies in the field of environmental physics related to energy generation, renewable energies, energy storage and their impact on public health, and on environmental safety.
- Research and development in the field of low carbon energy technologies and of energy saving in industrial technologies.
- Interdisciplinary research on complex functional materials and nanometer-scale structures, exploration of physical, chemical, and biological principles, their exploitation in integrated micro- and nanosystems, and in the development of characterization techniques.
- Dissemination of the results in international programs, education and industrial research.

SCIENTIFIC ADVISORY BOARD OF THE MTA CENTRE FOR ENERGY RESEARCH

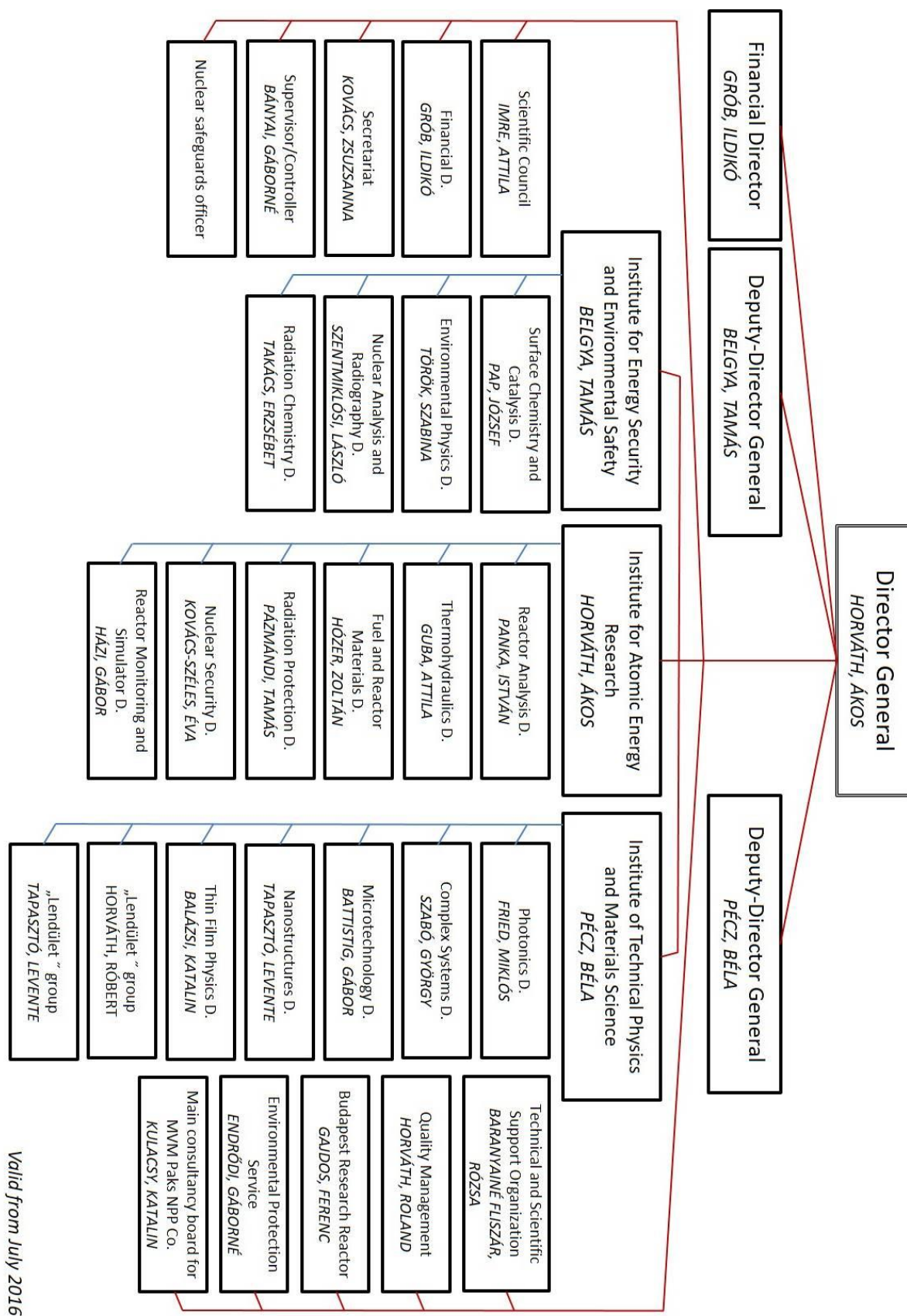
The board consists of five Hungarian and two foreign leading scientists. The last meeting of the board took place in Budapest, April 14, 2015. The management of EK presents usually an overview of the R & D activities in the previous year as well as tables containing financial data and analyses of human resources. The possibility of the measurement of the scientific output is in general discussed, too. There is a consensus, that real evaluation has to be based on several years. The R&D plans for the coming year and for the near future will be presented, too.

The board members usually comment the presentations and ask questions. The board suggested in 2015 EK to inform the president of the MTA on the problem that the insufficient number of qualified people might cause difficulties in the nuclear field in the future, especially taking into account the need due to government decision on new NPP units. The Board members commented that the activities of the recently joined Institute for Technical Physics and Materials Science should be harmonized with those of the two other institutes within the Centre. The Board suggested also preparing a more detailed vision of the future activities and presenting it at the next meeting.

Members of the Board:

- Prof. Dr. László Keviczky (Chair), MTA Institute for Computer Techniques and Automation
- Dr. Hervé Bernard, Deputy Chairman, Centre French Alternative Energies and Atomic Energy Commission (CEA)
- Dr. Maximilian Fleischer, Head of Department of Corporate Technology, Siemens AG
- Prof. Dr. Ádám Kiss, Eötvös Loránd University
- Dr. Zoltán Homonay, Head of Laboratory of Nuclear Chemistry, Eötvös Loránd University Mr. István Hamvas, Director General, Paks Nuclear Power Plant
- Dr. József Rónaky, Scientific Advisor, Hungarian Atomic Energy Authority

ORGANIZATION STRUCTURE OF THE MTA CENTRE FOR ENERGY RESEARCH



QUALITY MANAGEMENT

In order to achieve the highest quality of research, development, design, condition monitoring and valuation, engineering, contracting and managing in design, production, implementation and inspection, the Research Centre's quality management system has been continuously upgraded by the recommendations of ISO 9001 standard since 1994. Reviewing our QM system by integral audits and management reviews, evaluating improvement opportunities, maintaining project documentation, infrastructure, supporting communication, ensuring the competence of workers the management improves the Centre's QM system. For the new organization structure our Quality Policy has been renewed. Many new employees induced a need to upgrade our QM tuition practice. We organised the work and fire safety educations. Our QM system has been certified by Hungarian Standards Institution, IQNet, and MVM Paks NPP.



Certifications by Hungarian Standards Institution, IQNet, and MVM Paks NPP



Accreditation Certificate for Environmental Protection Service, and Nuclear Security Department

BUDAPEST RESEARCH REACTOR

One of the most important strategic large scale research facilities in Hungary is the Budapest Research Reactor (BRR). It serves the needs of an extensive and diverse scientific community by supporting R&D opportunities, helping innovation and providing a strong foundation for training and education.



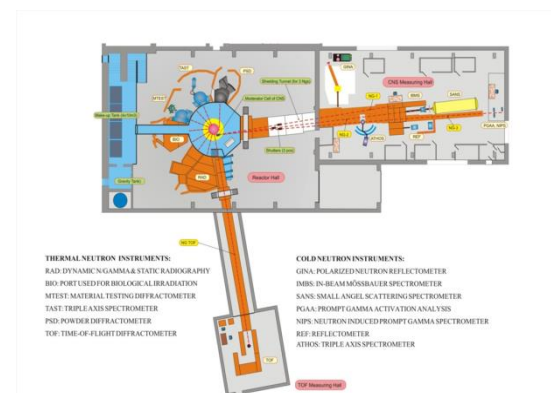
Bird's eye view of the Budapest Research Reactor

The BRR is a VVR-type reactor that uses light water as moderator and cooling fluid. The power of the reactor is 10 MW provided from low enrichment uranium fuel, and its main purposes – as established during the feasibility/functionality study - are: radioisotope production, production of thermal and cold neutron beams for research and applications in all areas, development of new functional materials and neutron activation analysis.

The core is designed to have about 10-11 reactor cycles per year, each having a cycle length of 10 days. We are committed to long-term safety and responsible operations, taking care of the wastes from the spent fuel coming from the reactor. Besides the temporary spent fuel storage pool, we also operate a long term spent fuel storage building for the physical and environmental separation between the reactor and the spent fuel storage.

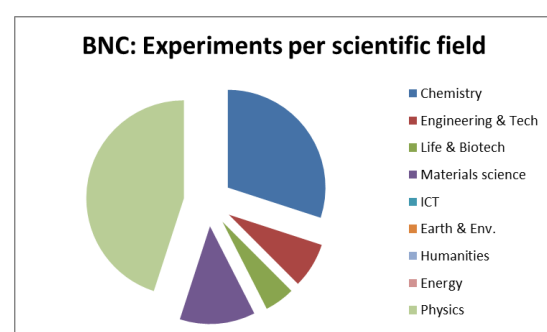


Top view of the research reactor



Layout of the BRR's facilities

The reactor is the centre of three kind of activities: e.g. research activities utilizing neutron beams, production of radioisotopes for industrial and research purposes and national and international training sessions. We are proud of our innovative flagship research topics, which are carried out with a network of neutron beam stations, including beam-lines of thermal neutrons, experiments on powder diffractometry, residual stress diffractometry, radiography, biological irradiations and beam-lines of cold neutrons for experiments on small angle neutron scattering, reflectometry, prompt gamma activation analysis and others. In accordance with recent worldwide trends, we are open to establishing new industrial relations, and supporting innovation. We aim to increase our competence on special topics, to implement new technologies and develop new materials, to promote and exploit our R&D capacity at the national and regional/international level. During the past years the BRR hosted several international schools on various technical and research topics, special trainings in the field of reactor physics, reactor operation, nuclear measurement techniques, and safety and environmental issues.



BRR is used by members of many scientific, medical, environmental and industrial communities, as well as several Hungarian Universities. Neutron beams are uniquely suited to study the structure and dynamics of materials at the atomic level. The Budapest Neutron Centre (BNC) coordinates the scientific utilization of the research reactor. Some of main research topics currently are:

neutron scattering, used to examine samples under different conditions such as variations in vacuum or pressure, high and low temperature, and magnetic field, modeling real-world conditions.

using neutron activation analysis, both prompt and delayed, it is possible to measure the concentration of elements in ppm and ppb levels of even small samples. Atoms in a sample are made radioactive by exposure to neutrons from the reactor. The characteristic gamma radiation each element emits can then be detected.

neutron activation is also used to produce different radioisotopes, widely used in industry and medicine, by bombarding particular elements with neutrons so that the target nucleus has a neutron added. For example Y-90 microspheres to treat liver cancer are produced by bombarding Y-89 with neutrons.

testing of materials for reactors; materials are subjected to intense neutron irradiation to study induced changes. For instance, some steels become brittle, and alloys exp. high-entropy alloys which resist embrittlement must be used in nuclear reactors.

production of radioisotopes for different applications.

applied research using neutron beams (neutron radiography, exp. cooling system of refrigerator or engine system of a car, tomography of different materials and items).

The BNC provides researchers with 15 neutron instruments; 13 instruments are installed directly on the horizontal beam ports of the reactor or to the thermal and cold neutron guides, while the other 2 are placed at the vertical irradiation channels. The instruments are supported by a variety of sample environments and data analysis and visualization capabilities.

The BNC provides access to the international neutron user community through a peer-review arrangement. Local scientists assist researchers and industrial users to find the appropriate neutron techniques that meet their research needs. The various neutron scattering instruments in BNC cater to a large number of users from Europe and has grown in strength and stature over the years.

BNC is a member of the European network of neutron centres, and a partner in the EU Framework Programme projects (NMI3-II, CHANDA, IPERION, SINE2020, ESS-BrighnESS, CERIC).

BNC is strongly committed to the training of future professionals. In cooperation with Hungarian universities (Budapest University of Technology and Economics, Eötvös Loránd University, Pannon University), BNC accommodates students for laboratory practice for studying nuclear-based techniques. A specialized course was developed for geology students at the Eötvös Loránd University to introduce nuclear analytical techniques into their education. To train young scientists in neutron physics and to attract new users, BNC organizes the Central European Training School on Neutron Scattering on a regular basis. The school provides insight into neutron scattering, element analysis and imaging techniques and their applications to study the structure and dynamics of condensed matter.

The Budapest Research Reactor is open to the public. Members of the local communities and high school and university students are invited to visit regularly and learn more about the amazing nuclear science possibilities available at BRR.



Researchers working at the Budapest Research Reactor

ENVIRONMENTAL PROTECTION SERVICE

In the past year the Environmental Protection Service (EPS) operated in compliance with the pertinent laws and orders. EPS is a functional unit of MTA Centre for Energy Research (MTA EK). In accordance with our main tasks, EPS took and measured environmental samples which were collected in the whole territory of the KFKI Campus.

In the year of 2015 we made several improvements in our laboratory equipment. We got one of our semiconductor detectors repaired which is used for measuring samples from environmental monitoring. We bought some radioactive sources and performed calibration procedures with these sources in order to make our detectors more sensitive to environmental control measurements.

EPS took part in the education of two groups of trainees of an international education course supported by the International Atomic Energy Agency (IAEA). They studied the operation of nuclear research centres and research reactors including the tasks of the environmental service.

Furthermore, we received 2 MSc students from Eötvös Loránd University of Sciences and Budapest University of Technology and Economics for their diploma thesis work.

Measurements of different type and sensitivity are performed by EPS for the analysis of radioactive materials including gamma-ray spectroscopy, selective alpha and beta counting and liquid scintillation spectrometry. We improved the measurement features of our in-vivo whole body counter; direct thyroid measurements are also available with the detector installed in the mobile laboratory.



Gáborné Endrődi
Head of Department
endrodi.gaborne@energia.mta.hu

New mobile laboratory unit



PROGRESS REPORT BY DEPARTMENTS



INSTITUTE FOR ATOMIC ENERGY RESEARCH

REACTOR ANALYSIS DEPARTMENT

In order to perform safety analyses of the new VVER-1200 reactors, the preparation and development of our own reactor physical code system KARATE have been started in 2015. The methodology of the preparation of few group cross sections for the new units was elaborated and verified by the SCALE code. The influence of resonance self-shielding of the isotopes of plutonium with higher mass numbers was also investigated but it was found that the new methodology is important mainly in case of MOX fuel.

The Department has been participating in the OECD NEA UAM ('Uncertainty Analysis in Modeling') benchmark. The survey of the uncertainties of the KALININ-3 VVER-1000 core calculations was carried out by the coupled KIKO3D-ATHLET code for a fresh core using the covariance matrices of basic cross sections. This task is also relevant for the new units from the safety margin's point of view. In order to take into account the influence of burnup, the development of the 'statistical' KARATE code system has been continued. The first results are promising in connection with the uncertainties of the power and burnup distributions. Supporting the criticality calculation methods of the spent fuel storage pool, a full core MCNP model of the core has been developed and the uncertainties of the calculated effective multiplication factors were investigated at hot zero power. It was pointed out that it is needed to take into account the uncertainties of the isotopic compositions, as well.

In 2015, several projects have been started within the frame of the Hungarian Sustainable Nuclear Energy Technology Platform and in connection with the Gen IV reactors. In the frame of an OECD NEA collaboration, the KIKO3DMG three-dimensional nodal code was prepared for the calculation of neutron physics in sodium cooled fast reactors. Temperature and fuel dependent cross sections were prepared and built into the code. KIKO3DMG was coupled with the ATHLET3.0 thermal hydraulics system code for kinetic calculations. It was demonstrated for different cases that the code system is able to calculate the most important, safety-related parameters like the reactivity feedback coefficients, the power peaking factors, delayed neutron fractions, etc. The coupled code system was successfully tested by a rod movement transient. In the frame of the V4 collaboration, the KIKO3DMG code has been prepared for the core calculation of the ALLEGRO - gas (Helium) cooled fast reactor demonstrator. Temperature and fuel dependent cross sections were prepared and built into the code. The parameters of the core were refined and an international benchmark was defined related to ALLEGRO. Safety-related parameters were determined and it was pointed out that the expansion of the materials plays an essential role in the reactivity feedback effects.

The research directions of the department was determined for many years by the former leader, Mr. András Keresztúri. His long term outstanding work in the field of neutron physics was also recognised by the Prometheus Award of the Hungarian Government. We are also thankful for his professional activities directing the department.

István Panka
Head of Department
panka.istvan@energia.mta.hu

THERMOHYDRAULICS DEPARTMENT

The experimental program on investigation of the efficiency of external cooling in the CERES Facility was continued. The ninth series of experiments had been performed, the influence of the flooding tube geometry at the sump model was investigated with different power distributions on the vessel surface. This work focused on the effectiveness of cooling with significant flow fluctuations which may lead to overspill from the sump, consequently loss of remaining coolant volume. The results show that the modelled circumstances do not lead to overspill.

The objective of the Joint Hungarian-Korean Laboratory (JHKL) is to advance scientific knowledge in three areas important for nuclear power plant safety: the effect of pressure waves on pressure vessel internals, the coolability of deformed fuel in a nuclear reactor core and coolant mixing in cold legs and downcomer, as well as to increase nuclear safety assessment capabilities via validation of computer codes. The scope of the activity includes performance and evaluation of tests in three test facilities of MTA EK: the PMK, the CODEX-COOL and the plexi model of the downcomer. Available computer codes at MTA EK and KAERI were applied with the aim to validate these tools for the given phenomenon. In support of the OECD ATLAS Project several pre- and post-test calculations was carried out.

As to the issue of coolant mixing in cold leg and downcomer stereoscopic Particle Image Velocity (PIV) measurement system was applied to produce high quality three-dimensional velocity profiles. FLUENT calculations performed indicate that maximum and minimum values of measured and calculated velocity component distributions are close to each other in all test cases.

The OECD PKL3 project investigates safety issues relevant for current nuclear power plants as well as for new design concepts by means. The tests performed in the PKL facility are complemented by experiments in the PMK facility. The aim of the first PMK test series was to study the propagation of pressure waves in the primary circuit following a large break in the system and their effect on pressure vessel internals, while the second PMK test addressed a station blackout scenario. Tests are performed in the facilities listed above with the aim to create a data base covering current safety-related phenomena.

The department participated in the preparation of the ALLERGO Design and Safety Roadmap in 2015. This document defines the tasks of each participant of the Visegrad Countries from the pre-conceptual design to the detailed design phase of ALLEGRO.

Critical Heat Flux (CHF) measurements were carried out at low flow low pressure conditions using the CHF experimental mockup built in the MTA EK ZR6 building. The collected data were analyzed and the CHF data points were identified and extracted. Five independent correlations – chosen from the literature – were compared with our measurement data.

The staff of the department is involved in giving lectures at the Budapest University of Technology.

Attila Guba
Head of Department
guba.attila@energia.mta.hu

FUEL AND REACTOR MATERIALS DEPARTMENT

The members of the Department participated in more than thirty domestic and international projects in 2015. The following examples are illustrating some of the most important results.

The mechanical properties of fuel rod claddings in different states and under different accident circumstances were studied in several experiments. The behaviour of E110 and E110G claddings under loss-of-coolant accident (LOCA) conditions was investigated in an integral test using the CODEX facility. The electrically heated seven-rod bundle was heated up to 900 °C and some of the fuel rods with high internal pressure ballooned and burst. Small-scale separate effect tests were performed in order to investigate the effect of pre-oxidation of Zr cladding on the failure of fuel rods under “air ingress” type reactor accident conditions. The load-bearing capability of the oxidized samples was analysed in a tensile test machine with ring compression tests.

In the framework of a Korean-Hungarian co-operation, the coolability of hexagonal VVER-440 type bundles was investigated during the reflood phase of LOCA events. The ballooning of fuel rods in the 19-rod bundle was simulated by special sleeves mounted on the rods. The high-temperature fuel rods were reflooded from the bottom. The results showed that the coolability of the bundle can be guaranteed even with a high degree of blockage, since the presence of ballooned sections does not prevent, only delays the cool-down process. The parallel by-pass line can also cause some short time delay in the cooling.

Different domestic and foreign numerical methods were used for the simulation of leaking fuel rods. The simulation period covered several years of operation of the four reactors at Paks NPP. The results can support decision making at the NPP on the further handling and storage of leaking assemblies. Additional analyses were carried out to evaluate the consequences of boiling in the spent fuel pool when leakers are stored there.

In the framework of structural integrity activities a new evaluation method was developed for the analysis of fracture mechanics measurements. These measurements supply the basis for the p-T curve that is used at the Paks NPP to control the cold overpressure mitigation system and is applied in the PTS (Pressurised Thermal Shock) analyses. The fracture mechanics measurements were precisely simulated with finite element methods. The results showed that the simulated results were much closer to the measured ones than in the earlier studies. It is intended to extend the new method to decrease the uncertainty of lifetime extension calculations using the data of additional low temperature measurements.

New research program was initiated in order to develop the optimal composition of concretes that will be used at the construction of new units at the Paks NPP. The experts of the Department started the development of numerical methods for the structural integrity analyses of the new VVER-1200 type reactors.

Zoltán Hózer
Head of Department
zoltan.hozer@energia.mta.hu

RADIATION PROTECTION DEPARTMENT

In year 2015, two colleagues left and two young researchers joined the Department. One of the colleagues spent one month as a guest scientist at the Max-Planck-Institute für Sonnensystemforschung (MPS) in Göttingen, Germany. Researchers from the Department participated in the CATHyMARA (Child and Adult Thyroid Monitoring After Reactor Accident) project. In 2015 the EK became a member of the NERIS Platform (European Platform on preparedness for nuclear and radiological emergency response and recovery). A Saudi Arabian researcher spent two months in our institute in the frame of an IAEA fellowship programme.

The 2015 Laurels for Team Achievement of the International Academy of Astronautics were given to the Rosetta Philae Lander Mission, including the experts of the Department working on the Dust Impact Monitor (DIM) and the Simple Plasma Monitor (SPM) instruments of the lander. This award is the highest team distinction of the Academy. Széchenyi Prize was

awarded to István Apáthy, electrical engineer, developer of the high voltage unit of the SPM instrument on Rosetta's Lander Philae. Széchenyi Prize is a state prize founded to honor the greatest scientists in Hungary alive today.

The Pille-ISS thermoluminescent dosimeter system developed at the former AEKI was successfully operated as part of the service system on board the Russian service module of the International Space Station (ISS). Manufacturing of a second flight model of the system got underway, which is going to replace the presently operating but expiring system on board. In the frame of the Rocket and Balloon Experiments for University Students programme of the European Space Agency (ESA), the REM-RED experiment was successfully performed in March 2015, in Sweden, in the beginning of the most intense geomagnetic storm within the last 10 years. In the REM-RED experiment Geiger-Müller counters of different sensitivities and orientations were used to quantify the cosmic ray intensity and to study its directionality for the first time during the flight of the REXUS-17 rocket up to an altitude of 88 km. Development of the ESEO-TRITEL three-dimensional silicon detector telescope continued in the frame of the European Student Earth Orbiter (ESEO) programme of the ESA. In the frame of the DOSIS-3D project organized by ESA and managed by the German Aerospace Centre, the radiation area monitoring inside the European Columbus module of the ISS continued; MTA EK participated with its own detector packages consisting of thermoluminescent and solid state nuclear track-etch detectors.

The evaluation of the calibration measurements of the whole body counter was finished. Detailed analysis of the results obtained between 2009 and 2014 of the environmental radiation monitoring system around Paks NPP was performed. The research in the field of dispersion of radioactive material in the atmosphere and in surface waters was continued. The work on developing an atmospheric dispersion model capable of estimating the environmental effects of a radioactive release outside of the vicinity of the source was also continued. Several calculations and analyses were performed supplying the operation safety of the Hungarian nuclear facilities.

Tamás Pázmándi
Head of Department
tamas.pazmandi@energia.mta.hu

NUCLEAR SECURITY DEPARTMENT

The year 2015 was the time for innovative developments and improvements in the field of nuclear forensics and in the establishment of international and national contacts and scientific cooperation. Several supporting R&D projects were carried out at the Department mainly for the Hungarian Atomic Energy Authority (HAEA), International Atomic Energy Agency (IAEA), Hungarian universities (e.g. Szeged University) and the Paks Nuclear Power Plant.

Development of the PTR-32 neutron coincidence device and in-field Laser Induced Breakdown Spectroscopy (LIBS) method for safeguards purposes, have been continued. The first prototype of the National Nuclear Forensic Library searching program was developed and established together with data of confiscated nuclear materials as well as nuclear fuel samples originated from Hungarian application. This topic is essential not only for Hungary and HAEA but is also a part of a Coordinated Research Project (CRP) of the IAEA.

In order to support the safeguards activities related to the nuclear materials, various measurement methods are under development and also in routine use in the Hungarian nuclear establishments. Measurements of enrichment of fresh fuel have been performed successfully at Paks Nuclear Power Plant in 2015, too. The experiments to study the burnup of the spent fuel have also been continued. Besides, corrosion study was carried out at the primary and secondary cooling system of the Power Plant.

Testing of huge, sensitive plastic scintillation detectors has been started at the test laboratory. The construction of static and dynamic gamma and neutron irradiation facilities and preparation of data collection system for testing has been also started.

MTA EK piloted a residential assignment in nuclear forensics where a qualified Slovakian scientist was placed for three month to the Nuclear Security Department. The assignment was organized by IAEA.

Several analytical techniques were used in our projects and to achieve the scientific results: mass spectrometry, gamma-spectroscopy, neutron coincidence technique at our Department and as additional methods from other departments: scanning electron microscopy, X-ray diffraction and X-ray fluorescence.

We organized the 20th Annual Meeting of the Nuclear Forensics International Technical Working Group in Budapest in June, 2015. The meeting was successful together with a small table-top exercise and a live demonstration with the mobile expert support team of the Nuclear Forensic Laboratory of MTA EK. The meeting was financially supported by the EU.

One member of the staff, Péter Völgyesi, successfully defended his PhD thesis at the Eötvös Loránd University in Budapest.

Éva Kovács-Szélés
Head of Department
eva.szeles@energia.mta.hu

REACTOR MONITORING AND SIMULATOR DEPARTMENT

In 2015, the Reactor Monitoring and Simulator Laboratory focused in particular on the refurbishment project of VERONA on-line core monitoring system of Paks Nuclear Power Plant (NPP). After successfully completing the first two phases of this project (development and installation of the new system in the first reactor unit), we also successfully participated as subcontractors in the tender of two significant I&C (Instrumentation and Control) reconstruction projects of Paks NPP: reconstruction of the rod control and reactor power controller system (RPCS project) and refurbishment of plant computer system (PCS project). Considering the RPCS project we have already finished our tasks in 2015, i.e. we have implemented the models of the new systems designed by SKODA JS in the full-scope simulator of Paks NPP and validated the new design in cooperation with the experts of the plant and the designer.

Considering the PCS project, the hard work is not over; in fact, it has only just begun with the design of the new system.

We also participated in two other important projects in 2015, as project leaders: design of a new reactivity monitoring system (RMR project), and establishment of the development of the environmental and radiation monitoring system (ERMS project) of Paks NPP.

The objective of the RMR project was to prove the wide-range applicability of a new type of neutron detector for reactivity monitoring. A new pilot system has been designed and installed in the 2nd unit of Paks NPP and a sequence of measurements has been performed to demonstrate the capabilities of the new detector. After successful demonstration, the management of the plant decided to apply the new detector types for reactivity monitoring not only during reactor startup but during fuel reloading, too. Based on our concept study, the design and implementation of a new complex reactivity monitoring system will be started in 2016.

In the EMRS project we coordinated the systematic revision of the present radiation monitoring system of Paks NPP by studying the resistance capabilities of system components against earthquakes and station blackout. Based on our investigation, we have prepared a technical description by redesigning and specifying all system components which need reinforcement to resist a design base earthquake and 72 hours power loss.

Based on our experiences in nuclear power plant simulation, we are developing a state-of-the-art graphical simulation environment, called SIMTONIA (SIMulation TOols for Nuclear Industrial Applications). This environment has already been applied successfully in above mentioned projects.

The laboratory, like in the past years, provided simulation exercises for students of Budapest University of Technology and Economics in 2015.

Considering our infrastructure, it is worth mentioning that our computer center has been completely renewed ensuring a solid technological basis for our future developments.

Gábor Házi
Head of Department
hazi.gabor@energia.mta.hu

INSTITUTE FOR ENERGY SECURITY AND ENVIRONMENTAL SAFETY

SURFACE CHEMISTRY AND CATALYSIS DEPARTMENT

Progress in 2015:

- New PhD students: Johanna Károlyi (dry reforming of methane) and Gergely Nagy (selective oxidations). PhD degree to Tímea Benkó (on maternal leave, gold catalysts in CO oxidation and selective glucose oxidation), MSc degree to Daniella Szülek (water splitting electrocatalysis), summer course to chemical engineers from the Jazan University (Saudi-Arabia)
- OTKA PD grant to Ferenc Somodi (promoted bimetallic catalysts) and postdoctoral scholarship to Dávid Sránkó (1 yr at Berkeley in 2016, electrocatalysis related to artificial photosynthesis), 3 year Bolyai János Scholarship evaluation to József S. Pap (excellent)
- Joint Research Activities/bilateral cooperations: Łukasz Szyrwił (Wrocław Medical University, homogeneous water splitting electrocatalysis), Róbert Horváth (EK-MFA, self-assembled electrode surfaces), University of Pannonia (Rita Skoda-Földes, heterogeneous catalysis)
- commissioned work for Bourns Automotive Co., Alcoa Zrt. and Paks Nuclear Power Plant (corrosion and other surface processes on metal surfaces)

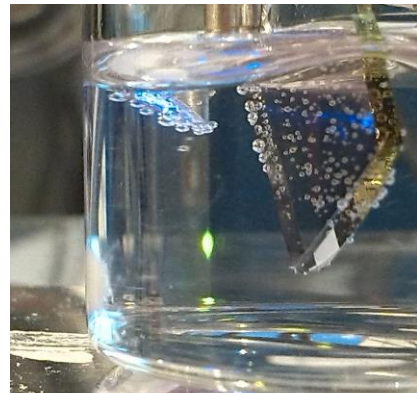
Most significant scientific achievements:

Water splitting: Two mononuclear Cu^{II} complexes with tetrapeptides incorporating a L-2,3-diaminopropionic acid (dap) branching unit were reported to undergo PCET and catalyse water oxidation. C-Terminal His extension of dap (L = 2GH) instead of Gly (L = 3G) lowered the pKa for Cu^{III}H-2L (9.36 vs. 9.98) and improved the TOF at pH 11 (24 vs. 53 s⁻¹) in water oxidation electrocatalysis. A three dimensional, quasi-tripodal new ligand, H-His-Dap(H-His)-His-NH₂ (3H) was also reported. This ligand offers new options in metal binding. A strategy was presented for the characterization of 3H focusing on the role of structural domains in Cu^{II} binding. Potentiometric, spectroscopic (UV-Vis, CD and EPR), mass spectrometric and electrochemical data indicated that in monomeric Cu^{II}-3H complexes the metal is bound with very high affinity due to the 3D branching.

We demonstrated the heterogenization of homogeneous water oxidation electrocatalysts in surface coatings produced by combining the substances with a suitable polyelectrolyte. The electrocatalysts i.e. Cu^{II}-3G and Cu^{II}-2GH were heterogenized by building composite layers on indium-tin-oxide (ITO) electrode surface. Optical waveguide light-mode spectroscopy (OWLS) has been applied to reveal the formation of a Cu-ligand/polyelectrolyte/phosphate coating. Electrochemistry employing coated ITO substrates indicated improved water oxidation electrocatalysis and dependence of this improvement on the presence or absence of a histidine ligand in the deposited Cu(II)-complexes. The results are under publication.

Activation of C1 molecules: the selective conversion of methane with carbon dioxide to yield hydrogen and carbon monoxide (dry reforming, DRM: CH₄+CO₂↔2CO+2H₂) was further investigated on nanostructured ZrO₂-supported bare or Na₂O-promoted Ni potential dry reforming catalysts. The Ni/ZrO₂ catalysts were prepared by a sol-based synthesis route, wet impregnation with the concomitant addition of NaHCO₃ and incipient wetness technique. The Ni nanoparticles in the fresh catalysts were smaller than 20 nm and the NiO on the Na₂O-promoted sample was the hardest to reduce. Diffuse Reflectance Fourier Transform Infrared Spectroscopy (DRIFTS) applied to detect the surface-adsorbed species in the presence of dry reforming mixture suggested that CO₂ activation at low temperature proceeds on the catalysts prepared by sol or incipient wetness techniques via transformation of bicarbonates→formates down to C_{ads}, while on the sodium-promoted ones through the conversion of surface carbonates at the metal-oxide interface assisted by the Na₂O promoter. Catalytic tests carried out with ¹²CH₄ and ¹³CO₂ reactants at 50 mbar pressure in a closed loop circulation system revealed the formation of ¹³CH₄ via surface methanation reaction in the case of sol sample. According to the temperature programmed oxidation measurements, there were 2 types of surface coke formed in the reaction: the easily oxidized one at around 300°C was composed of only ¹²C (originating from ¹²CH₄ reactant), while the other type of coke above 500°C was composed of both ¹²C and ¹³C and formed presumably from gas phase carbon monoxide products. The coke coming from the methane source was more reactive on the Na₂O-promoted samples having stronger metal-support interaction.

Wet catalytic oxidation: special attention was devoted to model catalytic reactions for wastewaters containing organic materials. We could successfully combine radiolysis with wet oxidation at elevated temperature and demonstrated its potentials on the solution of model substrate phenol. A comprehensive book chapter was published in „Wastewater Treatment Engineering” edited by InTech Open summarizing literature examples and industrial technologies. The catalytic wet oxidations were extended to catalyst comparisons by means of designed experimental plans, moreover, detailed surface and material analysis examinations. These were discussed in a paper in the „Journal of Industrial and Engineering Chemistry”. In this case the model substrate was N,N-dimethylformamide that is a frequently used solvent in chemical industry.



O₂ evolution from water by a Cu-catalyst at indium-tin-oxide anode.

József Sándor Pap
Head of Department
pap.jozsef@energia.mta.hu

RADIATION CHEMISTRY DEPARTMENT

The OH radical induced degradation of sulfonamide and penicillin derivative antibiotics was followed in dilute aqueous solutions. As pulse radiolysis experiments show, in the case of sulfa drugs the basic initial reaction is hydroxyl radical addition to the benzene ring, forming cyclohexadienyl radical intermediates. In aerated solutions these radicals transform to peroxy radicals. Among the first formed products aromatic molecules hydroxylated in the benzene rings or in some cases in the heterocyclic rings were observed by LC-MS/MS. Comparison of the COD and TOC results shows gradual oxidation. Simultaneously with hydroxylation, ring opening also takes place. The S atoms of the sulfonamides remain in the solution (ICP-MS measurements) after degradation, whereas some part of the N atoms leaves the solution probably in the form of N₂ (TN measurements). Degradation is accompanied by a high pH drop due to formation of SO₄²⁻, NO₃⁻ and smaller organic acids. The degradation goes through many simultaneous and consecutive reactions.

In the case of penicillines the predominant sites of the •OH attack are suggested to be the thioether groups, initially yielding an •OH adduct to the sulfur and the aromatic ring. This adduct to the sulfur converts to sulfur radical cation, which has three competitive reaction paths: (1) by deprotonation at the adjacent carbon α-(alkylthio)alkyl radicals form, which undergo disproportionation leading presumably to sulfoxide as main product; (2) via the pseudo-Kolbe mechanism it may transform to α-aminoalkyl radicals; (3) the radical cation can be stabilized through intramolecular S-O bond formation. Thiyil radicals were also present in equilibrium with α-aminoalkyl radicals. In the presence of dissolved oxygen, aromatic ring hydroxylation occurred along with complex reactions resulting in e.g. oxidation of the methyl groups. The penicillin scaffold is highly affected under free radical-induced oxidative conditions, the reactive β-lactam ring, however, remains mostly intact.

Superabsorbent hydrogels were prepared by gamma irradiation from aqueous solutions of carboxymethylcellulose (CMC) and acrylic acid (AAc) with varying CMC:AAc ratio. By partially replacing the CMC with AAc, the gelation increased and led to a higher gel fraction and lower water uptake. Moreover, the gelation required significantly milder synthesis conditions. Decreasing both the dose and the solute concentration in the presence of AAc led to gels with higher gel fraction and higher degree of swelling compared to pure CMC gels. Increasing the AAc content up to 10% proved to be very effective, while very high AAc content (over 50%) hindered the gelation.

The Laboratory has collaboration inside the campus with the Surface Chemistry and Catalysis Department and with the Nuclear Security Department. It cooperates with universities (Szeged University, University of Technology and Economics, Eötvös Loránd University, Óbuda University, Szent István University). László Wojnárovits gives lectures for Ph.D. students at Eötvös Loránd University and Erzsébet Takács at Óbuda University. Between August 29 and September 3 2015 the staff of the Laboratory organized the 13th Tihany Symposium on Radiation Chemistry, an international meeting with 170 participants from more than 30 countries. The proceedings of the symposium will appear as a special issue of Radiat. Phys. Chem. The guest editors of this issue are the senior scientists of the Laboratory.

One of the Ph.D. students, Renáta Homlok defended her theses in 2015. Another Ph.D. student, Gyuri Sági was awarded with the Attila Vértes Award.

Erzsébet Takács
Head of Department
takacs.erzsebet@energia.mta.hu

ENVIRONMENTAL PHYSICS DEPARTMENT

The mission of the Department is the complex evaluation of environmental impact of energy generation. In the beginning of the years 2000, the major interest was in large scale point sources like fossil and nuclear power plants. The Department strongly supported the comparison of environmental and social impact of life and fuel cycles. Human health was considered as most sensitive receptor of the impacts. The experimental group carried out field and laboratory studies for proper estimation of air pollution exposition. Fundamental research was carried out by the theoretical group for the proper estimation of exposition-response function of low-dose ionizing radiation (of nuclear cycle) and atmospheric particles (resulting of combustion of solid fuel). With the accession to European Community (EC) in 2004, Hungary complied with most air quality regulations of the EC.

The characterization of the health effects of low dose ionizing radiation or any environmental pollutant is one of the most important challenges of current radiation and environmental protection. The exploration of the basic mechanisms associated with the exposure to low doses of ionizing radiation and the characterization of the dose-effect curves at low doses received high priority at international level and also within our laboratory. One of our research topics is the characterization of the cellular-, tissue-, organ- and health effects of inhaled radon progenies. Other specific topics include low dose hypersensitivity, hyperplasia, cellular versus tissue reactions, individual sensitivity, role of spatial inhomogeneity of burden and role of dose rate. We develop complex numerical tools, such as mutation models, the stochastic respiratory tract deposition model and computational fluid dynamics based lung models. Our models are used also to characterize the burden of tobacco smoke, industrial-, urban-, therapeutic- and environmental aerosols. The research is conducted within large scale national and international projects and platforms. We are full members of the European Joint Programme for the

Integration of Radiation Protection Research Project, in addition the MELODI (Multidisciplinary European Low Dose Initiative) and EURADOS (European Radiation Dosimetry Group) Platforms. Occasionally, we irradiate biological samples in the Budapest Neutron Centre.

The Department has developed dedicated sampling and analyzing devices for airborne particulate matter and has experience in building air quality monitoring stations at industrial facilities (e.g. power plant and airport). Measurement of particulate and gaseous atmospheric components is possible by the monitoring station installed at the KFKI Campus. The department has developed a versatile X-ray fluorescence (XRF) laboratory. Occasionally, these studies are utilized for identifying local and remote sources of emission and determining potential dose consequences in co-operation with the Environmental Control Service of MTA EK.

In the last decade the problem of high level and long lived radioactive waste (HLW) was addressed in the Department in two main aspects: (i) conditioning of waste using vitrification and (ii) final disposal in deep geological repository.

With the support of the Swiss Contribution, the radionuclide retardation capability of the host rock of the potential Hungarian HLW repository is extensively studied jointly with Swiss scientists from Paul Scherrer Institute (PSI). The research is focused on characterization of sorption of cationic radionuclides on argillaceous rocks of the Buda Claystone Formation (BCF). The macroscopic wet chemistry tests are complemented with microscopic investigations in order to verify the mineral phases responsible for the radionuclide uptake and the uptake mechanism. Microspectrometry investigations have been performed at large international infrastructures such as synchrotron radiation (SR) laboratories. The capabilities of microbeam XRF have been increased by recent methodological developments at the XRF laboratory of the Department.

The year 2013 was a watershed for the Department since the former Atomic Energy Research Institute has changed the agenda facing the unprecedented increase of renewable energy sector all over the EC. Hungary, while complying with the renewable directive, is well behind the economic and technical potential in wind and photovoltaic (PV) energy. To facilitate the work in the field of renewable energy sources, the Department has expanded its human resources, employing young researchers with experience from the field of renewable energy. The mission of a newly established research group is to perform complex analysis of energy production, transmission and distribution, and consumption scenarios, in order to provide the lacking scientific background for long-term electricity and heat energy planning processes. The group also performs applied energy research contract work for industry, ranging from green data center infrastructure to energy related utilization of brownfield sites.

The staff of the Department –consist of scientists (physicists and chemists) and engineers.

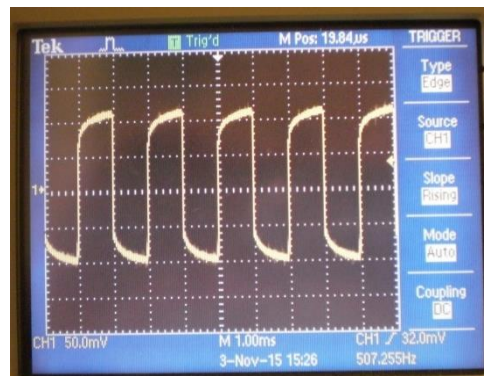
Senior scientists of the Department teach at different universities of Hungary mostly at science and engineering faculties (BME, ELTE, Pannon University, SZIE). The major instructed fields are: several subjects of radiation protection, power system engineering, electric power transmission, renewable energy sources.

Since 2006 the staff of the laboratory strongly participated in the conceptual and design studies of the world's most powerful neutron source, the European Spallation Source. This new facility, under construction in Lund (Sweden), will be up to 100 times brighter than today's leading facilities, enabling new opportunities for researchers in all scientific and engineering disciplines.

The major international partners are Karlsruhe Institute of Technology, Paul Scherer Institute and the JRC Institute for Environment and Sustainability. In the field of radiation protection and biological shielding our assigned group has a framework contract with the European Spallation Source.



Educational laboratory setup for measuring cooperation of solar photovoltaics, battery storage and supercapacitors.



Impulse discharge pattern of the battery.

Szabina Török
Head of Department
torok.szabina@energia.mta.hu

NUCLEAR ANALYSIS AND RADIOGRAPHY DEPARTMENT

In 2015, the Nuclear Analysis and Radiography Department continued to renew its staff, competences and infrastructure. The staff is now an ideal combination of experienced researchers, motivated Ph.D. students and an expert support team.

In addition to the already running transnational access programs, a new EU H2020 project called IPERION CH for cultural heritage science was successfully launched. The first experiments within the EU FP7 CHANDA collaboration were carried out to measure accurate nuclear data for Gen IV reactors. Long-term bilateral collaborations with IRMM JRC and LBNL were continued. A multilateral collaboration agreement with Hungarian museums was established.

In the past two years, significant progress was made in modernization of instrumentation, financed by successive Infrastructure Upgrade Initiative Grants of the MTA. At the RAD facility, after completing the transition to digital image acquisition, a new X-ray generator was installed and characterized this year. It allows complementary high-resolution X-ray and neutron imaging on the same object on a routine basis. The Octopus 3D reconstruction software was also upgraded. At the NAA laboratory, a state-of-the-art microbalance and concentration calculation software were purchased. All our facilities benefit from the new set of dose rate meters for beta, gamma and neutron detection. Cultural heritage and earth science research were boosted with new accessories to our handheld XRF device.

The department published about 30 papers and our staff delivered 26 oral presentations and posters. The highlights include a new series of in-beam catalysis measurements to study gas phase HBr and HCl oxidation on CeO₂, ZrO₂ and Ce-Zr-mixed oxide catalysts. Recent experiments hinted that the boron concentration of the NIST SRM 57B standard reference material was not accurate enough. Following our efforts, NIST published new data and certificate. We participated in the IAEA project "Research Reactor User Networks: Standardization of Neutron Imaging for Industrial Applications". PGAI experiments of new Zr-based fuel claddings after secondary hydridization were made for the direct mapping of their hydrogen content. The applicability of PGAI-NT method was demonstrated for the first time for nuclear safeguards purposes, in order to identify and quantify the uranium content of items placed in sealed lead containers. Silver artefacts were investigated by non-destructive methods as case studies for future participation in the "Seuso-project". The NAA laboratory participated in a Mo-99 production and a soil and plant sample analysis exercises organized by IAEA and TU Delft, where one of the best ratings was achieved. At RAD, the ANCARA supercritical water test loop was extensively utilized.

We participated in domestic and international training activities, such as Central European Training School on Neutron Scattering; PGAA undergraduate lab exercises for ELTE and BME; lecture series and lab training at ELTE: Advanced nuclear analysis methods and their applications in geochemistry research; PGAA, NAA and Neutron Imaging training materials for the IAEA Higher Education Programmes. Within CHANDA collaboration, we hosted a fellow from Turkey for 6 weeks training. L. Szentmiklósi received the best oral presentation award at the Modern Trends in Activation Analysis 14 conference.

*László Szentmiklósi
Head of Department
szentmiklosi.laszlo@energia.mta.hu*

INSTITUTE OF TECHNICAL PHYSICS AND MATERIALS SCIENCE

PHOTONICS DEPARTMENT

The main activity field of the Department is the development of non-destructive characterization methods and the R&D on integrated photonic systems. MFA Photonics Department is involved in the (EU FP7) UNION (Ultra-versatile Nanoparticle Integration into Organized Nanoclusters) project with the aim to develop tailored assemblies of nanoparticles to be used in the field of theranostics, thermoelectrics and lighting applications. The main parameters investigated are the size of the template particles, wettability of the substrate and the drying (temperature) kinetics. Due to the arrangement of the gold nanoparticles, electromagnetic hot-spots can be created that can be exploited in different spectroscopy techniques. With proper surface chemistry design, the ring-like structures can also be used to "focus" liquid dissolved molecules to accumulate at the hot-spots upon solvent drying.

Mesoporous silica thin films were patterned at the sub-micron scale utilizing the ion hammering effect in order to combine the advantages of mesoporous character and surface morphology, while preserving the interconnected pore system or creating laterally separated porous volumes surrounded by nonpermeable compact zones. Measurements confirmed that the majority of the porous volume can be preserved as interconnected pore system by the application of low ion fluence. By increasing the fluence value, however, separated porous volumes can be created at the expense of the total pore volume.

In an international collaboration (Hungary-Japan-Czech Republic) neutron irradiated reactor vessel steel samples were non-destructively analysed. The recently developed method (Magnetic Adaptive Testing, MAT) is based on the systematic measurement and evaluation of minor magnetic hysteresis loops. This method was suggested as a highly promising non-destructive alternative of destructive tests for monitoring structural changes in ferromagnetic objects. MAT introduces a large number of magnetic descriptors to diverse variations in non-magnetic properties of ferromagnetic materials, from which those, optimally adapted to the just investigated property and material, can be picked up. This year, satisfactory correlation between nondestructively measured magnetic descriptors and actual lifetime of the fatigued material was found. The method is able to serve as a powerful tool for indication of changes, which occur in structure of the inspected objects during their industrial service lifetime, as long as they are manufactured from ferromagnetic materials.

MFA Photonics Department is involved in 2 EU-projects („SEA4KET” and the ENIAC-2012-2 “E450DL”) to develop “Imaging Optical Inspection Device With A Pinhole Camera”. Using domestic and international project support, the prototype of the patented (USA, EU, Japan) imaging ellipsometric equipment „Industrial thin-film optical mapping tool” for „record size” 30 - 45cm diameter Si wafers, as well as for thin-film samples of the size of 60 - 90 cm is developed. Ellipsometry related information is available from the site operated by the Department: www.ellipsometry.hu

We used finite element simulations to calculate the optical response of rough surfaces. This way we can generate any surfaces for the investigation of the usually simplified optical models of ellipsometry or other characterization methods. In agreement with previous investigations on polysilicon samples, we found a correlation between the thickness of the effective medium layer and the RMS roughness. Our method also allows to investigate the limits of the effective medium approach in more detail.

MFA Photonics Department researchers have developed a special flow cell for plasmon-enhanced, internal reflection, multiple-angle of incidence *in situ* spectroscopic ellipsometry, which can be used to monitor interface processes with a high sensitivity ($\sim 40 \text{ pg/mm}^2$) and speed (less than 1 s for a full spectrum) in a broad wavelength range (350-1690 nm). The device was successfully applied to study protein adsorption, cell adhesion and polyelectrolyte deposition simultaneously on uncoated and titanium nanoparticle-coated gold surfaces.

*Miklós Fried
Head of Department
fried@mfa.kfki.hu*

COMPLEX SYSTEM DEPARTMENT

We have studied the decomposition of symmetric matrix games into four elementary interactions. The coordination games have been extended by additional neutral strategies preserving the order-disorder phase transition when the noise is increased, which is characteristic of the Ising models. We have studied a spatial social dilemma game in which beside unconditional cooperator (C) and defector (D) strategies we also introduced “informed” strategies: the latter are those who invest extra efforts to explore the aim of neighbours and behave accordingly. We could identify elementary relations between the four competing strategies in the governing food web, which revealed the existence of two three-strategy defensive alliances. We have shown that a direct evolutionary advantage of a strategy within a defensive alliance can be compensated by the other alliance through a faster internal rotation of its strategies. Thus, even though in the food web the informed defectors are superior to unconditional ones, the alliance whose defense relies on the weaker strategy can still prevail.

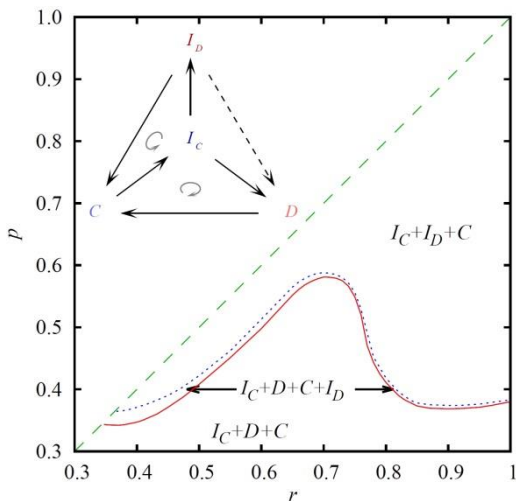


Figure 1 Full r - p phase diagram, as obtained at a specific cost value. Solid red line denotes continuous phase transitions from the very narrow but stable $I_C+D+C+ID$ phase to the stable I_C+D+C phase, while the dotted blue line denotes re-entrant continuous phase transitions to the stable I_C+ID+C phase. Dashed green line is the $p < r$ border.

Inset in the left-up corner shows the direction of invasion between the competing strategies (see arrows).

(Source: A. Szolnoki and M. Perc: Reentrant phase transitions and defensive alliances in social dilemmas with informed strategies, EPL 110 (2015) 38003)

The statistical physical investigation of dynamic processes on random graphs can be materially used in brain research and in the interpretation of social and biological phenomena. This emphasizes the study of slow processes (Griffiths phase) on hierachic and modular networks. Our numerical investigations showed power-law behaviour, which is typical of critical transitions in interconnection systems characteristic of the neural cells of the brain.

Members of our Department published 14 papers in 2015 in peer reviewed international journals and their previous work has received more than 1700 citations in 2015. They delivered 14 lectures at conferences and seminars. They also participate in education as lecturers at various universities in Hungary.

György Szabó
Head of Department
szabo.gyorgy@energia.mta.hu

MICROTECHNOLOGY DEPARTMENT

The main task of the Department is to carry out fundamental multidisciplinary research on new sensing principles, novel materials and nanostructures, innovative 3D microfabrication techniques, development, fabrication and functional validation of nano- and microsensors and integrated systems. The group runs 300 m² + 160 m² clean labs, class 100-10000, hosting the only complete Si-CMOS processing line and mask shop of Hungary along with assembly, packaging, electrical and mechanical test labs. The capacity of the microtechnology line is offered for SME-s and universities.

In the MEMS category 3D silicon force-microsensors were developed and adopted for laparoscopy devices and steering manipulators of surgical robots to measure tactile information as part of a European project (INCITE).

Micromotors for explosive gases sensitized with colloidal nanocatalysts were developed for stable and low power dissipation transducers in industrial use.

In the BioMEMS field novel microfluidic systems for point-of-care medical diagnosis were designed by the understanding of fundamental fluid-dynamic processes.

Microfluidic devices to be used in complex diagnostic systems were developed for the separation of liquid-suspended micro- and nanoparticles using their size, physical and chemo-biological properties.

In the NeuroMEMS field novel multi-channel electrode systems were developed for the monitoring of neural processes in the brain in form of both implantable and skull-surface attachable form, their excellent signal-transfer performance was verified with medics-biologist partners, a.o. in the frame of the National Brain research Program (NAP).

In the NEMS field the ordered growth of piezoelectric nanowires was solved in a European project (PIEZOMAT) for the fast and efficient spatial detection of fingerprint morphology. In the realization of the dense submicron array of sensing bunches of nanowire the electron-beam nanolithography competence obtained with MTA support in 2015 played a key role.

As a novel research topic in the NEMS field the optimisation of the heteroepitaxial layer structure of modern LED lighting diodes was started with a Taiwanese industrial partner (Epistar). The generally used, expensive ITO transparent conductive electrode was successfully replaced by the optimised, homogeneous large area atomic layer deposition of 3at % Ga doped GaZnO having a specific resistivity of $<3 \times 10^{-4}$ Ohm.cm.

Gábor Battistig
Head of Department
battisti@mfa.kfki.hu

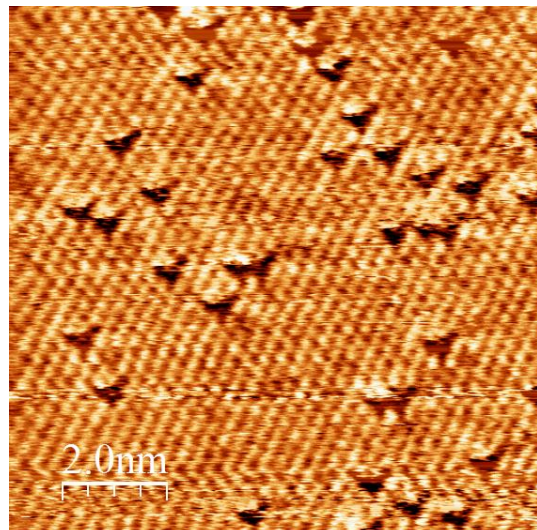
NANOSTRUCTURES DEPARTMENT

2015 was the first year of the Nanostructures Department within the Centre of Energy Research. From December 2015 Dr. Levente Tapasztó became the new head of the Department following Prof. László Péter Biró, the founding head of the Department. 15 research papers have been published in international peer reviewed scientific journals, including leading journals, such as *Nano Letters* and *Nature Scientific Reports*. The number of independent citations received by the members of the Department during 2015 was about 500. Gergely Dobrik and Péter Vancsó obtained their PhD degree. A new Scanning Tunneling Microscope has been installed in 2015, within the framework of the 2D Nanoelectronics "Lendület" project, which is the first low temperature (10K – 300 K) STM in Hungary.

3 new projects have been secured during the year: (1) ERC Starting Grant (L. Tapasztó), (2) "Graphene Flagship" WP7 Electronic Devices; Logic switches, (G.I. Márk & L.P. Biró), (3) OTKA K115724 (K. Kertész)

Major scientific achievements:

1. They have developed a novel method for the exfoliation of large-area 2D transition metal chalcogenide (TMC) crystals, providing single layers with lateral sizes of about two orders of magnitude larger than previously achieved. The novel exfoliation mechanism is based on the strong adhesion between atomically flat gold substrates and the surface chalcogenide atomic layer of the TMC flakes.
2. They observed for the first time a graphene "nanomesh". This is a new type of graphene superlattice with a concave geometry, which has been identified in atomic resolution STM images of graphene on Au(111) substrate.
3. MoS₂ sheets were grown by chemical vapour deposition (CVD) on highly ordered pyrolytic graphite (HOPG). The triangular MoS₂ flakes were shown to follow the crystallographic orientation of HOPG substrate. STM measurements revealed one-dimensional metallic edge-states. Besides, less than 20 nm wide MoS₂ nanoribbons were cut by STM nanolithography for the first time.
4. They were able to reveal the native defect structure of exfoliated MoS₂ single layers by atomic resolution STM investigations. By DFT calculations of defect-induced electronic states they were able to identify the sulfur atom vacancy origin of the experimentally observed defect sites.
5. They have investigated the variability of structural colour generated by photonic crystal type nanoarchitectures in the case of two common Lycaenid species living in Hungary. For the two investigated species the intensity and wavelength deviations were almost identical, this shows that the natural variability of the structural colour is very similar due to the colour-based conspecific recognition.



Atomic resolution STM image of a MoS₂ single layer, displaying a high native concentration of single sulfur atom vacancy defects (dark triangles)

Levente Tapasztó
Head of Department
tapaszto@mfa.kfki.hu

THIN FILM PHYSICS LABORATORY

www.thinfilms.hu

2015 was an important year in the life of the Laboratory, as they moved (together with the whole MFA) from the Research Centre of Natural Sciences to the Centre for Energy Research. As they were located even before on the same campus, they did not have to move physically. The research staff lead the work of 6 PhD students, one of them defended his Thesis (summa cum laude) in 2015. They worked in a wide international cooperation running a large EU FP7 project, another Materials ERA project, several bilateral projects with foreign parties and some national projects (OTKA). Their scientific results achieved in 2015 are listed below.

They have prepared graphene/ Si₃N₄ nanocomposite ceramics by hot isostatic pressing and spark plasma sintering. The graphene flakes are ordered into a preferential direction (determined by the mechanical deformation). The novel ceramics have a very low wear.

In order to develop biocompatible implants they successfully coated Ti implants by sputtered TiC/a:C coating in which all the titanium are bonded and its adhesion is very good. The bioactivity of implants is improved by electrosprayed nanosized hydroxyapatite prepared from biogenic based materials.

They could prove that irradiating LiNbO₃ crystals with high intensity laser pulses, a 3D matrix-structure can be created in which the irradiated regions are small discs of amorphised regions.

Low cycle thermo-mechanical fatigue experiments were carried out on reactor steel material. The structural investigations carried out by TEM have shown that above the half of the lifetime the dislocation mechanism of deformation is gradually completed by a grain(cell) boundary sliding mechanism, leading to further softening of the material and (possible) formation of micro-cracks.

For the first time they managed to show that within a nanoscale area graphene is able to build various Moiré superlattices with different curvature and convexity due to the near energetical degeneracy of them. The experimental results have been supported by DFT calculations.

They have developed and patented a new method for the combinatoric deposition of bimetallic alloys especially for transmission electron microscopy. They have developed bimetallic catalysis material which can be activated by visible light.

They developed two statistical methods to obtain additional information from diffractions alone starting with improved visualization of grain boundaries, dislocations and inclusions and ending with quantitative determination of the projected width of grain boundaries without taking images.

Members of the Laboratory took an active part in the organization of Multinational Congress on Microscopy (Eger, 2016. August 23-28). Professor Emeritus Péter B. Barna (very efficient member of the Laboratory) was honoured by the R. F. Bunshah Award (American Vacuum Society) recognizing his outstanding research in the field of thin films. Katalin Balázs was awarded by the Bolyai plakett for her outstanding research carried out in her Bolyai fellowship period.

Béla Pécz
Head of Department
pecz@mfa.kfki.hu

NANOBIOSENSORICS GROUP

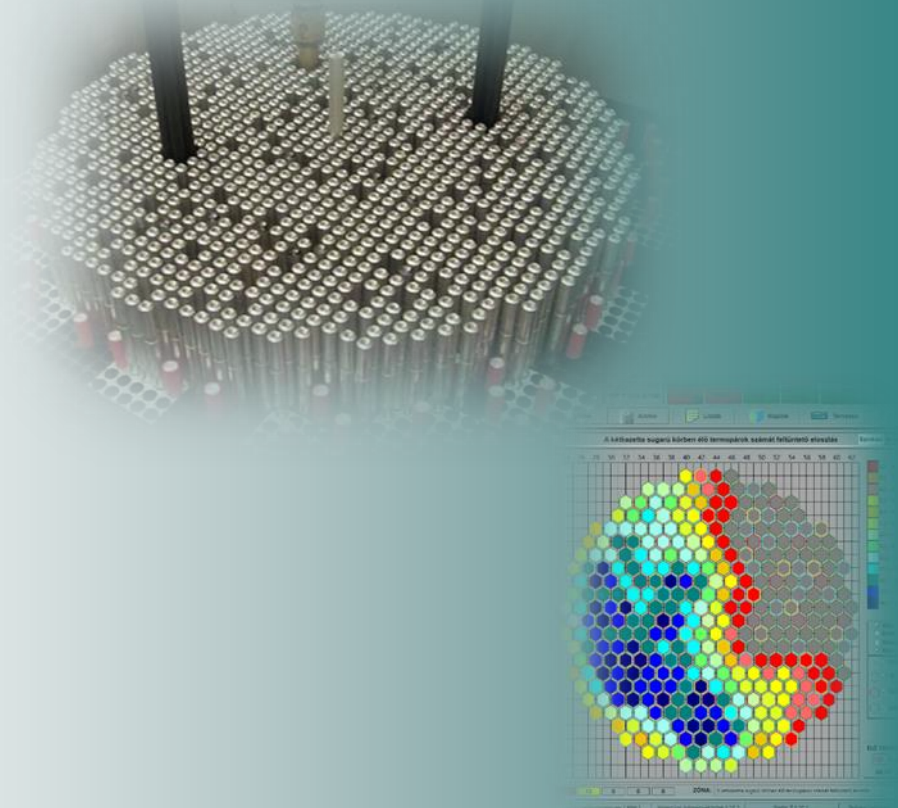
The Nanobiosensorics Group was established in 2012 in the framework of the Lendület (Momentum) Program of the MTA. The research program funds outstanding young researchers in Hungary in order to establish their own independent research groups. The research profile of the Nanobiosensorics Group is the development and application of label-free optical biosensors, the mathematical modeling of the relevant biological and biophysical processes. Building on their broad national and international collaborative network, the group conducts research in instrument development, monitoring of cell secreted extracellular vesicles, development of protein-based functional coatings, adhesion studies on human cancer and immune cells, and theoretical modeling.

In 2014, the ERC (European Research Council) Consolidator Grant application of the head of the research group received category "A" (:Fully meets the ERC excellence criteria and should be funded if sufficient funds are available) after the interview in Brussels, but the funding line did not reach this proposal due to budgetary constraints. However, using this achievement he could successfully apply for funding from NKFIH (National Research, Development and Innovation Office) in the framework of the ERC_HU call.

Outstanding research results of the Nanobiosensorics Group in 2015

- The Group developed methodologies which allow to design and fabricate nanometer scale ultrathin hydrogel layers with well-controlled surface structure to coat biosensor surfaces.
- In 2015 they published two successful applications of holographic microscopy to monitor cancer cell motility, migration, motility speed, and to examine the spreading of preosteoblast cells on nanostructured titanate coatings.
- In 2015 they focused on the molecular scale interactions between proteins and EGCg (epigallocatechin-3-gallate) with special focus on its limited stability and antioxidant properties, the observed biophysical effects of EGCg on various cell lines and cultures. The alteration of cell adhesion, motility, migration, stiffness, apoptosis, proliferation, as well as the different impacts on normal and cancer cells are all summarized in a prospective review article.
- They developed a computer vision-based robot applying a motorized microscope and micropipette to recognize and gently isolate intact individual cells for subsequent analysis, e.g., DNA/RNA sequencing in 1-2 nanoliters from suspension without immobilizing cells on the surface.

Robert Horvath
Head of Group
robert.horvath@energia.mta.hu



I. RESEARCH RELATED TO NPP'S



HUNGARIAN NUCLEAR RESEARCH PROGRAM - SUSTAINABLE NUCLEAR ENERGY TECHNOLOGY PLATFORM

Ákos Horváth

Objective

High levels of nuclear expertise and of nuclear safety culture are important pre-requisites for the long term use of nuclear power and its acceptance by the members of society. Starting from this recognition, the leaders of the Hungarian nuclear sector have identified and proposed strategic research and development objectives. In order to promote and organize the necessary nuclear research and development at the national level, the Hungarian Sustainable Nuclear Technology Platform was launched in 2010. Its main goal is to influence the agenda of nuclear energy research and development activities in Hungary and to participate in its implementation and coordination. MTA EK is the leading organization of the Platform.

Plans and goal

The pillars of the Strategic Research Agenda of the Platform are as follows:

- Preserving Hungarian nuclear power competence during the lifetime extension of the Paks nuclear power plant (four VVER-440 units);
- The construction and activation of new nuclear units;
- The closing of the fuel cycle and the development of Generation IV reactors.

This platform is necessary to meet the needs and necessities for energy generation in Hungary, and is influenced by the European energy developments as well. The above three goals answer the requirements of the nuclear industry and serve as a basis for its future development. The lifetime extension of the existing units requires the maintaining of the high safety level already reached and also should lead to some important further modifications, such as the refurbishment of the process control system. The government's decision concerning new units makes it necessary to concentrate on related issues. Therefore in order to reach the goals on the short and medium terms, the main supporters of the Platform are the Paks Nuclear Power Plant and the Hungarian Safety Authority.

Members and tasks

Five members of the Platform – MTA EK, BME NTI, MTA Atomki, OKH OSSKI, Nubiki Ltd – successfully applied for financial support from the National Office for Research, Development and Innovation. The tasks of the Hungarian Nuclear Research Program are based on the technical and scientific needs related to the adoption of the advanced nuclear technology in the country, e.g. preparing for the adoption of the closed fuel cycle in the second half of the century. Only the continuous research on reactor safety and the improvement of our knowledge on the processes in the reactors can ensure the maintenance of nuclear competence and its transmission to the younger generation.

The strategy concerning the nuclear fuel cycle is one of the hottest issues all over the world. The Institute participates in the V4G4 collaboration, represented by nuclear institutions from the Visegrád region. The main objective of V4G4 is to design and construct a demonstrator unit of a gas cooled fast reactor and build the necessary competence in the region. The Hungarian Nuclear Research Program is supporting the Visegrád national contributors in the period 2015-2018. An important additional goal of the project is the promotion and improvement of the Hungarian nuclear education system.

AGEING OF CONCRETE STRUCTURE'S MATERIALS

Tamás Fekete, Veronika Bartha, Károly Kovács, ÉMI Nonprofit Ltd.

Objective

Concrete structures are significant components of nuclear power facilities. They are designed to provide:

- Shielding against nuclear radiation and retaining of harmful radioactive material releases;
- Structural support to the mechanical and electrical systems and components; and
- Protection of the systems and components from the environment.

Studies of concrete aging usually use two classifications to group concrete structures. These are: safety significant and environmental exposure. Concrete structures that are classified as safety significant are called Category I concrete structures, according to the NRC terminology. Concrete structures classified as only providing protection from environmental exposure are called Category II.

Category I concrete structures perform one or more of the following safety-related functions:

- Radiation attenuation and shielding;
- Prevention of uncontrolled liquid or airborne radiation releases;
- Structural support for nuclear steam supply system and containment internal equipment;
- Structural support for redundant safety-related equipment;
- Structural support for heat sink equipment;
- Support for spent fuel pools;
- Protection of safety-related equipment from harmful environments; and
- Separation or "communication" function.

Category I structures are the ones most significantly influenced by the nuclear power generation process. Category II concrete structures of a nuclear power plant facility are considered to be conventional structures.

The durability and performance of concrete structures also depend on the severity of the environment in which the structure is located. The concrete structures directly around the reactor pressure vessel experience the majority of irradiation and temperature related degradation during the lifetime of a nuclear power plant (NPP).

The goal of the project is to produce a material database that is designed to contain reliable experimental data for the relevant compositions and material parameters of structural concretes planned for future installations.

Methods

As a first step, a literature review has been performed. Based on results of the literature review, a detailed experimental program has been developed. The scope of the experiments is to age different concrete specimens by various aging mechanisms (n - and γ -irradiation, thermal) up to different aging levels, equivalent to a number of years of operation of an NPP during long-term operation.

A plan for the relevant measurements has been developed. In the first phase of the project, detailed component analysis is planned using neutron activation analysis (NAA) and prompt gamma activation analysis (PGAA) at the Budapest Neutron Center, in order to discover those stock materials containing undesired elements (i.e. cement, gravel and other additives) from an irradiation activity point of view. Concrete specimens will be produced only from accepted stock materials. The neutron irradiation rig is planned to contain specimens with diameters up to ≈ 2 cm. The γ -irradiation and the thermal aging facility are planned for specimens with diameters up to ≈ 5 cm. The temperature at the center of the specimens will be held around 100 °C during irradiation.

Temperature, gamma heat, gas and water release, and dimensional change measurements are planned during the aging processes. Neutron fluence evaluation, remanent activity, volume change, and mass change measurements and mechanical tests will be performed after the irradiations.

Results

The literature review and international experiences led to the conclusion that the planned experimental program is feasible. There are no experimental results yet.

Remaining work

A detailed experimental program plan has been developed, the experimental facilities have to be developed and constructed, and after that the complete aging program has to be implemented. Finally the material tests have to be performed and the results of the program have to be evaluated.

RELEASE OF THE FUROM-2.1 VERSION. VERIFICATION AND INTRODUCTION OF AN EXTENDED DIFFUSION FGR MODEL

János Gadó, Ágnes Griger and Katalin Kulacsy

Objective

The objective of the work was the issue of FUROM-2.1 version which contains several new models and refinements. It also incorporates an extended fission gas release (FGR) model, which provides satisfactory simulation results for high burn-up fuel element in case of high temperature occurring ramp tests. The work was sponsored by MVM Paks NPP.

Methods

For the verification of the efficiency and compliance of the new FGR model, ramp-test simulations were carried out using some integral tests of Halden Reactor Project (HRP). After proper data handling and data reduction of the original raw data, the calculated (simulated) and measured values were compared.

Results

For moderate (low) burn-up and low temperature the MacDonald-Weisman's solution of the diffusion equation uses an effective diffusion coefficient fitted to measured data for the determination of the FGR. It turned out that in case of high burn-up and high temperature, instead of the traditional FUROM model the Turnbull's coefficient is more suitable to model the FGR process (Fig.1). This variation is acceptable, as Booth' solution (with the Turnbull's coefficient) and the approximation of MacDonald-Weisman converge to each other at high temperature while the incubation time of the fission gas release from the grains tends to zero.

Within the FUROM-2.1 code the validity and applicability limits of the extended FGR model were determined, as well as its automatic operation was ensured. The new FGR model was validated by comparing the code calculations with real measurements of some irradiated fuel rods from integrated tests (HRP) (Fig.2, Table 1).

The minor errors and uncertainties of FUROM-2.1 code version were eliminated and the actual code version was issued.

Table 1: Comparison of the errors in FGR in ramp simulations using the two diffusion models

| SAMPLES | traditional | Turnbull |
|---------|-------------|----------|
| Rod1 | -6.5% | +1.6% |
| Rod2 | -8.9% | +3.0% |

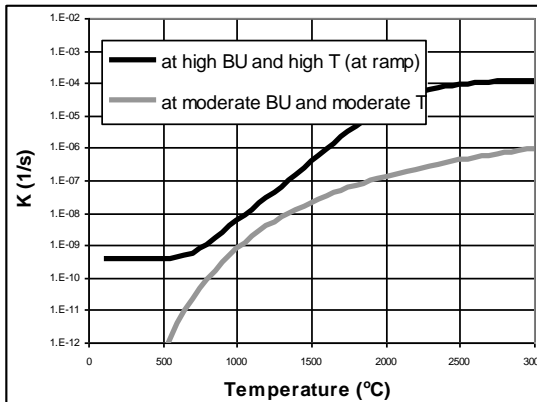


Figure 1: Comparison of diffusion coefficients

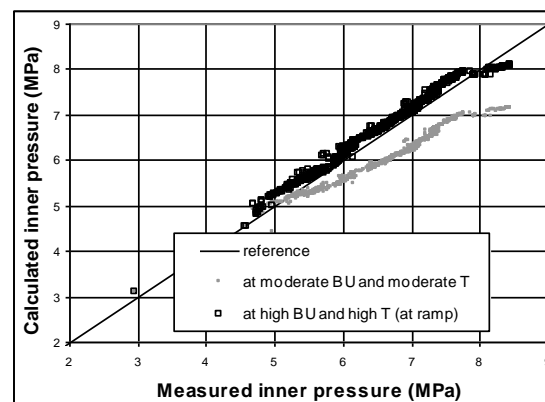


Figure 2: Results of FUROM-2.1 simulations

Remaining work

The validation report of FUROM 2.1 has to be finalised.

Related publications

- [1] J. Gadó, Á. Griger and K. Kulacsy: *Physical models of the FUROM 2.1 code*, MTA EK RAL-2015-985-01-01-M0, in Hungarian (2015)
- [2] Á. Griger: *Programmer's Guide to FUROM 2.1*, MTA EK RAL-2015-985-01-02-M0, in Hungarian (2015)
- [3] Á. Griger: *User's Guide to FUROM 2.1*, MTA EK RAL-2015-985-01-03-M0, in Hungarian (2015)
- [4] J. Gadó, Á. Griger: *Development of an extended diffusion fission gas release model*, MTA EK RAL-2015-985-02-01-M0, in Hungarian (2015)

SAFETY ANALYSIS OF ADVANCED FUEL RODS DURING 15 MONTHS CYCLES

Ágnes Griger

Objective

The objective of the work was the safety analysis of new fuel rod designs by using the FUROM-2.1 code. The new geometric parameters of the new designs are given in Table 1. The fulfilment of safety criteria was investigated for a large series of fuel rod histories in case of two new rod designs. The contractual work was ordered by MVM Paks NPP.

Methods

The fuel rod histories were taken from a library of the results of steady state reactor physical calculations performed for the 15 months fuel cycle. 166 challenging full life histories with high loads and load changes were selected. Initial conditions were varied in a conservative manner to test the fulfilment of the various safety criteria (centreline temperature, internal pressure, hoop stress, fuel stack and cladding axial and tangential deformations) in accordance with the fuel design safety rules approved by the Hungarian Atomic Energy Authority.

Results

In both new designs the cladding thickness is reduced compared to the standard design. It was found that in general the safety criteria are fulfilled with the applied conservatism. However, in several cases the maximum radial inward deformation somewhat exceeded the criterion as the low cladding thickness leads to higher inward creep. This experience calls the attention to the need of further considerations concerning the applied conservatism.

As an example, Fig. 1. and Fig. 2. show the axial cladding deformation and hoop stress as a function of rod burn-up, respectively. The criteria require that the axial deformation must not exceed 31.5 mm and the hoop stress must not exceed 280 MPa. Though the axial deformation is somewhat higher for the new designs than for the base case, the criterion is fulfilled for all the three cases.

Table 1: Parameters of fuel rod designs (all data in mm)

| Parameters | Base case | Design 1 | Design 2 |
|-----------------------|-----------|----------|----------|
| Pellet inner radius | 0.6 | 0.0 | 0.0 |
| Pellet outer radius | 3.80 | 3.81 | 3.91 |
| Cladding outer radius | 4.55 | 4.45 | 4.55 |
| Cladding thickness | 0.685 | 0.575 | 0.575 |

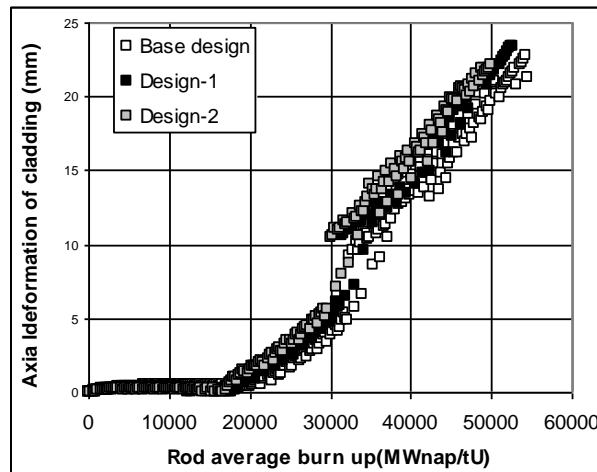


Figure 1: Comparison of axial deformations

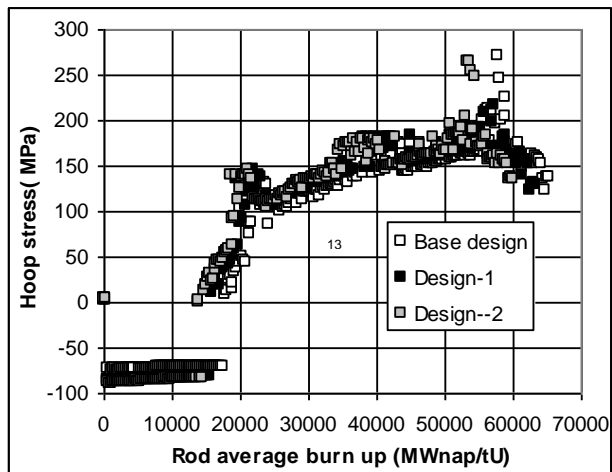


Figure 2: Comparison of hoop stresses

Remaining work

There is no remaining work.

Related publication

- [1] Á. Griger: Analysis of new fuel rod designs in the 15 months cycle, MTA EK RAL-2015-993-01-M0, in Hungarian (2015)

CODEX LOCA TESTS WITH E110 AND E110G ALLOYS

Zoltán Hózer, Imre Nagy, Mihály Kunstár, Nőra Vér, István Trosztel

Objective

The main objective of the experiment was the testing of E110 and E110G type fuel claddings under LOCA conditions.

Methods

The CODEX-LOCA-200 experiment was carried out in the CODEX facility with an electrically heated 7-rod bundle. Four rods had E110G cladding, while E110 alloy was applied in the other three rods. The fuel rods were internally pressurized at the beginning of the test. After the high temperature phase the bundle was cooled down by water injection from the bottom of the facility.

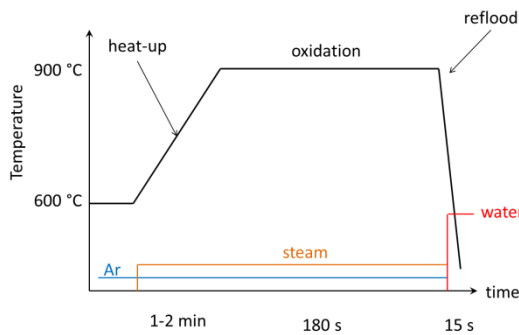


Figure 1: Selected temperature history of the CODEX-LOCA-200 test

The scenario was determined on the basis of Paks NPP safety analysis result for 200% large break LOCA scenario. The temperature history and initial pressure were selected according to the results of ATHLET and FRAPTRAN calculations. Additional supporting calculations were performed for the test with the ATHLET code.

Results

The test parameters conservatively covered the 200% LOCA reference scenario. The maximum temperature was 900 °C and the high temperature oxidation of Zr lasted for a longer time compared to the reference case. The internal pressure in the rods with maximum pressure reached 17-20 bars. Three out of seven rods failed due to ballooning and burst (Fig. 2).

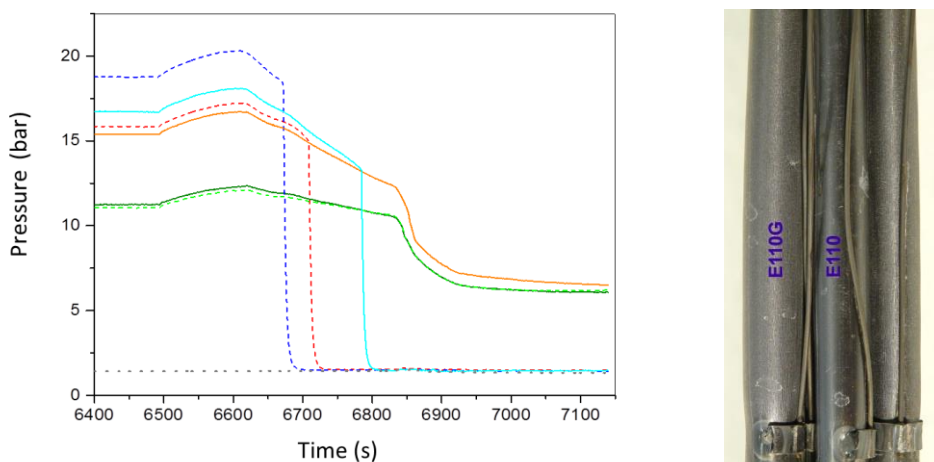


Figure 2: Pressure history of the fuel rods (left) and view of the CODEX-LOCA-200 bundle after the test (right)

Remaining work

The CODEX LOCA experimental program will be continued with three more tests in 2016 and 2017.

Related publication

- [1] I. Nagy, M. Kunstár, Z. Hózer, N. Vér, I. Trosztel: *Simulation of the 200% LOCA transient in the CODEX Facility*, MTA EK-FRL-2015-701-1-1-M0, in Hungarian (2015)

MECHANICAL PROPERTIES AND ANISOTROPY OF E110G ALLOY

Márton Király, Richárd Nagy, Zoltán Hózer, Margit Fábián, Lukács Szende, Károly Hufkó, Eszter Barsy

Objective

The main objective of the experimental series was the production of new data on the mechanical properties of the non-irradiated E110 and E110G type claddings and the evaluation of the anisotropy of E110G alloy.

Methods

High temperature facility was built to study the creep behavior of E110 and E110G cladding tubes (Fig. 1). The 100 mm long samples were placed horizontally into the high temperature furnace and were axially loaded with heavy lead weights. The deformation of the cladding samples was recorded by several methods. Inert atmosphere was kept in the furnace in order to avoid chemical reactions. The measured data were evaluated by analysis of variance (ANOVA).

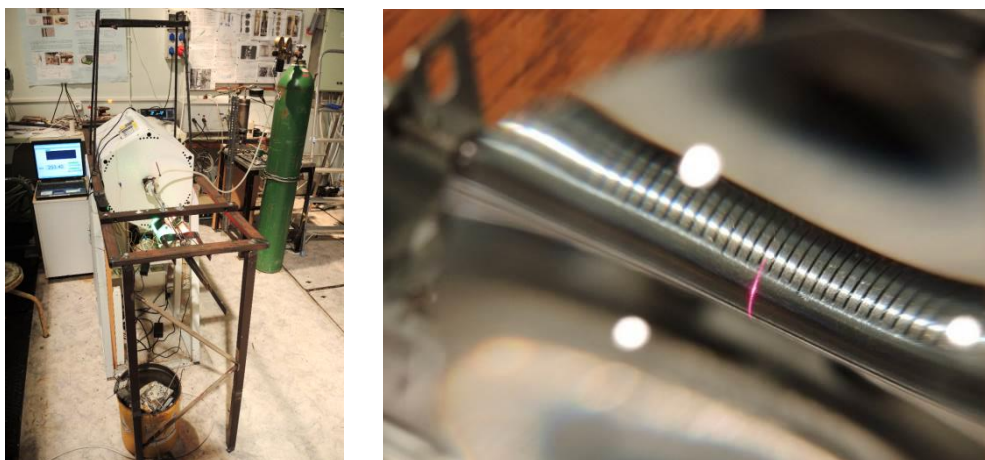


Figure 1: View of the creep test facility (left) and the E110G sample (right)

The mechanical properties – first of all ultimate tensile strength and creep data - were compared to the experimental data of other laboratories and to the numerical models built in the FUROM fuel behavior code.

Neutron diffraction was applied to study the anisotropy of the Zr alloys. The diffractometer uses neutrons from the tangential channel of the Budapest Research Reactor.

Results

The secondary creep rates were determined on the basis of creep tests carried out at 300 °C and 500 °C temperatures. The results indicated that the temperature and the load play the most important role in the creep process. The E110 and E110G samples showed very similar creep behavior in the investigated range of temperature. New optical methods were developed for on-line tracking the deformation of cladding tubes.

The new ultimate tensile strength data with pre-oxidation and hydrogen charging of E110 and E110G tubes can be used for further development, but the effect of high temperature treatment must be taken into account. The creep model of FUROM code can be validated against the new measured data.

The neutron diffraction examinations indicated that the E110 and E110G alloys have similar microstructure, texture and orientation. The anisotropy factors are practically the same for the two alloys.

Remaining work

Radial creep tests will be performed with E110 and E110G alloys.

Related publication

- [1] M. Király, R. Nagy, Z. Hózer, M. Fábián, L. Szende, K. Hufkó, E. Barsy: *Investigation of the creep behavior of E110G cladding at nominal and high temperatures*, MTA EK-FRL-2015-718-1-1-M0, in Hungarian (2015)

NUMERICAL SIMULATION OF TELESCOPE SIPPING EXAMINATION OF A LEAKING FUEL ASSEMBLY

Zoltán Hózer, Katalin Kulacsy, Péter Szabó, Richárd Nagy,

Objective

The telescope sipping (TS) procedure is applied at Paks NPP to identify leaking fuel assemblies. The VVER-440 assemblies cannot be dismantled at the NPP, and there are no tools for fuel examinations. It was expected that the numerical analyses of leaking assembly identification techniques could provide useful information on the characteristics of leaking rods.

Methods

The activity release during sipping test from assembly No. 77715 was simulated using the TSKGO computer code. The code calculates the activity inventory in the free volume of the fuel rod and estimates the release of different gaseous and volatile fission products during steady state operation in the reactor, storage in the spent fuel pool and transient (e.g. sipping test) conditions.

Several important input parameters could be determined from the NPP data. The date of the fuel failure was set to the 381st day of the assembly operation (at the beginning of the 29th cycle). The TS examination was executed 24 days after shutdown at the end of 31st cycle. The power history of each fuel element of the assembly was calculated by the NPP experts on the basis of operational data. Since the leaking fuel rod inside the assembly was not identified, all 126 rods of the assembly were simulated.

Based on the power history of the fuel elements in the leaking assembly, the amount of fission products released from the pellets to the free volume was calculated by the FUROM code. The TSKGO program took these results as input and determined the amount of fission products in the free volume of the leaking fuel element during normal operation.

Three series of calculations were performed for each of the 126 fuel elements, using different defect positions. The three positions were 5 cm, 125 cm and 245 cm from the bottom of the rod. The full length of the rod was 260 cm, 248 cm thereof filled with pellets.

Results

The calculated results show that the activity release during sipping tests is driven by the expansion of the gas volume inside the fuel rod, and the amount and composition of the released radioactive isotopes highly depend on the defect location.

Good agreement between measured and calculated data was reached in those cases when the defect was located at the bottom of the fuel rod. The best agreement was obtained for a fuel rod located halfway between the periphery of the assembly and the central tube. Since fuel inspection cannot be carried out at the power plant, this information on the defect location and rod power can be used to plan the further handling and storage of the leaking assembly.

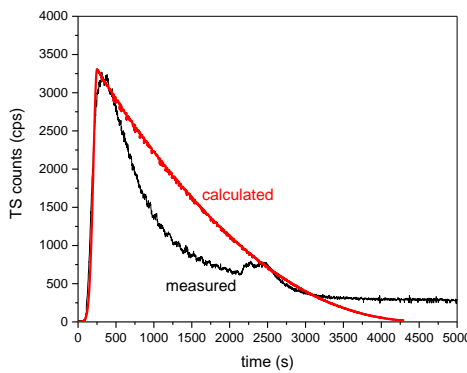


Figure 1: The calculated and measured counts during the TS examination.

Remaining work

The planned work has been completed.

Related publication

- [1] Z.Hózer, K. Kulacsy, P. Szabó: *Numerical Simulation of Telescope Sipping Examination of Assembly No. 77715*, MTA EK-FRL-2015-761-1-1-M0, in Hungarian (2015)

TRANSPORT OF LEAKING FUEL ASSEMBLIES TO DRY STORAGE FACILITY

Zoltán Hózer, Péter Szabó

Objective

The identified leaking fuel assemblies are nowadays stored in the spent fuel pool of the Paks NPP. The conditions of transport and long term storage of such assemblies in the dry storage facility must be established, since the leaking fuel assemblies sooner or later will have to be removed from the spent fuel pool. In the present work, the experts of MTA EK proposed criteria and a procedure for transportation of leaking fuel assemblies from the spent fuel pool.

Methods

The following information and aspects were taken into account during the development of criteria and procedure:

- Primary coolant activity concentrations (normal operation and shutdown transient) were used for the estimation of the number and burnup of leaking fuel rods.
- The results of telescope sipping examinations were analyzed in order to optimize the timing and the necessary number of such examinations and to determine the list of measured radioactive isotopes.
- Spent fuel pool coolant activity concentrations were used to develop proposals on the optimal storage time in the spent fuel pool. The effect of different manipulations in the pool on the release of activity from the leaking assembly and on the inventory of radioactive isotopes in the leaking fuel rod before removal from the pool was also taken into account.

Results

A special algorithm has been developed for the transport of leaking fuel assemblies to the dry storage facility. The procedure includes the following steps:

- 1) Evaluation of primary coolant activity concentration.
- 2) Estimation of the total number of leaking fuel rods in the core by the RING code.
- 3) Estimation of the burnup of leaking fuel rods.
- 4) Evaluation of transients with power change during normal operation, analyses of activity peaks (spiking).
- 5) Evaluation of shut-down transient, analyses of activity peaks (spiking).
- 6) Sipping tests during refueling, identification of leaking fuel assemblies.
- 7) Estimation of the number of leaking fuel rods inside the identified leaking assembly.
- 8) Analyses of potential UO₂ release (pellet fall-out) from the leaking rod.
- 9) Evaluation of the spent fuel pool coolant activity concentrations (measurements are taken after the placement of the leaking assembly into the pool).
- 10) Sipping test in the spent fuel pool to confirm the leaking assembly before transportation.
- 11) Measurements in the water of the transport container during the transport of leaking fuel assembly from the spent fuel pool to the dry storage facility.

The following data are necessary to initiate the transport of a leaking fuel assembly to the dry storage facility:

- a) Isotope inventory of the assembly. It must be determined on the basis of power history.
- b) The estimated number of leaking rods in the assembly.
- c) The estimated inventory of the selected radioactive isotopes dissolved in the water inside the leaking fuel rod at the beginning of storage period in the spent fuel pool.
- d) The estimated inventory of the selected radioactive isotopes dissolved in the water inside the leaking fuel rod at the time of transport (taking into account the manipulations and transients in the spent fuel pool).

Remaining work

The work will be continued when the first leaking fuel assembly will be transported to the dry storage facility .

Related publication

- [1] Z. Hózer, P. Szabó: *Development of criteria and procedure for the transport of leaking fuel assemblies to the dry storage facility*, EK-FRL-2014-964-01/01-M1, in Hungarian (2014)

CALCULATION OF LEAKING FUEL CHARACTERISTICS

Péter Szabó, Zoltán Hózer, Zsolt Kerner

Objective

Several numerical methods have been developed and are available for the characterization of leaking fuel rods in a nuclear reactor. In the framework of the present project, a systematic comparison of three methods was carried out using large number of primary coolant activity data from the Paks NPP. The main objective of the work was the review of applicability of these methods for the Paks NPP.

Methods

Three different numerical methods were applied:

- The RING code provides estimation on the number of leaking fuel rods and mass of tramp uranium on the basis of measured iodine, xenon and krypton activities in the primary water. The code is applied in the chemical expert system of Paks NPP since 2009.
- The WANO FRI index can be calculated using measured coolant activities of ^{131}I and ^{134}I isotopes. The FRI value of 19 Bq/g corresponds to a leaking fuel rod in pressurized water reactors.
- The Russian methodology was developed by the Russian fuel supplier. The algorithm uses the activity concentration of five iodine isotopes as input data and gives estimation of the number of leaking fuel rods.

In the calculation series the same technological parameters (e.g. primary water mass, reactor power, and water purification system characteristics) were used for all three methods.

Results

The calculated results in most of the cases showed well the presence or absence of leaking fuel in the core during the given cycle. The RING and the Russian methodology were less sensitive for the scatter of measured data, since they use more isotopes than the WANO FRI index.

The Russian methodology often overestimated the number of leaking fuel rods. The estimated mass of tramp uranium in the core significantly affects the estimated number of leaking fuel rods in this algorithm.

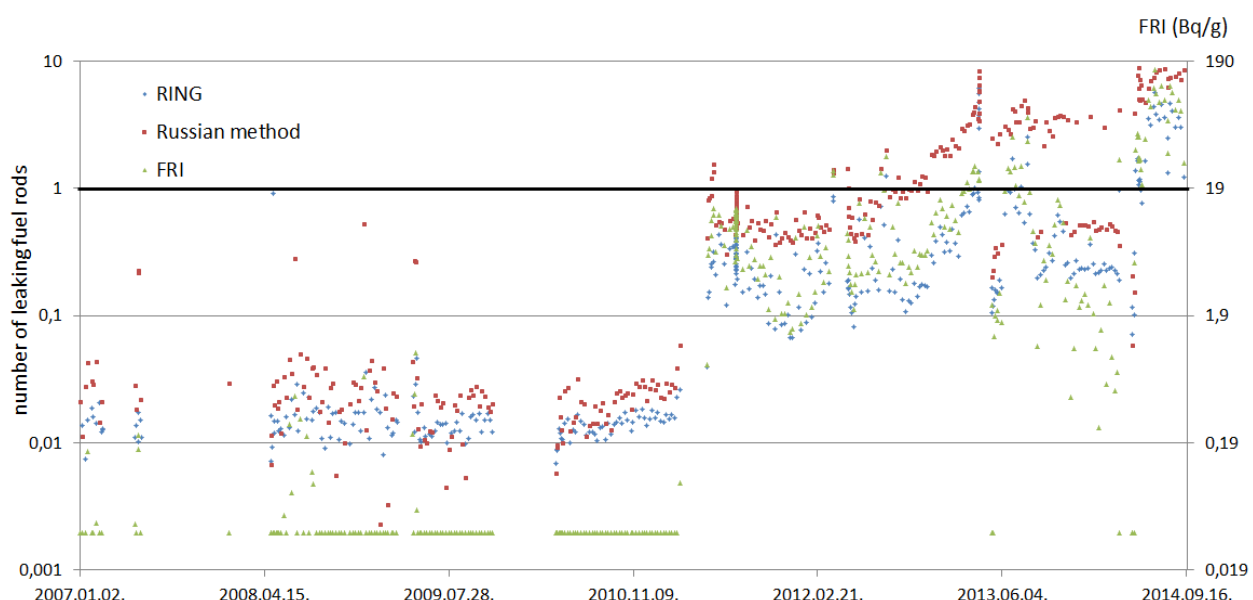


Figure 1: The calculated number of leaking fuel rods and the FRI index for unit No. 1 of Paks NPP

Remaining work

The planned work has been completed.

Related publication

- [1] Z. Hózer, P. Szabó, Zs. Kerner: *Application of the RING code, the WANO FRI and the Russian methodology for the calculation of leaking fuel characteristics*, MTA EK-FRL-2015-967-1-1-M0, in Hungarian (2015)

INVESTIGATION OF FUEL CLADDING EMBRITTLEMENT WITH A SEGMENTED TOOL

Márton Király, Richárd Nagy, Zoltán Hózer

Objective

The pellet-cladding mechanical interaction (PCMI) can lead to failure of fuel cladding. The prediction of such phenomena needs reliable models in fuel behavior codes. In order to support model development, mandrel test will be carried out with E110 and E110G cladding. The objectives for the first year of the project were the specification of segmented tool design and development of finite element numerical model for the simulation of mechanical test with this tool.

Methods

The international practice of mandrel testing was reviewed on the basis of literature data. The advantages and disadvantages of solution used in different laboratories were taken into account in the development of the new segmented tool.

The finite element model of the mandrel test was developed using the MSC.Marc-Mentat code, version 2005r3. The simulated mesh included 7680 elements for the zirconium ring and 8800 elements for one segment of the tool.

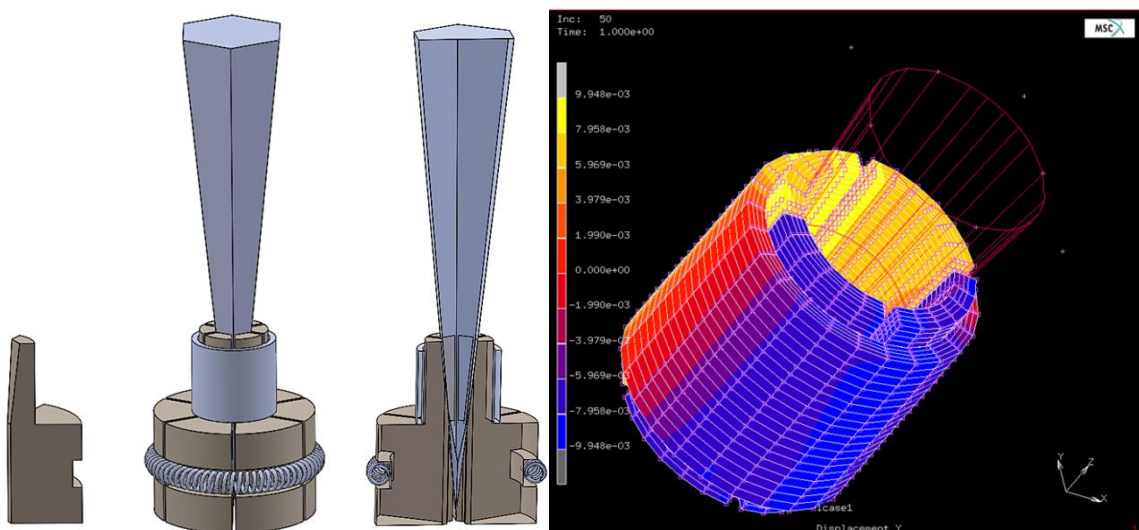


Figure 1: Drawing of the segmented tool design (left) and finite element model of the mandrel test with Zr sample (right)

Results

It was concluded that with increasing number of segments more uniform loads can be created on the cladding tube. Non-uniform loading will take place at the edge of the segments at the beginning of the tests. More uniform load patterns are expected at the end of the elastic region. Large number of segments can challenge the fabrication accuracy. For the above reasons, the optimal solution seems to be the six segment configuration.

The scoping calculations showed that the needle angle must be changed from 19.2° for 11.4°. However, with the smaller angle larger displacement will be necessary.

The present design of the segmented tool allows maximum 1.5 mm radial displacement, corresponding to 38% deformation. This range is enough for the planned experiments, for the plastic deformation of as-received samples starts roughly at 10% and in case of oxidized or hydrided samples at smaller deformation.

Remaining work

The experiments with the segmented tool will start 2016 with as-received samples. The testing of oxidized and hydrided Zr rings will be performed in 2017.

Related publication

- [1] M. Király, R. Nagy, Z. Hózer: *Investigation of fuel cladding embrittlement with segmented tool*, MTA EK-FRL-2015-989-1-1-M0, in Hungarian (2015)

EFFECT OF HIGH TEMPERATURE TREATMENT ON THE ULTIMATE TENSILE STRENGTH OF FUEL CLADDINGS

Márton Király, Márta Horváth, Zoltán Hózer, Tamás Novotny, Erzsébet Perez-Feró

Objective

Earlier experiments with oxidized Zr cladding samples showed significant changes in the mechanical properties of cladding materials after high temperature oxidation in steam. It was suspected that both oxidation and high temperature treatment are responsible for the changes. In the present work it was intended to identify the role of the thermal treatment without oxidation in the change of ultimate tensile strength (UTS).

Methods

The measurements were carried out with 2 mm long E110 and E110G cladding samples. The high temperature furnace was used for the treatment with inert (Ar) atmosphere. Several samples were slightly oxidized (up to 1-5% ECR) to complete the test matrix. The temperature of oxidation and treatment covered the 600–1000 °C range. The longest oxidation and thermal treatment times reached 7200 s.

Standard Instron tensile test machine was used for mechanical testing. The radial ring tensile tests were carried out at room temperature.



Figure 1: View of the Zr samples after thermal treatment at 1000 °C for 690 s in Ar atmosphere (left) and radial tensile test of a Zr ring (right)

Results

The thermal treatment at 600 °C practically had no effect on E110G alloy, while in case of E110 the UTS decreased. It can be suspected that the two alloys received different thermal treatments during the fabrication of cladding tubes.

At 800 °C the thermal treatment duration had significant effect on the UTS value. At this temperature the α to β phase transition takes long time, and obviously the short times were not enough for full transition.

At 900 °C the phase transition is much faster, for this reason the effect of duration of thermal treatment was not significant.

At 1000 °C the UTS of E110 cladding increased by 60% and that of E110G by 20-25%.

The comparison of oxidized and non-oxidized samples after the same duration and temperature of treatment showed that the thermal treatment had more significant effect on the change of UTS than the oxidation in the investigated range of parameters.

Remaining work

The planned work has been completed.

Related publication

- [1] M. Király, M. Horváth, Z. Hózer, T. Novotny, E. Perez-Feró: *Effect of high temperature treatment on the ultimate tensile strength of fuel claddings*, MTA EK-FRL-2015-980-1-1-M0, in Hungarian (2015)

RE-EVALUATION OF SURVEILLANCE SPECIMENS OF NPP PAKS

Attila Kovács, Márta Horváth, Ildikó Szenthe, Ferenc Gillemot

Objective

The design operational lifetime of four WWER-440 units of NPP Paks is 30 years. It has been extended up to 50 years. The operational lifetime extension was based on wide scale research and safety evaluation. The re-evaluation of the safe operation time was partially based on the traditional impact energy shift increase evaluation. The present development has been using fracture toughness data for the safe operational lifetime evaluation. The original surveillance program of the WWER-440 units had been designed in the 1970'th, and the radiation ageing monitoring specimens were irradiated and tested in the 1980'th. At that time the fracture toughness was not measured. The objective of the work is to reconstitute the remnants of the surveillance specimens and evaluate the fracture toughness properties for enhanced safety analyses for long term operation.

Methods

The remnants of the selected surveillance specimens have been transported into the hot cells of MTA EK. Each specimen remnant has been carefully identified, and pictures have been made on the fractured surfaces. The specimen remnants were stored in numbered boxes to avoid any mistake during the further work. The fractured end (deformed material) of the broken Charpy specimens have been cut off and sent back to NPP Paks for further storage. The remained 24 mm long archive material is used for reconstitution. First the weldment specimens have been tested, the lengths of the welding material measured, and the place of a new notch evaluated. The notch of the specimens has been prepared by spark erosion. Two end part have been welded by stud welding. The welding quality is carefully checked including the measurement of the heat affected zone. This zone must be narrow, not to affect the measured properties. The welded specimens are machined using remote controlled, NC machine in a semihot cell. All work phases had to be made in shielded area, remote controlled since the radioactivity of the irradiated surveillance specimens. Beside the reconstitution of the fracture mechanics specimens, small size tensile specimens have also been produced (see Figure 1). The fracture toughness specimens have been pre-fatigued and tested according to the ASTM-1921 standard. Both for the pre-fatigue and testing of fracture toughness and the testing of tensile properties several rigs, furnaces, cooling device and extensometers have been developed, since the specimens' sizes do not allow the use of standard ones. Figure 2 shows the high sensitivity extensometer used for pre-fatigue of the fracture toughness specimens.

Results

The two and four years long irradiated surveillance Charpy specimens of NPP Paks have been successfully reconstituted in 2015. The fracture toughness and tensile properties have been measured in the function of the temperature.

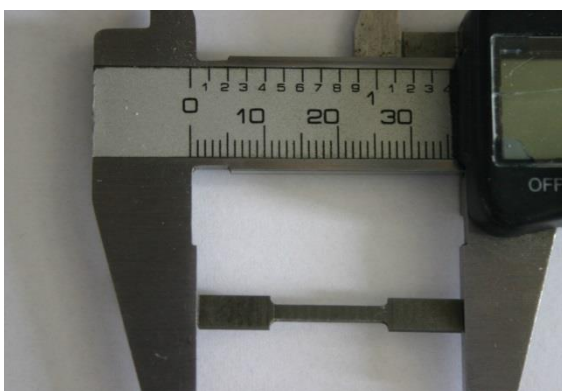


Figure 1: Small size tensile specimen produced from the reconstituted remnants of Charpy specimen

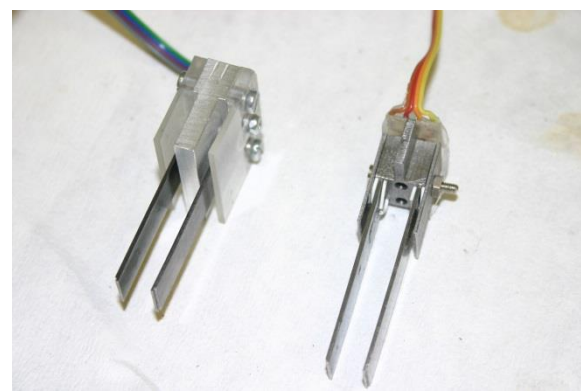


Figure 2: High sensitivity extensometer for pre-fatigue of the fracture toughness specimens

Remaining work

The tests have been evaluated in 2015, but the elaboration of the final report comparing the results with the former surveillance results are going on. Reconstitution of two further sets of specimens and testing them is the task for 2016. In 2016 also technology development of the so called J-R curve measurement is planned.

Related publication

- [1] F. Gillemot, M. Horváth, A. Kovács, I. Szenthe, N. Kresz, F. Oszvald: *Surveillance Program Extensions for Long Term Operation in WWER-440 reactor*, presented at the Workshop on surveillance of WWER reactors Rez, 14-15 October (2015)

HANDBOOK OF REACTOR MATERIALS

Ferenc Gillemot, Márta Horváth, Attila Kovács, Ildikó Szenthe

Objective

The as-received strength properties of the structural materials of nuclear power plants can be found in the relevant standards. However, during evaluation of safe operational time also the aged material properties require consideration. Aged (irradiation and thermal embrittled, etc.) properties are sometimes given in different codes, but not always. For safety and lifetime evaluation, fracture toughness data and physical properties are also required in as -received and in aged condition. These data generally are not given in standards and codes. The purpose of the handbook is to collect these data and provide them to the institutions and authorities dealing with safety and lifetime evaluation. Furthermore, the different books, literature etc. data many times are deviating, according to the data source. The main goal of the handbook is that all institutions should use the same material properties.

Methods

First the standard data are collected and the database extended with aged data from researches and from the literature. The data are evaluated, and selected values are printed in the handbook. The format is tables or/and diagrams.

Results

In 2015 the following chapters have been elaborated:

15H2MFA reactor vessel steel and its weldment

08X18H10T austenitic stainless steel and its weldment

WWER-440 reactor vessel cladding

As an example from the handbook, Figure 1. shows the yield strength of the 15H2MFA steel in the function of the irradiation fluence.

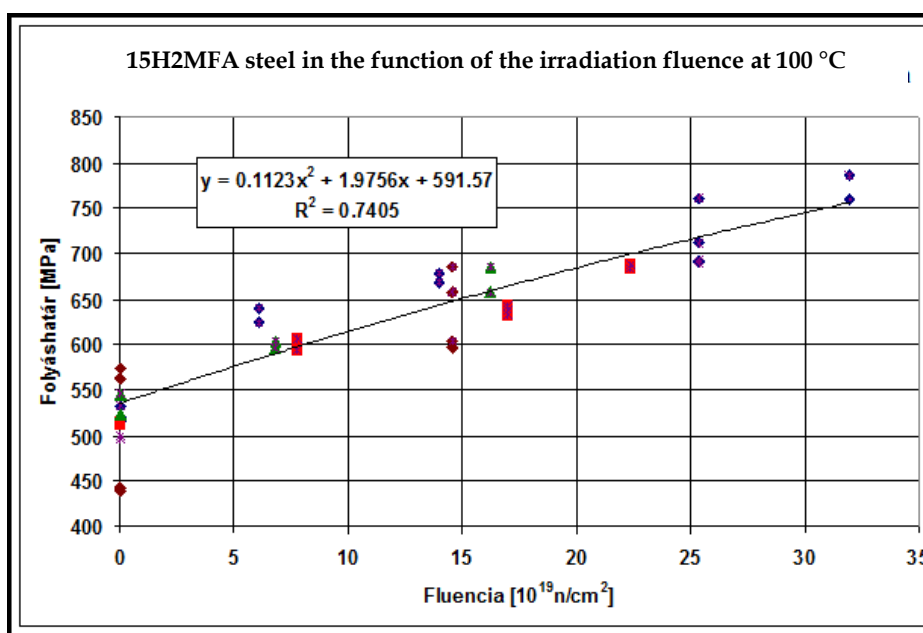


Figure 1. Yield strength of the 15H2MFA steel in the function of the irradiation fluence

Remaining work

In a nuclear power plant many structural materials are used. The elaboration of the handbook will be continued to include further relevant materials.

VALIDATION OF THE NEW TRANSURANUS CODE VERSION AGAINST BALLOONING-AND-BURST EXPERIMENTS

Eszter Barsy, Katalin Kulacsy

Objective

For the safe operation of nuclear fuel it is necessary to thoroughly understand the consequences of design basis accidents, such as a LOCA (Loss-of-Coolant Accident). The most common method for this is the use of numerical simulation, which must be validated by appropriate experimental data. The fuel behaviour simulation code used at MTA EK as a technical support organisation to the HAEA (Hungarian Atomic Energy Authority) is TRANSURANUS, and the up-to-date knowledge of the code is especially important considering the capacity expansion of the Paks Nuclear Power Plant. We therefore reviewed [1] the latest (as in 2015) code version (v1m1j14) against the one used earlier (v1m1j11). As the next step, we verified the simulation capabilities of the code using the experiments (on ballooning and burst) conducted at our Centre, on E110G cladding material under isothermal circumstances.

Methods

First of all, we inspected the changes mentioned in the manual and changelog of the code, and compared the source codes of the two versions of TRANSURANUS. Then we wrote the input files which contained all the relevant traits of the ballooning-and-burst experiments. This meant choosing the right nodalisation, boundary conditions, material properties, phase transition and burst criteria. This way we could compare not only the two code versions to each other (by running both with the same input) but also the code results to the experimental results.

Results

There were no modifications in the cladding behaviour modules between the two code versions, only minor changes in calculation precision due to the usage of Fortran 95. However, a new failure criterion was added.

The comparison of the two code versions regarding the experiments showed – as expected – identical results.

According to the comparison between the results of simulations and experiments, the burst time is estimated quite well (Fig. 1) and the burst pressure is estimated well by the code. The differences in results are mostly conservative, the code tends to underestimate the values of pressure and time of burst. The code was found to be suitable for modelling cladding behaviour under LOCA conditions.

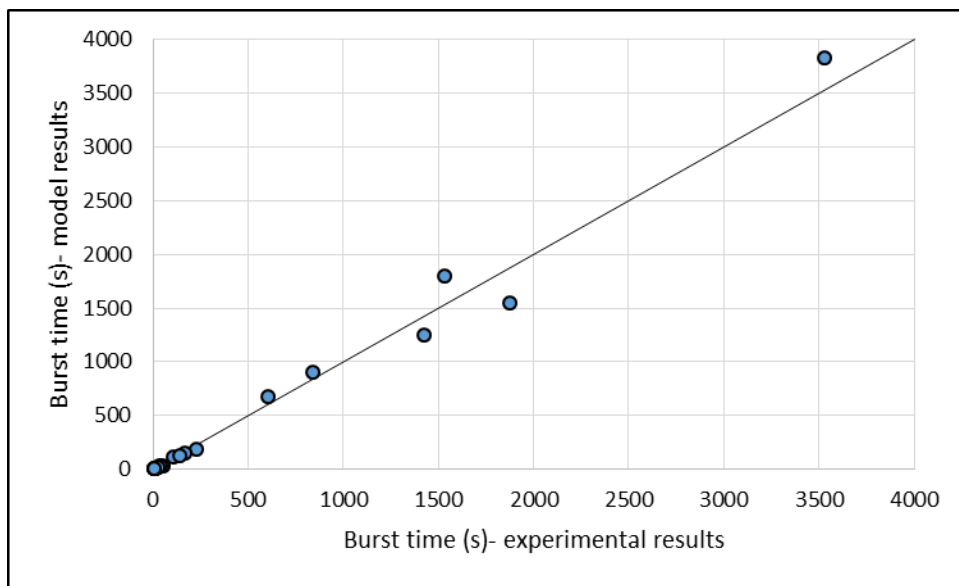


Figure 1: Comparison of experimental and simulation results, one point per sample (the closer a point is to the solid line, the smaller is the difference between the two results)

Remaining work

The project was finished in 2015.

Related publication

- [1] E. Barsy, K. Kulacsy: *Validation of the new TRANSURANUS code version regarding the ballooning-and-burst experiments in the Centre for Energy Research, HAEA report in Hungarian (2015)*

SIMULATION OF HALDEN LOCA TEST IFA-650.10

Katalin Kulacsy

Objective

Fuel behaviour simulation is essential to the safety assessment of all new core designs or fuel types, and code validation is essential to fuel behaviour simulation. In order to extend the validation database of the code FRAPTRAN used at MTA EK to simulate transients and accidents, the LOCA (loss-of-coolant accident) test IFA-650.10 performed at the Halden Reactor in the framework of the Halden Reactor Project was simulated.

Methods

The Halden test segment with a burn-up of 61 MWd/kgU was cut from a commercial 17x17 PWR fuel rod with Zircaloy-4 cladding, irradiated to an average burn-up of 56 MWd/kgU. The base-irradiation history was not very detailed, especially the axial distribution of the linear heat generation rate and fast neutron flux were missing. These data were approximately reconstructed on the basis of the final axial burn-up profile and the linear heat generation rate, respectively, using previous simulation experience. The base-irradiation history was simulated by the code FUROM and the results on the state of the fuel rod segment served as input to the code FRAPTRAN for the transient calculations.

During the LOCA test the axial temperature distribution was measured in five positions, but not at the location of the maximum temperature, as the thermocouple would have influenced ballooning and burst; measured temperatures were only available at least 10 cm away from the burst location. In addition, coolant circulation during the LOCA test was unpredictable, the relevant temperature profile had therefore to be interpolated without a physical basis, which caused a large uncertainty in the results. This was circumvented by running several simulations with different temperature profiles. The temperature of the gas in the large, unheated plenum of the test rod also gave rise to uncertainties.

Results

The two main quantities used to evaluate burst test simulations are burst time and burst pressure. Figure 1 presents the measured and the simulated evolution of the pressure inside the rod when the temperature profile was the most realistic, i.e. when the maximum temperature exceeded the temperatures measured by the nearest thermocouples by only 20-30 °C.

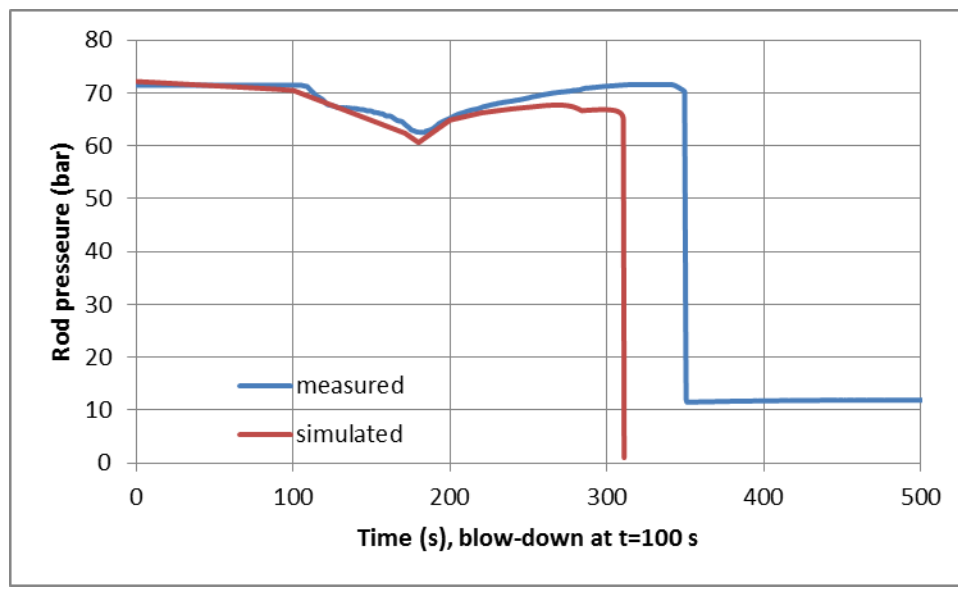


Figure 1: Simulated and measured rod pressures during the LOCA test IFA-650.10

The simulated burst pressure was in all runs lower than the measured value, which may be due to an inaccurate interpretation of the plenum temperature. The burst time simulated with the realistic temperature profile showed good agreement with the measurement: cladding temperature plays a crucial role in this result.

Remaining work

The work was completed in 2015.

Related publication

- [1] K. Kulacsy: *Simulation of Halden LOCA test and participation in fuel behaviour simulation activity*, MTA EK FRL-2015-982-1-1-M0 (2015), in Hungarian (2015)

SIMULATION OF THE HATAC RADIOACTIVE FISSION GAS RELEASE EXPERIMENT

Katalin Kulacsy

Objective

The code FUROM has been developed at MTA EK and used for steady-state fuel behaviour simulation for many years. It is our tool to assess the safety of new core designs and fuel types during normal operation and anticipated operational occurrences.

As the steady-state gap inventory of a fuel rod may provide a significant part of the activity release during an accident, the fission gas release module of the code was extended to radioactive nuclides in 2005, and the model was recently modified to achieve self-consistency. Although the thermo-mechanical simulation capabilities of the code have been validated against several measurements, data on the extent and kinetics of radioactive fission gas release are scant and have previously not been used. The experiment HATAC designed to provide on-line information on the release of both stable and radioactive fission gases was therefore simulated with the code FUROM.

Methods

Two segments with burn-ups of 35 and 48 MWd/kgU were cut from commercial 17x17 PWR fuel rods with Zircaloy-4 cladding irradiated to average burn-ups of 33 and 46 MWd/kgU, respectively. They were subjected to ten power transients each in approximately one year in the SILOE research reactor. Calculated fuel centreline temperatures in all the transients were above the Halden 1% threshold where significant fission gas release could be expected.

Base irradiation was simulated both for the full-length mother-rods and for the segments as if the segments were complete short rodlets. The missing parameters (e.g. the plenum volume) of the segments were adjusted in such a way that the pressures inside the rodlets match those inside the full-length rods. The history of the HATAC experiment was then added to the base irradiation history of the rodlets and the entire irradiation was simulated.

Results

- For radioactive nuclides, instantaneous releases and releases during each single transient are over-predicted by the code by one, sometimes two orders of magnitude.
- In spite of this, for stable nuclides the simulated cumulative stable fission gas release is one order of magnitude lower than the measured value.
- Measurements show release peaks at abrupt linear heat rate changes, i.e. at the beginning and end of each transient, which becomes more pronounced for transients occurring later in the series (see Fig. 1). These peaks are probably due to significant new crack formation in the fuel, which is not simulated by the code.
- Release due to increased cracking is much more significant for stable nuclides than for radioactive ones, as the former can accumulate between and during transients.
- Under VVER-440 operating conditions, such increased cracking due to abrupt, large power changes does not occur.

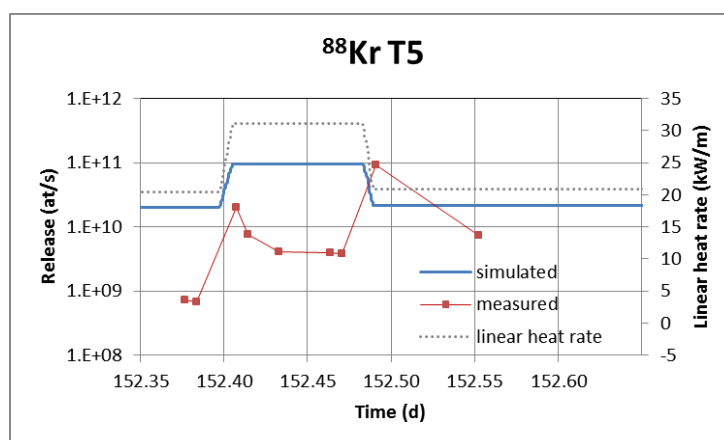


Figure 1: Simulated and measured release of ^{88}Kr during transient no. 5 of rodlet C1

Remaining work

The work was completed in 2015.

Related publication

- [1] K. Kulacsy: *Improvement and testing of radioactive fission gas release calculation methods through comparison with experiments*, MTA EK FRL-2015-986-01-01-M0 (2015), in Hungarian (2015)

SIMULATION OF THE HALDEN CREEP TEST IFA-699 FOR VVER CLADDING

Katalin Kulacsy

Objective

The code FUROM has been developed at MTA EK and used for steady-state fuel behaviour simulation for many years. It is our tool to assess the safety of new core designs and fuel types during normal operation and anticipated operational occurrences. Versions 2.0 and 2.1 were released in 2010 and 2015, respectively. One of the important modifications was a complete revision of cladding mechanics, including the extension of the creep model to anisotropic cladding materials.

The test IFA-699 performed at the Halden Reactor aimed at measuring the bi-axial creep behaviour of four cladding materials during periods of different stresses. One of the specimens was a tube made of the Russian cladding alloy E110. The behaviour of the E110 specimen was simulated using the mechanical models of versions 2.0 and 2.1 of the code FUROM in order to compare the old and the new models.

Methods

During the experiment, the specimen was subjected to different inner pressures for periods of time usually long enough to allow steady-state creep to develop. Compressive and tensile stresses were both tested. The diameter of the specimens was measured regularly.

The code FUROM can only simulate closed fuel rods with the evolution of the inner pressure according to the actual thermo-mechanical circumstances and fission gas release. However, the creep test was based on externally fed fill gas pressures. The relevant subroutines (thermal expansion, elastic deformation, irradiation growth and creep) of both code versions were therefore compiled into two stand-alone codes in order to simulate the experiment. Different combinations of isotropic and anisotropic models were tested for version 2.1.

Results

Figure 1 presents results for the most relevant case where the compressive tangential stress of -75 MPa was closest to the values experienced in a VVER-440 reactor before the fuel-to-clad gap closes. This stress was preceded by an unstressed state when the external and internal pressures were equal. After the first 100-200 hours of transient creep modelled by means of the strain hardening procedure, creep rate becomes constant (illustrated by the slope of the dashed line). The simulated and measured values show a very good agreement.

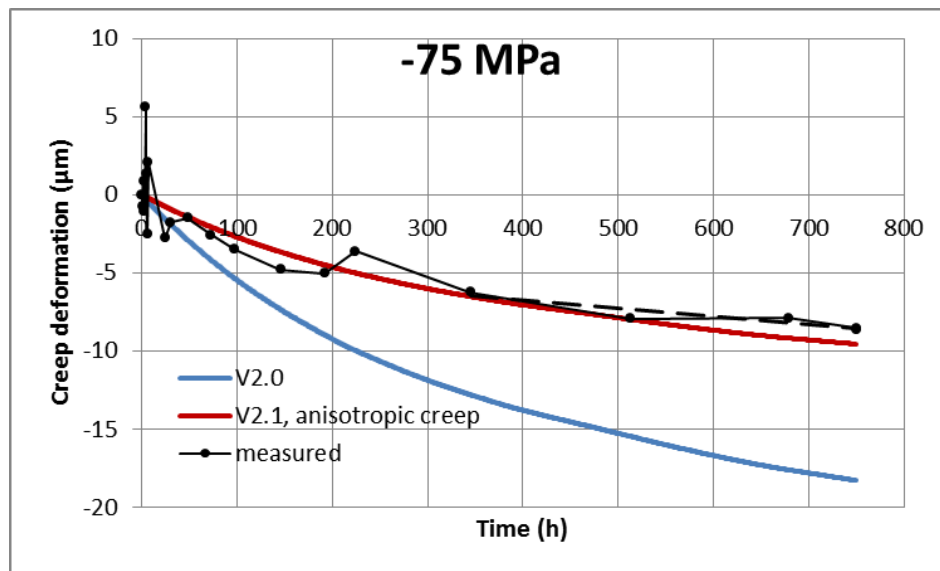


Figure 1: Measured and simulated creep during the first period of the test IFA-699

Version 2.1 of the code FUROM predicted lower creep rates than version 2.0 in all cases. For tensile stresses the simulated creep rates were typically lower than the measured ones, which gives conservative simulation results (higher stresses) during pellet-cladding mechanical interaction due to the slower relaxation of the cladding.

Remaining work

The work was completed in 2015.

Related publication

- [1] K. Kulacsy: *Post-test simulation of the Halden creep test IFA-699 for VVER cladding*, MTA EK FRL-2015-992-01-01-M0 (2015), in Hungarian (2015)

EFFECT OF PRE-OXIDATION ON THE AIR OXIDATION OF ZIRCONIUM

Erzsébet Perez Feró, Tamás Novotny, Márta Horváth

Objective

The oxidation and embrittlement of zirconium fuel cladding may occur in air ingress situations. In such cases, the oxide layer formed – prior to the air oxidation – on the surface of the cladding may have an impact on the further oxidation and on the mechanical properties of the cladding. The aim of our project was to determine the effect of the steam pre-oxidation on the high temperature air oxidation kinetics and the ductility of E110G zirconium cladding.

Methods

Two oxide layers with different thicknesses (3 µm and 10 µm) were produced on the surface of the E110G samples, in steam at 800 °C. The thickness and the quality of the formed oxide layer were measured by optical microscope. The pre-oxidised samples were oxidised in 10% air – 90% steam mixture and in 100% air at high temperature. The oxidations were carried out under isothermal conditions, preferably at 1000 °C, but a few tests were performed at 1200 °C. After the air oxidation, the oxidised specimens were examined in the ring compression tests. Some tests were also performed on E110 cladding – currently used in Paks NPP – and the results of the claddings were compared.

Results

The oxidation experiments show that there is a significant difference between the air oxidation kinetics of E110G and that of E110 claddings (Fig. 1). Nevertheless, the results clearly indicate that even a relatively thin (3 µm) oxide layer is able to decelerate the air oxidation of both claddings. The relatively compact oxide layer formed during steam pre-oxidation prevents reaching of oxidising atmosphere to the surface of the metal.

On the basis of the ring compression tests, the oxidised E110G shows more ductile behaviour compared to E110. The effect of the previously formed oxide layer on the embrittlement of the cladding is less significant than its impact on the oxidation.

It can be concluded that the oxide layer formed under normal conditions or in the initial phase of an air ingress accident – in case of the examined oxide thicknesses – would inhibit the degradation of E110G cladding. It is important to point out that the air-containing atmosphere under accident conditions – in spite of the protective effect of oxide layer – leads to a rapid oxidation and embrittlement of the zirconium cladding.

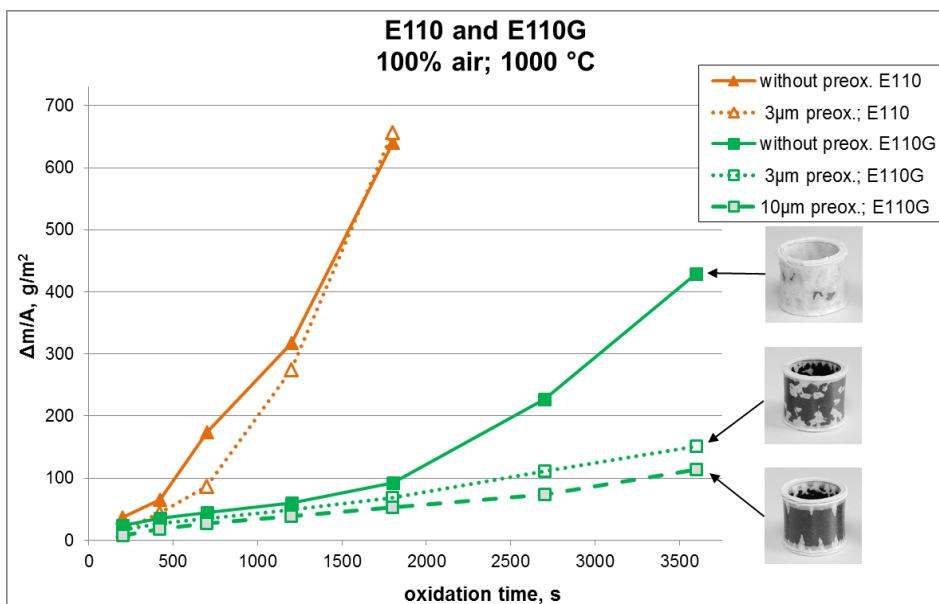


Figure 1: Oxidation kinetics of E110 and E110G alloys in pure air at 1000 °C

Remaining work

The work has been completed.

Related publication

- [1] E. Perez Feró, T. Novotny, M. Horváth: Vízgőzös előoxidáció hatása az E110G cirkónium ötvözettel – levegőbetöréssel járó atomerőművi balesetek esetén bekövetkező – magas hőmérsékletű oxidációjára, EK-FRL-2015-271-01/01, in Hungarian. (2015)

SECONDARY DEFECTS OF NUCLEAR FUELS – MODELLING OF HYDROGEN FORMATION INSIDE THE LEAKING FUEL

Emese Slonszki, Péter Szabó, Zoltán Hózer, Tamás Novotny

Objective

In this second part of the "Secondary defects of nuclear fuels" project we developed the TSKGO computer code so that can simulate the secondary failures. The TSKGO code earlier calculated only with mixture of helium-argon-krypton. However, our model calculates the amount of formed and accumulated hydrogen inside the leaking fuel rod.

Methods

If the fuel rod loses integrity, the water penetrates into it through the initial defect, where hydrogen is formed during the corrosion processes and the radiolysis. One part of hydrogen is picked up by cladding while another part of it can be released from the fuel. This is a very complex process that is affected by many factors. The hydrogen accumulation is confirmed by such examination where high hydrogen content was found, for the brittle parts of the fuel rod with secondary failure were broken. However, very few data of the corrosion processes inside the fuel rod, the rate of radiolysis and characteristic parameters of hydrogen absorption are available. Our model is developed based on three main sources:

- Literature overview and evaluation of models of primarily outside corrosion of Zircaloy-2 and Zircaloy-4 claddings considering published data of E110 cladding.
- Model developing for the calculation of effect of radiolysis based on theoretical considerations.
- Hydrogen pick-up of E110 alloy was estimated by aimed test series.

Results

TSKGO code models the leaking fuel elements processes. We made the model of simulation of formed hydrogen and built in the TSKGO code. The models of corrosion processes and the model of radiolysis were tested separately and after that we built them in the FORTRAN program. The amount of formed hydrogen is limited by the amount of water entering the fuel element. The released hydrogen appeared in the prescribed balance equation. The developed models must be assessed as the first approaching, since these models are adequate to estimate the amount of hydrogen which forms inside the leaking fuel element, but the validation of models is not possible due to very few measured data.

Our calculations have shown that the presence of hydrogen may be affected by the results of TS (telescope sipping) examinations. According to the calculations, release of iodine, caesium and noble gas by TS examination can be much higher if hydrogen accumulated inside the fuel rod. However, based on results of our calculations the position of assumed hole of the leaking fuel element can cause larger differences than the presence of hydrogen.

The calculations have pointed out that due to the accumulation of hydrogen in the zirconium, the cladding can become more brittle locally, which can lead to additional (secondary) damage in the reactor or the spent fuel pool.

Remaining work

This project is finished.

Related publication

- [1] E. Slonszki, P. Szabó, Z. Hózer, T. Novotny: *Modelling of hydrogen formation inside the leaking fuel*, MTA EK-FRL-2015-966-1-1-M1, in Hungarian (2015)

VALIDATION OF THE KARATE CODE SYSTEM AGAINST THE LATEST OPERATIONAL DATA AND STARTUP MEASUREMENTS

András Keresztúri, György Hegyi, Lajos Korpás

Objective

In the last decades, KARATE-440 was elaborated and developed continuously to calculate VVER-440 reactor cores by coupled neutron physical - thermal hydraulics models. The main goal of the calculations is the core reload design, however, certain safety analyses amenable to a static code can be analyzed also by KARATE-440. The program serves economic core reload design so that the limitations demanded by the safety analysis should be observed. The latter function is utilized for the periodic independent check of the Paks NPP core design. On the other hand, in the last years several modifications of the VVER fuel construction and the corresponding core design aiming at more economic fuel utilization - like for example Gd doped fuel - were introduced by Paks NPP which made further development of the models necessary. Having regard to the above situation, continuous validation from year to year against the latest operational and start-up measurements is indispensable for the establishment of the uncertainties and the margins for the calculated safety related frame parameters. In 2015, the cycles of Paks NNP realized in 2014 were used for the validation. An additional task was the comparison of the measured and calculated critical boron concentrations for the last three cycles of Paks NPP.

Methods

Model validation, comparison of the calculated and measured data.

Results

The following parameters were used for the validation

- core burnup dependent radial peaking factors based on the assembly-wise in-core temperature rises,
- core burnup dependent operational critical boron concentrations,
- critical boron concentrations measured at the Minimum Controllable Power,
- moderator temperature reactivity coefficients measured at the start-up procedure,
- integral and differential efficiencies of the control rod groups.

According to the validation results, there are no significant changes of the deviations from the measurements as compared to the earlier cycles. However, the detailed analysis in connection with the critical boron concentrations during the last three cycles showed a little bit higher differences between the measured and calculated values as usually. In spite of this fact, the overall agreement is good as it is demonstrated in Fig. 1. Additionally, it was concluded that KARATE code system produced very stable results during the last ten years, and the observed differences are acceptable taking into account the uncertainties of the calculations and measurements.

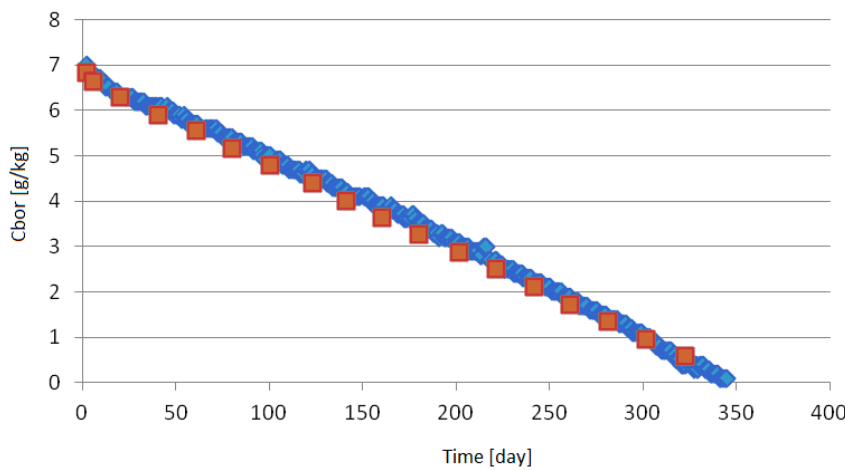


Fig. 1: Measured and calculated (squared symbols) critical boron concentration for Cycle 30 of Unit 2 depending on the time

Remaining work

Continuous validation of the KARATE code system against measurements.

Related publications

- [1] Gy. Hegyi, A. Keresztúri, L. Korpás: *Comparison of the KARATE 5.0 results with the measurements and C-PORCA calculations for the cycles of Paks NNP realized in 2014*, MTA-EK-RAL-2015-706/1-M0, in Hungarian (2015)
- [2] Gy. Hegyi, A. Keresztúri, L. Korpás: *Comparison of the measured and calculated critical boron concentrations for the last three cycles of Paks NPP's Units*, MTA-EK-RAL-2015-706/2-M0, in Hungarian (2015)

UNCERTAINTIES OF BURNUP DEPENDENT CELL CALCULATIONS AND OF ACTIVE CORE CALCULATIONS WITH THERMAL-HYDRAULICS FEEDBACK FOR VVER REACTORS

István Panka, György Hegyi, András Keresztúri, Csaba Maráczky

Objective

Best estimate codes without knowledge of uncertainties can not be used for safety evaluation. In the frame of the OECD NEA Uncertainty Analysis in Best-Estimate Modeling (UAM) cooperation, the final objective is to determine the uncertainties of the coupled reactor physics/thermal hydraulics LWR calculations at all stages. Phase-I of this benchmark deals with the survey of the uncertainties of the standalone neutronic calculations. At the beginning of this work, the uncertainties of the neutronic calculations at zero burnup were investigated in the benchmark. Later on, Phase-I has been extended for the burnt out case. Additionally, at the final stage, one of the problems to be analyzed is the Kalinin-3 benchmark problem from the point of view of the uncertainties in case of VVER reactors.

Methods

Concerning the statistical method, basically the algorithm elaborated earlier was used. At the first step, a sampling procedure for the selected isotopes and cross sections, and also for other relevant data (e.g. fission yields, reactor power, effective delayed neutron fractions) is performed many times and, subsequently, the elaborated statistical methodology is applied. Finally, one can get the estimated standard deviations and /or correlations matrices for selected target parameters.

Results

A PWR pin cell defined in the UAM benchmark was used for the investigations of the burnup dependence of the uncertainties of cell calculations using the MULTICELL module of KARATE code system. It was pointed out that the uncertainties of infinite multiplication factor are increasing with burnup mostly due to uncertainties of the considered ^{239}Pu reactions. At high burnup, the estimated standard deviation can reach 0.84 % - 0.94% values.

Concerning the core calculations, the Kalinin-3 benchmark data and the coupled KIKO3D-ATHLET code system were used for the assessment of the uncertainties in a VVER-1000 core considering fresh fuel. Both stationary and transient cases were investigated. It was pointed out that considerable uncertainties - related to the investigated outputs - are coming from the considered input uncertainties in case of fresh fuel. Additionally, it was also shown that the investigated target uncertainties are changing both in axial and radial direction (see Fig. 1) to a great extent and that is why three-dimensional analysis is needed to survey the uncertainties properly.

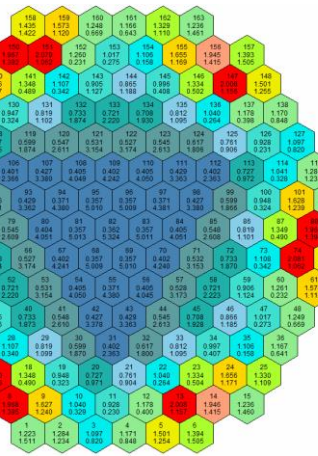


Fig. 1: Normalized radial power distribution and corresponding uncertainties (relative sigma in percent)

Remaining work

There is no remaining work. However, the OECD NEA UAM benchmark is still going on with new and updated tasks.

Related publications

- [1] I. Panka, Gy. Hegyi, Cs. Maráczky, A. Keresztúri: *Assessment of the uncertainties of coupled KIKO3D-ATHLET reactor physics/thermal hydraulics calculations by using the data of Kalinin-3 benchmark*, MTA-EK-RAL-2012-727/03/M0, in Hungarian (2014)
- [2] I. Panka, A. Keresztúri: *Assessment of the uncertainties of MULTICELL calculations by the OECD NEA UAM PWR pin cell burnup benchmark*, Kerntechnik **80**, 305-313, (2015)
- [3] I. Panka, Gy. Hegyi, Cs. Maráczky, A. Keresztúri: *Uncertainties of the KIKO3D-ATHLET calculations using the Kalinin-3 benchmark (Phase II) data*, Proceedings of the 25th AER symposium, ISBN 978-963-7351-25-9 (2015)

ELABORATION OF NEW VERSIONS OF THE GUIDES "FUEL DESIGN" AND "ACTIVE CORE" FOR NEW NPP UNITS

András Keresztúri, Zoltán Hózer, Tamás Fekete

Objective

It is a well established international tendency that more stringent requirements are applied for the new Gen3 nuclear power plants than for the older types, the latter ones running without serious problems for several decades. Therefore, a renewal activity of the documents comprising the licensing requirements was initiated by the Hungarian Atomic Energy Agency. First, the Nuclear Safety Regulations were modified, and in the second step the reissue of the related guides is foreseen. The work presented here was aiming at two special guides devoted to the fuel design and the procedures related to the active core.

Methods

Studying, correcting and writing.

Results

The proposals for more detailed guides have been prepared. The most important differences in comparison with the previous guides are as follows:

- The new guides detail the recommendations for the strength and structural analyses of the fuel assemblies.
- Before using the new fabricated fuel assemblies in the reactor, endurance tests are proposed and detailed.
- The new guides don't give the concrete criterion values necessary to avoid the fuel failure in case of the different mechanisms ("acceptance criteria"), the necessary procedure is detailed to derive them instead. In this respect, the necessary experiments and the well established mathematical statistical procedure is emphasized. The usual derivation of the DNB criterion specifying both the confidence level and the probability content is regarded as an example to be followed.
- The classification of the various fuel failure mechanisms is taking into account the new classification of the reactor states and initiating events.
- The proposals for the core monitoring and core design are more detailed.
- A special chapter is devoted to the monitoring and storing the assemblies containing failed fuel pins.
- The steps of the inspection procedure of the new fuel pins and assemblies in the factory are classified in a more detailed and consequent manner.
- The xenon oscillations are considered in connection with the requirements against the ex-core detectors.

Remaining work

There is no remaining work.

Related publications

- [1] A. Keresztúri, Z. Hózer, T. Fekete: *Fuel design for the nuclear power plants*, MTA EK-RAL-2014-792-01/M2, in Hungarian (2014)
- [2] A. Keresztúri, Z. Hózer: *Active core and fuel handling procedures in the nuclear power plants*, MTA EK-RAL-2015-972-02/M2, in Hungarian (2015)

MULTI-PHYSICS APPROACH OF THE SAFETY ANALYSIS HOT CHANNEL CALCULATIONS; DEVELOPMENT AND TESTING OF A GENERAL SOFTWARE FRAMEWORK TOOL

István Panka, András Keresztúri, Ádám Tóta

Objective

The hot channel calculation is the important final phase of the safety analysis because the fulfilment of the acceptance criteria is investigated here. In fact, it would require simultaneous application of several disciplines like reactor physics, thermal hydraulics, material science and mechanics.

Nevertheless, the traditional approach to this problem is that the applied calculations are focusing on only one or two disciplines while the influence of the other ones are taken into account in an approximate manner which can result in an insufficient coupling between the different disciplines.

Establishing an online coupling between the neutron physics, the fuel behavior and the thermal hydraulic codes would be unavoidable for the best estimate parallel handling of the processes important for the safety analyses.

Methods

The remedy of the problem outlined above can be based only on parallel tightly coupled and detailed models of all disciplines, which is called "multi-physics". The constituent models are depending on the specific problem to be solved. In the present work, we focus on the hot channel calculations of various transient events.

In the frame of the project, the most important processes – to be modeled in parallel – are the thermal hydraulics of the coolant, especially the mixing, the corresponding surface heat transfer process and the heat conduction inside the fuel pin, especially in the gap; moreover the feedback effects of the reactor physics. In 2015, development and testing of a general software framework tool to be applied for parallel running of the models were foreseen.

Results

The modeling tools intended to be used are as follows: ATHLET for the system thermal hydraulic, COBRA for the hot-channel thermal hydraulic and mixing, FUROM and FRAPTRAN for the stationary and the transient fuel behavior, KARATE for the stationary neutron physics and KIKO3DMG for the neutron transient calculations. The software framework to be filled with the appropriate modules is capable for both the stationary and the transient multi-physics calculations.

In 2015, the list of data to be exchanged between the modeling tools was finalized and a generalized software framework tool (MPHFtool) was developed using the MPI (Message Passage Interface) library to communicate between the parallel running modeling tools. MPHFTool was written in FORTRAN and implemented by using INTEL VISUAL FORTRAN compiler.

The tool consists of modules: the main one is the so called master module which controls the working of the sub-modules including the processing of data changes between the sub-modules. In the current versions, MPHFTool consists of maximum sixteen parallel running modules and each sub-module (except the master module) is based on the codes, modeling tools mentioned before. The working of the master module can be controlled by an input file and using this file MPHFTool is able to control stationary and transient calculations.

In order to test the elaborated software framework tool, the sub-modules were filled by simplified models representing the modeling tools mentioned before. In order to follow and characterize the processing of data changes and other features of the running of the modules, the history of the running of MPHFTool was recorded in a log file. Both stationary and transient calculations were successfully tested

Remaining work

The project has been completed.

Related publication

- [1] Á. Tóta, I. Panka, A. Keresztúri: *Development and testing of a general software framework tool for hot channel calculations*, MTA-EK-RAL-2014-951/2-M0, in Hungarian (2015)

SUPPLEMENTING THE KARATE CODE SYSTEM WITH THE RESONANCE SELF SHIELDING CAPABILITY FOR THE PLUTONIUM ISOTOPES

András Keresztúri

Objective

The revision of the resonance self-shielding treatment in the MULTICELL spectral code of KARATE became necessary due to the recent and future application of MOX fuel in the Gen4 and PWR reactors. Another motivation is the burnup increase in the Gen3 reactors. It was found that the resonance self-shielding treatment in KARATE is to be supplemented for the Pu-240, Pu-241 and Pu-242 isotopes.

Methods

The number of the energy groups in the spectral codes is not more than hundred (or a few hundred), therefore application of special treatments based on the equivalence theory is necessary in these programs to take into account the flux decrease in the vicinity of the resonances, which are sharp in comparison with the energy width of the groups. The NJOY and PEACO codes were applied for generating Doppler broadened point-wise cross sections for various temperatures and using them in the further transport calculations, the latter ones performed in ultra-fine energy representation. The parameters of the equivalence theory were fitted to match the results of the transport calculations. The Bell factor – connecting the homogeneous and heterogeneous transport cases – played essential role in this procedure.

Results

The fitted parameters of the equivalence theory depending on the temperature, the background dilution cross section and the Dancoff factor were built in a special library of the MULTICELL spectral code, moreover, special subroutines were developed to provide the self-shielding factors. The test calculations have shown that the resonance self-shielding of the above - mentioned three isotopes can influence the multiplication factors and burnup chains in case of MOX fuel. For higher burnup of UOX fuel the influence is not negligible either. Figure 1 shows the shielding factors obtained for the epithermal capture of the Pu-240 at various temperatures and Dancoff factors.

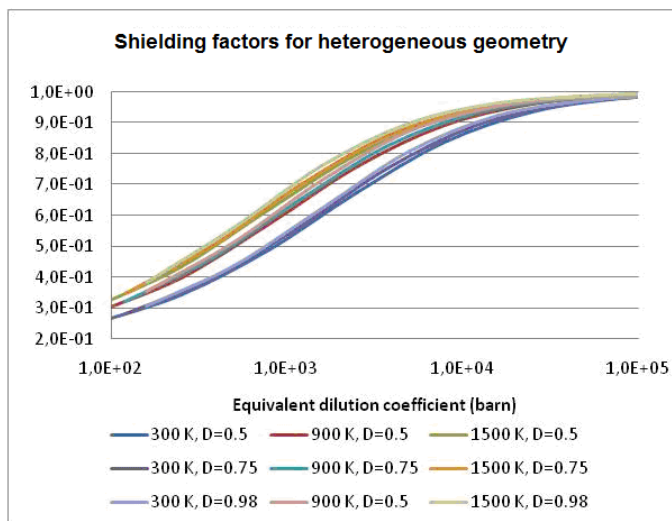


Figure 1: Shielding factors for the epithermal capture of Pu-240 at various temperatures and Dancoff factors

Remaining work

There is no remaining work.

Related publication

- [1] A. Keresztúri: *Calculation of the resonance self-shielding of the Pu-240, Pu-241 and Pu-242 isotopes in the KARATE code system*, MTA EK-RAL-2015-978/M0, in Hungarian (2015)

DEVELOPMENT AND TESTING OF STATISTICAL VERSION OF THE KARATE CODE SYSTEM

István Panka, György Hegyi, Csaba Maráczy, Emese Temesvári

Objective

The safe and at the same time economically competitive utilization of the recent and future nuclear installations can only be based on well-established reserves, "margins" responsible for the correctly evaluated uncertainties, which must be applied both for the normal operation and the accidental conditions. That is the reason of the increasing demand from nuclear research, industry and regulation for best estimate predictions provided with their confidence bounds.

From time to time, newer fuel types are introduced at Paks NPP. As an example and a consequence of this fact, according to the core design calculations, the 15 month cycle lengths at Paks NPP will result in higher burnup values of the assemblies and the fuel pins, consequently smaller but well-validated burnup margins lead to significant economic advantages.

In order to support the well-validated evaluation of safety-related margins, it was decided to elaborate the "statistical version" of the KARATE code system which will also be useful for the uncertainty evaluation of other, directly not measured parameters such as the power peaking factors of the fuel assemblies and pins. The final goal is to reduce the safety margins of the so called "frame parameters" as far as possible.

Methods

Concerning the statistical method, basically the algorithm elaborated by us in the frame of OECD NEA UAM ("Uncertainty Analysis in Modeling") benchmark was used. At the first step, a sampling procedure for the selected isotopes and cross sections, and also for other relevant data (technological data, reactor power) is performed many times, and subsequently, the elaborated statistical methodology is applied. Finally, one can get the estimated standard deviations and / or correlations matrices for selected target parameters.

Results

KARATE involves all the libraries and computer programs which are needed to perform fuel cycle calculations and fuel cycle design. The calculation is grouped into 3 levels. The levels involved in KARATE include cell level to provide a cell library, assembly level to provide homogenized assembly library and to calculate pin powers in selected assemblies, global level to determine criticality parameters and power distributions.

A level is connected to the higher one through parameterized data libraries; these libraries provide a part of the input data for the higher level. A level is connected also to the lower one, usually boundary condition is provided for a "Lupe"-like calculation.

Because the libraries play essential role in providing the connections between the levels, they – together with the input and output of each calculation step – must be taken into account according to the statistical treatment in the frame of the Monte Carlo sampling of cross sections, technological data, etc. This procedure was elaborated in 2014.

In 2015, further development of the highest, nodal-wise level of the statistical KARATE code system was carried out. Using the updated code, preliminary investigations were performed in order to demonstrate the applicability of the elaborated methodology during burnup, using large number of sampled input sets of the corresponding parameters. In order to take into account the influence of burnup, the investigations were performed for an equilibrium cycle of Paks NPP considering the newest, 4.7% averaged enriched fuel type and 15 month cycle length.

The first results are promising in connection with the uncertainties of the power and burnup distributions. The corresponding uncertainties were decreased during the burnup. Concerning the results related to the effective multiplication factor, it was concluded that the effect of input uncertainties in connection with the cross sections and technological data should be separated to see clear their impact during the burnup.

Remaining work

There is no remaining work scheduled for 2015, although the investigations will be continued in 2016, as well.

Related publications

- [1] Gy. Hegyi, Cs. Maráczy, I. Panka, E. Temesvári: *Elaboration of the spectral and reflector calculations parts of the KARATE code system*, MTA EK-RAL-2014-789/M0, in Hungarian (2014)
- [2] Gy. Hegyi, Cs. Maráczy, I. Panka: *Development of the highest, nodal-wise level of the statistical version of KARATE code system, demonstration of the applicability*, MTA EK-RAL-2015-988/M0, in Hungarian (2015)

USING HZP STATES OF PAKS NPP FOR THE VALIDATION OF BURNUP CREDIT CALCULATIONS, ELABORATION OF A DETAILED FULL CORE MCNP MODEL

István Panka, György Hegyi, Gábor Hordósy, Csaba Maráczky

Objective

The subcriticality analysis of a spent fuel storage facility is strongly influenced by the uncertainty of the calculated multiplication factor (k_{eff}) due to the uncertainties of nuclear cross section data. Traditionally, this uncertainty was determined from comparison of calculated and measured k_{eff} values for a number of critical experiments.

This approach can easily be applied to cases with fresh fuel, because there are a number of publicly available critical experiments with fuel enrichment, moderator, geometry etc. similar to the storage facilities. However, when burnup credit is applied in the subcriticality analysis i.e. the change of reactivity due to the change of composition with burnup is considered, the problem arises that there are no such published critical experiments where the fuel composition is similar to the composition of the spent fuel.

A possible solution is to determine the discussed uncertainty by calculation using the covariance data of the cross sections and use the HZP (Hot Zero Power) states of operated NPP's for checking the calculations. In this case, an additional task is to assess how representative are the considered HZP states for the storage facility in connection with the fuel composition.

Methods

Concerning the statistical method, a Monte-Carlo type, sampling based methodology was used. At the first step, a sampling procedure for the selected isotopes and cross sections is performed many times, and subsequently, the elaborated statistical methodology is applied. Finally, one can get the estimated standard deviations or the results can be evaluated using the Wilks' method in case of small sampled values. In the latter case, the calculations can usually be characterized by tolerance intervals with 95%/95% probabilities.

Results

In 2015, the full core MCNP model was developed and the elaborated model includes the reflector zone, as well. First, real HZP states of Paks NPP were calculated by the new model. These results correspond to the so called best-estimate calculation. After that, the elaborated statistical methodology based on the Wilks' method was applied to determine the uncertainties of the effective multiplication factors. In the present investigations, the composition of the fuel was taken from the best-estimate KARATE calculations, which means that the effect of uncertainties of the compositions was not taken into account in this study.

In connection with the effective multiplication factor, the first results are promising (see Table 1), although it was concluded that it is also needed to take into account the uncertainties of the isotopic compositions to cover the measured values with higher probabilities. It was concluded that the statistical version of the KARATE code system, which is being developed parallel with this project, could be used for this purposes in the near future.

Table 1: Mean values and uncertainties of the effective multiplication factor for some HZP states

| | Mean | 95%/95% lower limit | 95%/95% upper limit |
|-------------------|---------|---------------------|---------------------|
| Cycle 22, Unit I | 0.98305 | 0.97019 | 0.99227 |
| Cycle 23, Unit I | 0.99007 | 0.97745 | 0.99904 |
| Cycle 17, Unit IV | 0.98575 | 0.97325 | 0.99473 |

Remaining work

There is no remaining work scheduled for 2015, although the investigations are planned to be continued using the results of the statistical version of KARATE code system.

Related publications

- [1] Gy. Hegyi, G. Hordósy, Cs. Maráczky, I. Panka: *Using HZP states for the validation of burnup credit calculations, Part 1, MTA-EK-RAL-2015-976/M0*, in Hungarian (2015)

IMPLEMENTATION AND VALIDATION OF THE NEW ROD CONTROL AND REACTOR POWER CONTROL SYSTEM OF PAKS NPP USING THE FULL SCOPE SIMULATOR

József Páles, Tamás Fogd, Gergely Makai, Gábor Házi

Objective

In 2015 Paks NPP carried out a public procurement procedure for reconstruction of the instrumentation and control (I&C) of the rod control and the reactor power controller systems (RCS and RPCS). The purpose of the reconstruction was to improve the RCS and RPCS with respect to instrumentation and control to today's standards by applying modern methods and solutions and by ensuring that the safety and reliability criteria related to the planned extension of the nuclear plant's lifetime (expected length of extension: 20 years) are met. SKODA JS was awarded by end user in the procurement procedure and MTA EK as a subcontractor to SKODA JS took part in the project by focusing on the simulator related activities. In particular, MTA EK was responsible for the implementation and integration of the simulator models of the new control systems to the full-scope training simulator of Paks NPP. Beside the implementation of the new models, we also supported the verification and validation procedure of the new systems, including their human-machine interface by performing tests (together with the staff of Paks NPP) on the simulator to demonstrate the vitality of the new system.

Methods

In the full-scope simulator of Paks NPP most controller models are implemented by the graphic modelling system GRASS developed by our Institute in the late 90's. However, some specific systems, including the original RCS and RPCS are still modeled by Fortran codes developed in the late 80's. The new I&C systems are modern digital ones, therefore new models were also implemented in the GRASS modelling environment. The implementation of models were carried out in four phases. First, the logic schemes of the new RCS and RPCS provided by SKODA JS were implemented and tested in SIMTONIA (SIMulation TOols for Nuclear Industrial Applications), which is a new, modern graphics simulator development platform of MTA EK. Since SIMTONIA is able to export its logic schemes in the format of GRASS, the offline tested logic schemes were exported into GRASS in the second step. In the next phase, the new models were coupled with other models of our full-scope simulator and the factory acceptance tests (FAT) were carried out using our touch-screen based virtual control room interface. After successful FAT, the new models have also been integrated into the simulator of Paks NPP and the controllers have been validated using the new user interface of the real control room (implemented by MVM OVIT) in the framework of site acceptance tests (SAT).

Results

The new RPCS models have been validated by a sequence of tests including: tests of operation modes (manual, automatic: N, T, SZ), transients (change of power, turbine trip, main circulation pump trip), interactions with the reactor protection and turbine control system and malfunctions. Considering the new RCS, the validation focused on operation modes (single rod and group movement), behavior of the new system during scram and malfunctions. Fig. 1 shows our touch-screen based virtual control room in action during the validation phase of the project. The application of the virtual control room interface in the SAT phase proved to be very useful, since almost all functions of the new systems could be tested in our Institute.

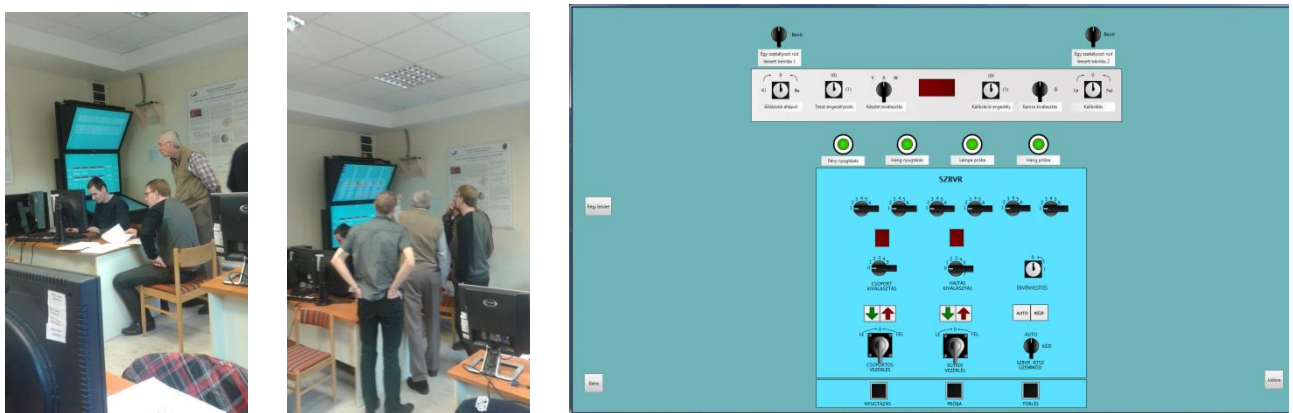


Figure 1: Touch-screen based control room in action - working together with the experts of SKODA JS and Paks NPP

Remaining work

Both FAT and SAT were performed successfully in the end of 2015. There is no remaining work.

Related publication

- [1] J. Páles: *SZBVR-RTSZ reconstruction, implementation of the new system in the simulator (in Hungarian)*, EK-RMSZL-2015-970-01/01, in Hungarian (2015)

VERONA 7.0 THE NEW CORE MONITORING SYSTEMS OF PAKS NPP

Gábor Házi, Csaba Horváth, Gergely Makai, József Páles

Objective

In 2012, Paks NPP decided to change its operational practice extending the fuel cycles from 12 to 15 months using new type of fuel assemblies. Some preliminary calculations revealed that the amount of on-line core monitoring calculations increases has significantly due to this change. It is also turned out that the increasing amount of computational work cannot be managed by the old hardware and software platforms of the on-line core monitoring system VERONA 6.2, while keeping the same high level availability of the system as before. Since the development tools of VERONA became also obsolete in the last decade, the management decided to initiate an overall reconstruction of the system. In 2014, Paks NPP carried out a public procurement procedure for the reconstruction of the VERONA and MTA EK, the winner of the tender, started to work on the reconstruction at the end of 2014.

Methods

The required major developments in the new system can be briefly summarized as follows:

- application of a new generation of proven hardware solutions (DELL PowerEdge R730 servers and thin clients), software platform (Windows Server 2012 R2), and software development tools (Visual Studio 2014, Embarcadero XE7, Visual Fortran Composer XE 2013),
- intensive application of VMware virtualization technology,
- extension and acceleration of reactor physics calculations using Graphics Processing Units (GPU),
- replacement of the Intellution's iFIX based process monitoring system by SIMTONIA based data displaying.

Results

Software and hardware developments had been carried out at the end of 2014 and the final touch was done in June of 2015. The factory acceptance tests (FAT) of the new system were started in the summer of 2015 in our Institute. During FAT, the new version of the system (VERONA 7.0) working together with the full-scope simulator (VERONA-s) was validated first. It was followed by the FAT of the so-called VERONA test system (VERONA-t) and the system of the 3rd reactor unit (VERONA-3). After successful FAT, VERONA-s and VERONA-t were installed in September in Paks NPP, site acceptance tests (SAT) were carried out successfully and one month trial period was started with the new systems. The new system was installed in the 3rd reactor unit in November during the regular one-month maintenance period of the unit. The system has been in operation since then. Fig. 1 shows the main screen of the new system implemented by using SIMTONIA.

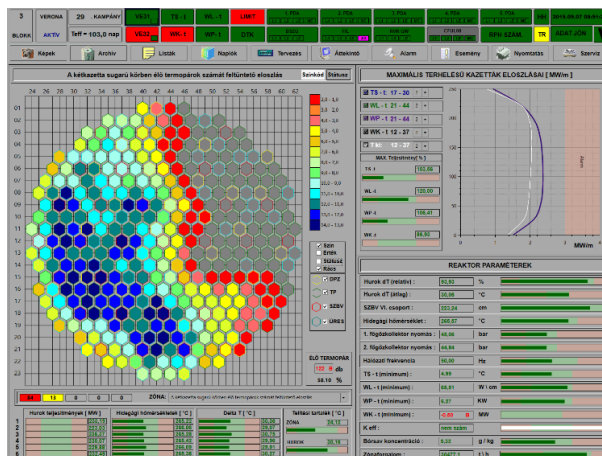


Figure 1: Main screen of VERONA 7.0

Remaining work

The new system has to be installed in the 1st, 2nd and 4th reactor units in 2016, during the regular maintenance period of the units.

Related publication

- [1] G. Házi, J. Páles, I. Pós, Z. Kálya, T. Parkó, Cs. Horváth, G. Makai, Á. Vécsi, M. Ignits, T. Fejes: A GPU accelerated nuclear reactor core monitoring system in virtual machines, submitted to Advances in Engineering Software

IMPROVEMENT OF THE RESISTANCE OF THE ENVIRONMENTAL AND RADIATION MONITORING SYSTEM OF PAKS NPP AGAINST EARTHQUAKES AND STATION BLACK OUT

Gábor Házi, Tamás Pázmándi, Sándor Deme

Objective

After the events in Fukushima Daiichi NPP, resistance of NPPs against station blackout and earthquake was in the focus of the stress tests performed all over the world. In line with this fact, the Hungarian authority decided to request revision of the capabilities of resistance of systems, which play role in the prevention or mitigation of the consequences of accidents, against these two key events. The revision included the investigation of the environmental and radiation monitoring system (ERMS) of Paks NPP. Although a reconstruction and reinforcement of ERMS against power loss and earthquake was accomplished in 2004, taking into account its central role in severe accident management, a decision was made to further improve the capabilities of this system. Paks NPP asked MTA EK to prepare a Technical Description for the development of ERMS, specifying all actions needed to assure the availability of the key components of ERMS after a design basis earthquake and power loss for 72 hours.

Methods

Based on the design base criteria and the maintenance experience gathered in the last decade, all components of ERMS have been systematically revised and several activities were identified as particularly relevant to achieve the desired availability of the system.

Results

The following major conclusions were drawn during the preparation of the Technical Description:

- Additional gamma dose power (BITT sensor) and air flowrate (EGE sensor) meters have to be installed (in earthquake and power loss resistant way) in the channel of chimneys.
- The software of the propagation calculation of released radioactive materials has to be renewed (to apply e.g. the measurements of the new severe accident measurements system).
- The present data acquisition systems of the environmental stations have to be replaced by Programming Logic Based (PLC) solution and they have to be unified in each station.
- The capacity of the present storage batteries have to be increased roughly with a factor of three (the original design base criterion requested 24 hours availability).
- The present UHF radios of the environmental stations and the radios of the two base stations have to be replaced using a new, integrated radio-modem type solution.
- An autonomous data acquisition computer has to be installed (in earthquake and power loss resistant way). This computer has to gather all information needed for propagation calculation from the environmental stations by UHF and send the measurement and calculated results to the Technical Support Center via microwave.
- In the "A" type environmental stations (9 stations, roughly 3km far away from the plant), the present organ iodide detector and spectrum analyzer have to be replaced with a new combined detector, which has temperature stabilization.
- The three "V" type stations (which measures the activity of inlet and outlet water of the NPP) have to be reinstalled into earthquake proof containers.
- The "U" type stations (18 BITT sensors in the area of the plant) have to be supplemented with UHF communication (beside the present RS232 communication channels).

Remaining work

There is no remaining work.

Related publication

- [1] G. Házi, S. Deme, T. Pázmándi, J. Jánosy, T. Benis, E. Korcsmáros, K. Varga, P. Káposztás: *Reconstruction of the environmental and radiation monitoring system – Technical Description*, EK-RMSZL-2015-981-01/01, 000000I02105-KFA, in Hungarian (2016)

PILOT PROJECT FOR THE RECONSTRUCTION OF TWO NEUTRON MONITORING SYSTEMS AT PAKS NPP

Gábor Házi, Zoltán Dezső, Sándor Kiss, Sándor Lipcsei, Tamás Parkó, István Pós

Objective

The Reactivity Monitoring System (RMR, Hungarian acronym) and the Refuelling Neutron Monitoring System (ÁNER, Hungarian acronym) of Paks NPP are aged and need to be reconstructed. Since both systems are based on neutron flux measurements, the new system is to be served by the same detectors and measurement instrumentation. Additionally, a full-range system is required, i.e. the detectors and the connected instrumentation should span the full range of neutron flux measurements from 0% to 100% reactor power.

Methods

In order to span the full neutron flux range, the Photonis CFUL08 detector was chosen. The same type is used by the Reactor Protection System (RVR, Hungarian acronym), but the conversion unit could not handle the current mode of the detector. Therefore a new electronic interface had to be developed for the full neutron flux range. The new interface works with all three modes of the detector: impulse, Campbell (AC) and current (DC) mode. First a prototype was built, verified and calibrated at the BME (Budapest University of Technology and Economics) Training Reactor. Then a pilot system was installed at Unit 2 of Paks NPP. Based on the measurements, the interface was further refined and the final verifying measurements were performed at Unit 3.

Results

RMR-Pilot was used to make parallel measurements with the current RMR system during the start-up period of a fuel cycle. It was found that the measurements with the new and the old system agree well (see Fig. 1).

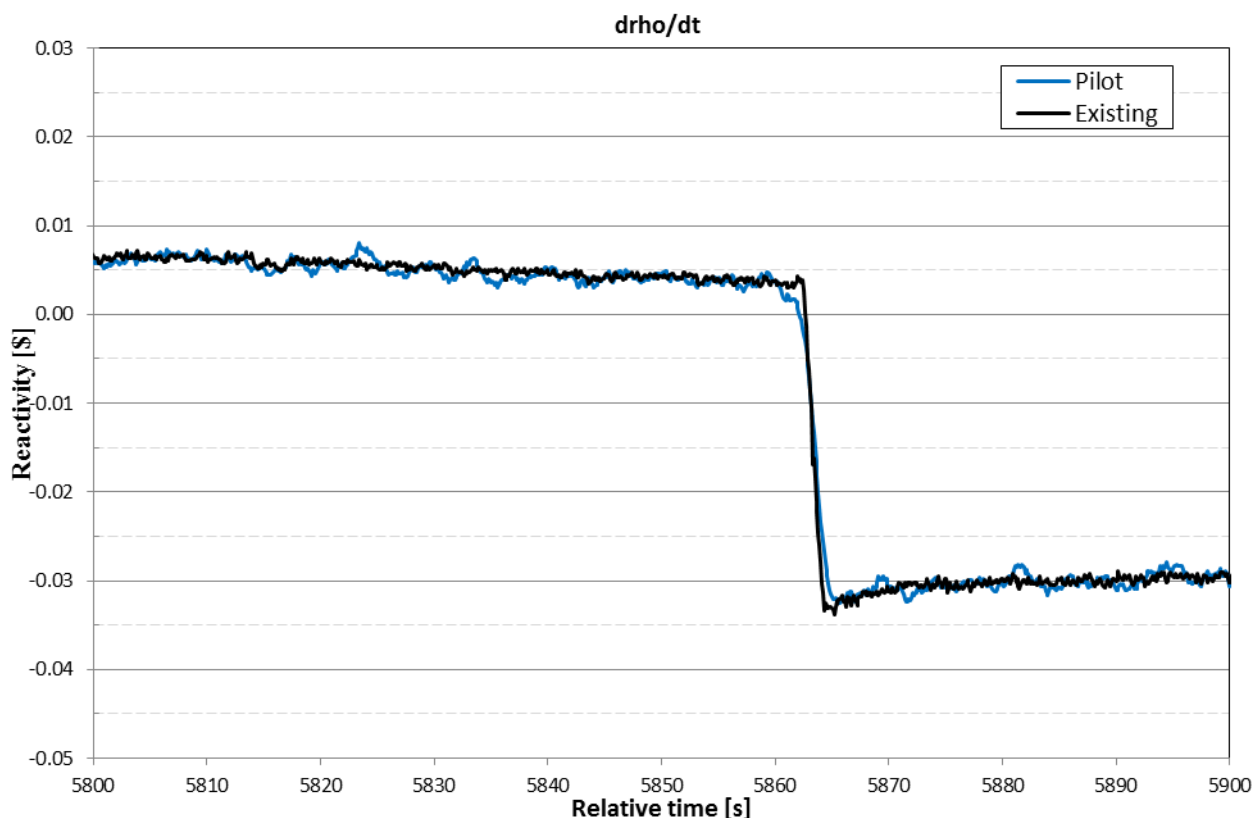


Figure 1: Reactivity calculated from the measurements with the existing and with the pilot system

Remaining work

Based on the experiences with the pilot system, a new RMR-ÁNER system will probably be built.

REACTOR NOISE DIAGNOSTICS MEASUREMENTS AND MAINTENANCE OF THE PAZAR MEASUREMENT SYSTEM AT PAKS NPP

Sándor Kiss, Zoltán Dezső, Károly Krinics, József Láz, Sándor Lipcsei

Objective

Regular reactor noise diagnostics measurements have been performed at Paks NPP (Nuclear Power Plant) since 2000. They were also continued in the present year, and the maintenance of the measurement system PAZAR (Paks Autonomous Noise Data Acquisition System, Hungarian acronym) was also carried out. PAZAR systems are fed with analogous signal sets of the VERONA systems (VERONA is a Core monitoring System for VVER type NPPs). Main part of our activity is monitoring the distribution of the coolant velocity in the core, and monitoring of vibration of the core internals.

Methods

Monitoring is performed using SPND (Self Powered Neutron Detector) chains installed in 36 fuel assemblies of the core.

Regular measurements were performed monthly. Long term (1 day to 2 weeks) measurements were also carried out, usually two times per month. All measurements were taken to the Centre for Energy Research for further processing. The evaluation of recorded data was performed off-line by means of PAZAR-K (evaluation software for the measurements acquired by PAZAR). Beyond the statistical evaluation of the regularly measured noise signals, a large subset of the detector signals was continuously monitored for transients.

Cooling units of the measurement system PAZAR were renewed and additional electrical power supply units were obtained for the system.

Results

Noise data archive was extended with the measurements of the present year.

According to the evaluated data, the average core coolant velocity was quite stable during the year, only usual small fluctuations could be observed at all four reactor units. As an example, the average coolant velocity of Paks NPP, Unit 2 is shown in Fig. 1.

The possible vibrations of core internals were also investigated, but no such anomalies were observed in 2015. Reports were compiled for the plant from all measurements.

Files with transient events were collected and classified by events.

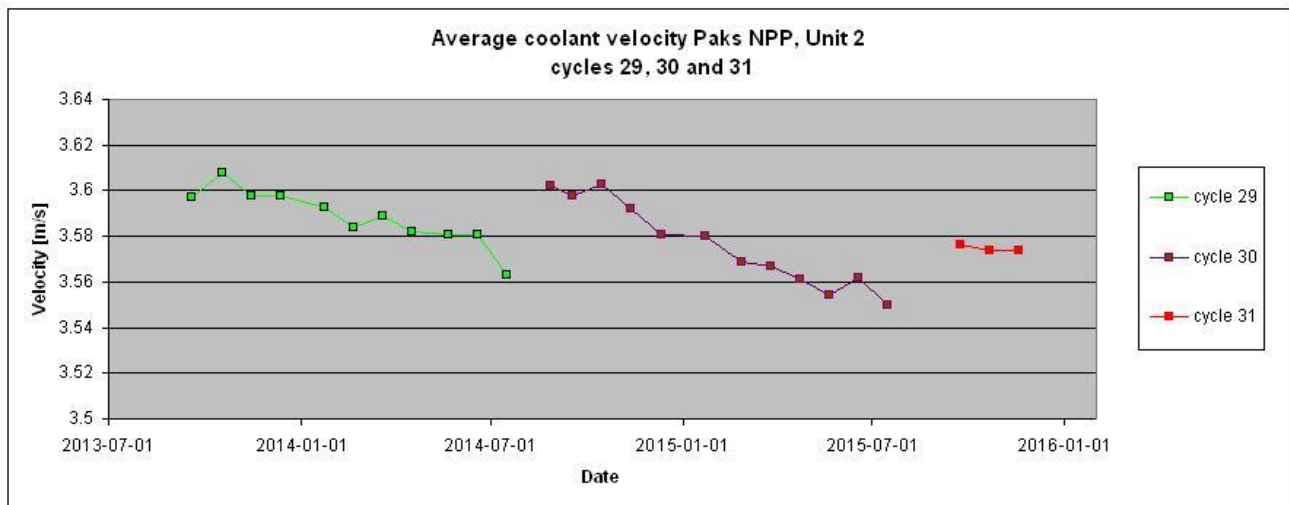


Figure 1: Average coolant velocity Paks NPP, Unit 2

Remaining work

Regular noise diagnostic measurements and collection of transient events will be continued in 2016.

ANALYSIS OF PROPAGATING TEMPERATURE PERTURBATIONS IN THE PRIMARY CIRCUIT OF PWRs

Sándor Kiss, Sándor Lipcsei

Objective

Neutron noise induced by temperature perturbations circulating in the primary circuit of PWRs (Pressurized Water Reactors) can be used to measure the velocity of the coolant passing through the reactor core or even to provide an estimation of the MTC (Moderator Temperature Coefficient of the reactivity). Temperature perturbations arising in the primary circuit and travelling with the coolant pass through the reactor core before disappearing due to the significant attenuation effect of the steam generators. Consequently, perturbations passing through the core are fed back with a time delay according to the circulation period of the coolant. The present paper aims at investigating these fluctuations.

Methods

Temperature perturbations circulating with the primary coolant as well as their ratio and feedback properties are investigated using noise data measured at nominal power of a VVER-440 reactor. An average, one-loop model is introduced to improve the through-core correlation between the inlet and outlet temperature measurements. The sources, frequency dependence and life cycle of the perturbations are determined using a kind of spectrum decomposition method. The investigation is based on the analyses of APSD and CPSD (Auto and Cross Power Spectral Density, respectively) functions between the temperature noise measured in the hot and cold legs of the primary circuit as well as at the core outlet.

Results

It was found that at nominal power the RMS (Root Mean Square) ratio of the hot and cold leg temperature noise is nearly constant during a fuel cycle. Similarly, the shape of the APSDs does not change.

There are two main sources of the temperature perturbations: the steam generator and the reactor. The ratio of the perturbations coming from the different sources changes along the primary circuit. The ratios of the components are shown along the loop at a specific frequency like in Fig. 1 at 0.1 Hz. In the reactor vessel there are two main sources of the perturbation: the reactor core and the upper plenum. Perturbations arising in the reactor core are typically under 0.25 Hz, while higher frequency components mainly originate from the upper plenum.

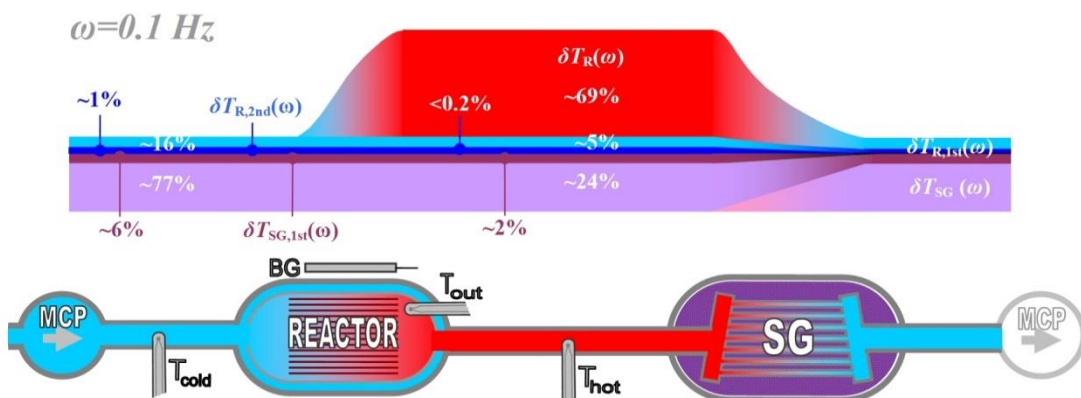


Figure 1: Relative magnitudes of temperature fluctuations arising and circulating in the primary circuit at 0.1 Hz (MCP: Main Circulating Pump, SG: Steam Generator, BG: compensation cable used as Background Detector)

The feedback through the circulation of the primary coolant was found to be about 8%, consequently it cannot be neglected: in spite of the strong attenuation effect of the steam generators on the temperature noise, at least one round of coolant circulation has to be considered.

Remaining work

The paper shows that the feedback effect caused by the propagating temperature perturbations in the primary circuit of a PWR is not negligible; therefore it may influence the interpretation of standard reactor noise diagnostics measurements. This effect can be investigated in a following work.

Related publications

- [1] S. Kiss, S. Lipcsei: Analysis of Propagating Temperature Perturbations in the Primary Circuit of PWRs, Annals of Nuclear Energy 85, 1167-1174 (2015)

DEVELOPMENT OF INTERACTION TECHNIQUES FOR A VIRTUAL CONTROL ROOM

B. Katalin Szabó

Objective

In an earlier project, we have created a 3D virtual model of the control room of the Paks Nuclear Power Plant. This control room model, which runs in the Blender Game Engine, has been integrated with our full-scope simulator. Conventional devices (keyboard, mouse), game controller and touchscreen have been used for input.

Our current project aims at using novel, touchless interaction devices to operate the virtual control room, in order to create an experience as "real" as possible for the operators/trainees who use the simulator (but do not have a physical replica of the real control room). They should be able to move within the virtual control room and operate the switches and pushbuttons. For this, it is necessary to display a 3D representation of the user's hand. This hand model should mimic the behaviour of the user's hand as well as possible, and it should be able to interact with the 3D models of the switches and pushbuttons.

The objectives for 2015 were:

- Finish the integration of the Leap Motion hand motion sensor device into the virtual control room model
- Work out the interaction of the 3D hand model with the simulated switches and buttons in the virtual control room
- Develop the hand model further
- Integrate the Kinect motion sensor device into the virtual control room model

Methods

The data provided by the Leap Motion sensor drive a simple hand model which is an armature in the Blender Game Engine.

Results

The Leap Motion device has been fully integrated. We have found that its use is quite computer-intensive, and, that it is reasonably accurate and thus usable for our purposes.

We have worked out a simple gesture recognition method with which we are able to determine whether a twisting movement of the hand (when interacting with a switch device) is clockwise or counter-clockwise.

Our simple armature model of the human hand is capable of following the movements of the user's hand. The main bones of the fingers are represented in the model. (The dimensional accuracy is not complete yet, and, for the time being, the bones are visualized with simple cuboids.)



Figure 1: Leap Motion device, hand, hand model



Figure 2: The hand model approaching a pushbutton.
The integration of the Kinect device is underway.

Remaining work

Finish the integration of the Kinect device. Optimize the use of computer resources.

Make a more realistic-looking 3D hand model.

Make a demo setup in which navigation within the control room is possible with at least one motion sensor device.

Try out (and, if possible, integrate) a head-mounted display (preferably Oculus Rift, when the commercial version becomes available).

SAFEGUARDS MEASUREMENTS AT PAKS NPP

István Almási, Zoltán Hlavathy, András Kocsonya, Péter Völgyesi, Gergely Dósa

Objective

- The aim was to verify the enrichment of freshly arrived fuel assemblies using a routine method developed earlier, before they are loaded into the reactor core.
- IAEA and EURATOM expect the Nuclear Power Plants to be able to verify their nuclear material's inventory. For additional verification we provide an independent series of measurement with the Spent Fuel Attribute Tester (SFAT) developed earlier.

Methods

Fresh fuel measurements were carried out in the fresh fuel storage at Paks NPP by a 95 cm³ HPGe (high purity germanium) detector (for the outer fuel pins of the assembly), placed on the detector holder rack at the half-height of the assembly, and by a 20 mm³ CZT (Cadmium-Zinc-Telluride) detector (for the inner pins), placed into the assembly's central hole. Enrichment verification relied on the measurement of the 186 keV energy gamma-rays of U-235, as compared to reference assemblies of 1.6 and 2.4% enrichment. The expected intensity ratio at 186 keV between the homogenous and profilised (from 3.8% nominal enrichment the fuel assemblies contain pins with different enrichment – the outer pins have lower enrichment) assemblies were determined by Monte Carlo calculation.

The SFAT is comprised of a 500 mm³ CZT detector with a lead shielding and a closed tube hanging below the detector unit using the water of the cooling pond as collimator. When the bottom of that tube approaches a standing fuel assembly only that particular assembly will be measured. As the activities of the fission products overwhelm those of fuel materials only the radiation of the formers can be detected. The 662 keV energy ¹³⁷Cs peak was detected from the irradiated fuel with 1 - 15 years cooling time, whereas ¹³⁴Cs peaks (605, 795 keV) were detected from 1- 5 years cooling time assemblies.

Results

Fresh fuel measurements

Recently we had to check profilised fresh fuel assemblies with nominal enrichment of 4.7 %. The calculated apparent enrichment for the inner and outer pins was 4.95 and 4.35 %, resp., determined by Monte Carlo (MCNP5) simulation. The measurements resulted in values of 4.91 ± 0.04 and 4.35 ± 0.006 %, resp. Three fuel assemblies of 4.2 % nominal enrichment were measured for comparison.

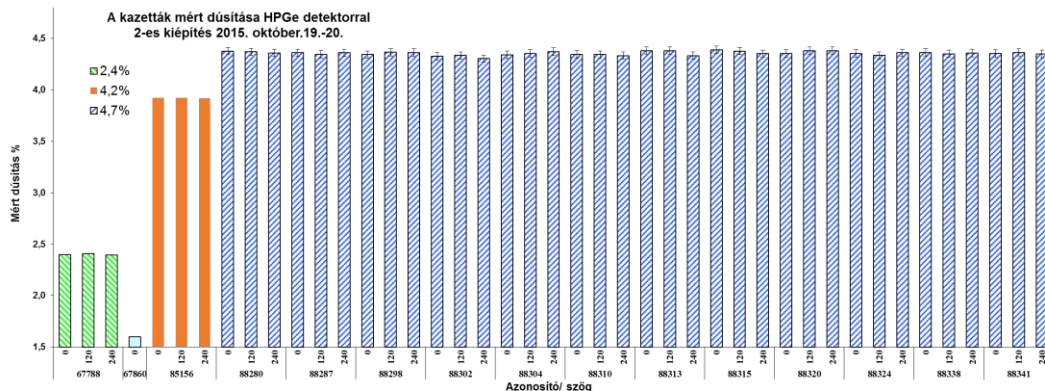


Figure 1: Measured enrichment of fuel assemblies for outer pins measured by HPGe

The ratio and intensities of Cs peaks are characteristic to the burnup and cooling time of the spent fuel assemblies. If these values agree well with usual values, the verification is acceptable. Co-60 peaks could be observed as well.

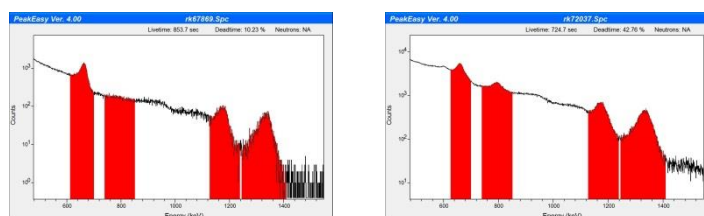


Figure 2-3 Spectra taken with CZT 500 detector after 4 and 10 years cooling time, resp.

Remaining work

The work will continue according to the terms of the contract.

ANALYSIS OF CORROSION PARTICLES ORIGINATED FROM THE PRIMARY AND SECONDARY COOLING SYSTEM OF PAKS NPP

Éva Kovács-Széles

Objective

Between Centre for Energy Research and Paks Nuclear Power Plant (NPP) there is a research contract which specifies analysis of corrosion particles originated from the primary and secondary cooling systems of the reactors to detect the origin or source of corrosion. For determination of the nature of these particles (size, morphology, activity, elemental composition, etc.), several different techniques are used.

Methods

In this work numerous parameters of particle samples originated from the block No. 1 from stopping and starting period were determined using different analytical techniques: morphology by optical microscopy (OM) and scanning electron microscopy (SEM), activity by gamma-spectrometry, ^{63}Ni and ^{55}Fe content by liquid scintillation technique, corrosion products (Fe, Co, Ni, Cr, Zr, Ag) by inductively coupled plasma mass spectrometry (ICP-MS), calculation of the specific activity and the residence time of the particles in the reactor zone, analysis of the filtered particles and also the filtrates.

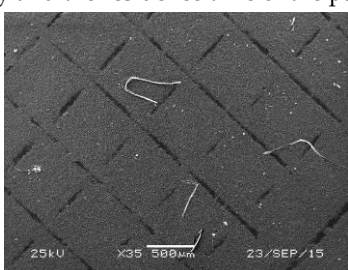


Figure 1: Particles from organic materials and fibres

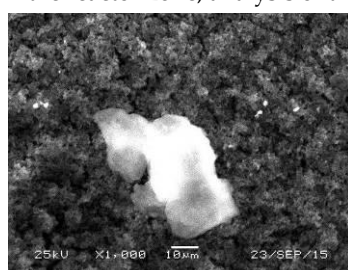


Figure 2: Iron-oxide particle

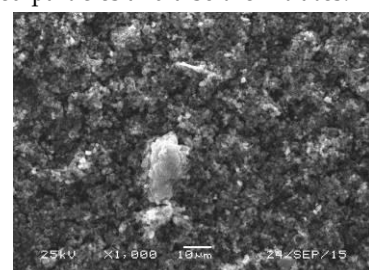


Figure 3: Zr-containing particle

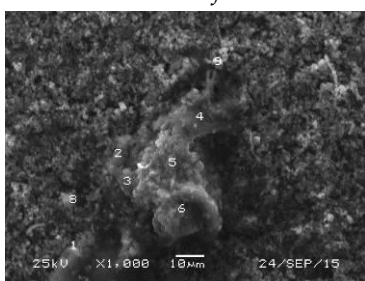


Figure 4: Silicate-containing particle

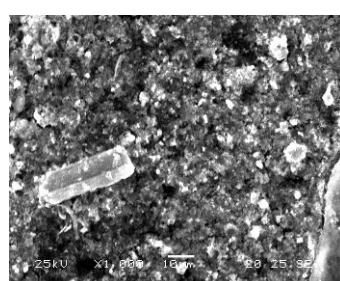


Figure 5: High iron content particle

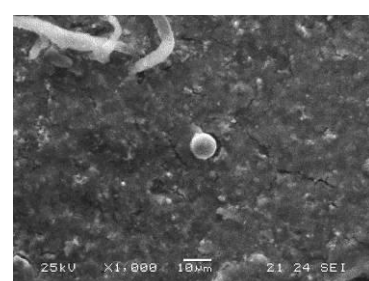


Figure 6: Round particle, probably a particle of ion-exchange resin

Results

During this work several particles originated from the primary and secondary cooling system of Paks NPP (block No. 1) were investigated. Some pictures taken by SEM can be seen in Fig. 1 and Fig. 2.

The investigated samples contained more silicate particles and in all of the samples Fe-oxides were also found. Main components of the samples were: Fe, Cr, Fe-Cr-Ni-oxides. Zr was found in samples originated at the stop period of the reactor. The second element which can be found in the highest concentration is the Mn. Ni and Mn can be found in the solved fraction, Fe is dominant in the colloid phase. Amount of Cr and Ag is significantly less in the samples. Following the speciation analysis: ^{51}Cr , ^{59}Fe and ^{95}Zr can be found in particles, Mn-54 in the solved phase, ^{58}Co , ^{60}Co and $^{110\text{m}}\text{Ag}$ in different chemical forms.

Determination of residence time by using the specific activity of the shorter half-life isotopes ($^{60}\text{Co}/\text{Co}$, $^{55}\text{Fe}/\text{Fe}$ and $^{54}\text{Mn}/\text{Fe}$) seems shorter than 50 days.

Remaining work

This work was a part of an ongoing research project for Paks Nuclear Power Plant, therefore the analysis of the particles is continuing in the future.

Related publication

- [1] É. Kovács-Széles: *Analysis of corrosion particles originated from primary and secondary system of NPP*, research report for Paks Zrt., EK-SBL-2015-766-02 (2015)

MEASUREMENT OF SPENT FUEL ASSEMBLIES FROM THE PAKS NUCLEAR POWER PLANT

Péter Völgyesi, István Almási, Zoltán Hlavathy, András Kocsonya, László Lakosi

Objective

The application of High Resolution Gamma-ray Spectrometric (HRGS) analysis to spent fuel is a useful tool to optimize fuel operation, to detect possible burnup anomalies, verify burnup calculations and to support nuclear inventory (Safeguards). This non-destructive method can also be applied to characterize the assemblies used in longer (1.5 year) burnup campaigns. In our previous burnup studies, where the $^{134}\text{Cs}/^{137}\text{Cs}$ ratio was used, a 2% measurement uncertainty was achieved. The main objective of our present study was to further decrease the uncertainty with longer measurements and to develop an independent method which can determine the cooling time of the assemblies based on the other nuclides in the measured spectra.

Methods

The measurements were carried out at Paks Nuclear Power Plant using a 45 cm³ HPGe detector placed behind a collimator built into the concrete wall of the service pit. The spent fuel assemblies were transported to the measurement position and moved up and down as well as rotated under water in front of the collimator hole by the refueling machine. Assemblies of 3.82% and 4.2% enrichment cooled for 0.9, 1.9, and 2.9 y were measured at 3 or 4 positions along their length for 1200 s on 3 to 5 of their 6 sides. Nine assemblies were analysed which were classified into 3 groups (3 each) based on their burnup and cooling times. One extra assembly with different burnup and cooling time was also studied. Gamma rays of ^{134}Cs and ^{137}Cs were registered. Their activity ratio reflects well the burnup, taking into account their irradiation history and decay times. Activity ratios were determined using the main gamma lines of ^{134}Cs (605 keV and 796 keV) and the 662 keV line of ^{137}Cs by the intrinsic calibration method. In order to get a spectrum with better statistics, 81 measurements were added together to give a sum spectrum, from which the presence of other fission products were identified in the assembly.

Results

The same three sides (in hexagonal symmetry) of assemblies in the different groups were compared (Figure 1) to determine the Cs-ratios. One group showed differences in burnup, whereas the other two groups did not. The representativeness can be deduced from the standard deviations in the ratio for each side, which varied between 0.7% and 1.4%. For the ^{137}Cs alone the standard deviations varied between 3.3% and 4.3%. Based on these results it can be concluded that the Cs-ratios showed less uncertainty than the values calculated from ^{137}Cs only, so they are less sensitive to the measurement geometry [1]. The sum spectrum indicated the presence of ^{154}Eu , ^{95}Zr , ^{95}Nb , ^{110}mAg , ^{144}Ce , ^{106}Ru which can potentially be used to determine cooling times and plutonium amount [1].

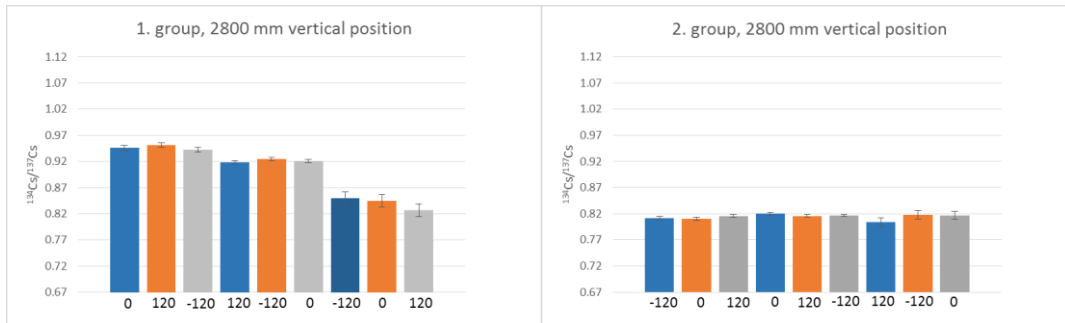


Figure 1: The $^{134}\text{Cs}/^{137}\text{Cs}$ ratios of two groups (1st and 2nd group) at 2800 mm vertical coordinate measured in different angular orientations. The assemblies were taken from different sectors of the reactor in equivalent positions. They were rotated to 0, 120, -120 degrees, or their cyclic permutations, in order to compare the same sides relative to the reactor core. One colour indicates one assembly.

Remaining work

A wide range of assemblies with different cooling time and burnup should be analysed to verify the method developed to determine independently the cooling times and the plutonium amount. The central nodes (central area) of the assemblies represent the most information due to the relatively constant burnup of this area. The relation between the uncertainties of burnup and Cs-ratio should be assayed under different operation parameters and cooling times. Further experiments are necessary to reduce the uncertainty of the measurements as well as to improve the calculations.

Related publication

- [1] P. Völgyesi, I. Almási, A. Kocsonya and Z. Hlavathy: *Burnup measurement of nuclear assemblies*, OAH MMT report, OAH-ABA-12/15-M in Hungarian (2015)

ASSESSMENT OF THE SOURCES OF METEOROLOGICAL DATA FOR THE PAKS NPP SITE

Lilla Hoffmann, Tamás Pázmándi, Péter Szántó

Objective

In order to perform atmospheric dispersion calculations, meteorological data are needed. For the Paks NPP site several sources of weather data are available. Measurements are made at the meteorological tower and a SODAR (both situated on the site) and at a meteorological measuring station near the site operated by the Hungarian Meteorological Service (OMSZ). Weather prediction data calculated using the ALADIN code by the OMSZ are also available.

The aim of this project was to compare these sources of weather data with respect to their applicability for atmospheric dispersion modelling.

Methods

The radiological effects of an accidental release from a nuclear facility can be estimated by dispersion modelling codes. These codes use the source term, weather data and various other (e.g. environmental, site and habitual) parameters as input, calculate the dispersion of the activity in the environment, and based on that, estimate the dose consequences of the release. During the modelling of the dispersion, the dry and wet deposition as well as the radioactive decay and progeny should also be considered.

In the case of an atmospheric radioactive release the main sources of the dose burden are

- cloudshine (external dose caused by contents of the radioactive plume),
- groundshine (external dose caused by the radioactive material deposited on the ground),
- inhalation (internal dose caused by the inhalation of the contents of the radioactive plume), and
- ingestion (internal dose caused by the ingestion of food produced in the area affected by the plume).

The main weather parameters of the atmospheric dispersion models are the wind speed, the wind direction, the precipitation and the stability parameter (e.g. Pasquill categorization, Monin-Obukhov length).

In order to compare the meteorological data obtained from the available data sources, one-month-long datasets of the above mentioned parameters were assessed during July of 2015. To assess the effect of the differences in the weather parameters on the estimated doses, sensibility analyses were performed using the SINAC program.

The SINAC program system (developed in the EK) is used to model the spread and deposition of radioactive material emitted into the atmosphere in the case of a potential accident at a nuclear power plant.

Results

The time resolution of the data measured by the SODAR and the meteorological tower is 10 minutes, while that of the data measured by the OMSZ station is 1 hour. The OMSZ station data are not available on-line, and therefore they cannot be used for on-line calculations in emergency situations.

The correlation between wind speed and wind direction data provided by the SODAR and the meteorological tower is good regarding dispersion modelling. The correlation of the measured precipitation data was also sufficient, although the assessed time period was extremely dry.

The parameters used for calculating the Pasquill categories were also assessed. The availability of the fluctuation of the wind direction was sufficient in the case of the meteorological tower. The availability of the fluctuation of the wind direction obtained with the SODAR was significantly lower, especially the datasets for 50 m and 120 m height over the ground. The OMSZ station and the prediction data did not contain parameters capable of being used for calculating Pasquill categories.

In summary the meteorological tower proved to be the most reliable data source. If the tower's data are not available, the SODAR can be used as a secondary data source. The OMSZ station and the ALADIN data do not contain information about the atmospheric stability; therefore they alone cannot be used to perform atmospheric dispersion calculations.

Remaining work

The assessment will be performed again with a one-year time period in order to obtain results for a wider variety of weather situations.

EXPERIMENTAL INVESTIGATION OF THE EFFICIENCY OF EXTERNAL COOLING IN THE CERES FACILITY

György Ézsöl, Gábor Baranyai, Valér Gottlasz, Attila Guba

Objective

A research program has been going on at the Centre for Energy Research to give scientific support to the in-vessel corium retention in the Paks NPP. Ninths series of experiments had been performed for highly influenced by the flooding tube geometry at the sump model and different power distributions on external vessel surface. This report, however, focuses on the effectiveness of cooling flow rate by significantly fluctuating in forward or backward direction and the axial heat flux distribution obtained from ASTEC code calculations. It was experienced in the former experiments that effectiveness is decreasing by increasing the coolant temperature up to saturation, changing the flow pattern in the critical gap region and the amount of backward flow rate was not enough to increase the coolant mass.

Methods

The measurements have been performed in the CERES facility, which is a scaled-down model of the external reactor vessel cooling, intended to apply in the Paks NPP, with 1:40 scaling ratio for the vessel external surface and 1:1 for the elevations, giving the driving force for natural circulation. To obtain coolant conditions relevant to the objective, the power to the elliptic bottom part of the vessel was 48 kW obtained from ASTEC, with hot critical gap size of 9,7 mm and the minimum diameter of the flooding sump model outlet was Ø 44.7 mm.

Results

As a result of these measurement conditions, the coolant enters the critical gap region of cooling channel at saturated circumstances.

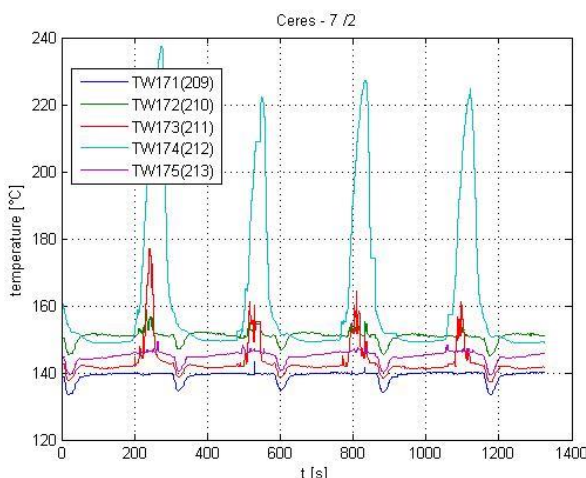


Figure 1: External surface temperatures

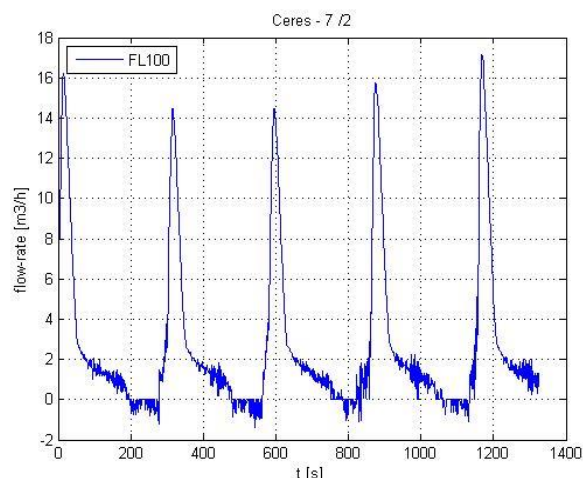


Figure 2: Flooding flow rate

Figures show wall temperatures at the elevation of lower part of critical gap and the flooding rate in the facility. Elevation of wall temperatures TW 171 and TW 172 is at the level of 1500 mm from the bottom. As shown, there is a stable cooling of vessel wall with a maximum value of 511 K and the backward flow rate was about 1 m³/h. Consequently, in spite of the decreasing of flooding flow rate being highly influenced by the flooding tube geometry at the sump model, the wall cooling is effective and it is not limited by the heat flux in the bottom part of the vessel in real heat flux ranges.

Remaining work

The CERES tests supplied important data for code validation; the findings were incorporated to the ASTEC calculation. The work has been finished.

Related publication

- [1] Gy. Ézsöl, G. Baranyai, V. Gottlasz: *Experimental investigation of the efficiency of external cooling in the CERES Facility*. Research Report EK-THL-2015-932/02/M0, in Hungarian (2015)

SILVER MEASUREMENT IN PRIMARY WATER, CHEMICALS AND STRUCTURAL MATERIALS

Zsolt Kerner, Éva Kovács-Széles, Nóra Vajda

Objective

Presence of trace quantities of silver in the primary water loop of a pressurized water reactor can produce radioactive ^{110m}Ag contamination which contributes to the collective dose of the personnel. ^{110m}Ag activity concentration is easily measurable. It is typically monitored in the plants. On the other hand, chemical measurement of the silver traces in a concentrated boric acid solution (like the primary coolant) is requiring some complex procedure. However, systematic measurement of silver is necessary to identify the source and understand the transport process.

In this work a novel method of chemical measurement of silver based on separation on CL resin and High Resolution Inductively Coupled Plasma Mass Spectrometry (HR-ICP-MS) technic is described. Silver concentration in primary water during the transients was measured. Silver content of structural materials of primary circuit and chemicals fed to the water was also determined.

Methods

Silver is measurable with high sensitivity ($\text{DL} \approx 1 \text{ pg/L}$) by HR-ICP-MS technique. It requires samples with low salt concentration (< 0,1 %) and low acidity, e.g. 0.1 M nitric acid. Chemical separation is necessary for silver measurement from primary water. TrisKem International® CL resin is known for fixing silver ions selectively and quantitatively from 1 M H_2SO_4 . We have found high distribution ratios in nitric and hydrofluoric acid solutions. Complete elution of silver is not possible, so the extractant has to be eluted and digested by hot 14 M HNO_3 . Yield of the process – determined by gamma spectrometry – was > 90%. Possible interfering elements (Pd, Au, Pt) are typically not contained in plant samples.

Silver can be analyzed in primary water, structural materials, chemicals, deionized water, swipe samples and spent ion exchange resin also after appropriate pretreatment based on this method.

Results

Silver concentration and ^{110m}Ag activity concentration are changing in different way during the start-up of the reactor (Fig. 1). Nuclear grade chemicals (boric acid, potassium hydroxide and hydrazine) containing silver are present in negligible quantity. The silver content of main structural materials of the VVER reactors (08H18N10T type stainless steel and Zr-Nb alloys) is 150-200 ppb. Considering the low corrosion rate of these materials, only a few milligram silver can be realized to the whole primary circuit in a year.

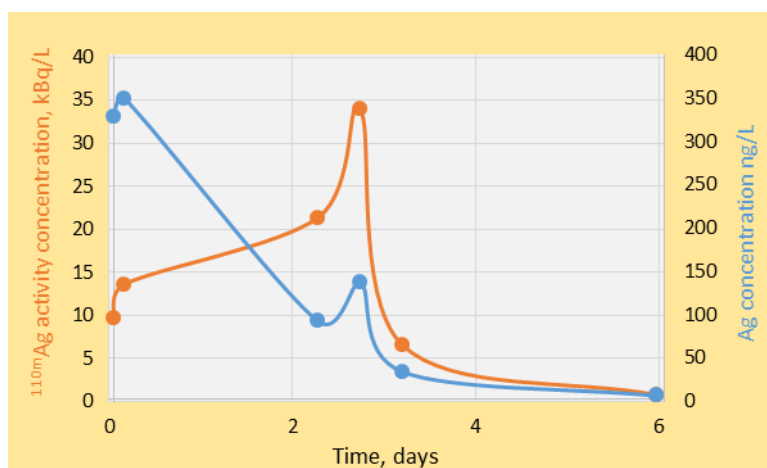


Figure 1: Silver concentration and activity concentration during the start-up of the reactor

Remaining work

Further measurement of silver content in the primary water during transients and determining the quantity of the silver stored on the surfaces of the primary circuit are planned.

Related publication

- [1] Zs. Kerner, É. Kovács-Széles, N. Vajda: *Silver measurements in primary water*, International Conference on Radioanalytical and Nuclear Chemistry, Abstract No. 446, Budapest (2016)

KINETIC MEASUREMENT OF CONTAMINANTS ACCUMULATION ON STAINLESS STEEL SURFACE AT HIGH TEMPERATURE

Zsolt Kerner, István Almási, András Kocsonya

Objective

On the surfaces of a nuclear reactor and its cooling system some corrosion products and other contaminants can be accumulated from the water phase and can dissolve or come off in the form of particles. For the description of the transport processes of contaminants which take place in the primary loop it is necessary to understand the elementary steps of them and to determine the rate's dependence on the circumstances (e.g. temperature, pH, concentration). In this work a novel experimental setup was designed and built for following the quantity of the accumulated contaminant on a stainless steel surface in a flowing system at temperature up to 300 °C.

Methods

Solution containing a radiotracered contaminant (e.g. ^{110m}Ag) was pressed to a steel capillary by a high pressure pump (Shimadzu LC-20AD). A 1 m long section of the capillary was coiled up in a copper block heated up electrically. The pressure in the capillary was kept constant by a back pressure regulator (EQUILIBAR EB1HP1). The accumulation process was followed by gamma spectrometry: the activity of the contaminant in the capillary was continuously measured using a High Purity Germanium (HPGE) detector, ORTEC digiDART analyzer and GammaVision software. The setup was built from commercial parts (Fig. 1).

pH dependence of the silver accumulation from boric acid solution was determined at 300 °C. Silver concentration in the solution was 2.5 mg/L. After approximately one week, base solution was added to detect the dissolution of the silver.



Figure 1: Photo on the experimental setup

Results

Measured data are shown in Fig. 2. The accumulation process is much faster at pH=7 than in acidic solution. The dissolution is also faster at higher pH.

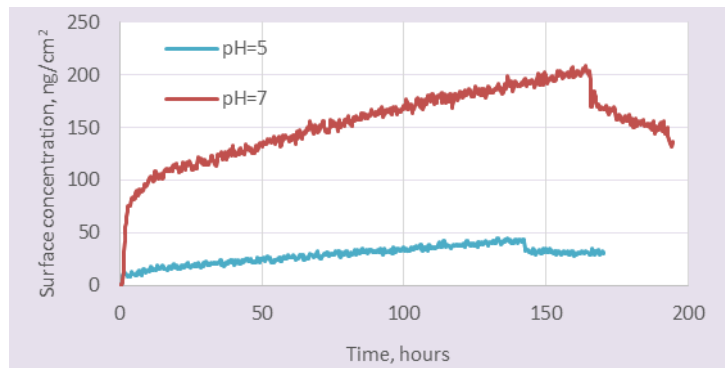


Figure 2: Silver concentration on the surface of the stainless steel capillary

Remaining work

The constructed setup can be used to measure the kinetics of accumulation of corrosion and fission products, examining temperature transients and optimizing decontamination techniques. Determining of silver accumulation kinetics at different temperature and concentrations is planned for the next period of time.

IN-SITU GAMMA-SPECTROMETRY AT BLOCK 2 OF PAKS NPP

András Kocsonya, Péter Völgyesi, István Almási, Zoltán Hlavathy

Objective

In-situ gamma-spectrometry is applied to characterise the activated corrosion products deposited to the inner surfaces of main facilities of primary loop of Paks NPP. These measurements support the monitoring the corrosion processes in the primary loop, and help to plan and reduce the collective dose of maintenances. Besides the corrosion products, the applied technique is suitable to detect several fission products as well, which are indicators of assembly leakage.

Methods

The measurement points were designated by the NPP. In case of pipes, 4 points were analysed on each of six loops. In case of steam-generator, 16 points were measured along the side of the outer surface of the device. Although the measurement on the ion-exchanger was originally requested by the NPP, due to the change of the resin before the date of measurements this device was not measured, according to the modified request of the NPP.

The method of measurement was almost identical to those developed in the previous year. A Canberra GLP2020 HPGe planar detector was applied for the primary loop pipes, while an Ortec SGD GEM 3615 coaxial HPGe detector with built-in tungsten shielding was applied for the steam-generator measurements. Spectra were collected by an ORTEC "Digidart" multichannel analyser controlled by a laptop PC. The applied collimators and supports were designed and manufactured in the Institute. The diameter of the collimators can be decreased by inserts. Typical measurement times were 15-20 minutes/point in case of pipes, while ~1 hours at the steam generator. A background spectrum was recorded at each measurement point by inserting a plug into the collimator. Spectra were evaluated by the GammaVision and FitzPeaks codes. Surface activity concentrations were calculated by an own-developed spreadsheet table.

The detectors were calibrated for all applied measurement geometries by ^{137}Cs and ^{152}Eu point-like sources in the Laboratory. Gamma-dose rates were measured by a Rotem TELEPOLE WR 4-0027-30 telescope.

Results

The dominant radionuclides are ^{58}Co and ^{60}Co . Besides these nuclides ^{51}Cr , ^{54}Mn , ^{59}Fe , ^{65}Zn , $^{110\text{m}}\text{Ag}$, and ^{124}Sb were detected. As a fission product, only ^{134}Cs was detected.

The measured activity concentrations were compared to the results of previous years. Activity of ^{124}Sb shows significant increment at several measurement points. The activity of certain nuclides is not homogenous comparing the loops. $^{110\text{m}}\text{Ag}$ activity is definitely higher at loop 1. The origin of the detected discrepancies is discussed together with the chemists of the NPP. The most contaminated point of the pipes is the point 2 (incoming "warm" pipe, between the valve and steam-generator) of loop 4, where the majority of activity is originated from ^{58}Co and ^{60}Co . The increment is reflected in the yearly change of activities (Fig 1). In case of the steam-generator, the activity concentrations are rather uniformly distributed. The dose rate is definitely decreasing at the medium section, due to the wall thickness (13.5 cm/7.5 cm, Figure 2).

Contrary to the previous year, all designated points could be measured, since no inaccessible points were found.

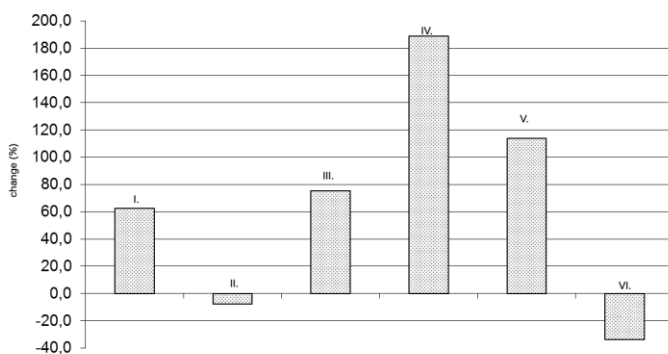


Figure 1: Change of surface activity concentrations compared to the previous year.

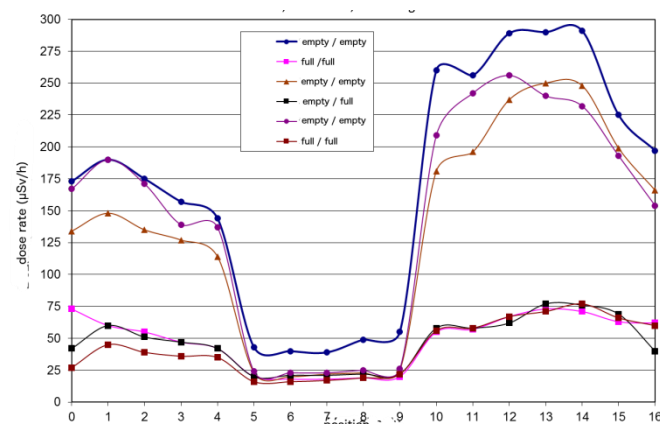
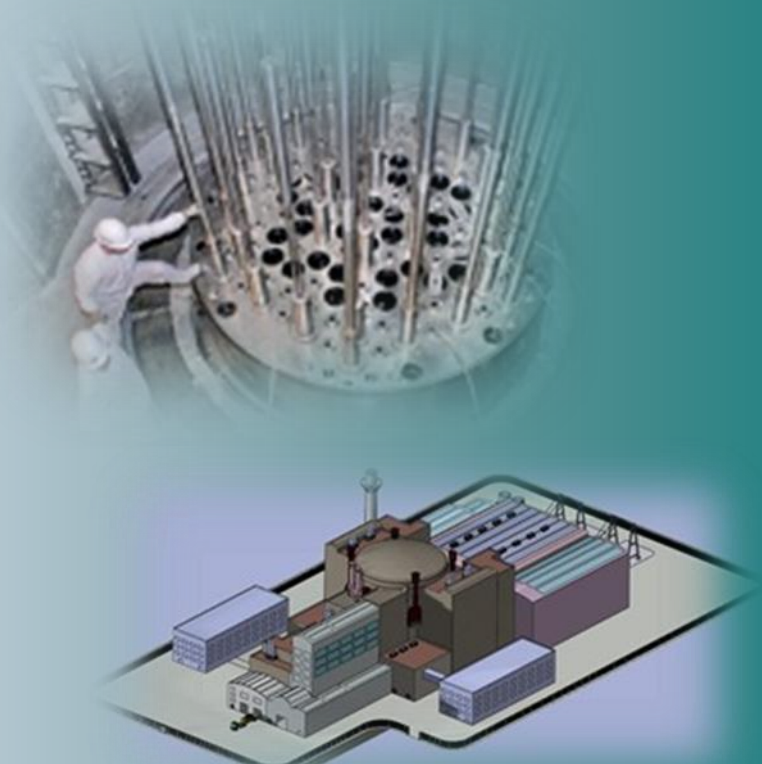


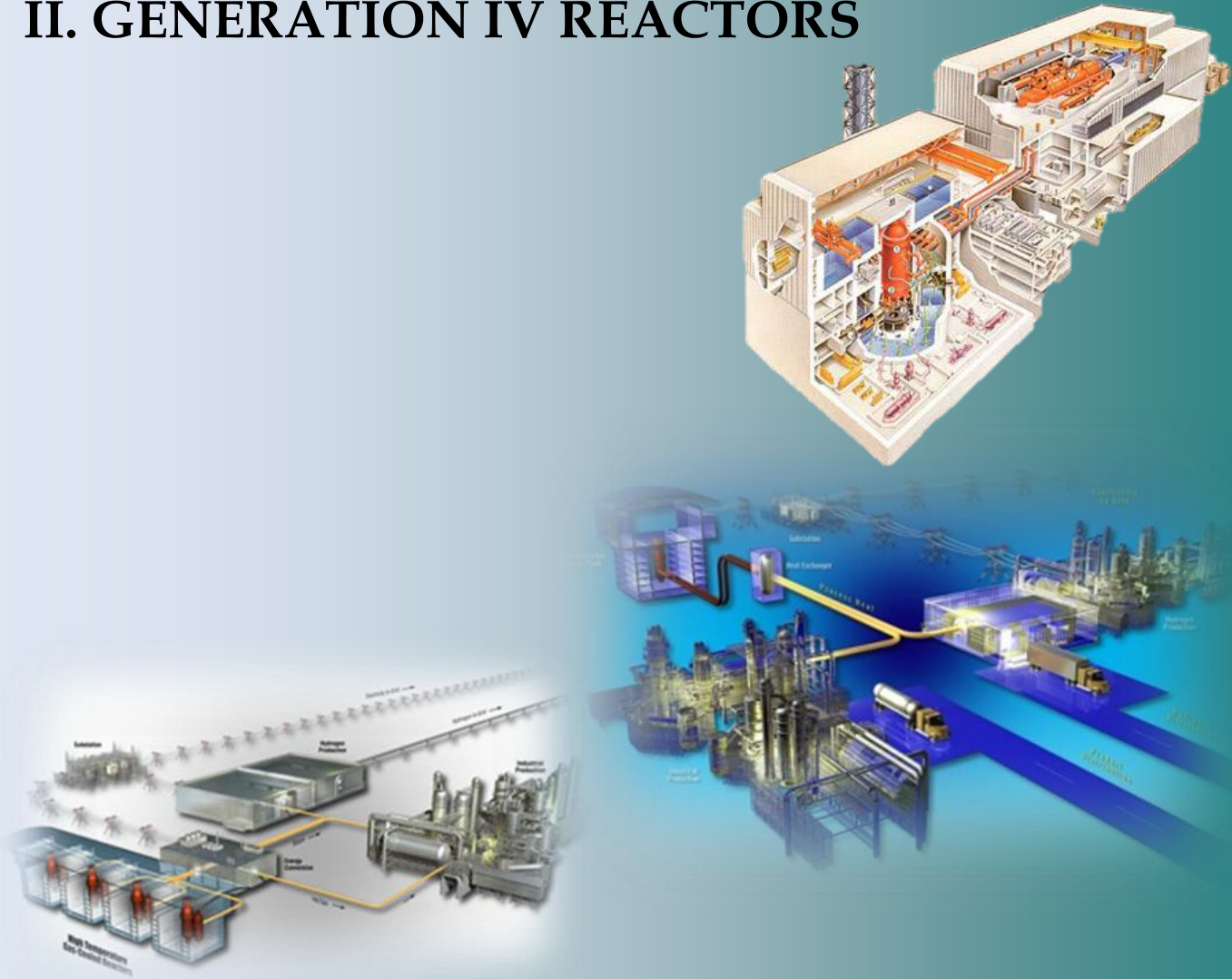
Figure 2: Dose rates on surface of the steam-generator.

Remaining work

Since Paks NPP converts to using 15 month operation cycle, in the future only 3 maintenance periods are scheduled per year. According to the agreement between the University of Debrecen and MTA EK, the in-situ gamma-spectrometry analysis of corrosion products in the primary loop main facilities remains at the University. However, analyses of other primary loop devices are required by the NPP. The measurement experiences can be applied to those future tasks. Special focus will be devoted to analysis of $^{110\text{m}}\text{Ag}$, the origin of which is unknown.



II. GENERATION IV REACTORS



THE ALLEGRO PROJECT

János Gadó

Objective

Corresponding to the European initiative on launching research in the field of Generation IV nuclear reactors, the nuclear research institutes of the Visegrad 4 countries and the French CEA started a co-operation on the development of the Gas Cooled Fast Reactor demonstration reactor ALLEGRO in 2010. The final objective of the co-operation is to build up and operate this reactor but the construction has to be preceded by a long period of research and development related to various technological issues and the design of the reactor has to be prepared in several steps. ALLEGRO can start operation not earlier than in 2030.

Methods

The ALLEGRO Project Preparatory Phase was launched by the consortium of the nuclear research institutes of the Visegrad 4 countries (V4G4) in 2015. In the preparatory phase of the ALLEGRO Project (2015-2025), the conceptual design will be elaborated and the necessary research-development-qualification tasks will be executed. During the design of ALLEGRO the usual design methods will be applied. By 2018, a pre-conceptual design will be elaborated using the existing CEA 2009 Design with the necessary additions and modifications. Design additions and modifications are motivated by the safety concerns related to the CEA 2009 Design. After 2018 the conceptual design will be elaborated (by 2025) which will be the basis of submitting the construction license application. Elaboration of the detailed design, construction, commissioning and operation will be a task of a new consortium.

Results

In order to begin the design of ALLEGRO, a Design and Safety Roadmap was created [1]. This Roadmap gives the technical specification of 47 tasks, including leader and participating organizations, deadlines and costs (in man-months). The execution of the various tasks was started in the framework on national programs, like the Hungarian National Nuclear Research Program.

The safety of the reactor is of primary importance. A book chapter was prepared [2] on the safety issues and concerns. Reports on the safety requirements and objectives and on the connections between design and safety are almost finalized.

Remaining work

As it was mentioned above, even the Preparatory Phase of the ALLEGRO Project requires efforts for several years. The Hungarian contributions (to be provided by MTA EK, NUBIKI and BME NTI) cover several aspects of design and safety.

Related publications

- [1] B. Hatala, P. Dařilek, R. Zajac, L. Belovský, P. Vacha, P. Hajek, K. Rózicky, A. Przybyszewska, J. Gadó, A. Keresztúri, Z. Hózer, I. Tóth, G. Mayer and A. Vasile: *ALLEGRO Design and Safety Roadmap*, V4G4-001 (2015)
- [2] J. Gadó: *Safety of the European Gas Cooled Fast Reactor*, in Safety of Generation IV reactors, IAEA publication in print, Edited by E. Corniani

IMPROVING THE PHYSICAL MODEL OF THE FUEL CYCLE SIMULATION CODE SITON

Áron Brolly

Objective

In the past years a fuel cycle simulation code called SITON (SImulationTOol for modelling the Nuclear fuel cycle) has been developed in our Research Centre. This year the following improvements were envisaged: extending number of tracked nuclides; reactors operating with different types of fuels; fuels having different parts with different discharge burn-up and composition. The first improvement allows calculation of activity, decay heating and radiotoxic inventory in the facilities and also enables modelling of thorium-based fuel cycles. The second and third improvements refine the physical model and ease usage of the code, while they prepare the basis for more sophisticated reactor models.

Methods

For the first improvement all fission product nuclides having atomic number between 60 and 170 and half life greater than 30 days were collected. This first compilation was filtered by examining the fission product yield of each fission product for several possible fissile nuclides. After that, decay chains of the filtered nuclides were established and condensed, i.e. data (like activity, decay heating) of short-lived decay daughters were merged into that of their long-lived parents. Concerning actinides, virtually all of them were taken into account except the short-lived ones. Selection criteria for the decay daughters of actinides included high branching ratio besides reasonable half life as well. Having compiled new actinide nuclides, their decay chains were also condensed using the same principles as for the fission products. For the second improvement taking into account of reactor cycles is necessary. Identification of the different fuel types loaded into the reactor in one cycle is also necessary. This calls for a new element in the physical mode which describes the cycle of the reactor. Furthermore, some parameters stored in the current model in the fuel type, like effective full power days and number of cycles the fuel spends in the core, have to be moved into this new cycle element. For the third improvement the current hierarchy of nuclide - material - fuel - package was revised. The planning phase, used to survey events in the fuel cycle, was also revised.

Results

For the first improvement a flexible and general solver was implemented using the rational Chebyshev approximation. The internal calculation time step for the method was tuned to the half lives of the new set of nuclides. In order to be able to integrate the new solver into the current implementation of SITON, a new interface layer was also created. Tests of the new solver showed that the calculation time of the new solver heavily depends on the implementation: FORTRAN 77 versus Fortran 90. For the second improvement key points to be changed in the physical model and in its implementation have been identified. It was found that the package ID, used to identify material travelling through the front-end plants, has to be extended to take into account the different fuel types in one batch. For the third improvement it turned out that it interferes with the second improvement. It was found that the package ID has to be further extended in order to take into account different parts of the fuel having different discharge compositions. It was also found that the current nuclide - material - fuel - package hierarchy has to be completely rebuilt and re-implemented. The reason for this is that Fortran 95, the programming language of the current implementation, does not support natively object-oriented concepts. This lack in the current implementation was overcome by extra coding emulating these features, however this solution will not be sufficient for the new layer hierarchy.

Remaining work

For the first improvement decreasing or optimisation of the calculation time is needed. This is a key point to be able to use the solver for evaluating long-term impact of fuel cycle waste within the code. For the second and third improvement complete reimplementation of the corresponding parts of the model is needed.

Related publication

- [1] Á. Brollya, M. Halász, M. Szieberth, L. Nagy, S. Fehér: *Physical model of the nuclear fuel cycle simulation code SITON*, Annals of Nuclear Energy **99**, 471–483 (2017)

THE ALLIANCE PROJECT---PREPARATION FOR ALLEGRO - IMPLEMENTING ADVANCED NUCLEAR IN CENTRAL EUROPE

Ákos Horváth

Objective

Nuclear reactors with a fast neutron spectrum (fast reactors) are to be developed and deployed in the future to make the use of nuclear energy sustainable by solving the closure of the fuel cycle. The Gas cooled Fast Reactor (GFR) has been selected as an alternative reactor type to the Sodium Fast Reactor which is to be tested as a prototype in the 2020s.

The ALLEGRO facility is intended to be a demonstration reactor hosting GFR technological experiments, but also as a test pad of using the high temperature coolant of the reactor for generating process heat for industrial applications. MTA EK has coordinated the EURATOM financed FP7 ALLIANCE project which was launched in 2012 with the aims

- to put together information on the feasibility of the construction, on the assessment of design needed following the GEN IV requirements and to produce documents on the preliminary design, environmental impact, site identification, consortium and licencing issues,
- to serve not only as a technical guide for future steps, but also to develop explanatory arguments for national and EU decision makers, whose political and financial support will be needed for further development of the GFR demonstrator.

Methods

Three nuclear research institutes of the Central European region (ÚJV, Řež, Czech Republic; MTA EK, Budapest, Hungary; and VÚJE, a.s., Trnava, Slovakia) agreed in 2010 to start a joint project aiming at the preparation of the basic documents in order to form the basis for a later decision on the construction and operation of the ALLEGRO gas cooled fast reactor in one of the countries. CEA, France has supported this effort in various ways, especially by transferring the documents of the earlier design efforts to the project participants. NCBJ, Świerk, Poland, joined the project in 2012, so now ALLEGRO is supported by all four Visegrad-4 (V4) countries.

Results

A new strategy for developing the ALLEGRO reactor was prepared, and accepted by the four Partners in 2015. The main components of this strategy are: (a) to reduce the ALLEGRO power from 75 MWth to 10 MWth and to find the optimum core configuration (switch from MOX to UO₂); (b) to optimize nitrogen injection (launch time, duration) and the backup pressure in guard containment; (c) to increase the main blowers inertia to avoid short term peak temperature for the LOCA+ blackout case and/or to develop a design with a gas turbine in the secondary side coupled to the primary blowers (this is the solution also advised for GFR).

The ALLEGRO consortium is represented by V4G4 Centre for Excellence, a legal entity registered in Slovakia. The main goal of V4G4 is to establish R&D facilities to investigate fuel development issues, helium technology related problems, issues related to structural materials and to construct a non-nuclear 1:1 mock-up of ALLEGRO. V4G4 is aimed at generating experimental results in the new facilities for developing the gas cooled fast reactor demonstrator ALLEGRO. If the financing can be ensured, experiments, system qualification and other preparatory works will by 2018 provide the governments of the V4 region a sound basis to decide on launching the design, licensing and construction of the ALLEGRO reactor, on selecting the site of the reactor and on financing and governance matters.

Remaining work

The ALLIANCE Project ended in 2015, after 36 months. The unfinished work on the development of ALLEGRO is continuing in the framework of V4G4, the EU VINCO project and other national programs.

DEVELOPMENT OF METHODOLOGY AND COMPUTER CODES FOR FAST SPECTRUM REACTOR CALCULATIONS

András Keresztúri, György Hegyi, István Pataki, Emese Temesvári, Ádám Tóta

Objective

Nuclear reactors with fast neutron spectrum (fast reactors) are to be developed to make the use of nuclear energy sustainable by carrying out the closure of the fuel cycle. This observation led to the decision in MTA EK to focus on developing tools and methodology necessary for the core design and transient analysis needs for two representative designs, namely the Sodium Fast Reactor types specified in an OECD NEA project and the gas cooled ALLEGRO demonstrator.

Methods

Code development and verification by taking part in international calculation exercises.

Results

- Participation in the cooperation organized by the OECD NEA aiming at determination of the methodological uncertainties of the neutronic core design calculations. Two reactor sizes of 3600 MW and 1000 MW and three fuel types, namely oxide, metal and carbide, were selected.
- The KIKO3DMG 3D nodal code was developed for the core design and dynamic transient analysis. The shape function calculation was improved by developing a new SP3 algorithm for the accurate treatment of flux and scattering anisotropy enhanced in the fast spectrum reactors.
- Coupling the KIKO3DMG code to the ATHLET3.0 thermal hydraulic code.
- Dynamic calculations of reactivity initiated accidents by using the coupled KIKO3DMG-ATHLET3.0 code.
- Evaluation of the uncertainties originating from the nuclear data. The results are shown in Table 1.

Table 1: Uncertainties of basic safety parameters of the Sodium Fast Reactor core design originating from the nuclear data

| | Effective multiplication factor | Effective delayed neutron fraction (%) | Control rod worth (\$) | Void effect | Void effect (\$) | Doppler effect (1/K) |
|-----------------|---------------------------------|--|------------------------|-------------|------------------|----------------------|
| Uncertainty (%) | 1.77 | 0.74 | 1.87 | 16.78 | 16.97 | 5.40 |

Remaining work

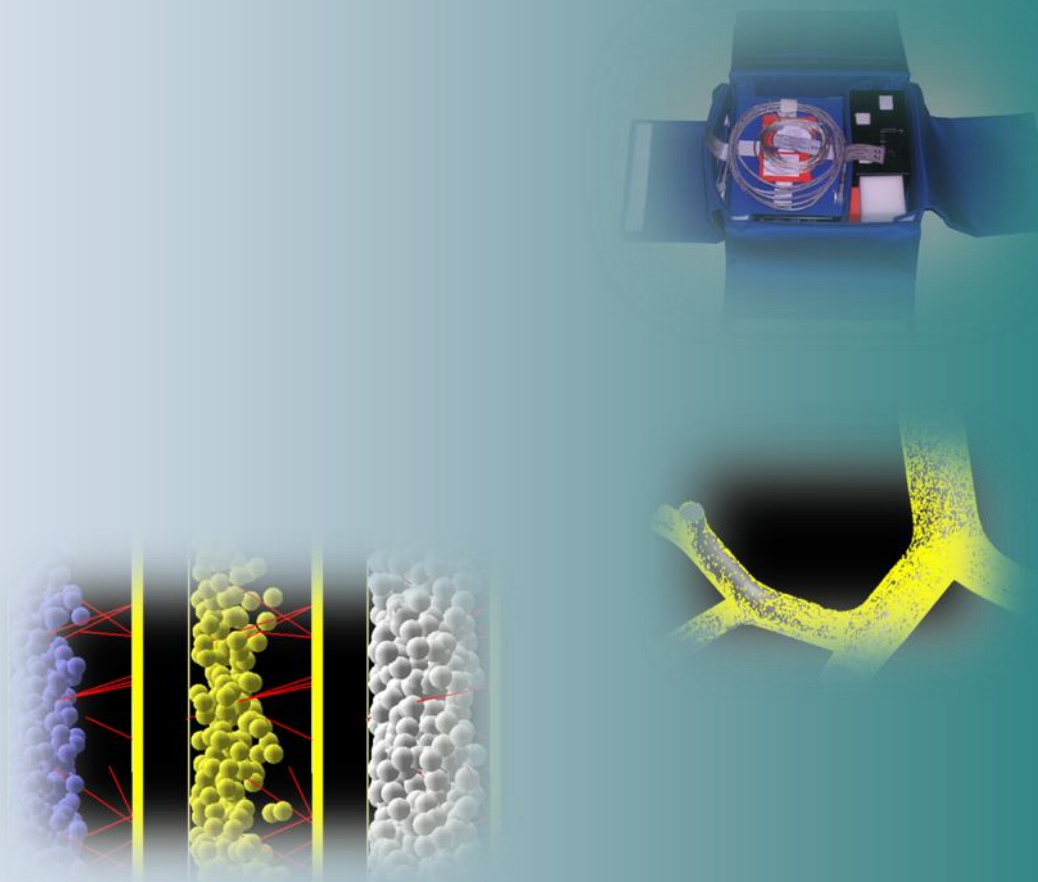
The project lasts more years.

Related publication

- [1] Gy. Hegyi, A. Keresztúri, I. Pataki, E. Temesvári, Á. Tóta: *Preparing activity for fast spectrum reactors calculations*, EK-RAL-2015-207-01/01, in Hungarian (2015)



III. HEALTH PHYSICS, SPACE DOSIMETRY



THE PILLE THERMOLUMINESCENT DOSIMETER SYSTEM ON BOARD THE INTERNATIONAL SPACE STATION

*István Apáthy, Sándor Deme, András Gerecs, Attila Hirn, Tamás Pázmándi, Péter Szántó,
Balázs Zábori*

Objective

Exposure of astronauts to ionizing radiation is a key risk factor in long-duration space flights. The Pille space-qualified thermoluminescent dosimeter (TLD) system developed by a predecessor of the MTA Centre for Energy Research (MTA KFKI AEKI) provides accurate and high resolution absorbed dose data. The Pille-ISS system launched in August 2003 to the Russian segment of the International Space Station (ISS) is operated in cooperation with the Institute for Biomedical Problems (IBMP) in Moscow in the frame of a bilateral contract. The objective of the Pille project is the evaluation and interpretation of on-board data, maintenance of the on-board system and the further development of the system.

Methods

TLDs are passive detectors that record the total absorbed dose from ionizing radiation over the course of the exposure. At readout, the TLD is heated while emitting visible light proportional to the dose, which is converted to an electrical quantity, amplified, measured and evaluated by a reader. Currently, Pille-ISS consists of 8 original dosimeters transported to the ISS in 2003, 4 dosimeters delivered in 2009 and a TLD reader. The dosimeters are located at different places in the ISS and read out monthly by the astronauts. Two of them are dedicated to extravehicular activities (EVAs) as well and the twelfth dosimeter is permanently inserted in the Pille reader and read out automatically every 90 minutes, providing high resolution dosimetry data. During coronal mass ejections of the Sun impacting also the Earth, certain dosimeters serve for individual monitoring of the astronauts with read-outs once or twice every day. For on-board sensitivity analysis, from time to time all Pille dosimeters are located on panel No. 327 for a while, and the quasi-homogeneous radiation field at that position is used as natural radiation source. The duration of the exposition is about two weeks. The correction factors for the individual dosimeters are then calculated from the results of the sensitivity measurements.

Although the Pille-ISS reader is fully operational and it performs correctly without any degradation or malfunctioning, its warranty has expired and the unit needs to be replaced.

Results

Manufacturing and assembling of the new Pille reader was finished.

In year 2015, approximately 6000 measurements were performed with the Pille-ISS system on board the ISS. The data obtained between May 2014 and March 2015 were evaluated, analysed, interpreted and presented at scientific conferences.

Interpretation of the data from the experiment investigating the shielding effect of a "protective curtain" using four Pille dosimeters was finished. Hygienic wipes and towels containing water were stored in the protective curtain located at the wall of the crew cabin providing an additional shielding thickness of about 8 g/cm^2 water-equivalent matter. The average shielding effect of the water filled protective curtain was found to be $24 \pm 9\%$, which is in good agreement with the results of measurements performed with other TLD systems as well as simulations performed by the international partners [1].

The development of a new type of Pille dosimeter with reduced shielding for EVAs was also continued.

Remaining work

Calibration, acceptance tests and delivery of the new Pille flight hardware is going to be performed in year 2016. Evaluation and interpretation of the measurement data produced by the on-board Pille-ISS system will continue.

Acknowledgement

The authors wish to acknowledge the precious help provided by the colleagues at IBMP and RSC Energia. Manufacturing and assembling of the new Pille reader and the five additional dosimeters are funded by the Ministry of National Development through contract No. IKF/375/2015-NFM_SZERZ).

Related publication

- [1] P. Szántó, I. Apáthy, S. Deme, A. Hirn, I. V. Nikolaev, T. Pázmándi, V. A. Shurshakov, R. V. Tolochek, and E.N. Yarmanova: *Onboard cross-calibration of the Pille-ISS Detector System and measurement of radiation shielding effect of the water filled protective curtain in the ISS crew cabin*, Radiation Measurements **82**, 59 (2015)

DUST, PLASMA AND MAGNETIC FIELD MEASUREMENTS ON COMET 67P/CHURYUMOV-GERASIMENKO

István Apáthy, Attila Hirn

Objective

Lander Philae of the European Space Agency's Rosetta mission, aimed at the in situ investigation of a comet nucleus for the first time in history, was deployed to the surface of the comet 67P/Churyumov-Gerasimenko (67P/C-G) on the 12th of November 2014 at a heliocentric distance of 2.99 AU. The objective of the complete Rosetta mission is to study the origin of comets and the relationship between cometary and interstellar material and its implications with regard to the origin of the Solar System. In year 2015, the evaluation and interpretation of the data collected during the Separation, Descent and Landing (SDL) and the First Science Sequence (FSS) phases of the lander mission by the instrument packages on board Philae was finished. Planning of the scientific program for the Long Term Science phase was also performed.

Methods

MTA EK was participating in two of the nine scientific experiments aboard the Lander. The first one, DIM (Dust Impact Monitor, see Fig. 1) is a part of the small instrument package SESAME (Surface Electrical, Seismic and Acoustic Monitoring Experiments) for determining the mechanical and electrical properties of the comet's surface; the second one, SPM (Simple Plasma Monitor) is a part of another small instrument package known as ROMAP (Rosetta Lander Magnetometer and Plasma Monitor) which complements the plasma packages on board the Rosetta Orbiter.

DIM employs 3x3 piezoelectric sensor segments made of PNZT7700 (Pb, Ni, Zr, Ti) and mounted on three faces of a cube to measure the flux of submillimetre- and millimetre-sized dust and ice particles emitted from the nucleus. From the signal properties measured by the associated electronics, the mass and the speed of the impacting particles can be calculated assuming given density and elastic material properties. The relation between the measured impact rates (N in s^{-1}) and the particle flux (Φ in $m^{-2}s^{-1}sr^{-1}$) in the measurement range of the sensor is given by $N = G\Phi$, where G is the geometric factor of the detector in m^2sr . The geometric factor of the DIM sensor was calculated assuming an isotropic ambient flux of the submillimetre- and millimetre-sized particles. For the measurement intervals when no particles were detected, the maximum true impact rate was calculated by assuming Poisson distribution of the impacts, and it was given as the detection limit at 95% confidence level. The shading by the comet environment at the final landing site Abydos was estimated by simulating the pattern of illumination on Philae and consequently the topography around the lander. Calculations were also performed with the Grain Impact Analyser and Dust Accumulator (GIADA) Performance Simulator (GIPSI) to simulate the expected fluxes on the DIM instrument during the descent of the lander. GIADA is an experiment on the Rosetta orbiter devoted to the measurements of the physical properties of cometary dust grains in orbit around the nucleus.

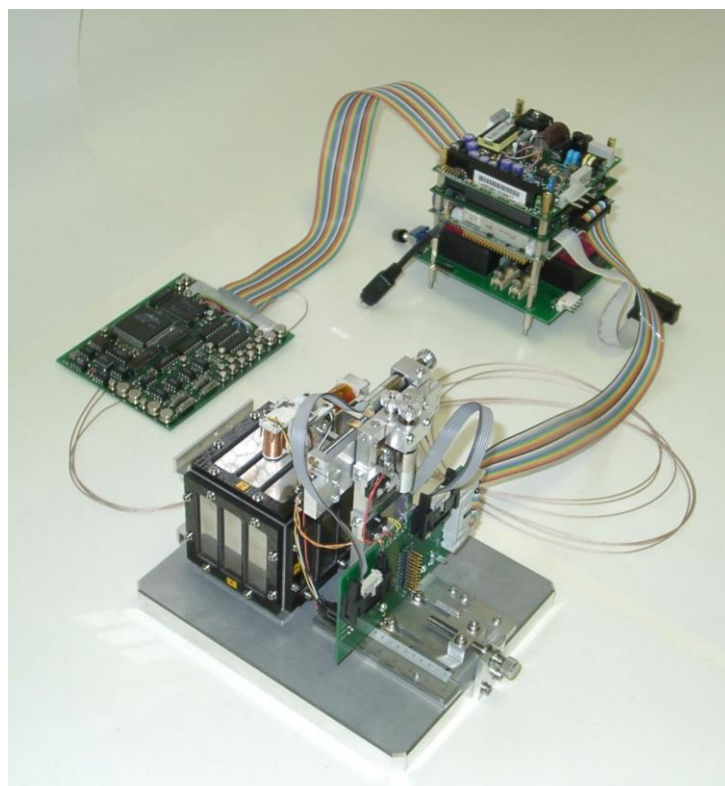


Figure 1: The DIM sensor and its ground support equipment used for calibrations on ground

The SPM sensor is a type of electrostatic, hemispherical E/Q analyser having 2 ion channels and 1 electron channel. It is mounted on the end of a short boom and it contains a Faraday cap as well. The energy range of the instrument is 0-12.6 keV for ions with a resolution of 3%, and 0-4.5 keV for electrons with a resolution of 10%; the field of view of the sensor is 140°x150° for ions and 8°x15° for electrons. It is able to determine the major solar wind parameters like density, speed, temperature, and flow direction. The scientific objective of the instrument is the characterisation of onset of the comet activity and the evolution of its interaction with the solar wind. The nature of this interaction is considered to depend on the solarwind activity as well as the location in the Solar System because the outgassing rate from a comet increases as it approaches its perihelion.

Both the orbiter and the lander are equipped with fluxgate magnetometer instruments. The magnetometer of the Rosetta Plasma Package, RPC-MAG serves as a solar wind monitor for the ROMAP magnetic measurements taken during descent, hopping and landing on the nucleus. The combined measurements on board the two spacecraft allow separation of the field of local sources from external field variations.

After completing the FSS phase, due to the low power on board, Philae entered into hibernation. As comet 67P/C-G got closer to the Sun, the illumination conditions improved significantly and the Lander woke up. Several attempts were made to establish stable radio contact between the lander and the orbiter and the scientific planning of a possible Long Term Science phase also continued. The operation plan was prepared based on the telemetry data received after the wake-up of the lander and the inputs provided by the lander instrument teams.

Results

DIM was operated before Philae's separation from Rosetta at altitudes between approximately 8 and 23 km from the nucleus surface. In this mission phase DIM was significantly obscured by structures of Rosetta, and no particles were detected. During Philae's descent to its nominal landing site Agilkia, DIM detected one approximately millimetre-sized particle at an altitude of 2.4 km. This is the closest ever detection at a cometary nucleus by a dedicated in situ dust detector. The material properties of the detected particle are compatible with a porous particle having a bulk density of approximately 250 kg/m³. At Philae's final landing site, Abydos, DIM detected no particle impacts. [2]

Based on measurements performed with DIM, we calculated the upper limit of the flux of particles in the measurement range of the instrument in the order of 10^{-8} - 10^{-7} m²s⁻¹sr⁻¹ during descent. An upper limit of the ambient flux of the submillimetre- and millimetre-sized dust and ice particles at Abydos was estimated to be 1.6×10^{-9} m²s⁻¹sr⁻¹ on the 13th and the 14th of November 2014. Considering particle speeds below escape velocity, the upper limit for the volume density of particles in the measurement range of DIM was constrained to 10^{12} - 10^{11} m⁻³. Results of the calculations performed with the GIPSI tool on the expected particle fluxes during the descent of Philae were compatible with the non-detection of compact particles by the DIM instrument. [3]

SPM was operated from the first touch-down during the complete FSS phase. From the first touch-down until the final landing Philae was permanently rotating which prevented it to measure the solar wind direction. After the final landing the SPM sensors were shadowed in the direction of the Sun. The Faraday cap provided measurement results which were very similar to the measurements of the RPC instrument of the Orbiter.

The magnetic field measurements obtained during the multiple landing of Philae demonstrate that 67P/C-G is unmagnetized. If comet 67P/C-G is representative of cometary nuclei, magnetic forces are unlikely to play a role in the accumulation of planetary building blocks on scales > 1 m, which is in the critical diameter range 10^{-1} to 10^2 m. [1]

Remaining work

The work on the project has been finished.

Acknowledgement

The Hungarian contribution to DIM and SPM was co-funded through PRODEX contracts and by the Government of Hungary through European Space Agency contracts No. 4000107211 and 4000107212 under the Plan for European Cooperating States (PECS).

Related publications

- [1] H.U. Auster, I. Apáthy, G. Berghofer, K. H. Fornacon, A. Remizov, C. Carr, C. Güttler, G. Haerendel, P. Heinisch, D. Hercik, M. Hilchenbach, E. Kührt, W. Magnes, U. Motschmann, I. Richter, C. T. Russell, A. Przyklenk, K. Schwingenschuh, H. Sierks and K. H. Glassmeier: *The Nonmagnetic Nucleus of Comet 67P/Churyumov-Gerasimenko*, *Science* **349**, 6247, aaa5102 (2015)
- [2] H. Krüger, K. J. Seidensticker, H.-H. Fischer, T. Albin, I. Apáthy, W. Arnold, A. Flandes, A. Hirn, M. Kobayashi, A. Loose, A. Péter and M. Podolak: *Dust Impact Monitor (SESAME-DIM) Measurements at Comet 67P/Churyumov-Gerasimenko*, *Astronomy and Astrophysics* **583**, A15 (2015)
- [3] A. Hirn, T. Albin, I. Apáthy, V. Della Corte, H.-H. Fischer, A. Flandes, A. Loose, A. Péter, K. J. Seidensticker and H. Krüger: *Dust Impact Monitor (SESAME-DIM) on board Rosetta/Philae: Millimetric particle flux at comet 67P/Churyumov-Gerasimenko*, *Astronomy and Astrophysics* **591**, A93 (2016)

MONITORING THE EFFECTS OF RADIOACTIVE RELEASES IN HUNGARY

Tamás Pázmándi, Péter Szántó, Péter Zagyvai

Objective

Our goal was to introduce the types, scopes and systems of measurements and evaluations which are suitable for monitoring normal and off-normal releases of nuclear and radiological facilities as well as for environmental occurrence and dispersion of such releases.

Methods

In the course of our work the array of required monitoring data and participating organizations were assessed and reviewed in order to obtain data in planned, existing and emergency exposure situations as defined in the recommendations of the International Commission on Radiation Protection (ICRP) Publication 103 for promoting the estimation of dose consequences of the general public in these situations. New publications of the International Atomic Energy Agency (IAEA) with new recommendations were elaborated and evaluated including safety standards, safety requirements, safety guides and technical reports and documents as well. Another series of items for review and evaluation work was focussed on the directives, regulations and recommendations of the European Union compiled in accordance with ICRP and IAEA concepts. The characteristics and features of the present radiation monitoring systems and networks of Hungary were reviewed.

Results

On the basis of consequences drawn from the review of the international and domestic situation of monitoring concepts and practices, recommendations were elaborated and presented in order to promote the improvement of the Hungarian radiation monitoring system toward a well-established, concerted structure with neither missing areas nor redundancies.

The structure of the system for the evaluation of the radiation situation was worked out. The system is capable of handling the measurement data obtained from the Hungarian radiation monitoring network. It is also capable of performing model calculations in order to give assumptions of the dose consequences of the release in the early phase, or to help to reassess the situation in the late phase of the emergency.

Remaining work

The next step of the work is to create a decision support system for monitoring the effects of radioactive releases based on the concept elaborated in the present project.

ACCEPTANCE CRITERIA FOR SAFETY ANALYSES: APPLICATION OF ATMOSPHERIC RELEASE CRITERIA

Barbara Brockhauser, Tamás Pázmándi, Péter Szántó, Péter Zagyvai

Objective

In order to eliminate uncertainties from the modelling of environmental transport it has been stated in the most recent years that emission criteria should be used for the limitation of environmental effects in the area around nuclear facilities. For this aim, introduction of the criteria should be investigated, methods suitable for the determination of the criteria for nuclear facilities should be analysed for design-basis accidents and beyond-design-basis-accidents, and conditions for the application in practice should be stated. The final goal of the project is to create a draft version of guidelines on application of the release criteria.

Methods

In the first year of the project the Hungarian regulations on deterministic safety assessments related to airborne radioactive releases were summarized, and the international reports and recommendations were overviewed. The basis of a method was established in agreement with the Hungarian legal environment and the international recommendations. Calculations and sensitivity assessments were performed in order to determine which parameters play a larger and which play a less important part in the results.

Based on the result of the first part of this project, the site parameters of Hungarian nuclear facilities playing an important role in determining the release criteria were defined. The available data were collected or the data sources were defined. The parameters for which different assumptions and/or approximations should be used for design-basis conditions and design-extension conditions events were also specified.

Results

As a result of the work a draft version of guidelines on application of the release limits was created.

Remaining work

This work is finished.

FURTHER DEVELOPMENT OF THE SINAC PROGRAM

Sándor Deme, Lilla Hoffmann, Emese Homolya, Tamás Pázmándi, Péter Szántó

Objective

The SINAC program system is used to model the spread and deposition of radioactive material emitted into the atmosphere in the case of a potential accident in a nuclear power plant. The expected contamination of the environment is estimated fairly precisely nearby the source, but beyond that, the reliability of SINAC is significantly reduced.

The aim of this work was to improve the models of the SINAC program in order to provide more reliable results further away from the release point. During the work, a method to calculate the environmental distribution of radioactive material outside the urgent protective action zone was determined. Models for calculating the internal and external dose were also developed in order to replace the semi-infinite dose models used by the previous versions of SINAC.

Methods

Calculation methods used in the Hungarian and international regional and large-scale atmospheric dispersion models are summarized. These methods are suitable to analyse the environmental contamination beyond the urgent protective actions zone. The Autoscale method is applied instead of constant time steps for the propagation of the puffs. The effective wind vector is determined for the description of atmospheric advection for 12 vertical levels used by the AROME. Application of Monin-Obukhov similarity theory instead of Pasquill categories for the description of atmospheric dispersion was proposed.

In the new model, dry deposition is determined as a function of the deposition velocity, where the surface roughness is also taken into account. In the case of wet deposition, the wash-out coefficient is used and a new type of precipitation, the graupel is taken into account.

The new model for dose calculation takes into account the activity distribution of every single puff individually. This method provides more accurate results than the semi-infinite dose models.

Results

Algorithms for the development of advection, dispersion, and deposition calculation models were worked out. The models for calculating internal and external doses were also improved.

Using the new models, the next version of SINAC will be suitable to provide reliable results up to 100 km from the source.

Remaining work

In the next phase the development of the models for early and late phase protective measures will be performed. Validation and comparison of the results of the new version of the SINAC program with results of other atmospheric dispersion programs are planned.

Following the appropriate validation the new models will be incorporated into the program.

A COMPREHENSIVE DOSE ASSESSMENT FOR NORMAL OPERATION AND ACCIDENTAL SITUATIONS

Lilla Hoffmann, Tamás Pázmándi, Péter Szántó

Objective

The European Committee revised its former recommendation on the use of Article 37 of the EURATOM Treaty and published a new recommendation (2010/635/Euratom C (2010) 6858) in 2010. The more detailed recommendation gave Hungary an opportunity to review the fulfilment of its obligation on data supply according to Article 37.

Methods

The Hungarian regulation was reviewed and it was shown that the system based on dose constraints and emission limit criteria can be fitted to the international practice. The dose burden of atmospheric and liquid releases from the Paks NPP for the population of the most affected neighbouring EU country was calculated for normal operation and for accidental scenarios as well.

The dose burden during normal operation was estimated by PC-CREAM 08 both for releases into the atmospheric and the hydroospheric environments. With the lack of an accepted model for short term aquatic releases, the PC-CREAM 08 programme was used, although it is basically suitable for estimating consequences of long term continuous emissions.

In the case of short term releases to the atmosphere, there is no accepted, validated program in use in the Hungarian

national practice that is able to make reliable calculations for larger distances. Therefore, when analysing atmospheric emissions, a combined application of two different programmes was used. Dilution between the source point and the receptor point was calculated with HYSPLIT. Then, knowing the atmospheric activity concentrations, the doses were calculated with SINAC software. For verifying the results additional calculations were performed with the SINAC and the PC-COSYMA programmes.

Results

Based on the estimations, the dose burden during normal operation in the most affected EU member state in case of aquatic and atmospheric releases were 11 nSv/y and 220 nSv/y, respectively. These values are four orders of magnitude lower than the natural background radiation level. Calculations were made for LBLOCA (large break loss of coolant accident) and PRISE (primary to secondary leakage) design basis accidents (DBA). In the case of an atmospheric release the results show that the radiation level in the most affected EU member state due to these events is one order of magnitude lower than the annual natural background. According to the Final Safety Analysis Report of Paks NPP no aquatic release should be assumed for DBAs. However, test calculations were made assuming that a portion of the atmospheric emission is washed out to the Danube. The results of these calculations show that for LOCA and PRISE events the radiation burden is 3.2 µSv and 0.1 µSv, respectively.

The main pathway regarding accidental releases was found to be the food chain. Doses caused by these events can be significantly and effectively decreased by countermeasures.

Remaining work

The project is finished. The models for the atmospheric transport of radioactive pollutants in present use in the Hungarian practice are only reliable for short distances; therefore, accuracy of the calculations would be improved with the integration of more suitable methods and models.

DOSE CONSEQUENCES OF A SEVERE ACCIDENT

Tamás Pázmándi, Csilla Rudas, Péter Szántó

Objective

During the assessment of a new nuclear site, the effect of external radiological incidents on the operation of the new units should be analysed. The most serious external radiological effect on the planned Paks 2 site is a severe accident of the Paks 1 NPP. The dose effect of a severe accident in Paks 1 NPP was assessed for the workers of the planned Paks 2 site.

Methods

The dose consequences were calculated for five discharge scenarios:

- a. Severe containment failure due to an earthquake.
- b. Discharge from an open reactor.
- c. Discharge from the spent fuel pool containing 706 fuel assemblies with 3100 kW of power. The reactor building remains intact, but the air ventilation systems are not working.
- d. Discharge from the spent fuel pool containing 436 fuel assemblies with 800 kW of power. The reactor building remains intact, but the air ventilation systems are not working.
- e. Discharge from the spent fuel pool containing 436 fuel assemblies with 800 kW of power. The reactor building is damaged; the air ventilation systems are not working.

Three meteorological cases were considered:

- 1) Extreme stable weather conditions: 1 m/s wind, dry weather, Pasquill F.
- 2) Typical weather: 2 m/s wind, dry weather, Pasquill D.
- 3) Extreme rainy weather: 2 m/s wind, 20 mm/h precipitation on the site, Pasquill D.

The calculations were performed with the PC-COSYMA program.

Results

Activity concentrations in the air and on the ground, external effective doses from the ground and the cloud, and committed effective dose from inhalation were calculated at 13 distances (100-1500 m) from the discharge point at 6 heights (0-50 m).

Remaining work

This work is completed.

COSMIC RAY RESEARCH USING SOUNDING ROCKETS

Balázs Zábori, Attila Hirn, András Gerecs, Sándor Deme, István Apáthy, Antal Csóke, Tamás Pázmándi

Objective

The sounding rocket experiment REM-RED was developed to operate on board the REXUS-17 rocket in order to measure the intensity of cosmic rays. The experiment was launched from the ESRANGE Space Center (68°N , 21°E) on the 17th of March 2015 at the beginning of the most intense geomagnetic storm within the preceding 10 years. The experiment provided the opportunity to measure the intensity of cosmic rays in the Polar Region up to an altitude of 88 km above sea level.

Methods

The experiment employed Geiger-Müller (GM) counters oriented with their axes perpendicular to each other in order to measure the cosmic ray intensity during the flight of the rocket. This measurement setup allowed performing direction-sensitive measurements as well. During the ascent phase the rocket was spinning and hence stabilized along its longitudinal axis looking close to the zenith direction. This phase of the flight was used for studying the direction dependence of the charged particle component of the cosmic rays.

Results

In comparison with earlier, similar rocket experiments performed with GM tubes at lower geomagnetic latitudes, significantly higher cosmic radiation flux was measured above 50 km. A non-isotropic behaviour was found below 50 km and described in detail for the first time in the Polar Region. This behaviour is in good agreement with the results of the TECHDOSE experiment that used the same type of GM tubes on board the BEXUS-14 stratospheric balloon.

Fig. 1 shows the count rates measured with the type ZP1210 GM tubes.

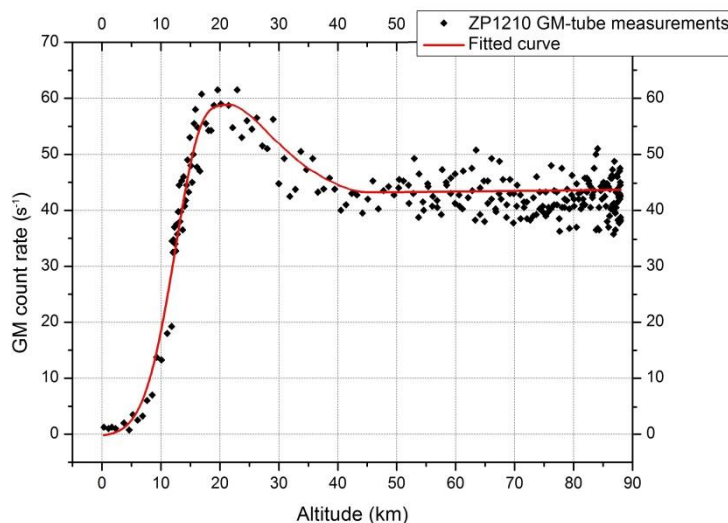


Figure 1: Count rates measured with the ZP1210 GM tubes as a function of flight altitude during the flight of the REXUS-17 rocket

The maximum count rates ($\sim 60 \text{ s}^{-1}$) measured with the REM-RED experiment were found at $23.6 \pm 1.0 \text{ km}$ altitude in agreement with earlier reports. Above 50 km the expected plateau was found with an average count rate of $42.28 \pm 0.35 \text{ s}^{-1}$ obtained from four ZP1210 GM tube measurements. The shape of the measured GM tube count rate profile as a function of altitude agrees well with the measurements performed by Van Allen in 1947–1948 using V-2 and Aerobee rockets at lower latitudes (41°N).

Remaining work

The experiment has been flown on-board the REXUS-17 sounding rocket successfully and all results were published.

Related publications

- [1] B. Zábori, A. Hirn, S. Deme, I. Apáthy and T. Pázmándi: *Characterization of cosmic rays and direction dependence in the Polar Region up to 88 km altitude*, Journal of Space Weather and Space Climate **6**, A12 (2016)
- [2] B. Zábori, A. Gerecs, Gy. Á. Hurtonyné, D. Bényei, F. Náczsi and T. Hurtony: *REM-RED cosmic radiation experiment on-board the REXUS-17 sounding rocket*, Proceedings of the 22nd ESA Symposium on European Rocket and Balloon Programmes and Related Research, ESA SP-730, 539-546 (2015)
- [3] B. Zábori et. al.: *REM-RED sounding rocket experiment to measure the cosmic radiation*, Proceedings of 66th International Astronautical Congress, IAC-15-D5.3.7 (2015) <http://www.videolan.org/vlc/download-ubuntu.html>

TRITEL SILICON DETECTOR TELESCOPE DEVELOPMENT FOR THE ESEO SATELITE

Balázs Zábori, Attila Hirn, András Gerecs, Sándor Deme, István Apáthy, Antal Csőke, Tamás Pázmándi

Objective

ESEO (European Student Earth Orbiter) is an educational satellite project of the European Space Agency (ESA) Education Office. Its aim is to place a spacecraft in a sun-synchronous, polar orbit to provide measurements of the radiation environment and to test technologies for future educational satellite missions. One of the scientific payloads will be a modified, satellite version of the TRITEL three dimensional silicon detector telescopes.

Methods

Due to significant spatial and temporal changes in the cosmic radiation field, radiation measurements with advanced dosimetric instruments on board space vehicles and satellites are extremely important. Since dose equivalent, which characterizes the stochastic biological effects of the radiation, was defined in terms of a LET (linear energy transfer)-dependent quality factor, determining the LET spectrum and the quality factor of cosmic radiation is necessary. For this reason, the development of a three dimensional silicon detector telescope (TRITEL) with almost uniform sensitivity was initiated in the MTA Centre for Energy Research. The instrument, comprising three mutually orthogonal, fully depleted passivated implanted planar silicon (PIPS) detector pairs, is capable of providing the LET spectrum and the average quality factor of the radiation as well as the absorbed dose and dose equivalent. With three orthogonal telescopes an assessment of the anisotropy of the radiation field might also be possible. Since the spectrum of the trapped radiation inside the South Atlantic Anomaly (SAA) is significantly softer, it is worth collecting the SAA and non-SAA spectra separately.

Results

In the year 2015 ESEO-TRITEL passed the Critical Design Review (CDR) phase. The main mission objectives and requirements have been identified according to the expected ESEO orbital parameters. The final mechanical design of the instrument has been provided with detailed mechanical and thermal simulation results in order to demonstrate the feasibility of the payload design. The ESEO-TRITEL engineering development activities have been closed by the end of 2015 and the qualification test campaign could be started (Fig. 1).

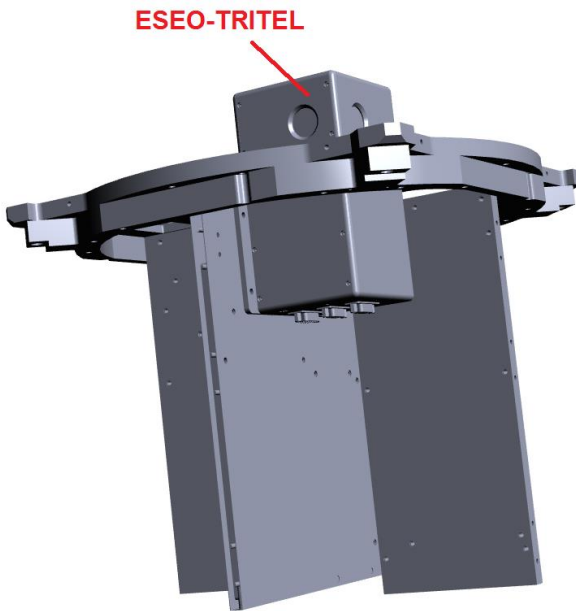


Figure 1: The ESEO-TRITEL payload attached to the structure of the satellite

Remaining work

Completion of the ESEO-TRITEL payload qualification test phase, manufacturing and assembling of the Flight Model, performing the payload Flight Model acceptance tests, launch and finally scientific operation and data evaluation will take place over the next few years.

Related publications

- [1] B. Zábori et. al.: TRITEL satellite version silicon detector development for the ESEO spacecraft, Proceedings of 66th International Astronautical Congress, IAC-15-A1.5.12 (2015)

DOSE MAPPING INSIDE THE ISS

Andrea Strádi, József K. Pálfalvi, Julianna Szabó

Objective

The measurements in the frame of the DOSIS-3D experiment (a European Space Agency program lead by the German Aerospace Center) continued in 2015. The aim of the project is to create a three dimensional dose distribution data base for the European Columbus Laboratory of the International Space Station (ISS).

Methods

Thermoluminescent detectors (TLDs) and solid state nuclear track detectors (SSNTDs) were applied by the MTA EK Space Dosimetry Group to investigate the dose contribution of the low ($< 10 \text{ keV}/\mu\text{m}$) and high ($> 10 \text{ keV}/\mu\text{m}$) Linear Energy Transfer (LET) cosmic radiation. The plastic detector boxes consisted of two SSNTDs and six TLDs (half of them was made of ^{6}Li enriched MTS-6 material, the other half was ^{7}Li enriched MTS-7). In each phase there were thirteen boxes in eleven fixed locations (ten single boxes and a set of three boxes, arranged in the three directions of space, see Fig. 1) inside the module.

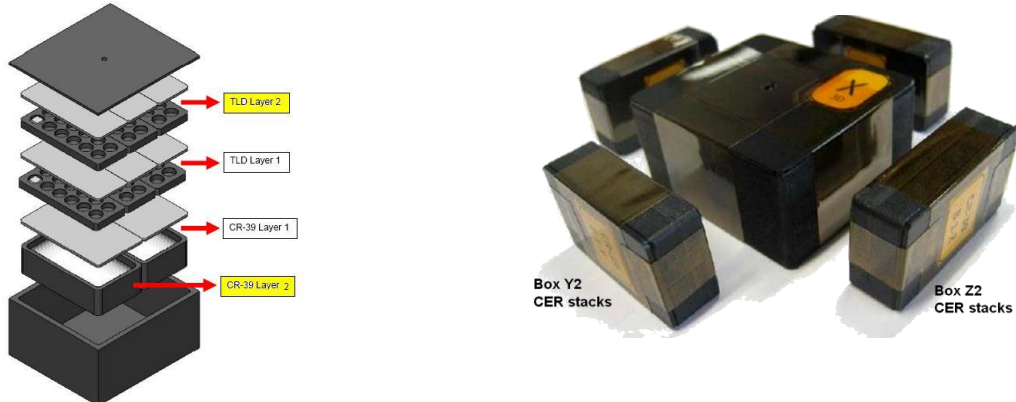


Figure 1: Left: A single detector box which contained the TLDs (TLD Layer 2 marked with yellow) and the track detectors (CR-39 Layer 2 marked with yellow). Right: The 3-dimensional arrangement of the boxes.

Results

During the comparative evaluation of the first 6 phases we found that the dose rates are higher in the boxes mounted on the aft side (rear side) of the Columbus module. Dose rates detected by track detectors are presented in Fig. 2. The TL measurements showed the same distribution, as the other participants' results.

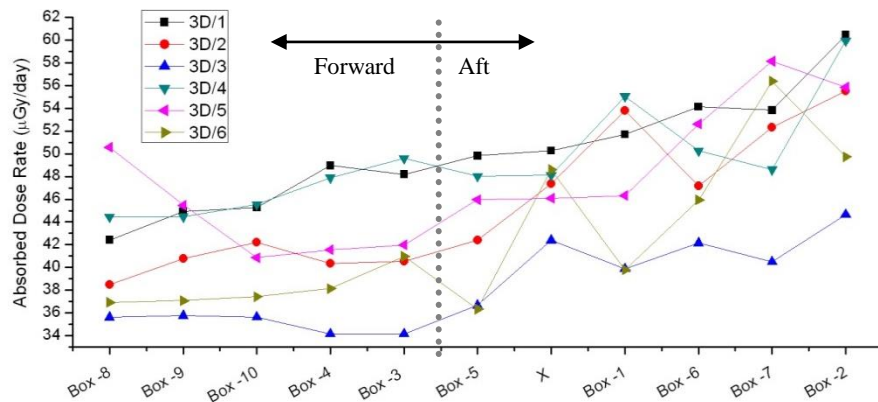


Figure 2: Absorbed dose rates in $\mu\text{Gy}/\text{day}$ of the high LET part ($> 10 \text{ keV}/\mu\text{m}$) of cosmic radiation between 2012 and 2015.

The trend is presumably caused by the west-to-east movement of protons, which are reaching the spacecraft from the rear side while the ISS is passing through the South Atlantic Anomaly (SAA) region.

Remaining work

The DOSIS-3D project is planned to be continued until the end of the 24th solar cycle (2018).

Related Publications

- [1] A. Strádi, J. Szabó, J. K. Pálfalvi, G. Reitz, T. Berger and B. Przybyla: 3D Dose Distribution Measurements by Passive Detectors in the Columbus Module, 20th Workshop on Radiation Measurements for the International Space Station, 8–10 September 2015, Cologne, Germany.

NUMERICAL MODELLING OF THE BIOPHYSICAL EFFECTS OF LOW DOSE IONISING RADIATION AND INHALED AEROSOLS

*Imre Balásházy, Balázs G. Madas, Árpád Farkas, Ágnes Jókay, Péter Füri, Lívia Hanusovszky,
Emese Drozsdik, Blanka Czitrovszky*

Objective

For this year, three research objectives were undertaken: (i) the development of a stochastic lung deposition model in three directions, namely, to enable the model to compute regional deposition densities in the human respiratory system, • to treat mass size distributions, and, • to handle large number of input parameter series, (ii) the elaboration of a computational fluid dynamics based bronchial clearance model to properly describe the trajectories of 50 – 500 nm diameter deposited aerosol particles which can penetrate through the epithelium due to the special properties of the mucus layer, (iii) the mathematical modelling of the cellular hypersensitivity observed in surviving cell fractions at low doses of ionising radiation.

Methods

The stochastic lung model applies Monte Carlo methods to generate the geometry of airways and to compute deposition of inhaled aerosols. In the planned developments: • a method was elaborated to compute the surface of the airways, • the correlation between number and mass size distributions of particles was described, and • an algorithm was implemented to handle large number of input data. Flow fields of mucus layer were computed by computational fluid dynamics techniques. Nanoparticles deposited on the mucus layer were tracked by accounting for inertial and diffusion effects. The main assumption of modelling low dose hypersensitivity is that the tissue tends to minimise the number of mutations by decreasing cell survival at low doses and by increasing it at higher doses.

Results

The computed regional and total airway surface areas were in good agreement with anatomical data from the literature. Thus, deposition densities can be computed realistically based on particle deposition fraction distributions along the airways. Calculated regional deposition density values strongly decrease with airway generation number, that is, to the direction of the deep regions of the lung. Average bronchial deposition density is two orders of magnitude higher than the average acinar one.

The mean residence time of deposited nanoparticles in the airways is higher than that of the larger particles, which may significantly increase the radiation burden caused by radioactive nanoparticles. Due to the special structural and physiological properties of mucus, deposited nanoparticles behave differently compared to micron-size particles. They encounter mucus viscosities up to three-four orders of magnitude lower than their micrometer sized counterparts. On the other hand, the fraction of radon progenies which is prone to mucociliary clearance in the bronchial airways decreases by the decrease of the diameter of the carrier particle. These findings have direct impact on future lung microdosimetry and risk assessment.

We applied the principle that survival of cells upon radiation exposure is determined by minimizing the mutation rate. It results in local minima in surviving fractions. However, these minima are observed in computations at higher doses than measured experimentally. If the spontaneous rate of the induction of pro-mutagenic lesions is considered, minima in survival fractions are observed at lower doses. It means that this principle provides a qualitative explanation for low dose hypersensitivity. In addition, simulations are in agreement with those experimental data which show multiple minima in surviving fractions. The results suggest that the slope characterizing the dose dependence of mutation induction is lower at low doses than at high ones.

Remaining work

The stochastic lung model will be further developed in the next years to compute activity and dose distributions of radioactive particles in the human respiratory system.

Related publications

- [1] I. Salma, P. Füri, Z. Németh, I. Balásházy, W. Hofmann and Á. Farkas: *Lung burden and deposition distribution of inhaled atmospheric urban ultrafine particles as the first step in their health risk assessment*. Atmospheric Environment **104**, 39-49 (2015)
- [2] Á. Farkas and I. Balásházy: *Development and application of a complex numerical model and software for the computation of dose conversion factors for radon progenies*. Radiation Protection Dosimetry **164**, 278-290 (2015)
- [3] Á. Farkas, Á. Jókay, P. Füri, I. Balásházy, V. Müller, B. Odler and A. Horváth: *Computer modelling as a tool in characterization and optimization of aerosol drug delivery*. Aerosol and Air Quality Research **15**, 2466-2477 (2015)
- [4] B. G. Madas, L. Hanusovszky and E. Drozsdik: *Low dose, high sensitivity: the basic assumption of radiation protection and the cellular hypersensitivity*. Magyar Tudomány, 62-67 (2016)

MODELLING OF AEROSOL DRUG DEPOSITION IN THE AIRWAYS

Árpád Farkas, Imre Balásházy, Ágnes Jókay, Péter Füri, Blanka Czitrovszky

Objective

The general objective of the work was to study the transport and deposition of aerosol drugs within the airways of patients suffering from obstructive pulmonary diseases. In this year, the specific aim was to develop and apply a computer model to simulate the airway deposition of some selected commercialised aerosol drugs in the case of COPD (chronic obstructive pulmonary disease) patients.

Methods

Breathing parameters of 25 healthy volunteers and 11 COPD patients in different stages of disease severity were measured during their inhalation through different inhalation devices mimicking aerosol drug intake. Physical parameters of dry powder aerosol drugs influencing particle deposition were gathered from the open literature. A self-developed validated lung model has been applied to calculate the amount of drug depositing in different anatomical regions of the airways.

Results

Figure 1 summarises the results of aerosol drug deposition modelling. The dose deposited in the upper airways (ET) and in the lungs (LUNG) is expressed as a percent of metered dose (the mass of drug dispensed in the inhaler). The average deposited doses of seven marketed dry powder aerosol drugs for different patient groups (KND - non-smoking control group, KD - smoking control group, CS - stable COPD patients, CAE - COPD patients with acute exacerbation) are depicted. According to the simulation results, there are significant differences in terms of regional aerosol drug deposition distribution among the different drugs. While average deposition efficiency of a drug in the lungs (as the target region) of different groups was quite similar for some drugs, deposition of other drugs was patient-group specific. Our results emphasize the need for patient-group and even individual specific drug selection in the future. Carefully validated numerical models can be a powerful tool in individualised drug choice and in the optimisation of aerosol drug delivery.

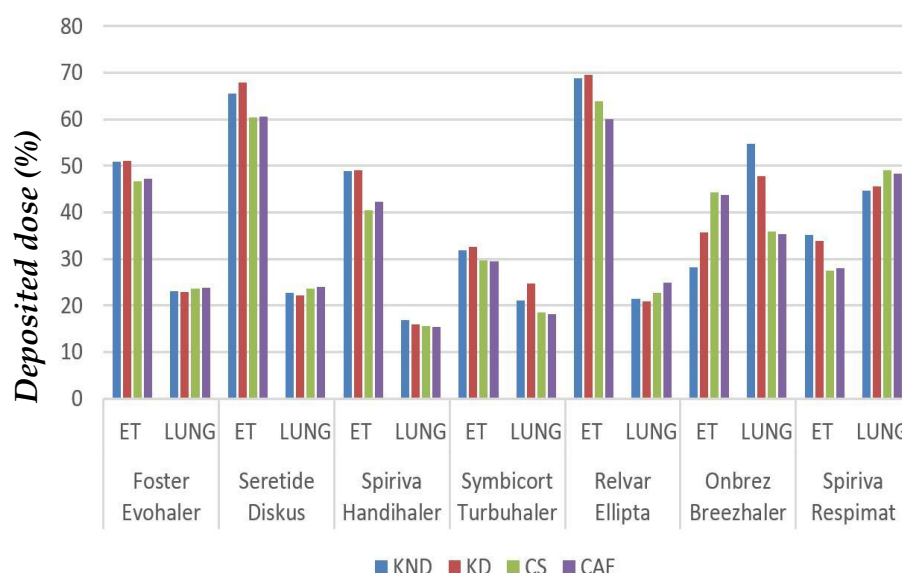


Figure 1: Deposited doses expressed as a percent of metered dose of different dry powder aerosol drugs in the extrathoracic (ET) and lung regions of the airways of different target groups (KND - nonsmoking control group, KD - smoking control group, CS - stable COPD patients, CAE - COPD patients with acute exacerbation)

Remaining work

The work has been completed within the KTIA_AIK_12-1-2012-0019 project. The project ended in 2015, thus there is no remaining work.

Related publications

- [1] Á. Farkas, Á. Jókay, P. Füri, I. Balásházy, V. Müller, B. Odler and A. Horváth: *Computer modelling as a tool in characterization and optimization of aerosol drug delivery*, Aerosol and Air Quality Research **15**, 2466-2474 (2015).
- [2] Á. Jókay, Á. Farkas, P. Füri, A. Horváth, G. Tomisa, I. Balásházy: *Computer modelling of airway deposition distribution of Foster NEXThaler and Seretide Diskus dry powder combination drugs*, European Journal of Pharmaceutical Sciences **88**, 210–218 (2016)

DEVELOPMENT OF LABORATORY MICROSCOPIC X-RAY FLUORESCENCE SYSTEM FOR METAL UPTAKE STUDIES ON ARGILLACEOUS ROCKS

Felicián Gergely, János Osán, B. Katalin Szabó, Szabina Török

Objective

Laboratory scale microscopic X-ray fluorescence (micro-XRF) plays an increasingly important role in various fields where multielemental investigations of samples are indispensable. In case of geological samples, the reasonable detection limits (LODs) and spatial resolutions are necessary to determine the trace element content in microcrystalline level. In order to fulfil these requirements, hardware and software development was performed towards a versatile laboratory micro-XRF system allowing various options of X-ray sources and detectors. The analytical performance of the system was tested in order to find the optimal experimental configuration in terms of sensitivities and LODs for selected elements in loaded petrographic thin sections. The method was applied to sorption studies involving thin sections prepared from cores of Buda Claystone Formation (BCF) which is a potential site for a high-level radioactive waste repository in Hungary. Cs(I), Ni(II) and U(VI) ions were chosen to represent fission and corrosion products as well as hexavalent actinides in the sorption experiments. Micro-XRF elemental maps and the related correlation coefficients between the loaded ions and the representative elements of the main rock components were investigated. For Cs(I) and Ni(II), low-power iMOXS source with polycapillary and silicon drift detector was found to be the best configuration to reach the optimal LOD values. Laboratory micro-XRF was found to be an excellent tool to identify the responsible key minerals for the uptake of Cs(I). In case of nickel, careful corrections were needed because of the relatively high Ca content of the rock samples. The results were compared to synchrotron radiation (SR) micro-XRF.

Methods

Petrographic thin sections were sliced from the selected argillaceous rock sample; they were mounted onto 350 µm thick high purity silicon wafers and polished by 0.25 µm diamond paste to reach an average thickness of 45-55 µm. Ib4-Cs sample was steeped into a 0.1 M NaCl solution where the initial concentration of Cs(I) was 3.6×10^{-4} M. Thin sections of an area of ca. 1 cm² were stirred into 40 ml solution at pH 7. Sample Ib4-Ni was treated with 40 ml modeled and synthesized porewater solution containing 10^{-4} M Ni(II).

In order to generate a microfocused beam, a low-power air cooled modular (iMOXS, Rh anode) and a high-power water cooled X-ray source (HPS; Cr, Mo and W anode) were used in laboratory scale micro-XRF. The diameter of the focal spot of the microbeam was between 20-90 µm depending on the source and the energy. Polycapillary optics and Peltier-cooled Si drift detector (SDD) with an active area of 30 mm² were used to the measurements. The stepsize varied between 20-25 µm. The total time for scanning was around 15 hours for a typical sample area. The measurement process is computer controlled by an in-house developed software specifically designed for the system. It controls the sample stage, the spectrum acquisition process and displays the optical image of the sample. The control software was developed under LabVIEW environment.

The SR experiments were performed at the FLUO beamline of the ANKA storage ring (Karlsruhe, Germany). The white beam of a bending magnet was monochromatized by a W/Si multilayer double monochromator ($\Delta E/E = 10^{-2}$). An SDD was used to collect fluorescence spectra. The micro-XRF elemental mapping on samples treated with Ni(II) and U(VI) were performed at a primary beam energy of 17.5 keV, using a compound refractive lens for focusing a beam down to a spot size of 2×5 µm². Because of the high iron content of the rock sections, micro-XRF elemental mapping of samples treated with Cs(I) was performed at the energy of 6.91 keV below the Fe-K absorption edge. A Fresnel zone plate was used as a focusing element, providing a 3×8 µm² spot size. Elemental maps were recorded for the adsorbed element (Cs, Ni, U) as well as for the major and minor elements of the rock (e.g. K, Ca, Fe, Pb), using a 5 µm stepsize and 4-6 s counting time per pixel. For Ni(II), additional SR micro-XRF measurements were performed at HASYLAB Beamline L (Hamburg, Germany) using a spot size of 22 µm at 17.5 keV. Elemental maps were collected using a stepsize of 20 µm and 1 s counting time per pixel.

Results

To determine the metal uptake of petrographic thin sections expressed as surface covering is not straightforward because the exciting X-rays might penetrate much deeper into the bulk resulting in overlapping characteristic lines of major or minor elements (K, Ca, Ti, Fe). LOD is an important criterion of analytical performance for each element. Generally, different settings are needed to reach the best LOD for the light, medium-heavy and heavy elements. LOD values for Cs, Ni and U are listed in Table 1.

Table 1: LOD values (1000 s) for nickel, caesium and uranium by HPS, iMOXS and SR micro-XRF setups

| | Limit of detection [µg/g; ppm] | | | | | |
|----|--------------------------------|-------|------|-------|------------|------------|
| | HPS | | | iMOXS | Syncrotron | |
| | Cr | Mo | W | Rh | 6.91 keV | 17.478 keV |
| Ni | 27.9 | 27.4 | 7.5 | 8.5 | n.d. | 0.5 |
| Cs | 23.57 | 174.8 | 68.3 | 35.2 | 1.4 | 19.2 |
| U | n.d. | 105.8 | n.d. | n.d. | n.d. | 0.3 |

Based on the LOD values calculated for different experimental configurations of the developed laboratory micro-XRF system, it was demonstrated that optimal excitation and detection conditions can be selected for 2D mapping of different elements of interest in geological samples such as petrographic thin sections. This was achievable due to the versatility of the system with easily exchangeable X-ray sources, capillary optics and X-ray detectors. Low-power iMOXS source with polycapillary at the excitation side and SDD at the detection channel was found to be the best configuration to achieve the necessary LODs for a wide range of elements especially for Cs. For application of laboratory micro-XRF to sorption studies on argillaceous rock thin sections, the results showed that laboratory scale measurements are excellent for identifying K-illite as the main mineral phase responsible for Cs(I) uptake (Fig. 1).

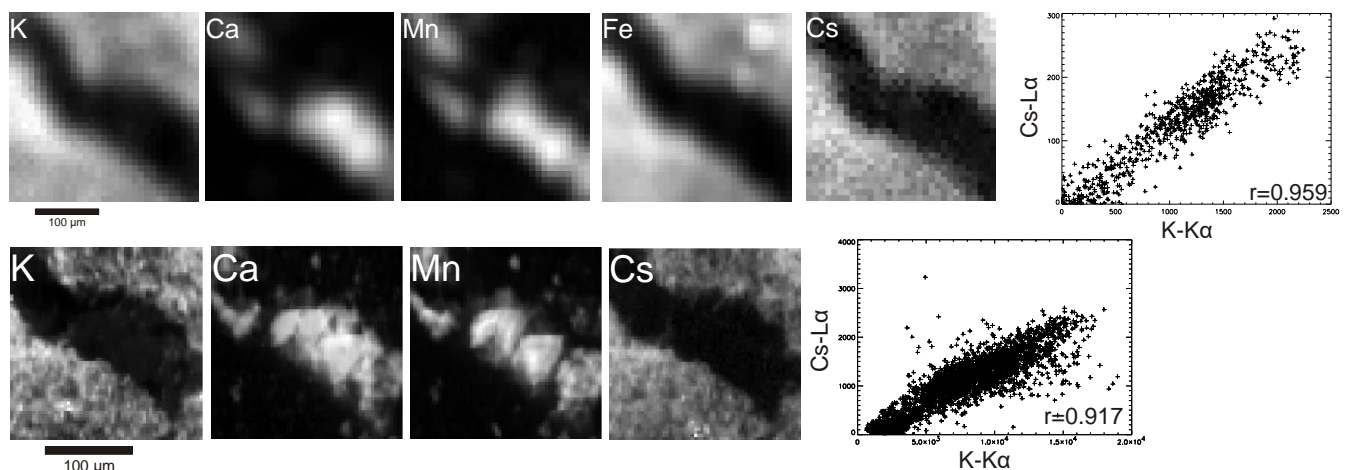


Figure 1: 2D distribution maps of selected elements using Rh anode (iMOXS, top) and SR at ANKA FLUO beamline (bottom) from an area of Cs-Ib4 sample with the relevant scatter plots of characteristic X-ray counts of Cs versus K

Although the relevant surface covering is near the LOD for nickel, an appropriate correction of the sum peaks due to the high Ca content of the studied rocks yielded a reasonable correlation coefficient between Ni and elements representing clay minerals (Fig. 2). For all elements of interest, laboratory micro-XRF was found to be an excellent tool for pre-selection of sample areas for detailed SR investigations due to the easy re-location of the areas based on the elemental maps collected using the laboratory set-up [1].

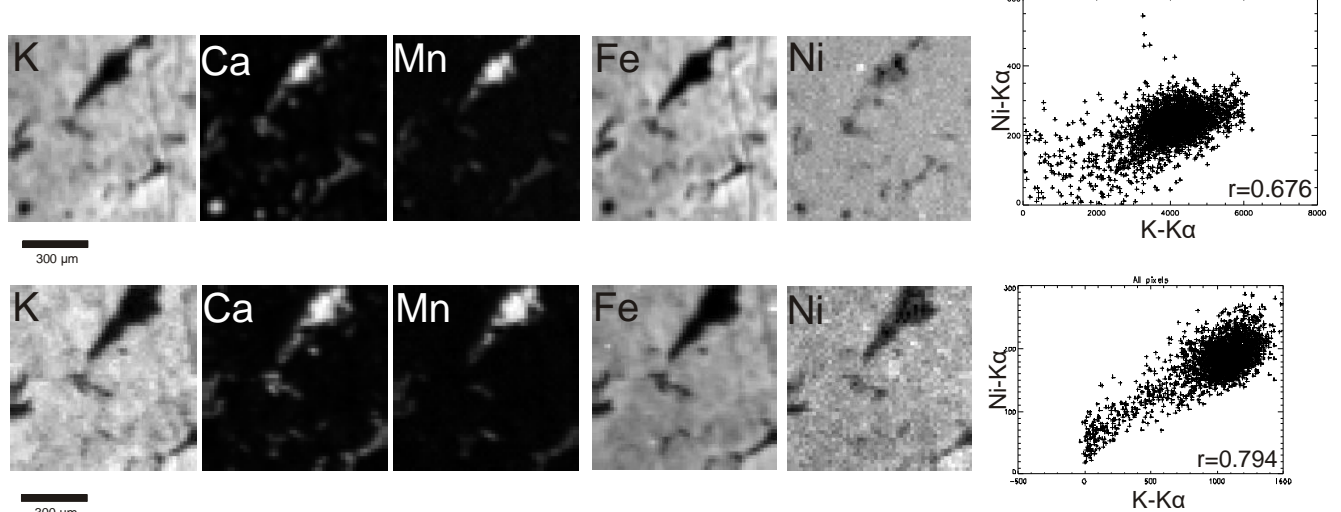


Figure 2: 2D distribution maps of selected elements using Rh anode (iMOXS, top) and SR at HASYLAB Beamline L (bottom) from an area of Ib4-Ni sample with the relevant scatter plots of characteristic X-ray counts of Ni versus K

Remaining work

Comparison of macroscopic and microscopic studies of the uptake representative ions by BCF, with verification of the uptake mechanism applying X-ray absorption spectrometry techniques.

Acknowledgement

The research leading to these results has received funding from the Swiss-Hungarian Cooperation Programme through Project n° SH/7/2/11. We acknowledge the Synchrotron Light Sources ANKA and HASYLAB for provision of instruments at their beamlines and thank Rolf Simon and Karen Appel for their great help. The courtesy of the Public Limited Company for Radioactive Waste Management (PURAM, Hungary) for providing the samples for analysis is also appreciated.

Related publication

- [1] F. Gergely, J. Osán, B.K. Szabó and Sz. Török: *Analytical performance of a versatile laboratory microscopic X-ray fluorescence system for metal uptake studies on argillaceous rocks*, Spectrochimica Acta Part B **116**, 75-84 (2016)



IV. NUCLEAR SECURITY, NON PROLIFERATION



CHARACTERISING OF NEW, UNKNOWN URANIUM SAMPLES

András Kocsonya, László Lakosi, Zsuzsanna E. Mészár, Katalin Tálos, Éva Kovács-Széles

Objective

The 17/1996. (I. 31.) governmental decree designates the Centre for Energy Research for the identification and characterisation of unknown (seized) nuclear materials. In order to fulfil this obligation but also for taking part in nuclear forensic research, the professional skills of the laboratory should be kept on state-of-art level. To evaluate the skills of the laboratory, inter-laboratory exercises and proficiency test are organised by the Nuclear Forensic (NF) International Working Group (ITWG). In course of the report period two international exercises were completed:

- Collaborative Materials Exercise 4 (CMX-4) where three low enriched uranium samples had to be characterised
- Galaxy Serpent Table Top Exercise (TTX) is a web-based virtual exercise that focuses on the development and application of national nuclear forensics libraries (NNFL's).

Methods

In frame of the CMX4 exercise three samples were distributed among the participant laboratories. Two of them were pellets, while the third one was a black powder. A hypothetical scenario is attached to the samples. Not only the characterisation and analysis of the samples were to be done, but their common origin should have been confirmed or rejected. Analyses were performed according to recommendations of IAEA Technical Guidance: Nuclear Forensics Support (Table 1): 24 hours, one week and 2 months reports are submitted.

Table 1: Analyses recommended by ITWG

| Report period | Analyses |
|---------------|--|
| 24 hours | characterisation of the package of samples, collecting traditional evidences, physical characterisation, photography, surface contamination, dose-rate, measurements with hand-held devices, isotopics by gamma-spectrometry |
| 1 week | gamma-spectrometry: isotopics, age, signatures of reprocessed character, scanning electron microscopy (SEM), X-ray diffraction (XRD), mass-spectrometry (LA-ICP-MS) |
| 2 months | mass-spectrometry: age-dating, trace elements (rare earth), signatures of reprocessed character (Pu content by chemical separation) |

The analyses focus on physical, chemical, structural, morphological, elemental and isotopic attributes of the samples. The analyses were partly performed in the laboratories of the Nuclear Security Department, but some analytical techniques were available at other departments of the Institute.

The Galaxy Serpent Exercise consisted three consequent phases:

1. Building up a National Nuclear Forensic Library (NNFL) of a hypothetical country.

This phase covered the processing of a large data set containing documents of individual radiation sources. First the aspects of the library structure should have been developed, then the attributes of sources were uploaded.

2. Identification of a radioactive source out of regulatory control, where analysis results are provided.

3. Identification of a source affected in a radiological dispersal device.

In course of phase 2 and 3, scenarios of hypothetical events were provided including the results of on-site and laboratory measurement. Identification was performed upon the database established in phase 1. The evaluation and interpretation of the available documents were task of the participants, including the revealing of confusions and resolving them.

Results

Analysis results of the CMX4 exercise were compared and discussed at the Data Review Meeting in 2015 March in Karlsruhe. According to the published history of the samples two of them are from the same production batch, while the third one was different. Our results were corresponding to the consensus value. The critical inter-comparison of the applied analytic methods and devices have shown several strengths or weaknesses of the techniques facilitating the spread of good practices. Lessons learned and other observations are published in "After Action Report".

In course of the analyses and interpretation an intensive discussion were started among the participating laboratories, which usefully facilitated the work and improved the inter-laboratory connections. The identification of the possible sources focused on determination of "key-parameters", which can effectively distinguish the potential candidates from others. After finishing the reporting period of the phases, a version by the organisers was circulated. Accordingly, our concept and methods were proper, which resulted in acceptable results.

In some cases inconsistencies or contradictions were revealed among the supplied data, however, this was characteristic to a real situation, where false results or misinterpretations similarly occur.

Remaining work

The exercises are finished, but the publication of the results is in progress. CMX-5 exercise is expected in autumn of 2016.

Related publication

- [1] L. Lakosi, A. Kocsonya, T.C. Nguyen, H. Ramebäck and T. Parsons-Moss: *Gamma Spectrometry in the ITWG CMX-4 Exercise*, submitted in 2016 Journal of Radioanalytical and Nuclear Chemistry.

EFFECTIVE CONTAINER INSPECTION AT BORDER CONTROL POINTS

András Kovács

Objective

Efficient non-intrusive inspection (NII) of containerised freight is increasingly critical to trade and society due to smuggling, illegal immigration and illicit trafficking of drugs, explosives, nuclear and radioactive materials, chemical and biological warfare agents and radioactively contaminated goods. Nowadays the quantity and quality of container inspection is not suitable from a societal security point of view, since no single inspection technology can effectively cope with the present challenge. A consortium has therefore been established to apply for a Horizon 2020 EU project to work out new methods and/or to improve already used ones, to help customs officials to analyse their needs, and to design integrated solutions and optimise the container inspection by deploying comprehensive, cost-effective container NII solutions that will more effectively protect EU sea- and land-borders. The project will also address detection levels, false alarm levels, throughput, health and safety issues and logistics. The project, called C-BORD (effective Container inspection at BORDer control points), involving 18 technology developers, controllers and end-users from 9 countries (France, Germany, Italy, Hungary, Poland, Norway, The Netherlands, United Kingdom, Belgium) has been approved and started in June, 2015. The main goal of the three and a half year's long project is to try out all presently developed technologies in 3 countries addressing the requirements of big seaports, small seaports and mobile landborder. This latter one will be performed in Hungary at a non-EU landborder.

Methods

The C-BORD Toolbox will include five complementary innovative detection technologies, including improved X-rays, target neutron interrogation, photofission, sniffing and passive detection. X-ray systems will be improved by combining different horizontal and vertical views as well as automatic pattern recognition. A tagged neutron inspection system will be applied in mobile units taking care about radiation protection issues. Photofission technology will be developed to detect special nuclear material (SNM) using high energy linear accelerators. Evaporation based detection technologies will also be used in mobile systems complementing X-ray imaging. Recently developed passive detection RPM (radiation portal monitors) will be further improved and integrated in comprehensive NII applications.

Results

MTA EK was given various tasks in the C-BORD project. Our centre is responsible (1) for the assessment of the improved X-ray scanning technology to test e.g. the improved material discrimination of the system and (2) for the assessment of the photofission technology to test the detection level of SNM. These tests will be performed at the development laboratories as well as at the test research facility of the centre. MTA EK will also utilize its new test laboratory for the tests of the different developers before the final trial takes place. The most significant task of MTA EK is the leadership of Work Package 11 (WP11: UC Mobile checkpoints – Integration & Field trials), where, in cooperation with the Hungarian National Tax and Customs Administration, the C-BORD subsystem (RPM, Sniffer and X-ray unit) will be tested with prepared and regular containers at a Hungarian – non EU landborder crossing place.

Since the project started only last year, during the past months, only the preparation work to prepare the field validation protocol has been initiated. At the same time gamma and neutron detectors were deployed into an operational field-survey and first-response mobile laboratory vehicle for in-field operations. Tests of another combined gamma AND neutron detector system have also been started using various radioactive and nuclear materials in the new testing laboratory of MTA EK according to the relevant ANSI standard.



Figure 1: The detector test laboratory and the mobile laboratory of MTA EK

Remaining work

Continuation of the work is in progress. The project is planned to finish at the end of 2018, and until then the R&D, and the test and validation procedures will be performed according to the determined milestones.

DEVELOPMENT OF A FAST, SELECTIVE, MORE SENSITIVE SAMPLE PREPARATION METHOD FOR IN-FIELD LIBS MEASUREMENTS FOR SAFEGUARDS PURPOSES

Éva Kovács-Széles

Objective

The aim of this work was to develop a fast, selective and sensitive sample preparation method for in-field analysis of liquid samples using Laser Induced Breakdown Spectroscopy (LIBS) technique. The method is simple and rapid enough, and should be applicable even for safeguards and nuclear forensic purposes. The sample preparation method is built on a pre-concentration step using different types of extraction chromatographic separation resins which can improve the selectivity and the sensitivity of the analysis. Method is applicable for analysis of uranium, thorium or caesium in different matrices.

Methods

For the selective sample preparation, four different extraction chromatographic resins were tested. The first three are useful for separation of actinides (e.g. especially uranium or thorium) from different sample matrices. CS resin is for separation of caesium. As a model matrix the so-called "leechate" originated from different parts of a nuclear power plant (NPP). It contains different elements (e.g. B, K, Mg, Na) in higher amount and other elements in much lower concentration (e.g. Cu, Fe, Co, Cr, etc.). If there is an undeclared activity at the NPP, it is also possible to present uranium in these samples but in very low concentration, therefore sensitivity increasing of the technique is essential. Finally three resins were found useful. Another task was to develop and test different sample presentation methods for

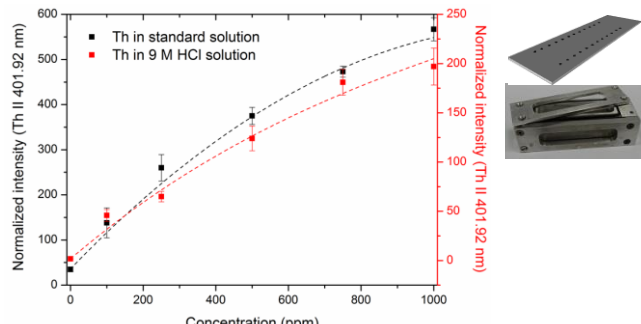
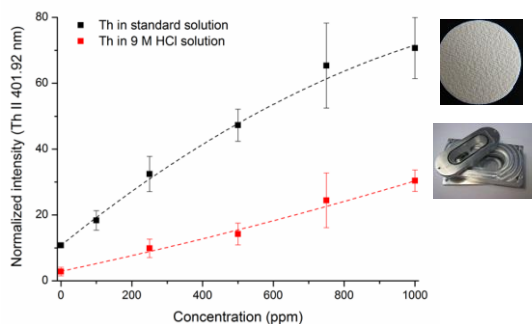
LIBS analysis. One was the classic closed cell LIBS analysis using glass fiber filter and microscope slide with pockets as basic surface for sample drying. Another technique was to analyse the resin particles directly, as well as extraction in a lab-on-a-chip system.

Results

Selectivity and pre-concentration factors of the resins and recovery for U, Th and Cs were analyzed using different LIBS sample presentation methods. Calibration and quantitative analysis using the technique was also carried out. In Figure 1 two examples for Th calibration using different LIBS sample presentation methods and a table with pre-concentration factors and better detection limits obtained can be seen.

| Resin | Recovery (%) | Recovery RSD (%) |
|---------|--------------|------------------|
| Uranium | | |
| TRU | 98.1 | 1.54 |
| Thorium | | |
| TEVA | 91.5 | 1.51 |
| Cesium | | |
| CS | 71.39 | 5.92 |

Table 1: Recovery of the elements using different resins



| Element | Matrix | LOD (ppm) with filter with enrichment | LOD (ppm) with microscope slide with enrichment |
|---------|-------------------------|---------------------------------------|---|
| Uranium | 0.1 M HF and 0.01 M HCl | 5 | 4 |
| Thorium | 9 M HCl | - | - |
| Cesium | 5 M NaOH | 1 | - |

Figure 1: Calibration curves for Th using different LIBS sample presentation techniques and the pre-concentration factors

Remaining work

Continuation of the topic and further development for fast in-field sample preparation and analysis of liquid samples using a kit device and using lab-on-a-chip technique is in progress.

Related publication

- [1] É. Kovács-Széles: *Development of a fast, selective, more sensitive sample preparation method for in-field LIBS measurements for safeguards purposes*, OAH MMT research report, OAH-NBI-ABA-37/15-M (2015)

ESTABLISHMENT OF A NUCLEAR FORENSIC DATABASE FOR SPENT NUCLEAR FUEL

Éva Kovács-Széles, István Almási, Gergely Dósa, Zoltán Hlavathy, András Kocsonya, Csaba Tóth, Péter Völgyesi, Cong Tam Nguyen, László Lakosi

Objective

The analysis and identification of the source of spent nuclear fuel is an important area of nuclear forensics. The risk of terrorism is increasing due to growing illicit trafficking and the growing amount of nuclear materials which are no longer under regulatory control. Revealing the provenance of nuclear fuel is a complex process involving the interpretation of analysis results and comparing them to library data. Due to the importance of spent fuel assay, the Nuclear Forensics International Technical Working group periodically organises experimental and virtual interlaboratory exercises where the participants can test and improve their professional skills.

Methods

A comprehensive study of analytical methods used to characterise spent fuel is being performed. Both destructive (DA) and non-destructive methods (NDA) are discussed. The irradiation history of fuel is described by three parameters: initial enrichment, burn-up, and cooling time.

Two groups of NDA methods are considered, namely active and passive methods. Passive methods involve gamma-spectrometry and neutron counting. Active methods use an external (pulsed or continuous) neutron source to induce fissions. Gamma-spectrometry is a widely used method of characterisation. Burn-up measurements based on ^{137}Cs activity or the $^{134}\text{Cs}/^{137}\text{Cs}$ ratio determination are used to support the optimisation of fuel usage. However the detection and analysis of other fission products can give additional information on the life-cycle of the fuel and its original composition. For instance, LEU and MOX fuels can be distinguished by the $^{134}\text{Cs}/^{154}\text{Eu}$ ratio. Methods suitable for determining the original enrichment are described in the literature. Another significant group of non-destructive methods is the comparison of experimental results with those of simulation codes.

Destructive methods often require chemical sample preparation. The preparation procedure usually involves the solution of the sample followed by chemical separation. Typically, liquid extraction and chromatography techniques are applied. However the opening of a fuel assembly and the chemical steps involve significant radiation protection risk. In order to reduce this risk, these steps must be performed in special laboratories equipped with dedicated hot-cells. The analysis techniques are alpha-spectrometry, liquid scintillation spectrometry, and mass-spectrometry.

To identify the provenance of a fuel sample, analysis results are compared with nuclear forensic library data. Data obtained from the SFCOMPO database is discussed. This database contains the data of spent nuclear fuels of 14 light-water (7 pressurized water +7 boiling water) moderated reactors. The isotopic composition (actinides and fission products) is included in the database, since this is considered as the most characteristic parameter of the spent fuel. Correlations are analysed between burn-up and uranium isotope / total U ratio, which are characteristic to the reactor type.

Candidate nuclides for monitoring plutonium production are discussed. The fission yield of $^{106}\text{Ru}/^{106}\text{Rh}$ is definitely higher for plutonium than uranium.

Results

Our own measurement results on spent fuel of the Paks NPP were analysed according to the methods discussed above. Correlations were discussed between fission products measured by gamma-spectrometry. Samples with different burn-up and cooling time could be separated by using appropriately chosen nuclide groups.

The concept of spent fuel categorisation by different provenance depends on the proper selection of a key parameter, which distinguishes the fuel according to the aspect taken into consideration. Referring to the 15 month operation cycle introduced in Paks NPP, detectable differences were revealed between assemblies used in 12 and 15 month operation cycles. As an illustration, a computer code was developed which simulates the $^{106}\text{Ru}/^{106}\text{Rh}$ production in VVER-440 assemblies.

The described DA and NDA methods are applied to a portion of an EK-10 fuel assembly which was used at the training reactor of the Budapest University of Technology. Gamma- and mass-spectrometric results are in good agreement with each other and the known history of the sample.

Remaining work

In the next period we intend to focus on establishing the Hungarian national nuclear forensics library based on our experience with interlaboratory exercises and using existing databases. Gamma spectrometric analysis of spent fuel assemblies is to be performed in order to try to determine the burn-up history by comparison of simulation results to experimental ones.

DEVELOPMENT OF NATIONAL NUCLEAR FORENSICS LIBRARY

Éva Kovács-Széles, László Lakosi

Objective

Nuclear and other radioactive materials were smuggled across Europe following the break-up of the Soviet Union. Illicit trafficking of nuclear and other radioactive material is a subject of serious concern due to the radiological hazard to the public and the environment as well as the security risks associated nuclear and other radioactive material out of regulatory control. Nuclear forensic science was born to examine these materials, and combines techniques of nuclear and material sciences. The most important aim of these investigations is to determine the specific "signatures", which characterize the given material, and reveal the possible origin of the sample. Availability of these data characteristics, the experiences indicate that it is difficult to determine the origin and history of unknown samples without comparison of data from known samples to facilitate the identification. To increase confidence in determining the origin and history of questioned materials, analysis of numerous comparison samples with different origin is necessary. Another necessary element is the development by States of a National Nuclear Forensics Library to aid in national level comparisons of material out of regulatory control.

Methods and Samples

In this project more analytical techniques were used for analysis of confiscated material as well as nuclear fuel samples of Hungarian application, which are available at the Nuclear Forensic Laboratory of MTA EK (scanning electron microscopy (SEM), gamma spectrometry (GS), mass spectrometry (MS)). The most important and informative characteristic parameters (signatures) were analyzed. Results were compared. A database with searching function as a first prototype of a National Nuclear Forensic Library has also been developed and tested using the analytical data of the project.

Results

SEM is considered as a useful tool to determine the shape, pattern and bulk composition of uranium pellets. GS and MS techniques are capable to determine the enrichment and age of the samples. However, samples with less than 2% U-235 enrichment cannot be measured by GS. Our results show that beside the very accurate and widely used MS method the GS is also a reliable technique to be used for the characterization of uranium pellets. These methods supplement each other as it can be seen in the results which show good agreement. The Pb-isotopic results of the studied samples show good correspondence with the isotopic ratios of Russian Pb-ores, hence their origin can be identified. The database generated by these analyses can be used as an important part of the Hungarian National Nuclear Forensic Library in the future.

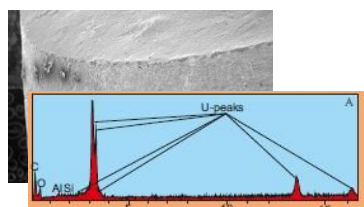


Figure 2: SEM picture and spectrum of a sample

| Sample-ID | HPGE | | ICP-MS | |
|-----------|------------------|------|------------------|------|
| | U-enrichment (%) | ± | U-enrichment (%) | ± |
| Sample-1 | - | - | 1.60 | 0.09 |
| Sample-2 | 2.00 | 0.02 | 2.00 | 0.09 |
| Sample-3 | 3.52 | 0.03 | 3.52 | 0.09 |
| Sample-4 | 4.31 | 0.03 | 4.32 | 0.35 |
| Sample-5 | 9.88 | 0.07 | 9.92 | 0.30 |

Table 1: U-enrichment of the samples

| Sample-ID | HPGE | | ICP-MS | |
|-----------|------------|----|------------|------|
| | Age (year) | ± | Age (year) | ± |
| Sample-1 | - | - | 40.91 | 1.92 |
| Sample-2 | 31 | 13 | 36.87 | 1.21 |
| Sample-3 | 34 | 6 | 43.02 | 1.79 |
| Sample-4 | 43 | 5 | 48.43 | 1.91 |
| Sample-5 | 56 | 3 | 54.0 | 2.03 |

Table 2: Age of the samples

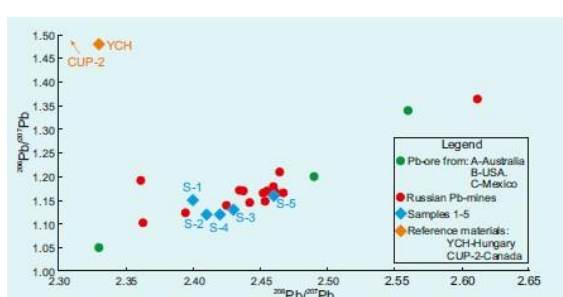


Figure 3: Pb isotopic ratio of the samples

Figure 4: Admission page of the National Nuclear Forensic Library System

Remaining work

Further development of the Library system with extension capabilities is in progress. Further aim is to analyze different types of nuclear materials originated from confiscations and also from Hungarian use (e.g. uranium and thorium-containing chemicals). Data will be uploaded into the Library system.

Related publications

- [1] É. Kovács-Széles: *Establishment of a National Nuclear Forensic Library by analysis of confiscated nuclear materials*, OAH MMT research report, OAH-NBI-ABA-40/15-M (2015)
- [2] É. Kovács-Széles and L. Lakosi: Progress Report on Coordinated Research Project (IAEA-CRP: J02003) with title: „Identification of High Confidence Nuclear Forensics Signatures for the Development of National Nuclear Forensics Libraries”, (2015)



V. RENEWABLE AND FOSSIL ENERGY PRODUCTION



DECOMPOSITION OF HYDROGEN SULFIDE OVER HDS CATALYSTS

Tamás Ollár, Tibor Szarvas, Pál Tétényi

Objective

Alumina supported transition metal sulfides (TMS) like MoS₂ and WS (with or without promoters Ni and Co) catalysts are widely used in hydrodesulfurization. In 2014, during the sulfidation of catalysts, we noticed that elementary sulfur was produced. It appeared that there was catalytic decomposition of hydrogen sulfide. This mechanism has importance in energy related and environmental chemistry. Because of this result, we thought in this type of catalysts could be useful for degradation of hydrogen sulfide. Our main goal was to optimize reaction conditions to promote this pathway. Our second aim was to find the reason of the linear correlation of the sulfur exchange capacity and thiophene conversion over MoS₂ catalysts.

Methods

A flow-system catalytic reactor equipped with a special unit for microanalysis was applied for the study of the sulfur production of H₂S decomposition reactions at atmospheric pressure in the stream of nitrogen gas of different rates in the temperature range of 573–653 K. The amount of catalyst: 50 mg.

Results

Until June 2015 we managed to build a reliable system for the investigation of hydrogen sulfide decomposition to hydrogen and sulfur. This system allows the investigation of new potential catalysts of the hydrogen sulfide decomposition reaction. At first we investigated how the supporting material (aluminium oxide) behaves among reaction conditions. In case of aluminium oxide we did not detect sulfur production but on the cooler part of the reactor cube water drops appeared during H₂S exposure and it is possible that adsorption of H₂S excludes oxygen as: H₂S+O→H₂O+[S]. As a result of the interaction of hydrogen sulfide with aluminum oxide at 653 K, the adsorbed species of H₂S can be formed as HS⁻ and produces H₂O.

Sulfidation of Mo, NiMo and CoMo catalysts produced elemental sulfur, but this production was only 1-3% of the initial amount of sulfur, however, decomposition ratio linearly increased with the temperature. This result shows that in case of higher temperature decomposition ratio can be higher [1].

This year we investigated thiophene adsorption mechanism, and we found a new type of adsorption, e.g., adsorption taking place via exchange of the surface atom, in case of our system this means sulfur exchange.

We have a reliable method for testing the decomposition of hydrogen sulphide. On the basis of our results, next year we can use catalysts which are made in our laboratory, like nano Ni and NiFe and nano Au, Au-Cu catalysts.

In case of thiophene HDS we already pointed out [2] that the sulfur exchange plays important role in the mechanism. During the investigation of adsorption of thiophene over ³⁵S sulfided MoS₂ catalyst, the absence of H₂S indicates that the adsorption takes place through sulfur exchange and sulfur vacancy is not necessary. To monitor the exact amount of hydrogen sulfide we built a gas chromatograph, and installed a TCD detector. We want to supplement our experimental results with theoretical calculations and we started co-working on that with Zoltán Hajnal from MFA.

In 2015 we were finishing an article with Prof. Hancsók from University of Pannonia, "On the Correlation in Between Sulfur Exchange Capacity and Hydrodesulfurization Activity of Molybdenum- or Tungstene-sulfide Based Supported Catalysts". Submission is in progress.

Remaining work

Investigation of hydrogen sulfide decomposition over Pt and PtPd catalysts started in November of 2015.

Related publications

- [1] T. Ollár: *Catalytic decomposition of Hydrogen Sulfid*, Falling Walls Lab, Sopron, 2015 szeptember 10. (2015)
- [2] Z. Varga, T. Ollár, T. Szarvas, P. Tétényi and J. Hancsók: *The particular characteristic of the active sites of MoS₂, WS₂ catalysts in Thiophene HDS*, submitted to Topics in catalysis (2016)

WATER OXIDATION – INITIAL STEPS

József S. Pap, Mounir Chamam, Dávid F. Sránkó, Zsolt G. Kerner

Objective

Water oxidation catalysis was launched in 2014 as a strategic experimental research directive. The reaction itself: $2\text{H}_2\text{O}(\text{f}) \rightarrow \text{O}_2(\text{g}) + 4\text{H}^+(\text{aq}) + 4\text{e}^- (E^\circ = 1.23 \text{ V})$ is a great challenge in catalysis and subject to intense research due to its importance in renewable water splitting to H₂ and O₂. Our long term objective is to find catalysts that can be made part of a complex (photo) electrocatalytic water splitting system. Three directions of research were initially chosen: (1) Ru-diimine complexes, a) catalytic properties in homogeneous solution, b) anchoring options on supports, c) design and synthesis of photosensitizers (PS). (2) Design and synthesis of ligands for Ru-based metal organic frameworks (MOFs) to test in water oxidation. (3) Synthesis and characterization of Cu-complexes for catalysis and looking into their anchoring options on electrode surfaces a) with diimine ligands, b) with branched peptides.

Methods

Surface-anchored Ru-diimines were investigated by X-ray photoelectron spectroscopy (XPS), X-ray diffraction (XRD) and transmission electron microscopy (TEM). Peptides were synthesized by an improved solid phase method. Several spectroscopic techniques (UV/VIS, circular dichroism - CD, electron paramagnetic resonance - EPR), electrospray ionization mass spectrometry (ESI-MS) and electrochemistry were applied to characterize the Cu-peptide catalysts. Electrocatalytic tests were run by cyclic voltammetry (CV) or controlled potential electrolysis (CPE), and dioxygen evolution was monitored by a fluorescent probe.

Results

(1) NiFe-LDH (layered double hydroxide) samples were modified with a molecular photosensitizer (PS) by using a terephthalate linker. The layered structure can accommodate molecules either by surface adsorption or intercalation. The NiFe-LDH acts both, as support for the PS and as catalytic material. A novel Ru(II)-diimine PS was successfully included into a NiFe-LDH-terephthalate-Ru(II)-diimine assembly and was tested by visible light activation. The results (moderate activation) were reported at an international conference and the work continued during the period January 2016–December 2016 at (University of California, Berkeley) by Dávid Sránkó. One homogeneous Ru-diimine catalyst was characterized in detail by means of structure, electrochemical properties and WOC capabilities. An M.Sc. diploma work with an excellent grade was defended by Daniella Szűlek on this topic.

(2) This topic is currently ceased due to the lack of external funding (OTKA) and adequate human resources.

(3) New Cu-complexes were characterized and some were tested in water oxidation electrocatalysis. Square wave voltammetry (SWV) was applied to obtain precise E (potential) vs. pH diagrams and pK_a (negative logarithm of the acid dissociation constant) values for the Cu^{III} and/or the Cu^{II} complex. CV and CPE allowed characterization of catalytic abilities. We concluded that proton couple electron transfer (PCET) steps played a role in reaching the oxidized states and C-terminal histidine extension (instead of glycine) of 2,3-L-diaminopropionic acid (L-Dap) lowered pK_a for the Cu^{III} form and improved turnover frequency (TOF) at pH 11 ($\sim 2\times$). We explained differences by means of histidine aided PCETs in the course of catalysis that can occur by several effects (for instance, by cation π -interaction with protons). In addition to the papers, one conference poster was presented at ISHHC17.

Remaining work

The results in point (3) inspire us to commence extended studies with branched peptides which will be the main focus in upcoming years (see also the report of topic 126). Due to the high modularity of these ligands, such compounds can be the draft horse for basic research in this field (Fig. 1), even though they are inherently less robust than heterogeneous systems. The fragment-by-fragment modifications of the peptides lead to new SINGLE SITE CATALYSTS, each unit can be extended to construct 1st gen. METALLODENDRIMERS that allow cooperation between various numbers of different Cu-sites, polyelectrolytes help in ANCHORING CATALYSTS TO SURFACE and this process can be followed by Optical Waveguide Lightmode Spectroscopy (OWLS) - to name only the directions explored so far.

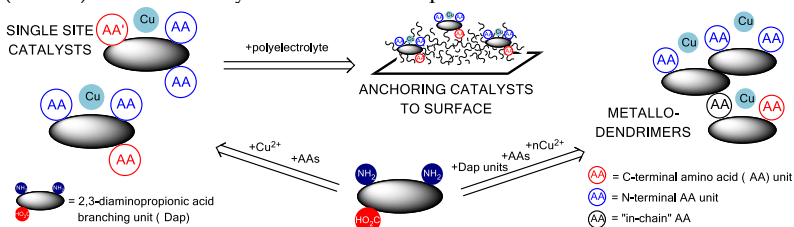


Figure 1: Explored applications of Cu-peptide complexes in water oxidation catalysis

Related publications

- [1] J. S. Pap, Ł. Szrywiel, D. Sránkó, Z. Kerner, B. Setner, Z. Szewczuk and W. Malinka, *Chem. Commun.* **51**, 6322 (2015)
- [2] Ł. Szrywiel, J. S. Pap, Ł. Szczukowski, Z. Kerner, J. Brasun, B. Setner, Z. Szewczuk and W. Malinka, *RSC Adv.* **5**, 56922 (2015)

SELF-ASSEMBLY OF CATALYTIC SURFACES

József S. Pap, Róbert Horváth, Inna Székács, Mounir Chamam, Dávid F. Sránkó, Zsolt G. Kerner, Enikő Farkas, Gabriella Gál, Róbert Schiller

Objective

Our aim was to explore possible ways to anchor layers of molecular catalysts for electrocatalytic water oxidation (WOC) by using polyelectrolytes to an ITO electrode surface, and moreover to characterize and test these surfaces in the WOC reaction. In this way, the advanced expertise of R. Horvath in real-time surface analysis at MFA and that of J.S. Pap at FKKL in WOC could be exploited in order to create unique knowledge in the application of advanced materials for the benefit of the strategic experimental research goals of MTA EK.

Methods

Optical Waveguide Lightmode Spectroscopy (OWLS, real-time detection of layer build-up), electrochemical OWLS (EC-OWLS, real-time detection of surface density under electrolysis conditions), X-ray photoelectron spectroscopy (XPS, surface microanalysis), atomic force microscopy (AFM, surface topology), Kelvin Probe (KP, work function, e.g., the amount of energy needed to release electrons from a material's surface), cyclic voltammetry (CV, prompt analysis of electrocatalytic response under various conditions), controlled potential electrolysis (CPE, diffusion controlled catalytic conditions) and fluorescent probe (dioxygen evolution).

Results

In a previous study two structurally characterized Cu(II)-branched peptide complexes involving 2,3-L-diaminopropionic acid (L-Dap) as a junction unit were reported (with ligands 3G = H-Gly-Dap(H-Gly)-Gly-NH₂ and 2GH = H-Gly-Dap(H-Gly)-His-NH₂) to promote water oxidation electrocatalysis at high pH (>10) in a phosphate electrolyte. These complexes were used as discrete building units of multicomponent layers on an indium-tin-oxide (ITO) surface in combination with selected polyelectrolytes (poly(L-lysine) = PLL for Cu-3G and poly(allylamine hydrochloride) = PAH for Cu-2GH) in the presence of phosphate in a pH range of 7.5-10.5. Layer-by-layer (LbL) evolution of sequential Cu-ligand/polyelectrolyte/buffer coating on indium-tin-oxide (ITO) and silica could be monitored by OWLS and the modified surface was investigated by means of XPS, AFM (in progress). EC-OWLS under optimized conditions (pH 10 and polarization of +1.1 V of the ITO vs. Ag/AgCl), where the Cu-3G and Cu-2GH content can be expected to initiate water oxidation, revealed changes in the coating upon alternating positive-zero-positive etc. polarization (Fig. 1, left). The dynamics of changes showed that after initial loss of mass from the surface, steady-state conditions occur. Independently, cyclic voltammetry (CV) and controlled potential electrolysis (CPE) studies in pure electrolyte with ITO electrodes sequentially pre-treated in Cu-ligand/polyelectrolyte/buffer solutions that mimic OWLS conditions yielded results in support of improved electrocatalysis on coated vs. neat ITO (Fig. 1, right). One conference poster was presented at ISHHC17 that included some of these results. This work presents an analysis and test procedure for electrode activation with molecular catalysts that are capable of secondary interactions with polyelectrolytes.

Remaining work

It turned out that only specific polyelectrolytes under specific conditions help in anchoring molecular catalysts to an ITO surface and this process can be followed by OWLS. The results are now being written up into a manuscript that will be sent to a journal with an "advanced applied materials" profile. Some measurements are in progress (AFM and KP). New ligands are available that were designed based on the above results. Also, new Cu-ligand/polyelectrolyte combinations will be tested next year.

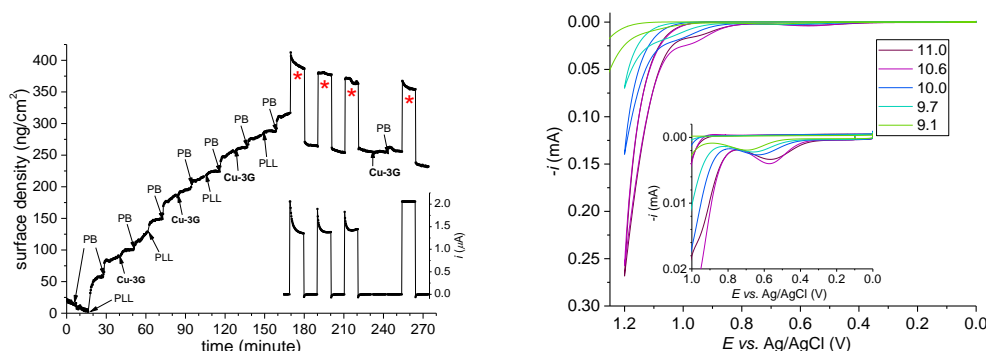


Figure 1: On the left: typical EC-OWLS plot showing the build-up of LbL catalyst material on ITO (PB: phosphate buffer, PLL: poly-L-lysine, Cu-3G: molecular catalyst) and concomitant CPE tests (red asterisks stand for CPE at 1.1 V vs. Ag/AgCl, inset shows corresponding current traces). On the right: current responses recorded at different pH values (as indicated by the legend) on a Cu-3G/PLL(PB)-ITO and the shift of the blowup of the Cu(III)/Cu(II) response from the surface adsorbed Cu-3G with pH (inset).

VISIBLE LIGHT PROMOTED AEROBIC BENZYL ALCOHOL OXIDATION ON ALUMINA SUPPORTED AU-CU CATALYSTS

Andrea Beck, Gergely Nagy, József Sándor Pap, András Deák, Dániel Zámbó, György Sáfrán, Károly Lázár and László Wojnárovits

Objective

Literature examples from the last 5-6 years show that the combination of plasmonic gold or silver nanoparticles (NPs) with wide-band gap semiconductors such as titanium dioxide and cerium dioxide can lead to an enhanced photocatalytic activity in the visible range due to the strong surface plasmon resonance (SPR) excitation of such metal NPs. Our alumina supported Au and bimetallic Au-Cu catalysts were tested in visible light irradiated photocatalytic aerobic benzyl alcohol oxidation and compared with a titania (Degussa P25) supported Au catalyst.

Methods

Wet-chemically derived bimetallic Au(0.9 wt%)Cu(0.3 wt%)/Al₂O₃ was prepared by different approaches, namely by co-reduction (Au&Cu) and sequential reduction of the two metals (Au→Cu and Cu→Au), corresponding monometallic Au(3.6 wt%)/Al₂O₃ and as a reference Au(1.8 wt%)/TiO₂ produced by deposition precipitation with urea were studied. The Au(Cu) particle sizes and the SPR bands were characterized by HRTEM and diffuse reflectance UV-vis spectroscopy, respectively. For better understanding of the differences in the SPR bands and structure of the different Au-Cu(O_x) NPs, optical simulations were performed based on boundary element methods for different size Au NPs with or without Cu, Cu₂O or CuO shells. Catalytic performance was assessed after calcination (400°C/air/1h) in aerobic benzyl alcohol oxidation reaction. The conditions were as follows: 5mL 0.1 M benzyl alcohol in toluene, O₂ oxidation agent (bubbling, 1 atm), 27°C, stirring with magnetic stirrer (1200 rpm), 25 mg catalyst (in case of Au/TiO₂ 30 mg). Each catalyst was measured in two parallel experiments, under irradiation at 530 nm (by Asahi Max-303 Xenon 300 W light source with band pass filter) and without irradiation, respectively. Samples of the reaction mixture were filtered and analysed by GC at certain time intervals. Beside benzaldehyde only benzyl benzoate was detected as product.

Results

The Au(Cu) mean particle sizes of the different samples in the calcined state were in the 1.8-3.1 nm range (Au/Al₂O₃: 2.0±0.6 nm, Au&Cu/Al₂O₃: 1.8±0.4 nm, Au→Cu/Al₂O₃: 2.6±0.8 nm, Cu→Au/Al₂O₃: 2.7±0.9 nm, Au/TiO₂: 3.1±0.8 nm). The SPR peak position of Au-Cu/Al₂O₃ samples and Au/Al₂O₃ varied between 522 and 528 nm (CuO_x/Al₂O₃ showed almost no extinction in the 400-550 nm region), in case of Au/TiO₂ it was 570 nm. According to the simulated spectra of different size spherical Au NPs, the SPR peak position does not change in the 3-5 nm size range, while the CuO_x oxide shell causes a significant redshift of the SPR band. Based on the UV-vis, HRTEM and earlier XPS results, in the calcined samples presence of bimetallic nanoparticles consisted of Au(Cu) metallic core with some Cu₂O and CuO decoration is suggested (CuO_x separated from Au(Cu) NPs is also possible).

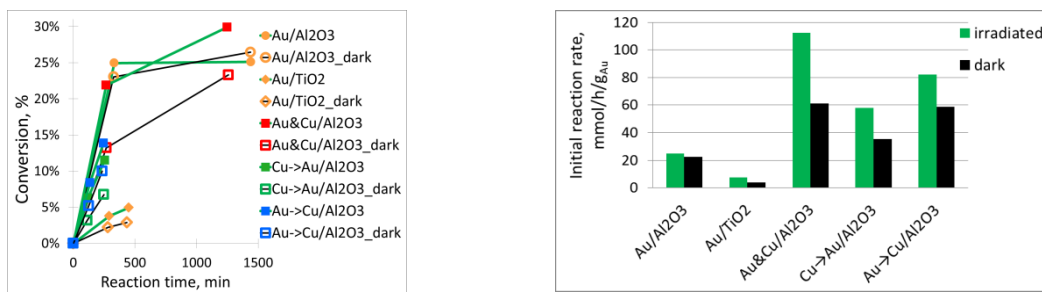


Figure 1: Benzyl alcohol oxidation irradiated (530 nm) (—) and non-irradiated (—)

As presented in Fig. 1, all three Au-Cu/Al₂O₃ samples, like also Au/TiO₂ show significant activity increase on the irradiation by light of 530 nm wavelengths, but in case of Au/Al₂O₃ there is no difference between irradiated and non-irradiated reaction conditions. The extent of the photoeffect of the bimetallic Au-Cu/Al₂O₃ samples is smaller, however, their catalytic activity is much higher than that of the Au/TiO₂, and it depends on the structure of the bimetallic catalyst. The photoeffect observed is possibly in relation with the interaction of SPR excitation of Au(Cu) and the semiconducting copper oxides.

Remaining work

The demonstration that introduction of Cu into/onto alumina supported Au NPs producing Au-CuO_x bimetallic nanoparticles generates catalysts with photocatalytic effect under 530 nm irradiation in aerobic oxidation benzyl alcohol opens further research directions. For example, the effect of concentration, size and structure of gold and copper oxide (Cu₂O, CuO), structure of their interface, extent of alloying gold with copper, support material, the reaction temperature, the energy range and intensity of irradiating light on the plasmonic photocatalysis are worth studying on the one hand to improve the photocatalytic performance under visible and sunlight, on the other hand to better understand the governing parameters.

AU-CONTAINING BIMETALLIC CATALYSTS IN HIGHLY SELECTIVE AEROBIC OXIDATION REACTIONS

Andrea Beck, Gergely Nagy, Dávid Sránkó, László Borkó, Zoltán Schay, Antal Tungler

Objective

Gold-based catalysis for aerobic selective oxidation processes is an environmentally and economically viable process for producing a wide range of useful chemicals from alcohols and carbohydrates, which are important biomass derived feedstocks. Alloying gold with other metals, synergistic effect can be obtained acquiring advantages in activity, selectivity and durability of the catalysts. In the frame of our OTKA project #101854, we are investigating Au-Ag, Au-Cu, Au-Ru and Au-Ir bimetallic systems in selective oxidation of glucose and benzyl alcohol as model substrates.

Methods

Bimetallic AuCu (Au&Cu, Au->Cu, Cu->Au) and corresponding monometallic nanoparticles were produced by aqueous phase reduction (co- or sequential reduction of the two metals) with NaBH₄ and stabilization with polyvinyl alcohol (PVA) or sodium citrate, followed by adsorption on Al₂O₃ or SiO₂ supports. After calcination (400°C/air/1h) and subsequent reductive (350°C/H₂/30min or 500°C/H₂/2h) or inert (500°C/Ar/2h) atmosphere heat treatments, the catalysts were characterized by UV-vis, HR-TEM (performed by G. Sáfrán, MFA), XRD (by I. Sajó, University of Pécs), XPS, CO adsorption followed by FT-IR spectroscopy, and tested in benzyl alcohol (BzOH) oxidation (typically 30 mL 0.1 M BzOH/toluene, in several cases with addition of K₂CO₃, 15-30 mg catalyst, 80 °C, 1 atm O₂ bubbling, stirring by 1200 rpm, analysis by GC in 10 minutes time intervals). Beside benzaldehyde only benzyl benzoate was detected as product.

Results

Particle size effect was studied in Au&Cu/Al₂O₃ (Au/Cu=1/1 atomic ratio, 0.9 wt% Au) and Au/Al₂O₃ (1.8 wt% Au) systems. Two different size PVA and one citrate stabilized Au&Cu sols derived catalysts contained Au(Cu) particles of 1.8, 2.2 and 4.2 nm mean diameter, respectively, both in calcined and reduced (at 350°C) states. From corresponding monometallic Au sols calcined samples of 1.8, 2.8, 3.6 nm average size Au particles were produced. The turn-over frequency (TOF: converted BzOH/surface Au atom/min) of Au/Al₂O₃ increased with increasing Au size. In case of Au&Cu/Al₂O₃, the order of TOFs calculated supposing the same Au/Cu atomic ratio both in the particles and on their topmost layer, was also the same. However, these Au/Cu ratios could not be measured and can be different regarding the different preparation and segregation depending likely on the particle sizes. For all three sets of alumina supported Au&Cu and Au catalysts, the bimetallic ones were more active than the monometallic ones related to the same gold content (Cu/Al₂O₃ was not active under the same reaction conditions). SiO₂ supported AuCu and Au were much less active than the analogous Al₂O₃ supported samples.

During the benzyl alcohol oxidation deactivation was detected, and the reaction almost stopped at much below 100% conversion. The conversion reached could be enhanced by increasing the catalyst/substrate ratio, or addition of base, K₂CO₃ in case of both bimetallic Au&Cu on both Al₂O₃ and SiO₂ and monometallic Au/Al₂O₃, while the selectivity of benzaldehyde was kept above 90% (in case of silica support at higher selectivity). Strongly adsorbing benzoic acid forming in very small amount (not detected by GC analysis) may block active sites. This could be diminished by added base and also by Cu-oxide.

According to the earlier HRTEM studies, AuCu/Al₂O₃ prepared by PVA stabilized sols (Au/Cu=1/1) contained low Cu content alloyed AuCu particles (Au/Cu>8/2) depending on the preparation approach and pretreatments. The rest of the copper decorated the Au(Cu) particles or located separately from gold, typically in form of oxide, except after reduction treatment that reduced Cu to metal or Cu₂O (that easily reoxidizes on air contact) as XPS measurements suggested. For increasing alloying of Au and Cu 500°C/H₂/2h reduction treatment was applied. The activity of the various Au-Cu catalysts decreased in different extent accompanied by slight sintering. The activity of Au/Al₂O₃ was also lowered by the high temperature reduction and in the same extent by similar treatment in Ar. The dehydroxylation of the catalyst surface may play a role in activity loss.

Remaining work

Regarding the great difference between the activity and selectivity of the silica and alumina supported systems and the advantageous role of base addition, the support effect will be studied with special attention to the acid-base properties.

Related publications

- [1] G. Nagy, T. Benkó, L. Borkó, T. Csay, A. Horváth, K. Frey and A. Beck: *Bimetallic Au-Ag/SiO₂ catalysts: Comparison in glucose, benzyl alcohol and CO reactions*, Reaction Kinetics Mechanisms and Catalysis **115**, 45-65 (2015)
- [2] G. Nagy, T. Benkó, D.F. Sránkó, L. Borkó, Z. Schay, G. Sáfrán, O. Geszti and A. Beck: *Bimetallic Au-Cu/Al₂O₃ Catalysts in Selective Aerobic Oxidation of Glucose and Benzyl Alcohol*, 12th European Congress on Catalysis - EuropaCat-XII, Kazan, Russia, 30 August - 4 September 2015, Abstract Book 1383-1384 (2015)
- [3] G. Nagy, D.F. Sránkó, L. Borkó, Gy. Sáfrán, O. Geszti and A. Beck: *Bimetallic Au-Cu/Al₂O₃ catalysts: Synergetic effect in aerob benzyl alcohol oxidation*, MKE 2. National Conference, Hajdúszoboszló, 31 August - 2 September (2015)

CORRELATION BETWEEN ACTIVITY AND COKE FORMATION ON NICKEL-BASED DRY REFORMING CATALYSTS

Anita Horváth, Miklós Németh, Johanna Károlyi, Ferenc Somodi, Dávid Sránkó, Zoltán Schay

Objective

The selective conversion of methane with carbon dioxide yields hydrogen and carbon monoxide as reaction products in equimolar ratio (dry reforming, DRM: $\text{CH}_4 + \text{CO}_2 \rightleftharpoons 2\text{CO} + 2\text{H}_2$). Nanostructured ZrO_2 -supported bare or Na_2O -promoted Ni catalysts were further investigated as potential dry reforming catalysts. Structural differences between the samples were studied and the catalytic transformations were followed to spoor the fate of different carbon species.

Methods

The Ni/ ZrO_2 catalysts were prepared by a sol-based synthesis route (1%Ni_{sol}), by wet impregnation with the concomitant addition of NaHCO_3 (1%Ni_{impNa} and 3%Ni_{impNa}) and by the incipient wetness technique (3%Ni_{IW}). Structural investigations were carried out by X-ray powder diffraction (XRD), X-ray Photoelectron Spectroscopy (XPS) and Transmission Electron Microscopy (TEM). Reducibility of Ni oxide species was studied by Temperature Programmed Reduction (TPR) experiments. Diffuse Reflectance Fourier Transform Infrared Spectroscopy (DRIFTS) was applied to detect the surface-adsorbed species during CO chemisorption at room temperature or in dry reforming mixture up to 500°C. Temperature-programmed or isothermal dry reforming experiments were done i) at atmospheric pressure in plug flow reactor with 70% CH_4 +30% CO_2 mixture (in excess methane) or ii) at 50 mbar total pressure in a closed loop circulation system using labeled $^{13}\text{CO}_2$. Subsequent temperature programmed oxidation (TPO) measurements were carried out to compare the reactivity of deposited carbon in both plug flow and circulation catalytic systems.

Results

The Ni nanoparticles in the fresh catalysts were smaller than 20 nm and could be reduced below 600°C with a TPR peak maximum being the highest for the Na_2O -containing catalysts. Strong and stable monodentate and bridged carbonates for impNa samples, while bicarbonates and formates on IW and sol catalysts were detected during in situ low temperature DRIFTS-DRM measurements. Thus, CO_2 activation at low temperature is suggested to proceed on IW and sol samples via transformation of bicarbonates→formates down to C_{ads} , while on the impNa samples through the conversion of surface carbonates at the metal-oxide interface assisted by the Na_2O promoter. During atmospheric catalytic tests in plug flow reactor, the 3%Ni_{impNa} sample was the most active and stable catalyst, while the 3%Ni_{IW} showed the most pronounced deactivation. The amount of surface coke was less for the latter sample and composed of carbon nanotubes and filaments. Experiments carried out with $^{12}\text{CH}_4$ and $^{13}\text{CO}_2$ reactants at 50 mbar pressure revealed on the 1%Ni_{sol} $^{13}\text{CH}_4$ formation already at around 400°C during the temperature ramp. This labeled methane can form from $^{13}\text{CO} + \text{H}_2$ or $^{13}\text{CO}_2 + \text{H}_2$ via surface methanation reaction that proceeds through $^{13}\text{C}_{\text{ads}}$ intermediate species. Thus, CH_4 dissociation seems to be faster and less surface oxygen species are available on 1%Ni_{sol}. There were 2 types of surface coke formed in the reaction and removed as $^{12}\text{CO}_2$ and $^{13}\text{CO}_2$ during the subsequent TPO measurements: the easily oxidizable one at around 300°C was composed of only ^{12}C (originating from $^{12}\text{CH}_4$ reactant), while the other type of coke above 500°C was composed of both ^{12}C and ^{13}C , and formed presumably from gas phase carbon monoxide products. The coke coming from the methane source was more reactive on the Na_2O -promoted samples having stronger metal-support interaction. To sum up, optimal distribution of Na_2O and Ni particle size were attained in the 3%Ni/ ZrO_2 catalyst resulting in a moderate methane dissociation rate accompanied with a fast enough carbon gasification due to the 0.7 wt% sodium oxide promoter. The amount, structure and reactivity of surface coke must be all known to understand the dry reforming performance of a Ni catalyst.

Remaining work

The project will be finished at the end of 2016.

Related publications

- [1] M. Németh, Z. Schay, D. Sránkó, J. Károlyi, Gy. Sáfrán, I. Sajó and A. Horváth: *Impregnated Ni/ZrO₂ and Pt/ZrO₂ catalysts in dry reforming of methane: Activity tests in excess methane and mechanistic studies with labeled $^{13}\text{CO}_2$* , Appl. Catal. A.: Gen. **504**, 608-620 (2015)
- [2] M. Németh, Z. Schay, D. Sránkó, J. Károlyi, Gy. Sáfrán, I. Sajó and A. Horváth: *Mechanistic studies with labeled $^{13}\text{CO}_2$ on Ni/ZrO₂ and Pt/ZrO₂ dry reforming catalysts*, 12th European Congress on Catalysis, poster, Kazan, Russia, 30 August - 4 September, (2015)
- [3] M. Németh, J. Károlyi, F. Somodi, D. Sránkó, Z. Schay and A. Horváth: *Comparison of different Ni/ZrO₂ catalysts in CO₂ reforming of methane using isotope-labeled experiments*, 17th International Symposium on Relations between Homogeneous and Heterogeneous Catalysis, poster P69, Utrecht, July 12-15, (2015)
- [4] M. Németh, Z. Schay, D. Sránkó, J. Károlyi, Gy. Sáfrán, I. Sajó and A. Horváth: *A metán száraz reformálásának vizsgálata hordozós katalizátorokon*, MKE 2. Nemzeti Konferencia, előadás, Hajdúszoboszló, aug. 31 - szept. 2, (2015)

SUPPORTING THE INTEGRATION OF RESIDENTIAL SOLAR PHOTOVOLTAICS WITH THE USE OF HYBRID ENERGY STORAGE

Károly Bodnár, Endre Börzsök, Csaba Dücső, Bálint Hartmann, Veronika Oláhné Groma, Erika Tunyogi

Objective

The objective of the research is to identify the potential advantages of battery-supercapacitor hybrid energy storage systems over conventional battery energy storage, when applied at residential level, supporting the integration of solar photovoltaics. It is also to be examined, whether the use of the hybrid system is capable to extend the cycle lifetime of the batteries, thus decreasing the levelized cost of electricity (LCOE) in the system.

Methods

The laboratory setup consists of two separate systems, where one is a stand-alone battery and the other is a hybrid system. Sonnenschein SB 12/60 A gel batteries, a PB-300 charger and a 58F 12V Maxwell supercapacitor were used. The discharge patterns are generated by a Gwinstek PEL-2002 programmable electronic load. Measurement data (voltage, current and temperature of the battery and the supercapacitor, time) are recorded by a NI-USB 6341 OEM data acquisition card. Three measurement setups are created: initial condition measurement of the batteries with constant current charging and discharging, and pulse load discharging of the battery-supercapacitor hybrid system. In the latter case 9 discharge pulses are generated with uniform duty cycle, then the measurement is taken during steady state operation.

The research tasks in connection with the use of energy storage include condition measurement of the batteries, which provides us the opportunity to examine the effect of various operation strategies on the state and the expected lifetime of the battery. Both charge and discharge characteristics of the batteries are recorded, taking into consideration the effect of the supercapacitor as well.

The research tasks in connection with solar energy generation include the analysis of measurement data, logged on site at KFKI Campus, between 1 July 2014 and 26 February, 2015 with a temporal resolution of 15 minutes. Effects of different meteorological parameters (global, direct and diffuse radiation, humidity, temperature) are also taken into consideration. These data are compared to residential electricity consumption data, to determine the coincidence of production and consumption, which values can be used to determine the typical charge and discharge power of the energy storage system.

Results

Electricity generation data of the solar photovoltaic system has been analysed in detail. Average daily electricity generation was 6.24, 5.50, 8.03 kWh, with a maximal value of 23.98, 21.46, 25.58 kWh, in case of system #1, #2 and #3, respectively. These electricity generation patterns were compared against residential consumption data, thus typical daily charge-discharge operation could be determined. These values can also be interpreted as if the battery was discharged with different C ratings during the day. By generating the probability density function of the 15 minute average discharge currents, we estimate the number of cycles when discharge current will equal different C ratings during the lifetime.

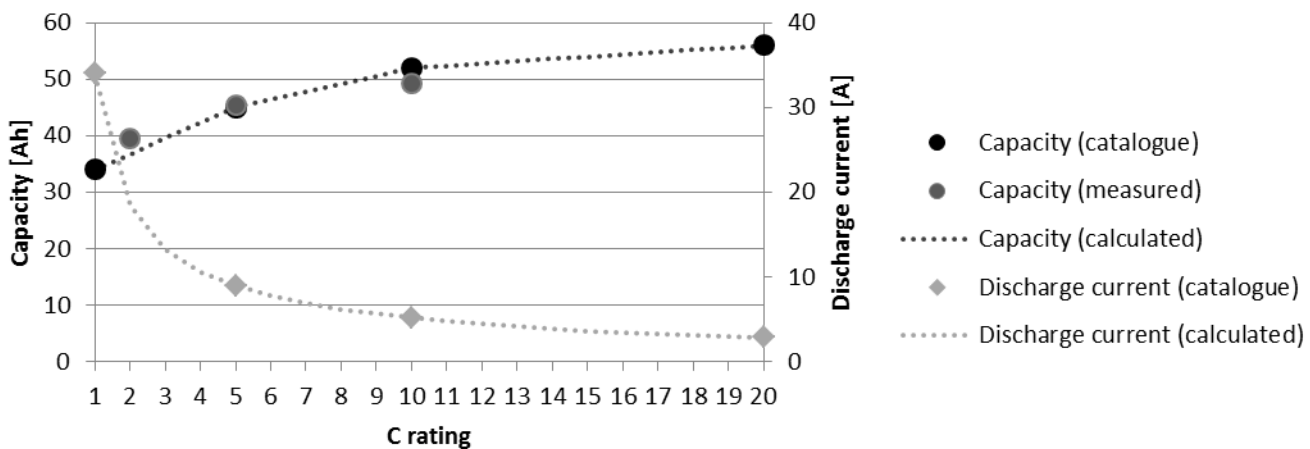


Figure 1: Result of initial condition measurements (C_2 , C_5 and C_{10}) plotted against catalogue data

Remaining work

Due to unexpected shortages of the human resources (participation of three researchers was time-limited) and delayed procurement of devices, measurements aiming to determine the lifetime differences between the stand-alone battery and the hybrid system are to be finished in 2016. A proposal will also be prepared on the future educational and demonstration use of the laboratory setup.

SURVEYING METHODS FOR DEVELOPMENT OF RENEWABLE ENERGY POTENTIAL

Bálint Hartmann, Attila Talamon

Objective

The objective of the KEOP 7.9.0/12-2013-0017 „Energy map (E-map)” project is to create a national scale “energy map”, which provides a foundation for the programming period of 2014-2020 in source-planning and implementation works by containing the summary of the regional energy data from all available statistical databases, as well as providing input data for planning by sectors using geospatial methods. The current renewable energy related primary databases are not suited to be used for a territorial data report, and the available applications do not contain the necessary information for responsible decision making. The present project aims to create a methodology in sync with the main European Union and national regulations and strategical documents, which is suitable to survey the theoretical, technological and economic potential of different renewable energy sources on a micro-regional level.

Methods

The initial estimation data of renewable energy sources are similar, as they are based on easily measured physical parameters (radiation energy, wind speed, water flow, and geothermal gradient). Thus the theoretical potential calculated from the aforementioned data is suited to quantify the physically available amount of energy. The base set defined by the theoretical potential can be used in developing several subsets.

One of these subsets is the ecologically sustainable potential (potential of different type of renewable energy and their ecological aspects), which is a definition closely connected to the goals of the project. It specifies the known energy amount which the already existing, as well as future projects can depend on. Another commonly used subset of the theoretical potential is the economic potential, which in accordance with its name quantifies the amount of renewable energy that can be utilized cost-efficiently. The intersection of the economic and ecological sets is called, in short, the sustainability potential, which is sustainable from both economic and environmental points of view. In addition to the above terms the convertible potential should be mentioned, which shows the proportion of energy demand that can be served by the available sources and known technologies.

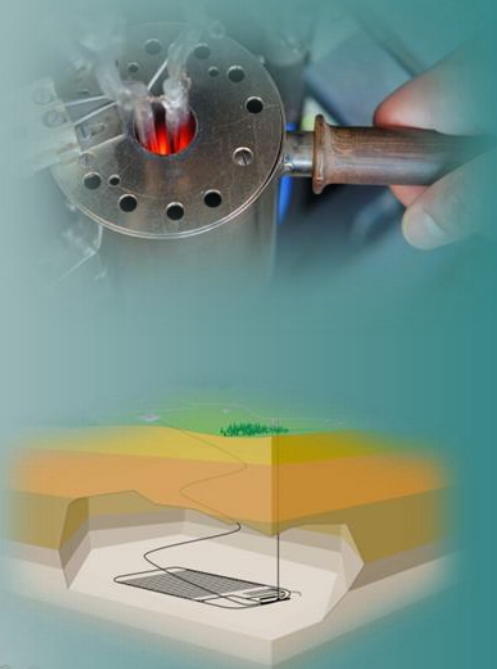
Results

The output information was used to create an interactive map, which can support the future projects and responsible decision making related to sustainable energy planning.

Related publication

- [1] A. Talamon, V. Sugár and B. Hartmann: *Fine adjustment of heating system design parameters considering the Urban Heat Island Effect in case of Hungary*, 2016 International Conference on Engineering and Natural Science – Summer Session Conference (2016.07.12-14.)

VI. ENERGY SAVING AND ENVIRONMENT STUDIES



DEVELOPMENT OF HIGHLY ENERGY-EFFICIENT DATA CENTRE INFRASTRUCTURE

Endre Börcsök, Csaba Farkas, Bálint Hartmann, Szabina Török, Veronika Oláhné Groma

Objective

The design of a complex power supply infrastructure and the satisfaction of the concentrated high energy demand is a constant challenge for data centre owners. Furthermore, economics of the operation and ideas of sustainability are getting lately more and more attention. A new concept was created: green data centres are designed to minimize the effect on the natural environment. One of the primary goals of such units is to decrease the energy needs both for the computing infrastructure and the supporting systems (e.g. thermal management), which can be achieved by increasing the efficiency of processes and/or by integrating renewable energy sources.

The research is based on ongoing development cooperation between the MTA Centre for Energy Research and Persecutor Ltd., supported by the Hungarian Government's "PIAC_13" programme. The project aims to develop a new, highly energy efficient data centre infrastructure, which is able to supply IT needs at a high-level, while minimizing power losses and exploiting the potential of locally available renewable energy sources. Two focus areas are the use of energy storage in data centres and decreasing power losses in the distribution and power conversion infrastructure. After extensive review of the literature, evaluation criteria are defined in both topics to allow the future owner of the data centre to properly compare different technology and topology options.

Methods

The project is well-aligned to the international trends, aiming to develop green data centre infrastructures. The difference is that in our case energy efficiency related to the information and communication technology (ICT) is not part of the investigations, and infrastructure issues are put into focus. The first phase of the project defined the boundary conditions of the research by evaluating possible energy sources and infrastructure location taking into consideration both strengths and weaknesses. The general energy model of a data centre was also defined, and a map of future locations was generated. These are later utilised, when evaluating the use of different energy sources based on their nature and local availability.

The second and third phase of the project laid more emphasis on technical questions of the research; technological processes, operational models, installed equipment and materials are selected. Possible use of energy storage was examined from several aspects, like efficiency, lifetime and maturity. Tools to decrease power in the distribution infrastructure were selected.

Results

Results considering energy storage has shown that means of both heat and electricity storage could be successfully applied in a data centre environment to decrease peak needs and to significantly decrease operation costs of the infrastructure. Results considering power losses have clearly proven that the majority of losses is generated by low loading of the elements of the technological chain, especially the UPS.

Remaining work

The final phase focuses on the implementation of the results of previous phases. Detailed proposals are elaborated for selected geographical locations, determining maximal and optimal size of the data centre infrastructure.

Related publications

- [1] B. Hartmann and Cs. Farkas: *Energy Efficient Data Centre Infrastructure – Development of a Power Loss Model*, Energy and Buildings **127**, 692–699 (2016)

HYDROXYL RADICAL REACTION WITH MONURON

Viktória Mile, Ildikó Harsányi, Krisztina Kovács, Tamás Földes, Imre Pápai, Erzsébet Takács, László Wojnárovits

Objective

The present work focuses on the aromatic ring hydroxylation of monuron using quantum chemical calculations because previously the experimental results established that the main (initial) process of decomposition of monuron is the reaction between monuron and $\cdot\text{OH}$ forming hydroxycyclohexadienyl radical.

Methods

The computational analysis was performed using Density Functional Theory (DFT) methods. Becke's three parameter hybrid functional was used with the Lee-Yang-Parr correlation extension, generally known as B3LYP. The standard 6-311G++(d,p) basis set was applied for geometry optimizations. In all cases, the nature of the located stationary points was verified through vibrational frequency calculations. The electronic energy was refined by single-point energy calculations at the B3LYP/6-311G++(3df,3pd) level. The Gibbs free energies are reported for $T = 298.15$ K. The calculations were performed with the Gaussian program package. In some cases, the Solvation Model Density (SMD) solvent model was applied in order to model the aqueous media.

Results

The computed Gibbs free energies ($\Delta_r G$) and free energy barriers (ΔG^\ddagger) of hydroxylation reactions on the aromatic ring (in gas phase) are collected in Table 1. All reactions are found to be clearly exergonic. The thermodynamic preference of product formation is exceptional for $\cdot\text{OH}$ attack in the *para*-position. The barriers vary between 30 and 42 kJ mol⁻¹ except for *ortho*2 reaction, where ΔG^\ddagger of hydroxylation is significantly lower. These results point to very fast reactions. In the *ipso*-, *ortho*- and *meta*-reactions, simple addition with hydroxycyclohexadienyl type radical formation takes place. Based on lower energy barriers and Gibbs free energies, the *ortho*-addition is preferred to *ipso*- and *meta*-addition in agreement with the experimental results obtained for smaller molecules containing electron donating group similar to monuron.

Table 1: Thermodynamic, kinetic and structural properties of $\cdot\text{OH}$ reactions with the aromatic ring of monuron at 298.15 K. $\Delta_r G$: Gibbs free energy, ΔG^\ddagger : activation free energy (relative to reactants), d_1 and d_2 : C- $\bullet\text{O}$ distance in the transition state and in the product, respectively.

| Possible positions of attack. | Position | $\Delta_r G / \text{kJmol}^{-1}$ | $\Delta G / \text{kJmol}^{-1}$ | $d_1 / \text{\AA}$ | $d_2 / \text{\AA}$ |
|-------------------------------|----------------|----------------------------------|--------------------------------|--------------------|--------------------|
| | ipso | -30.2 | 42.3 | 2.01 | 1.42 |
| | ortho 1 | -35.5 | 31.5 | 2.00 | 1.44 |
| | ortho 2 | -40.3 | 16.1 | 2.12 | 1.46 |
| | meta 1 | -19.2 | 38.8 | 2.00 | 1.45 |
| | meta 2 | -20.8 | 32.1 | 2.02 | 1.45 |
| | para | -155.9 | 39.5 | 2.07 | 1.26 |

The results obtained for the *para*-reaction strongly depend on whether the calculations were carried out for gas phase reactions, or the solvent effect was also considered. The presence of solvent modifies the relative energies significantly, through a stabilization mechanism of the formed radical or product and affects the outcome of the reaction as well. Without using the implicit water model, the end product of *para*-reaction is a phenoxyl type radical (HCl elimination). Applying the water model, OH/Cl substitution takes place. In a subsequent reaction, a phenoxyl type radical may form (Cl elimination). According to the experimental results, the yield of phenoxyl radicals is estimated to be somewhat smaller than the yield of chloride release.

Remaining work

To provide more insight into the mechanism further calculations are necessary, paying special attention to the effects of water medium. Similar calculation in case of anilin, fenol, fenuron, diuron are in progress (few calculations are required). The summary of these calculations will be published soon.

Related publication

- [1] K. Kovács, S. He, V. Mile, T. Földes, I. Pápai, E. Takács and L. Wojnárovits: *Ionizing radiation induced degradation of monuron in dilute aqueous solution*, Radiation Physics and Chemistry **124**, 191–197 (2016)

VITRIFICATION – DEVELOPMENT OF GLASS MATRICES FOR HIGH-LEVEL RADIOACTIVE WASTES

Margit Fábián, Felicián Gergely, János Osán

Objective

The final and safe storage of radioactive waste materials is nowadays an existing problem to be solved urgently. The most feasible and accepted way for storage of high-level radioactive waste (HLW) is the vitrification process, where the active elements are melted and poured into glass form.

Methods

During the project more than 15 glass samples were successfully prepared using a high-temperature furnace that was put into operation last year. The glasses were melted under atmospheric conditions, at temperatures between 1350 and 1450°C in platinum crucibles. The atomic structure of the glasses was studied by diffraction and spectroscopic techniques. The elemental composition was verified by X-ray fluorescence method. Pressed pellets prepared from the crushed samples were investigated using molybdenum anode X-ray tube and molybdenum secondary target. The nominal and the measured values were found to be the same within ~1%. Neutron diffraction (ND) experiments were performed on the PSD neutron diffractometer ($\lambda_0=1.068 \text{ \AA}$) at the 10 MW Budapest research reactor in the momentum transfer range $Q=0.5-10 \text{ \AA}^{-1}$. Data were corrected for detector efficiency, background scattering and absorption effects. The total structure factor, $S(Q)$ was calculated by local software packages. The ND experimental $S(Q)$ data have been simulated by the reverse Monte Carlo (RMC) method, which is a widely used effective tool to model disordered structures. The RMC minimizes the squared difference between the experimental $S(Q)$ and the calculated one from a 3-dimensional atomic configuration.

Results

Simple and multi-component borosilicate and molybdate glassy samples were studied. Based on the experience of our previous studies, new glassy samples were synthesized with the so-called 'Matrix' of composition 55SiO₂-10B₂O₃-25Na₂O-5BaO-5ZrO₂ (mol%); into which the model compounds were added as oxides. The first series contained 90 (70) w% Matrix and 10 (30) w% UO₃, CeO₂ or Nd₂O₃. Another successful preparation was the sample series with UO₃ added to the matrix; the final glassed contained 10, 20, 30, 35 and 40 w% UO₃. Transuranium elements are not available, therefore lanthanides chemically modeling them were used. Ce stays for the hazardous radioactive Pu, while Nd for Am and Cm. Samples were prepared from oxides: SiO₂ and B₂O₃ (¹¹B isotope) are strong network formers; Na₂O is a network modifier; BaO and ZrO₂ serve both as network modifier, glass and hydrolytic stabilizers. ND measurements indicate that the new compositions are stable glassy samples, no crystalline phase was detected. The convergence of the RMC calculation was good and the final $S(Q)$ matched very well the experimental structure factor (Figure 1). From the RMC simulation several first and second neighbour partial atomic pair-correlation functions, $g_{ij}(r)$ and coordination number distributions, CN_{ij} have been revealed with a fairly good stability and statistics. Figure 2 presents most important partial pair correlation functions, $g_{Si-O}(r)$, $g_{B-O}(r)$, $g_{U,Ce,Nd-O}(r)$ for the different concentrations. The atom pairs responsible for building up the glassy network show characteristic first neighbour distributions.

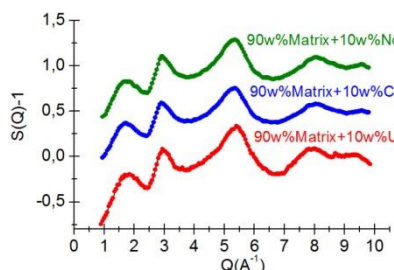


Figure 1: ND structure factor of glassy samples, experimental data (marks) and RMC simulation solid line.

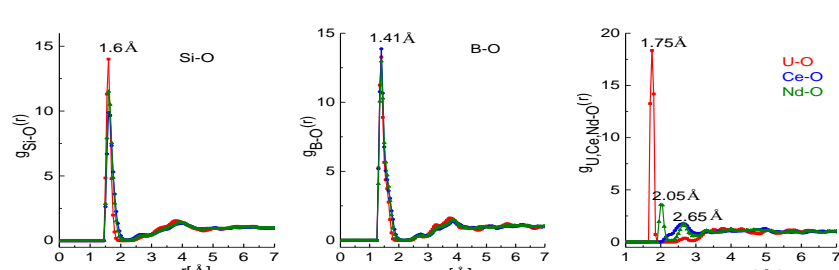


Figure 2: The Si-O, B-O and U,Ce,Nd-O partial atomic pair correlation functions from RMC modeling, for Matrix-10U (red), Matrix-10Ce (blue) and Matrix-10Nd (green).

Coordination number distributions were calculated from RMC modelling. The average oxygen coordination number around Si atoms is very close to 4, as proposed by the formation of tetrahedral units in the network. The average B-O coordination number suggests that the glassy network consists of trigonal and tetrahedral boron units. It was found that the first neighbour distances do not depend on the dopant. This result demonstrates that the basic matrix network structure is stable, the added U, Ce and Nd are structurally well integrated. Further data treatment for the new compositions is in progress.

For the high-concentration uranium samples we have established that the studied Matrix can incorporate maximum 40 w% UO₃. Samples containing 45 w% UO₃ became crystalline.

Remaining work

The evaluation of the chemical-physical glass properties and the leachability tests are in progress.

Related publications

- [1] M. Fabian and Cs. Araczki: Basic network structure of SiO₂-B₂O₃-Na₂O glasses from diffraction and reverse Monte Carlo simulation, Physica Scripta **91**, (2016)
- [2] M. Fábián: Managing nuclear waste 1-2., Fizikai Szemle LXV, **7-8**. 241-244 and **9**. 311-314 (2015)

PREPARATION, STRUCTURAL STUDIES AND OPTIMIZATION OF OXIDE GLASSES FOR HIGH LEVEL WASTE STORAGE APPLICATIONS

Margit Fábián

Objective

The aim of the project is to synthesize novel glass matrix for long term storage of radioactive waste materials, and to determine the atomic structure of these new glass compositions. Due to the hollow structure of glasses, the radioactive elements are linked into the network structure, and the dissolved radionuclides become strongly bonded to the glass and therefore become isolated from the biosphere. This report summarizes the activity of the 2nd year of an OTKA three years long project. As a first step, I established a small radiochemistry laboratory for preparation of glassy materials, the research in the past year was focused on the sample preparation and evaluation of experimental measurements.

Methods

The glassy samples were prepared by melt-quenching technique. The glasses were melted under atmospheric conditions, at temperatures between 1350 and 1450°C in platinum crucibles. Neutron diffraction (ND) experiments were performed at the 10 MW Budapest research reactor using the PSD neutron diffractometer, $\lambda_0=1.068\text{\AA}$, $Q=0.6\text{--}10\text{\AA}^{-1}$ and on the 7C2 diffractometer at the LLB-Saclay, $\lambda_0=0.726\text{\AA}$, $Q\sim16\text{\AA}^{-1}$. The powder specimens were filled in thin walled cylindrical vanadium sample holder. Data were corrected for detector efficiency, background scattering and absorption effects. The total structure factor, $S(Q)$ was calculated by local software packages. Simultaneous reverse Monte Carlo (RMC) simulation of the two diffraction data sets was applied to generate reliable 3D atomic configurations and, to calculate the partial atomic pair correlation functions, nearest neighbour distances and coordination number distributions. The RMC simulation box contained 10000 atoms and the usual constraints were applied, i.e. atomic density, cut-off distances and connectivity.

Results

During the work we studied simple and multi-component borosilicate/molybdate glasses. I had synthesized new glassy sample series containing lanthanides used as elements chemically representing actinides, which are difficult to access. I had deeply investigated the basic structure of molybdates which are also a possible structure for conditioning of HLW. The studied systems: $50\text{MoO}_3\text{-}25\text{Nd}_2\text{O}_3\text{-}25\text{B}_2\text{O}_3$, $(100-x)\text{MoO}_3\text{-}30\text{Nd}_2\text{O}_3\text{-}x\text{B}_2\text{O}_3$, $x=30, 50\text{ mol\%}$ and $x\text{MoO}_3\text{-}50\text{ZnO}\text{-}(50-x)\text{B}_2\text{O}_3$, $x=10, 20, 30\text{ mol\%}$. The fit of the RMC calculations was good, the final $S(Q)$ s matched very well the experimental ones, as shown in Fig. 1.

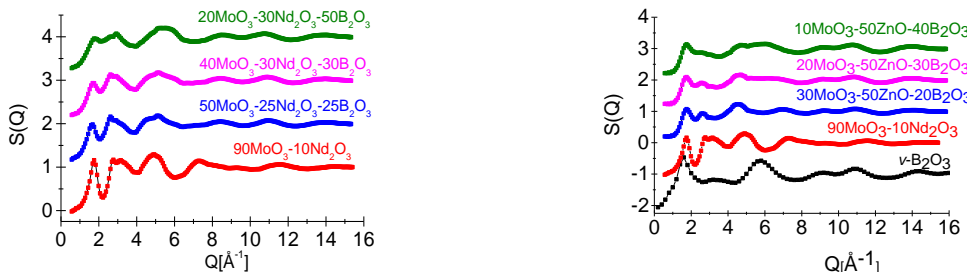


Figure 1: Neutron diffraction structure factor of molybdate samples. The binary $v\text{-B}_2\text{O}_3$ and $90\text{MoO}_3\text{-}10\text{Nd}_2\text{O}_3$ glasses are also displayed to help the interpretation of the observed changes: experimental data (symbols) and RMC simulation (solid line).

From the RMC modelling the partial atomic correlation functions $g_{ij}(r)$ and the coordination number distributions CN_{ij} have been revealed. In case of Mo-Nd-B system the ratio of $\text{MoO}_4/\text{MoO}_6$ increases with decrease of MoO_3 concentration. BO_3 and BO_4 groups are formed, and with increasing B_2O_3 content conversion of BO_4 to BO_3 takes place. Medium range order was established by mixed $\text{MoO}_4\text{-BO}_4$, BO_3 linkages besides the pronounced Mo-Mo and B-B second neighbour correlations. For the Mo-Zn-B system, it was found, that the first neighbour distances do not depend on concentration within error of limit. ZnO proved to be a network former, not a modifier as it is often reported in the literature for similar systems. From the analyses of the obtained structural parameters we have concluded that the glassy network is formed by trigonal BO_3 and tetrahedral BO_4 , MoO_4 , ZnO_4 groups. Concentration dependence was found for the BO_4/BO_3 fraction, it increases with increasing B_2O_3 content. We have concluded that only small amount of boroxol rings are present and it is supposed that the network is formed by organization of BO_3 and BO_4 groups into superstructure units. The BO_3 and BO_4 units are linked to MoO_4 or ZnO_4 , forming mixed ${}^4\text{Mo-O-}{}^3\text{B}, {}^4\text{Mo-O-}{}^4\text{Zn}, {}^3\text{B-O-}{}^4\text{Zn}$ bond-linkages. Significant medium-range order exists up to $\sim 7\text{\AA}$.

Remaining work

The next step will be the structure study of the new samples and optimization of glassy samples containing lanthanides as actinides elements.

Related publications

- [1] M. Fabian, E. Svab and K. Kiril: *Network structure with mixed bond-angle linkages in $\text{MoO}_3\text{-ZnO-B}_2\text{O}_3$ glasses: neutron diffraction and reverse Monte Carlo modelling*, *J. Non-Cryst. Solids* **433**, 6-13 (2016)
- [2] M. Fabian, E. Svab and K. Kiril: *Network structure of molybdate glasses by neutron and X-ray diffraction and reverse Monte Carlo modelling*, *Journal of Physics: Conference Series* **746**, 012068 (2016)

RAPID METHOD FOR SEPARATION OF ^{241}Am AND OTHER ACTINIDES ON DGA RESIN BY EXTRACTION CHROMATOGRAPHY

Márton Zagyvai, PhD student, Supervisor: Nóra Vajda, D.Sc., RADANAL Co. Ltd.
Consultant: László Szentmiklósi, Ph.D.

Objective

Our purpose was to develop new methods for separation of actinides for α -spectrometry which are faster than the procedures known from literature.

Methods

DGA® is a commercially available resin that contains N,N,N',N'-tetra-n-octyldiglycolamine on inert support. Am, U, Pu and Th are separated by extraction chromatography based on DGA resin. A previously applied method was simplified by omitting digestion and preconcentration steps before DGA resin separation. 200 mL of urine samples acidified with HCl to 4M were loaded on to a 0.5 g DGA column. α -sources of different actinides were prepared by coprecipitation with NdF₃; measurements were performed with Si α -detector. Model experiments with only one actinide were combined with LSC measurements. Method performance was checked by comparison. Effect of carbamide was investigated with ¹⁴C-spiked carbamide.

Results

A series of model separations were implemented. The method was not efficient for separation of Th but proved successful for Am, Pu and U (Table 1). The method was tested on urine samples taken from workers exposed to Am incorporation related to an incident at the Radioactive Waste Processing and Storage Facility (RWPSF) Püspökszilág (Table 2).

Table 1: Chemical recoveries of actinides in model experiments

| loading solution | spike | Recovery % | | | |
|---------------------|---------------|------------|-----|----|------|
| | | U | Th | Pu | Am |
| urine | Am-241 | | | | 6-80 |
| urine | Pu-241 | | | 67 | |
| urine | U-238 | 100 | | | |
| urine | Th-230 | | <10 | | |
| water | Am-241 | | | | 100 |
| water+2g carbamide | Am-241 | | | | 80 |
| water+10g carbamide | Am-241 | | | | 27 |
| urine | α -mix | 74 | 9 | 66 | 84 |

It was observed that Am was more difficult to be eluted from DGA resin in the presence of carbamide, the yield decreased with increasing amount of carbamide as an increasing part of the Am remained fixed on the column (Fig. 1). Using ¹⁴C-spiked carbamide it was confirmed that a part of carbamide was irreversibly fixed to DGA resin.

Remaining work

Conditions of direct separation of Pu and U from urine samples will be examined; rapid digestion methods (fusion, microwave digestion) will be developed for different matrices; separation of actinides will be examined for soil and sediment samples.

Related publication

- [1] M. Zagyvai, N. Vajda, E. Bokori and Zs. Molnár: *Rapid method for ^{241}Am -separation by DGA resin from human urine*, presentation at Őszi Radiokémiai Napok, 2015. in Őszi Radiokémiai Napok, ISBN 978-963-9970-59-5, 110 (2015)

Table 2: Intercomparison with urine samples originating from RWPSF personnel

| Exp. no. | ^{241}Am measured at the reference laboratory | | ^{241}Am measured in our laboratory | | |
|----------|--|----------|--|----------|------------|
| | mBq/l | unc. (%) | mBq/l | unc. (%) | recov. (%) |
| 10220 | 180 | 5 | 210 | 8 | 43 |
| 10984 | 4,98 | 7 | 12,3 | 24 | 75 |
| 11095 | 22,8 | 3 | 30 | 17 | 73 |
| 11238 | 55,6 | 3 | 50,3 | 11 | 45 |

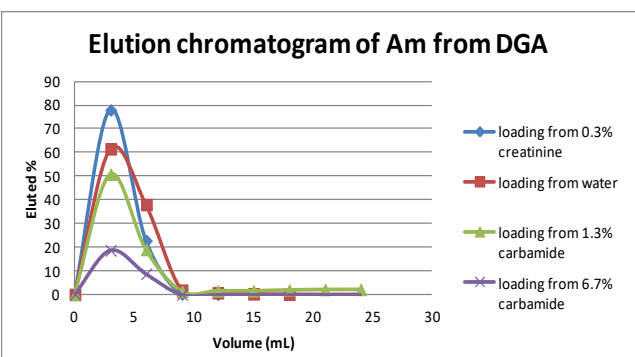


Figure 1: Effect of carbamide on Am separation



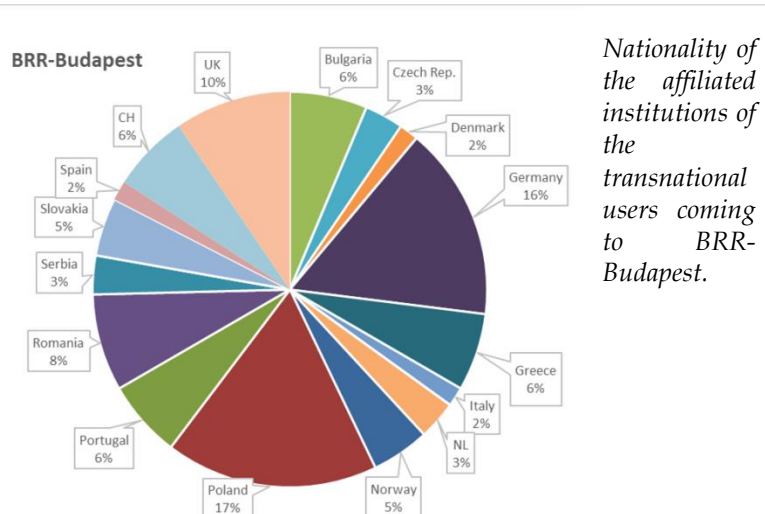
VII. RESEARCH REACTOR



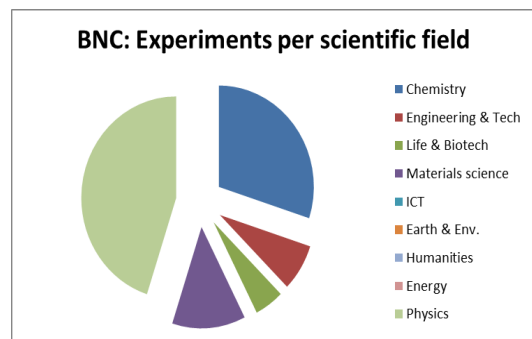
Budapest Neutron Centre - Scientific Utilization of the Budapest Research Reactor

Rózsa Baranyai

The Budapest Neutron Centre (BNC) coordinates the scientific utilization of the research reactor and makes available its facilities to the international neutron user community through the peer-review arrangement. BNC is a member of the European network of neutron centres and a partner in the EU FP7 Framework Programme NMI3-II - Integrated Infrastructure Initiative for Neutron Scattering and Muon Spectroscopy. 2015 was the last year of this 4 year programme. During this period a total of 63 users conducted 53 experiments requiring 317 days of beam time at BNC. Users came from almost 20 different countries to conduct experiments in Budapest, and stayed for an average of seven days.

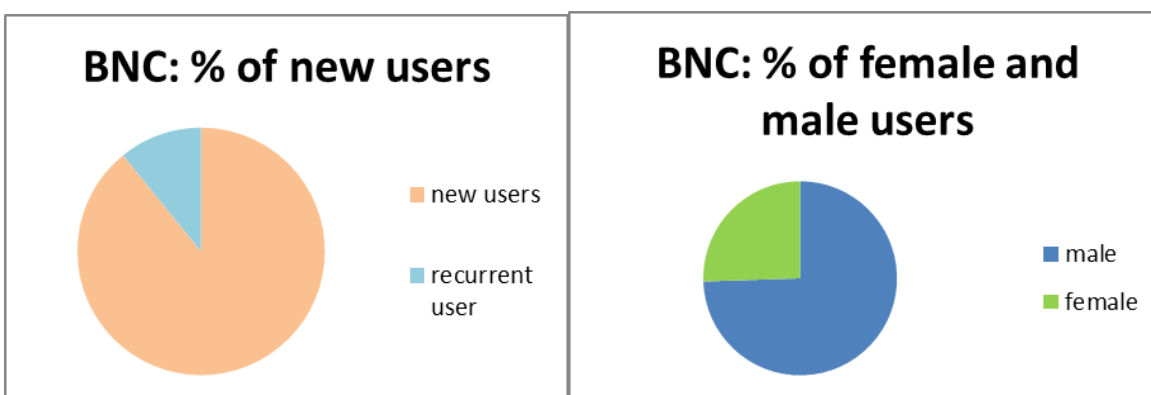


Nationality of the affiliated institutions of the transnational users coming to BRR-Budapest.



Majority of the projects carried out on BNC's facilities belongs to physics, chemistry and material sciences.

NMI3-II support attracted new scientists to BNC, with 83% of users using the facility for the first time. A quarter of the users were female, more than half of which were early-career researchers.



A total of 17 publications resulted from the experiments, till April 2016.

A significant development occurred in BNC's access programme since BNC joint to NMI3. We could adopt high standards in our operation which have already been introduced in the main European neutron centres. The proposal system and services provided to the users were improved and the result of this progress was that the number of proposals increased significantly.

Last year, two new EU supported programmes started; IPERION - Integrated Platform for the European Research Infrastructure ON Culture Heritage and SINE2020 - Science and Innovation with Neutrons in Europe in 2020. BNC is strongly involved in these programmes.

University education and professional training are important tasks for BNC. We focus on the training of the future professionals, for that reason we organize the Central European School on Neutron Scattering yearly. This school gives an introduction to the neutron techniques with a special emphasis on the hands-on-training at BRR's facilities.

In the frame of EERRI (Eastern European Research Reactor Initiative), BNC together with the Budapest University of Technology and Economics organized the 11th Group Fellowship Training Course on Research Reactors for 11 participants from developing countries. These nuclear training programmes are also supported by the International Atomic Energy Agency.

APPLICATIONS OF PROMPT GAMMA ACTIVATION ANALYSIS

Zsolt Kasztovszky, László Szentmiklósi, Boglárka Maróti, Szandra Szilágyi, Ildikó Harsányi

Objective

It was aimed to apply the prompt gamma activation analysis to determine the samples' elemental composition. Research was performed in the fields of catalysis, material science, geochemistry and archaeometry. Within the project, the activities related to an OTKA and the EU-funded NMI3-II projects were supported, too.

Methods

Principally, PGAA and NIPS facilities at a cold neutron guide of the Budapest Research Reactor were used to determine the elemental compositions of various samples. As complementary methods, NORMA and RAD imaging facility, in-situ catalytical characterization, and NAA were applied. A comparative study between PGAA, NAA and portable XRF has started on sets of obsidian and glass samples. The results are under evaluation.

Results

Chemical catalysis

- With a customized in-beam catalysis setup at the PGAA station, we are able to determine slight changes in the surface and bulk elemental compositions of catalytic materials in operation. These measurements are on-going since 2008, in close collaboration with the Fritz-Haber Institute, Berlin, and from this year on also with the ETH Zurich. This year we extended the scope to HBr oxidation and compared the results to earlier data for HCl reaction. The results were published [1].
- Composition of bimetallic SiO_2 supported Au-Cu catalysts and Ru and Ir containing Ti mesh monolith catalysts have been determined in co-operation with the Surface Chemistry and Catalysis Department (~25 spectra). Results are being published.

Material science

- In-situ chemical alteration has been measured on dental implantation material (Glass Ionomer Cements - GICs) that is already used in clinical practice or under development.
- Test measurement on orthodontic archwires made of Ti-Ni alloy was carried out.
- We analysed a set of LiNbO_3 samples by PGAA and NAA for Wigner FK.

Archaeometry

- Partly related to a project supported by the Hungarian Scientific Research Fund (OTKA), compositions of stone axes made of metamorphic rocks have been studied. A large set (more than 110) nephrite, serpentinite, greenschist, etc. archaeological and geological samples from Hungarian museums and from fieldwork have been analysed. The aim of the study is to identify the origin of the raw materials (i.e. provenance of the objects).
- A unique collection of radiolarite (a sedimentary rock type) raw material from Bosnia-Herzegovina has been measured and the data were incorporated to an expanding raw material database. New obsidian geological samples from Imbreg (Slovakia) have been collected and analysed, too.
- Earlier silver-coin, pottery and bronze measurements were published [2-4]
- A few silver artefacts has been investigated by various non-destructive methods (PGAA, in-beam NAA, NR, μ XRF, pXRF, PIXE) – as case studies for future participation in the "Seuso-project" [10].
- Compositions of a few archaeological iron objects (oriental knives and daggers) and ceramic fragments have been measured.

Geochemistry

- We have continued analysis of terrestrial lava flow samples from Antarctica (Deception Island) using PGAA in a framework with a Polish Scientific Cooperation. In the meantime, selected samples have been measured by NAA.
- With NAA and PGAA, we took part in an IAEA round-robin project on a set of WEPAL soil and plant samples.
- In cooperation with ELTE Institute of Geology, 6 bauxite samples have been analysed (MSc thesis of Péter Kelemen).
- A newly discovered rock from Cserhát, Hungary has been investigated. The rock is considered as peculiarity –due to its extremely high boron content that can be easily observed on neutron radiography image and by PGAA as well.

Remaining work

We wish to continue applications of PGAA related to thematic research projects (OTKA) and also ad hoc proposals coming from international TNA users (NMI3, IPERION CH, C-ERIC). Complementarity study of the available methods (PGAA, NAA, NR and XRF) requires further work as well.

Related publications

- [1.] M. Moser, G. Vilé, S. Colussi, F. Krumeich, D. Teschner, L. Szentmiklósi, A. Trovarelli and J. Pérez-Ramírez: *Structure and reactivity of ceria-zirconia catalysts for bromine and chlorine production via the gas-phase oxidation of hydrogen halides*, J. Catal. 331 128–137 (2015)
- [2.] J. Corsi, B. Maroti, A. Re, Zs. Kasztovszky, L. Szentmiklósi, M. Torbagyi, A. Agostino, D. Angelici and S. Allegretti:

Compositional analysis of a historical collection of Cisalpine Gaul's coins kept at the Hungarian National Museum, Journal of Analytical Atomic Spectrometry **30**, 730-737 (2015)

- [3.] V. Kiss V, K.P. Fischl, E. Horváth, G. Káli, Zs. Kasztovszky, Z. Kis, B. Maróti and G. Szabó: *Non-destructive analyses of bronze artefacts from Bronze Age Hungary using neutron-based methods*, Journal of Analytical Atomic Spectrometry **30**, 685-693 (2015)
- [4.] M.I. Prudêncio, M.I. Dias, C.I. Burbidge, Zs. Kasztovszky, R. Marques, J.G. Marques, G.J.O. Cardoso, M.J. Trindade, B. Maróti, F. Ruiz, L. Esteves, M.A. Matos and A. Pais: *PGAA, INAA and luminescence to trace the "history" of "The Panoramic View of Lisbon": Lisbon before the earthquake of 1755 in painted tiles (Portugal)*, Journal of Radioanalytical and Nuclear Chemistry **304**, AiP-7 (2015)
- [5.] S. J. Sztáncsuj, K.T. Biró, Zs. Kasztovszky, S. Józsa, K. Gmélíng and B. Maróti: *Lithic Implements At Ariușd (Erősd) A Preliminary Report*, Communications Archaeologiae Hungariae, 19-36 (2014)
- [6.] Zs. Kasztovszky and B. Maróti: *Ezüsttárgyak neutronos vizsgálatának lehetőségei és nehézségei*, Archeometriai Műhely **12**, 25-31 in Hungarian (2015)
- [7.] E. Starnini, Gy. Szakmány, S. Józsa, Zs. Kasztovszky, V. Szilágyi, B. Maróti, B. Voytek and F. Horváth: *Lithics from the Tell Site Hódmezővásárhely-Gorza (Southeast Hungary): Typology, Technology, Use and Raw Material Strategies during the Late Neolithic (Tisza Culture)*, Archäologie in Eurasien **31** 18. 2. **15**, 115-138. (2015)
- [8.] Zs. Mráv, Zs. Kasztovszky, Z. Kis, B. Maróti, I. Kovács, Z. Szőkefalvi-Nagy, Gy. Káli, K. Pánczél-Bajnok, L. Rosta and E. Mitcsenkov-Horváth: *Késő római ezüstleletek archeometriai vizsgálata*, Research Report in Hungarian (2015)
- [9.] S. Szakáll, F. Kristály, Zs. Kasztovszky and B. Maróti: *Vulkáni eredetű borátásvány a Cserhátból*, VI. Kőzettani és Geokémiai Vándorgyűlés Ópálos, 2015. szeptember 10-12. in Hungarian (2015)
- [10.] Zs. Kasztovszky, Z. Kis, B. Maróti, D. Párkányi, L. Szentmiklósi, I. Kovács, Z. Szőkefalvi-Nagy, Gy. Káli, K.P. Bajnok, L. Rosta and J. Osán: *Ezüst tárgyak archeometriai vizsgálata roncsolásmentes nukleáris módszerekkel - A Seuso kincsek kutatási programjához kapcsolódó nagyműszeres előkísérletek* – BNC Research report in Hungarian (2016)

PROVENANCE STUDY OF LITHIC RAW MATERIALS OF STONE TOOLS FOUND IN THE CARPATHIAN BASIN

Zsolt Kasztovszky, György Szakmány, Zsolt Bendő, Katalin T. Biró, András Markó, Bálint Péterdi, Szandra Szilágyi, Ildikó Harsányi

Objective

Prompt Gamma Activation Analysis (PGAA) has been successfully applied to investigate various lithic assemblages, chipped and polished stone tools made of obsidian, flint, radiolarite, and greenschist-metabasite varieties (high-pressure metamorphite, nephrite, serpentinite, greenschist). The absolute non-destructive feature of PGAA is highly capitalised in the study of intact museum pieces. The present report is about the fourth year of an OTKA* project, with a focused aim to map, analyse and characterise prehistoric resources, taking into consideration contemporary geographical and social endowments in the Central European region, as well as „long distance” raw material sources known to have played important role in the European prehistoric exchange network. The expected results will contribute essentially to the knowledge on the system of contacts of the prehistoric communities by fingerprinting, characterising and tracing important lithic resources like obsidian, radiolarite, flint, high-pressure metamorphites, serpentinite and nephrite. The originally four-year project has started in April 2012, and will finish – after one year extension – in 2017.

Methods

The research plan equally consists of geological sample collection on field work, conventional petrography (macroscopic and microscopic investigations), as well as instrumental analytical measurements. The leading analytical method applied is PGAA, mainly because of its absolutely non-destructive character. PGAA is applicable to quantify all the major components and some trace elements in the lithic material. It is unique in determination of the elements H and B. Occasionally we perform complementary measurements using portable XRF, INAA and EPMA. Other very important new method, the non-destructive SEM-EDX analysis was developed, partly in the framework of the current OTKA project. Besides PGAA, it has become a significant method to study the elemental and mineralogical composition of polished stone tools.

Results

In the fourth year of the present project, we have continued the work with PGAA investigations of archaeological and geological samples made of various rocks from Hungary and – thanks to field works organized within the project, from Romania and Bosnia. We have measured 123 polished stone objects (axes and hammers) made of serpentinite, hornfels, greenschist and blueschist, which have been selected from the historical Miháldy- and Ebenhöch collections exhibited in several Hungarian Museums. Most of the objects have been analysed by complementary SEM-EDX, too. Because of the lack of local raw material sources, these stone tools are considered as typical examples of long distance trade in prehistory. Thanks to the analytical results, in many cases their provenance was possible to identify, e.g. hornfels probably originate from the Apuseni mts. or from the Southern Carpathian.

We have finished the PGAA measurements of the obsidian and silex chipped stone tools from a Copper-Age culture of Erősd, which is represented in settlements of Eastern Transylvania and over the Carpathian mountains, Romania. In 2016, further 40 chipped stone archaeological pieces will be analysed by PGAA, which originate from the excavations in Borvízoldal, Málnásfürdő, Oltszem, Eastern Carpathians.

We have analysed an 18 samples set of radiolarite raw material, which has been collected during a field-work in Bosnia Herzegovina (Movrica, Maslovare-Teslic, Gracanica, Vranjak, Kozuhe and Stanic Rijeka sites). This unique study will contribute to the identification of “border-zones” of raw material supply for tool production in the prehistoric Carpathian basin.

Finally, we have performed a methodological study on a large selection of obsidian raw materials. We have analysed around 80 representative samples from the major European-Mediterranean sources by PGAA and portable XRF. Additionally, a limited 17 piece set was analysed by NAA at the BNC. We aimed to demonstrate the benefits and limitations of the above methods. The data evaluation and publication is in progress. A special variety of “mahogany” obsidian was studied in more details by Mössbauer-spectroscopy and electron-microscopy, too.

Altogether, approximately 200 samples – both artefacts and raw materials – have been measured on PGAA and NIPS-NORMA stations of the Budapest Research Reactor in 2015.

Remaining work

In the final year (2016), we wish to organize an on-field collection of raw materials in Slovakia and Austria to complete the analytical studies (PGAA, SEM-EDX, NAA), and finally to make our comparative database available for further research.

Related publications

- [1] B. Péterdi, Gy. Szakmány, Zs. Bendő and Zs. Kasztovszky: *Nefrit kőeszközök kőzettani vizsgálata roncsolásmentes módszerekkel: típusok, lehetséges nyersanyag-források azonosítása (előzetes eredmények)*, Miskolci Régészettudományi Konferencia, Miskolc, 2015.04.01-02. talk - in Hungarian (2015)
- [2] Zs. Bendő, Zs. Szakmány, I. Oláh, Zs. Kasztovszky, K. T. Biró and A. Osztás: *Nagynyomású metaofiolit nyersanyagú csiszolt kőeszközök magyarországi leletanyagokban*, Miskolci Régészettudományi Konferencia, Miskolc, 2015.04.01-02. talk - in Hungarian (2015)
- [3] B. Péterdi, Gy. Szakmány, Zs. Bendő, Zs. Kasztovszky, K. T. Biró and G. Gil: *Nephrite artefacts in Hungary - The present state of knowledge*, Abstract of 6th MSCC 6th Mineral Sciences in the Carpathians Conference Veszprém, Hungary, 16-19 May, 2015 - Acta Mineralogica-Petrographica, Abstract Series 9, 53 (2015)
- [4] Zs. Bendő, Gy. Szakmány, Zs. Kasztovszky, K. T. Biró, I. Oláh and A. Osztás: *High pressure metaophiolite polished stone artefacts from Hungarian archaeological localities and collections*, Abstract of 6th MSCC 6th Mineral Sciences in the Carpathians Conference Veszprém, Hungary, 16-19 May, 2015 - Acta Mineralogica-Petrographica, Abstract Series 9, 3 (2015)
- [5] Gy. Szakmány, Zs. Bendő, B. Péterdi, Zs. Kasztovszky and K. T. Biró: *Prehistoric "greenstone" artefacts from Hungarian archaeological localities and collections*, Abstract of 6th MSCC 6th Mineral Sciences in the Carpathians Conference Veszprém, Hungary, 16-19 May, 2015 - Acta Mineralogica-Petrographica, Abstract Series 9, 62 (2015)
- [6] B. Péterdi, Zs. Bendő, Gy. Szakmány, Zs. Kasztovszky, Sz. Szilágyi, I. Harsányi, V. Mile and K. T. Biró: *Serpentininit nyersanyagú csiszolt kőeszközök magyarországi régészeti leletanyagokban* - In: E. Pál-Molnár, B. Raucsik and A. Varga, (Eds.): *Meddig ér a takarónk? A magmaképződéstől a regionális litoszféra formáló folyamatokig*, 6. Kőzettani és Geokémiai Vándorgyűlés Kiadványa, Ópálos, 2015. szeptember 10-12, SZTE Ásványtani, Geokémiai és Kőzettani Tanszék, 93. in Hungarian (2015)
- [7] Gy. Szakmány, Zs. Bendő, S. Józsa, Zs. Kasztovszky, V. Szilágyi, B. Maróti, Sz. Szilágyi, E. Starnini and F. Horváth: *Hornfels nyersanyagú csiszolt kőeszközök magyarországi régészeti leletanyagokban* - In: E. Pál-Molnár, B. Raucsik and A. Varga, (Eds.): *Meddig ér a takarónk? A magmaképződéstől a regionális litoszféra formáló folyamatokig*, 6. Kőzettani és Geokémiai Vándorgyűlés Kiadványa, Ópálos, 2015. szeptember 10-12, SZTE Ásványtani, Geokémiai és Kőzettani Tanszék, 102-105. ISBN: 978-963-306-389-7. in Hungarian (2015)
- [8] Zs. Bendő, Gy. Szakmány, Zs. Kasztovszky, Sz. Szilágyi, V. Mile, I. Harsányi, K. T. Biró, A. Osztás and I. Oláh: *Nagynyomású metaofiolit nyersanyagú csiszolt kőeszközök magyarországi régészeti leletanyagokban* - In: E. Pál-Molnár, B. Raucsik and A. Varga, (Eds.): *Meddig ér a takarónk? A magmaképződéstől a regionális litoszféra formáló folyamatokig*, 6. Kőzettani és Geokémiai Vándorgyűlés Kiadványa, Ópálos, 2015. szeptember 10-12, SZTE Ásványtani, Geokémiai és Kőzettani Tanszék, 36-39 in Hungarian (2015)
- [9] Zs. Bendő, Gy. Szakmány, Zs. Kasztovszky, I. Harsányi, K. T. Biró, A. Osztás and I. Oláh: *Jadeitit és egyéb nagynyomású metaofiolit nyersanyagú csiszolt kőeszközök Magyarországon*, Az MTA X. Osztály Geokémiai, Ásvány- és Kőzettani Tudományos Bizottságának Archeometriai Albizottsága előadónapja Budapest, 2015.11.10. talk - in Hungarian (2015)
- [10] B. Péterdi, Zs. Bendő, Gy. Szakmány, Zs. Kasztovszky and K. T. Biró Katalin: *Magyarországon előforduló serpentinit nyersanyagú csiszolt kőeszközök kutatásának előzetes eredményei*, Kőkor Kerekasztal, Miskolc, 2015.12.11. talk - in Hungarian (2015)
- [11] Gy. Szakmány, Zs. Bendő, Zs. Kasztovszky, I. Harsányi, K. T. Biró and F. Horváth: *Contact metamorphic rocks as long distance import raw materials of Prehistoric polished stone tools in Hungary*, Abstract book of "Raw materials exploitation in Prehistory: Sourcing, processing and distribution", Faro, Portugal, 2016.03.10-12., 95 (2016)
- [12] Zs. Bendő, Gy. Szakmány, Zs. Kasztovszky, K. T. Biró, I. Oláh, A. Osztás and I. Harsányi: *Jades and related HP greenstone polished stone implements from Hungary*, Abstract book of "Raw materials exploitation in Prehistory: Sourcing, processing and distribution", Faro, Portugal, 2016.03.10-12., 94. (2016)
- [13] B. Péterdi, K. T. Biró and Z. Tóth: *Domoszló: Grinding stone and millstone production center in Hungary*, Abstract book of "Raw materials exploitation in Prehistory: Sourcing, processing and distribution", Faro, Portugal, 2016.03.10-12., 123 (2016)
- [14] S. J. Sztáncsuj, K. T. Biró, Zs. Kasztovszky, S. Józsa, K. Gmélíng and B. Maróti: *Lithic Implements At Ariușd (Erősd) - A Preliminary Report*, Communications Archaeologiae Hungariae 19-36 (2014)
- [15] Zs. Bendő, Gy. Szakmány, Zs. Kasztovszky, B. Maróti, Sz. Szilágyi, V. Szilágyi and K. T. Biró: *Results of non-destructive SEM-EDX and PGAA analyses of jade and eclogite polished stone tools in Hungary*, Archeometriai Műhely, XI. 4, 187-205 (2014)
- [16] B. Péterdi, Gy. Szakmány, Zs. Bendő, Zs. Kasztovszky, K. T. Biró, G. Gil, I. Harsányi, V. Mile and Sz. Szilágyi: *Possible provenances of nephrite artefacts found on Hungarian archaeological sites (preliminary results)*, Archeometriai Műhely, XI. 4, 207-222 (2014)

NON-DESTRUCTIVE ANALYSIS OF METALLIC SAMPLES USING PGAA AND COMPLEMENTARY METHODS

Boglárka Maróti, László Szentmiklósi, Tamás Belgya

Objective

To combine different non-destructive methods in the scientific analysis of valuable objects - including archaeological artefacts and material science samples -, in order to obtain the most reliable results considering the non-destructiveness and the representativeness of the applied method, and the immediate availability of the samples after measurement.

Methods

For near-surface compositional analysis, XRF technique was applied using the Olympus Delta Premium InnovX type handheld device. For the bulk elemental composition determination, prompt gamma activation analysis (PGAA) was used. Since PGAA is less sensitive for trace elements and minor components, different PGAA setups were tested examining the measuring time required and the performance of the analytical information. Different PGAA setups were compared in order to achieve the best signal-to-noise ratio. Pilot imaging experiments were carried out on pure metal samples and on certified alloy standards using the NORMA station with cold and thermal neutron beam in order to calculate and compare the linear absorption coefficients.

Results

Since Compton-background depends on the number of the high-energy peaks and their energy and intensity, the same radioactive sources (59 keV line of Am-241; 569, 1063 and 1770 keV lines of Bi-207) were used to assess the signal-to-noise ratio (where signal is the specific count rate in the peak and noise is the specific count rate in the background under the peak). Setup equipped with a good neutron and gamma shielding resulted in the best signal-to-noise ratio up to 1 MeV. The setup was successfully used to determine the elemental composition of Ru and Ir containing Ti mesh monolith catalysts.

If we have prior information about the examined samples, neutron imaging techniques can be indirectly used to estimate the compositional differences in a heterogeneous object. In order to reduce the disturbance effect of the neutron scattering, the metal sheets were placed to the neutron screen in close-geometry. The radiography images were corrected by the open beam images and the closed beam images using Igor Pro software, and an average of higher amount grey values were estimated using ImageJ software. We concluded that at least 1 mm thickness is necessary to achieve sufficiently precise data (Fig. 1 b). Pure metal sheets with different neutron absorption characteristics could be reliably distinguished (Fig. 1 a).

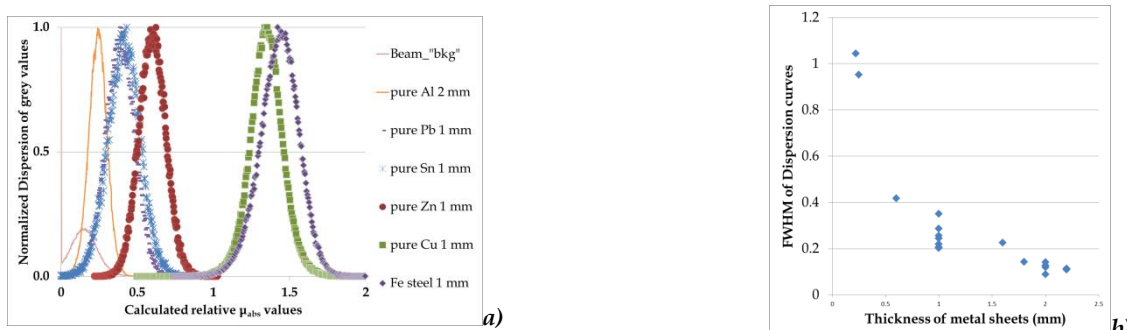


Figure 1: a) apparent linear absorption coefficient (μ_{abs}) values of several pure metals at the NORMA beamline, b) FWHM of the gray value distribution curves in function of the metal sheet thickness.

The composition (or differences in the elemental compositions) can be indirectly concluded from the calculated linear absorption coefficients.

Remaining work

To summarize the results obtained by different setups and techniques.

Related publications

- [1] J. Corsi, B. Maróti, A. Re, Zs. Kasztovszky, L. Szentmiklósi, M. Torbágyi, A. Agostino, D. Angelici and S. Allegretti: *Compositional Analysis of a Historical Collection of Cisalpine Gaul's Coins Kept at the Hungarian National Museum*. Journal of Analytical Atomic Spectrometry **30**, 730 (2015)
- [2] A. Tungler, E. Szabados, D. F. Sránkó, F. Somodi, B. Maróti and S. Kemény: *Wet oxidation of dimethylformamide via designed experiments approach studied with Ru and Ir containing Ti mesh monolith catalysts* Journal of Industrial and Engineering Chemistry **34**, 405-414 (2016)
- [3] B. Maróti, L. Szentmiklósi and T. Belgya: *Compton-suppressed low energy germanium (LEGe) detector for metal analysis by PGAA*, Abstract at 25th Seminar on Activation Analysis and Gamma Spectroscopy (SAAGAS), 02. 23-25. Aachen, Germany, (2015)
- [4] B. Maróti, L. Szentmiklósi and T. Belgya: *Application of a High-Resolution Germanium Detector in the Analysis of Metallic Samples* in: Szentmiklósi L (Edt.) Ószi Radiokémiai Napok. 80-85. (ISBN: 978-963-9970-59-5) / Vértes Attila Különdíj/ (2015)

RADIOGRAPHY AND TOMOGRAPHY AT CHANNEL NO. 2 OF BRR

Zoltán Kis, László Horváth, László Szentmiklósi

Objective

To develop multimodal (neutron, X-ray and gamma) imaging instrumentation and methodology at channel No. 2 of Budapest Research Reactor. The RAD radiography station gives a possibility to study relatively large objects, and to benefit from the complementary features of the different radiations.

Methods

In 2015 the RAD station has been upgraded by a *portable X-ray unit*. The new unit together with the older ones makes it possible to cover a wider voltage range (5-300 kV) than before. That is important for delicate imaging, e.g. thin materials as paintings, electronic parts, etc. *Reference samples* were imaged by neutrons at both RAD and NORMA stations to be able to compare the effects of the different neutron energy spectra. The completion of measurements with *two modalities* in delicate imaging was accomplished by fulfilling the requests from Hungarian National Museum to perform neutron and X-ray *imaging of historical bronze objects* (spearheads, a round shield). For the *ANCARA supercritical loop* neutron imaging was carried out in "wet" and "dry" conditions for the area around a thermocouple. "Wet" condition means that the loop was filled up with water during the heating process; "dry" condition means that the loop was heated in its empty state, without water. Subtracting the belonging dry image from the wet one creates theoretically an image showing (apart from some scattering effects) the water only.

Results

The basic parameters of the *new X-ray unit* have been measured. Moreover, the necessary *configuration setups* for the various imaging conditions (for the available screens with different optical and electronic setup of the RAD) were elaborated and standardized. The *reference samples'* investigations show that thicker materials with lower contrast could be imaged with comparable exposure times at the RAD and NORMA stations, respectively.

As a result from the *two-modality imaging*, the neutron image of a *spearhead* revealed that the hollow in the head is filled with different materials not seen in the X-ray images (Fig. 1). It means that all of them should be some kind of organic material, an important knowledge for the archeologist.

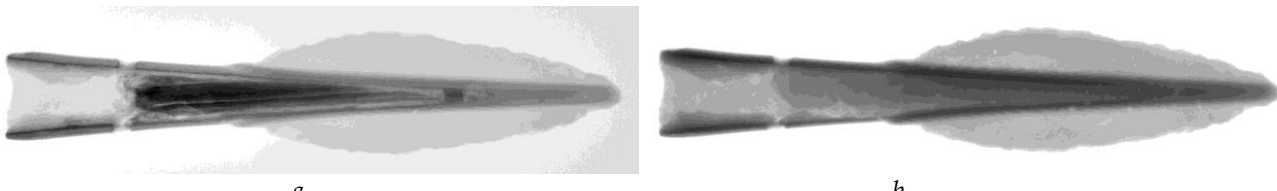


Figure 1: (a) The neutron (a) and X-ray (b) attenuation images of the bronze spearhead showing the different materials.

Theoretically the neutron attenuation is decreasing as the temperature of the materials increases. This behaviour was demonstrated with the evaluation of the successive neutron radiographic images of the *ANCARA loop* when its temperature and pressure were increased from 50 C to 355 C, and from 1 bar to 250 bar, respectively.

Remaining work

One of the main outcomes of the work with the new, high resolution imaging system was that the *vibration effects* from the reactor hall limit the reachable spatial resolution. The solution of this problem creates a new task for the future. The *neutron tomography measurements of the IAEA test objects* will be postponed next year because of the delay in sample's fabrication. To avoid the deterioration of the camera system, there is a need to use a *more thermal beam*. To fulfil this demand the characteristics of the neutron beam has to be changed by applying a sapphire filter. The purchase and the installation of the crystal were postponed.

Related publications

- [1] Z. Kis, L. Szentmiklósi, T. Belgya, M. Balaskó, L. Z. Horváth and B. Maróti: *Neutron based imaging and element-mapping at the Budapest Neutron Centre*, Physics Procedia **69**, 40-47 (2015)
- [2] Z. Kis and B. Maróti: *Report on the pilot PGAA and NR measurements of selected bronze objects from the Hungarian National Museum*, Kutatási jelentés, MTA EK-NAL-2015-141-1-1-M0 (2015)
- [3] Z. Kis and B. Maróti: *Report on the Pilot XRF and NR Measurements of a Selected Bronze Shield from the Hungarian National Museum*, Kutatási jelentés, MTA EK-NAL-2015-141-1-2-M0 (2015)
- [4] A. Kiss, M. Balaskó, L. Horváth, Z. Kis and A. Aszódi: *Experimental investigation of the thermal hydraulics of supercritical water under natural circulation in a closed loop*, Annals of Nuclear Energy **100**, 178–203 (2017)

SELECTED APPLICATIONS OF MÖSSBAUER SPECTROSCOPY

Károly Lázár, Sándor Stichleutner

Objective

Applications of Mössbauer spectroscopy are presented with primary aims on studying porous and nanodisperse systems.

Methods

Studies are primarily based on ^{57}Fe and ^{197}Au Mössbauer spectroscopies, complemented with other suitable techniques.

Results

^{57}Fe spectroscopy

Earlier results obtained on micro- and mesoporous ferrisilicates are summarized in a review article. Primary aim is laid on the comparison of close environments of iron in micro-, and mesoporous structures. In microporous systems the structure is dominantly crystalline, whereas mesoporous substances comprise amorphous regions as well. This feature is reflected in corresponding Mössbauer spectra, too [1]. Studies performed on microporous zeolite (LTA) have been complemented with another nuclear method, namely with positron annihilation studies on structural damages induced by 2.5 MeV proton irradiation [2]. Modification and thermal transformations of starting synthesis gel of iron-LTA were the subjects of another study. In particular, stages of formation of iron-mullite, a high temperature refractory material, were monitored in cooperation with colleagues from Ruder Boskovic Institute, Croatia [3].

Study of formation of iron oxyhydroxide aerogels has been commenced recently in cooperation with the colleagues from the Inorganic Chemistry Department of University of Debrecen. Low density and high specific surface area iron oxyhydroxide aerogels can be prepared by hydrolysis of iron salts carried out in organic solvents in presence of limited amount of water. For preparation of aerogels the organic media should be removed by extraction with supercritical carbon dioxide at the last stage. From our part, first stages of hydrolysis of $\text{FeCl}_3 \cdot 6 \text{ H}_2\text{O}$ were studied in various organic solvents, based solely on the six water molecules per iron, present in the starting crystals. Formation of transient components, stages of gel formation could be followed by recording Mössbauer spectra of frozen samples taken after different interval following the mixing of reaction components. The most demonstrative results were obtained in dimethylformamide. Namely, appearance of two transient components exhibiting exceptionally high quadrupole splitting values (1.3 and 1.6 mm/s) could be demonstrated in the 3 – 80 min interval of formation. Further, significant increase of the probability of the Mössbauer effect could also be observed simultaneously, attesting the progress of oligomerization of primary hydrolysis products. Specific surface area, HRTEM and X-ray studies were in good correspondence with the previous observations. For illustration, the “highlight” figure of Ref. [4] is shown in Fig. 1.

^{197}Au spectroscopy

Gold nanoparticles with 2-3 nm diameter have been stabilized in butyldithiol and were characterized by XRD, TEM, Raman, PAS, FTIR techniques as well. Three types of gold coordination can be distinguished in ^{197}Au spectra [5].

Related publications

- [1] K. Lázár and Á. Szegedi: *Dual, amorphous and crystalline characteristics in pore walls of mesoporous ferrisilicates*, Comprehensive Guide for Mesoporous Materials **2**, Nova Science Publ., 73–96 (2015)
- [2] L.A. Tuyen, E. Szilágyi, E. Kótai, K. Lázár, L. Bottyán, T.Q. Dong, L.C. Cuong, D.D. Khiem, P.T. Phuc, L.L. Nguyen, P.T.Hue, N.T.N. Hue, C.V. Tao and H.D. Chuong: *Structural effects induced by 2.5 MeV proton beam on zeolite 4A: Positron annihilation and X-ray diffraction study*, Radiation Physics and Chemistry **106**, 355–359 (2015)
- [3] I. Buljan, K. Lázár and C. Kosanović: *Preparation and spectroscopic characterization of iron doped mullite*, Croatica Chemica Acta **88**, 171-178 (2015)
- [4] I. Lázár, A. Szilágyi, G. Sáfrán, Á. Szegedi, S. Stichleutner and K. Lázár: *Iron oxyhydroxide aerogels and xerogels by controlled hydrolysis of $\text{FeCl}_3 \cdot 6\text{H}_2\text{O}$ in organic solvents: stages of formation*, RSC Advances **5**, 72716–72727 (2015)
- [5] K. Lázár, E. Kuzmann, S. Stichleutner et al.: *Butyl-dithiol functionalized Au nanocomposite studied by ^{197}Au Mössbauer and other methods*, ICAME 2015 Conference proceedings, 190 (www.icame2015hamburg.de/sites/site_icame2015hamburg/content/e218801/e260088/ICAME2015-All.pdf)

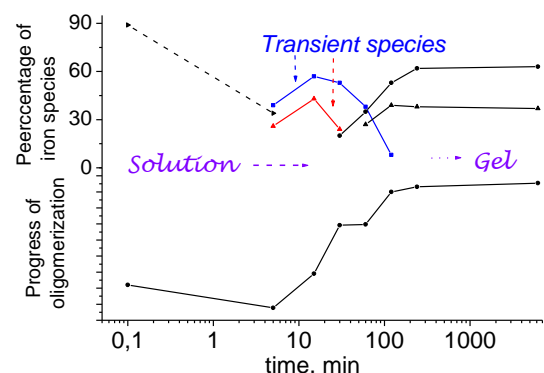


Figure 1: Progress of hydrolysis. Relative percentage of spectral components with appearance of transient species (top). Average probability of the Mössbauer effect in dependence of time (bottom).

PROGRESS IN SEPARATION-METHOD DEVELOPMENT OF LANTHANIDES AND MINOR-ACTINIDES

Dénes Párkányi, László Szentmiklósi

Objective

Radioactive lanthanide isotopes play important role in several fields, such as nuclear fission and nuclear medicine. Some of these nuclides have high fission yields, but they are difficult to measure (DTM) (e.g. Pm-147, Sm-151) due to lack of well-detectable gamma emission. Consequently, chemical separation is necessary to accurately determine them. The lanthanides show chemical similarity to minor actinides (e.g. Am), therefore lanthanide-actinide separation is an important aspect, too. In this year the main objectives were the method development and optimization of the separation process.

Methods

Tracer isotopes of lanthanides (e.g. La-140, Ce-141, Nd-147, Sm-153, Eu-152, Gd-153) were produced by neutron capture at vertical channels of BRR, using its high thermal-neutron flux ($\Phi_{th}=2.0 \times 10^{13} \text{ s}^{-1}\text{cm}^{-2}$), whereas Am-241 was obtained from a standard solution. The requested isotopes were mixed into a model solution. For separation, dyglicolamine (DGA) resin from Triskem was used, packed in a long (approximately $h=280\text{mm}$, $d=3\text{mm}$) separation column. During the year this column was covered from outside with a flow-water thermostat to keep the temperature of the separation column stable and adjustable.

The test isotope mixture was bound in the upper part of the resin in the column. After this step eluted fractions were collected (0.5–1.0 cm³ each). The binding solution was 3 M HNO₃, the elution solution was a diluted acid (0.5–0.1 M HNO₃ and/or 1.5–0.5 M HCl). Generally, the flow rate was 0.2 cm³ per minute.

The isotopes we used so far are well detectable with high-resolution gamma-spectrometry. Therefore the fractions were measured with an ORTEC PopTop 55195-P HPGe detector ("D5") in contact geometry (to increase detection efficiency and to reduce the acquisition time). The gamma spectra were evaluated with Hyperlab 2013.1.

Results

An experimental chromatogram from model solution of lanthanides and americium with the presented method is shown in Figure 1.

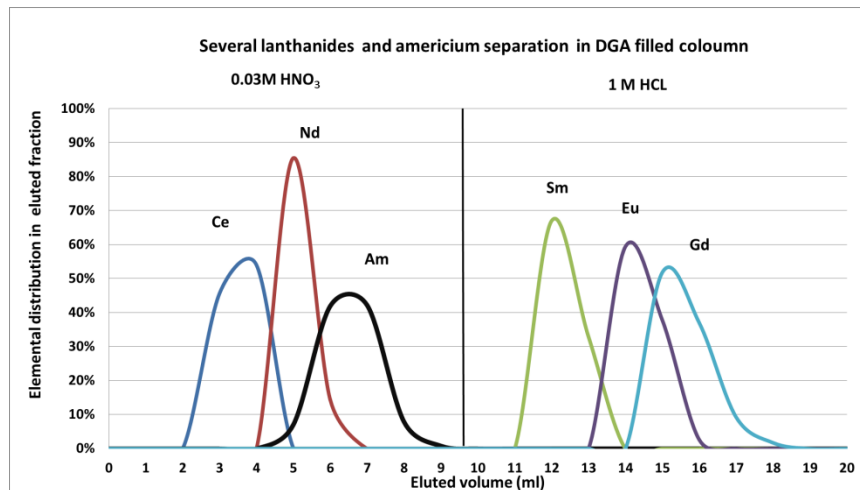
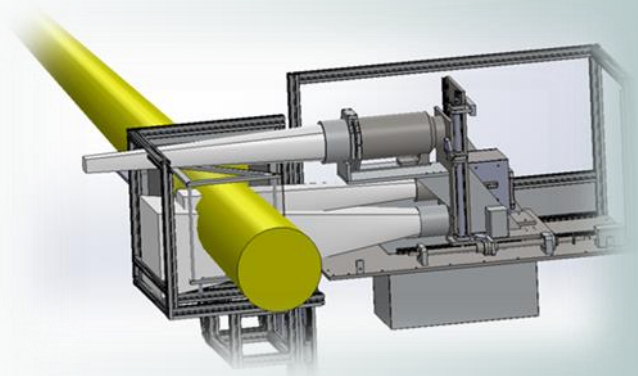


Figure 1: Elution curves for Ce, Nd, Am, Sm, Eu, Gd on the used DGA Column, $T=40^\circ\text{C}$, $v=0.2\text{cm}^3/\text{min}$

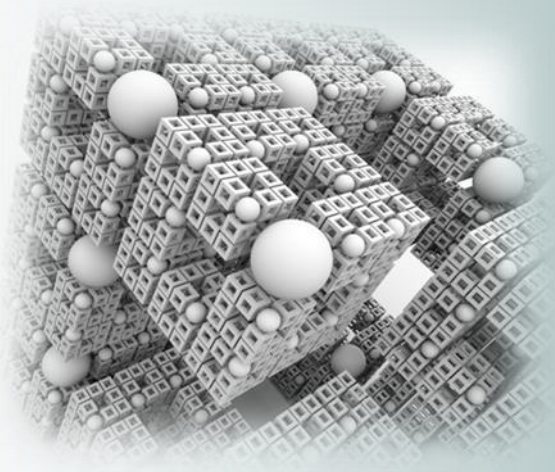
The experiences show that the separation of lanthanides and americium is possible with this rapid method, therefore the separation of long-lived and DTM (e.g. Am-241, Sm-151) nuclides seem quite promising.

Remaining work

Application of this or a similar method to real nuclear waste samples. The separation procedure makes possible to use even more sensitive radioanalytical detection of fractions, such as liquid scintillation counting (LSC) and alpha-spectrometry. Application of ICP-MS would also be useful, as the separation can resolve the main isobaric interferences (Pm-147 vs. Sm-147; Sm-151 vs. Eu-151). PGAA trial measurements of the liquid samples are also foreseen.



VIII. MISCELLANEOUS



EVALUATION OF FRACTURE TESTS USING ADVANCED MODELS

Tamás Fekete, Dániel Antók, Levente Tatár

Objective

The Reactor Pressure Vessels (RPVs) are the lifetime limiting components of a Nuclear Power Plant (NPP) and irradiation embrittlement is the leading ageing mechanism of them. Evaluation of the structural integrity of long term operating RPVs requires an adequate knowledge of fracture mechanical properties of their structural materials in various aged states. Knowledge of the fracture properties of structural materials depends on the evaluation methodology of the material tests. The original surveillance program produced fracture mechanical tests that served as a database for a lifetime extension, but these results now have to be supplemented by further measurement results in order to cover newer aspects of material characterisation required for the later phases of the Long Term Operation (LTO). The main reason of the claim for a need for new measurements is the rapid development of the theory and the numerical methods used for structural integrity calculations of RPVs. Structural integrity calculations are tools to evaluate the safety of flawed or damaged structures. Today, 3D RPV models are commonly used during Pressurised Thermal Shock (PTS) structural integrity calculations. PTS phenomenon can occur when in some accidental situations an extra quantity of cooling water flows into the RPV, causing severe overcooling of the vessel wall. A PTS event can cause a dangerous situation regarding the structural integrity of an RPV, because a high thermal gradient develops through the vessel wall, causing high thermal stresses, which are superposed on the stresses originating from internal pressure. The main goal of PTS calculations is to assess allowable service time of the RPVs from a PTS point of view. Today, there is a chance to bring more advanced theoretical and numerical methods into PTS calculation methodology. But today the evaluation of fracture tests according to current standards are still based on simplified theoretical models and numerical procedures. The inconsistency of the use of different models in the structural integrity calculations and in the evaluation of material tests is incorrect on a theoretical level. Furthermore, it can lead to inaccurate results regarding allowable service time of the RPV.

The goal of the project was to develop and verify an advanced methodology for evaluation of fracture tests, using the same theoretical models of continuum mechanics/thermodynamics and numerical methods that will be used for PTS structural integrity calculations in the future.

Methods

In the modeling part of the project, the methodology of calculations has been developed at MTA EK, applying the theory of configurational forces to fracture mechanics. The theory of configurational forces is a unified theory of nonlinear continuum mechanics and modern nonequilibrium thermodynamics with internal variables. According to the theory of configurational forces, the driving force on a crack tip can be described by the (generalized) J -integral in the case of a more generally behaving (i.e. elastic-plastic), materially inhomogeneous material, independent of the scale of deformation, so the theory can be used for solving problems with large deformations. A 3D finite element model has been developed for the fracture test specimen geometry (Figure 1.). Large deformation plasticity theory was applied in order to model effects of geometrical and material nonlinearities which are present in the system. Flow curves of structural materials were developed from tensile test results. Numerical calculations were performed using the Msc.MARC FEM code. In the experimental part of the project, tensile tests and fracture tests on 3 point bend fracture specimens had been performed.

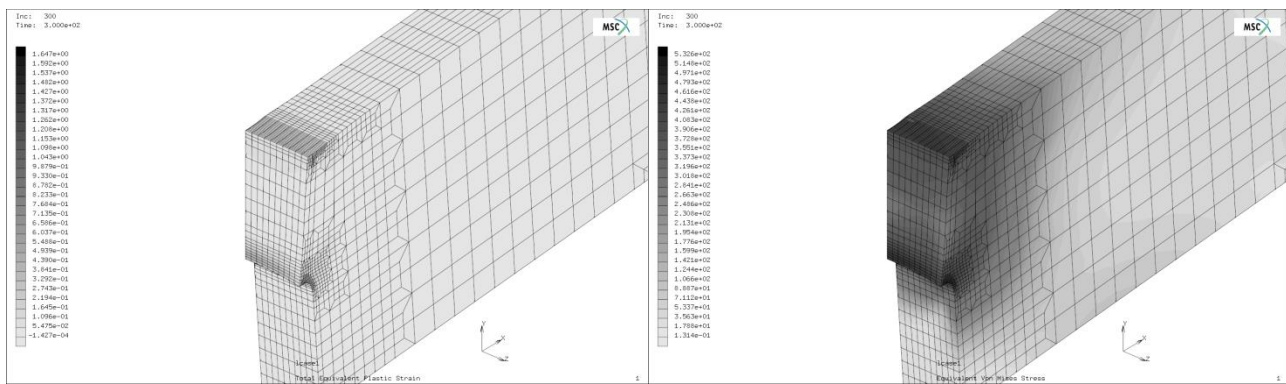


Figure 1: FEM model of a 3 point bend fracture specimen showing equivalent plastic strain field (left) and von-Mises stress field (right) during loading

Results

3D finite element models of the tensile specimens and of the 3 point bend fracture specimens have been developed and tested. During the experiments, tensile tests and fracture tests on 3 point bend fracture specimens had been performed. The experimental and numerical results show better agreement on larger deformation scales than do earlier models found in literature.

Remaining work

Further development of the newly developed methodology is planned using more general constitutive/material models.

AGE-DATING OF URANIUM SAMPLES

András Kocsonya, Cong Tam Nguyen, Koppány Pázmán, László Lakosi

Objective

Identifying provenance of unknown nuclear materials, the age of the sample is a unique signature. Traditionally, age-dating of uranium samples is done by destructive analytical methods, e.g. mass-spectrometry. A decade ago a non-destructive method based on gamma-spectrometry for age-dating of uranium samples was developed in our Department. Due to technical limitations, this method could mostly be applied for high-enriched uranium samples. The extension of the method to low-enriched uranium (LEU) samples depends on the available detection limits. In order to extend capabilities of the method to LEU samples and to improve sensitivity and accuracy, a high efficiency well-type HPGe detector was purchased and installed in 2014. The aim of this project was the extension of the method to lower enriched samples.

Methods

The method of age dating is based on determining the activity ratio of ^{234}U and its progenies. Due to technical reasons, the $^{214}\text{Bi}/^{234}\text{U}$ activity ratio is measured. Since nuclides to be measured are terrestrial radionuclides which occur in the environment and, moreover, ^{214}Bi is a radon-daughter, the proper background subtraction is crucial. The background level and its variance greatly define the available detection limit, therefore their reduction improve the detectability.

In order to reduce the radon-level in a low-background iron chamber, ventilation by N_2 gas of $\sim 1 \text{ m}^3/\text{day}$ flow rate was applied. The ventilated volume was separated within the chamber by polystyrene wall. Due to the applied gas-flow, the intensity of the 609.3 keV line of ^{214}Bi in the background and its variance were decreased.

Relative efficiency calibration was performed on a uranium-ore sample, in which the members of the ^{238}U decay chain are in secular equilibrium with each other. Absolute efficiency of the detector was also measured by single-line gamma emitters (^{58}Co , ^{54}Mn , ^{65}Zn , ^{95}Nb).

Well type detectors have rather large solid angle, consequently – in case of multi-line gamma-emitters with cascade decay (such as ^{214}Bi) – they have significant true gamma-gamma coincidence effect. In order to take into consideration the coincidenceloss, a direct measurement was made to determine the correction factor. A coincidence loss of 55% was measured for the 609.3 keV line if the sample was positioned in the bottom of the well, whereas it was 20 % at the upper surface of the detector cover (0 level).

Whereas the solid angle has a maximum if the sample is in the well, the coincidence effect is the largest here as well. Different measurement positions were tested regarding multiple aspects such as detection limit, signal-to-noise ratio, etc. Due to the two competitive effects mentioned above, the detection limit is nearly constant at a depth interval of -4 to 0 cm in the detector-well. The signal-to-background ratio shows a maximum at the 0 level.

Gamma-spectra were evaluated by the FitzPeaks code. In order to facilitate the calculations a special spreadsheet was constructed.

Results

A general problem of the validation of the method was that no uranium samples of certified age were available. Only samples of minimum age were available.

As first demonstration, an EK-10 nuclear fuel assembly with 10% nominal enrichment from the Training Reactor of the Budapest University of Technology was analysed. An age of 57 ± 6 year was obtained which is a reliable result and does not contradict to the known provenance of the sample. The three samples of the ITWG CMX4 exercise (2 pellets, 1 powder, 2-3% enrichment) were also analysed. Due to the young age of these samples, only upper limit could be determined.

A set of uranium samples, which are stored in the Institute, were analysed by this method. 7 samples are from seizures. 3 samples are from the stock of the Budapest Research Reactor, which are identical to the original fuels of the VVER-440 blocks of Paks NPP. The physical form of these samples were pellets. 3 samples are members of a uranium enrichment standard series (2-5-10%) from the National Bureau of Standards (NBS) in powder form. The date of delivery is known for this samples, however, it means only a lower limit of the age. Age of samples with enrichment >2.5% were determined successfully. For enrichment $\approx 2\%$ the age detection limit is ≈ 20 years. All of these samples were analysed by determining the $^{230}\text{Th}/^{234}\text{U}$ ratio by mass-spectrometry as well. The two results are in good agreement.

Remaining work

The scheduled work for the actual year is finished, however, some more ideas are not yet implemented. Further rejection of the radon-background should be tested by more intensive N_2 flow or by direct ventilation by filtered fresh air. Additional shielding can be tested later within the iron chamber. Due to the low intensities, the testing of these methods is time consuming. Long-term variation of the background could be monitored simultaneously with the measurements by an additional background detector. The implementation of these ideas is depending on the availability of human resources as well.

Related publication

- [1] A. Kocsonya, Zs. Kovács, C.T. Nguyen and L. Lakosi: *Gamma-spectrometric age-dating of uranium samples*, Proceedings of 37th ESARDA Symposium on Safeguards and Nuclear Non-Proliferation, Manchester, UK, 19-21 May (2015)

DIGITAL GEOMETRY

Attila R. Imre

Objective

Upon measurements of perimeter and area for two-dimensional patches, unavoidable errors caused by the violation of translation and rotation invariance can influence the obtained results. These errors are much higher for perimeters, therefore it is advisable to use area-based statistics to describe the size-distribution of patches. One of the "traditional" methods is the so-called Korcak-method. In this project, the result obtained from Korcak method is compared to other, fractal-based methods to show the difference between the various descriptions.

Results

The Korcak-law was one of the examples used by Benoit Mandelbrot to show that fractals are applicable to describe many natural objects and phenomena, and they are not only mathematical monsters. This law was first presented in an empirical form in 1938 for the statistical description of the size-distribution of various geographical objects, including lakes and islands by the Czech statistician, Jaromír Korčák. In the project, the history of the Korcak-theory was revealed. Also, the connection of the Korcak-description with other, fractal-based descriptions was investigated. It was shown, that although there are similarities between fractal-related laws and the Korcak-law, the Korcak-exponent is not directly related to fractal dimension. Therefore one can conclude that the measure introduced by Benoit Mandelbrot based on Korčák's empirical findings is not a fractal measure [1].

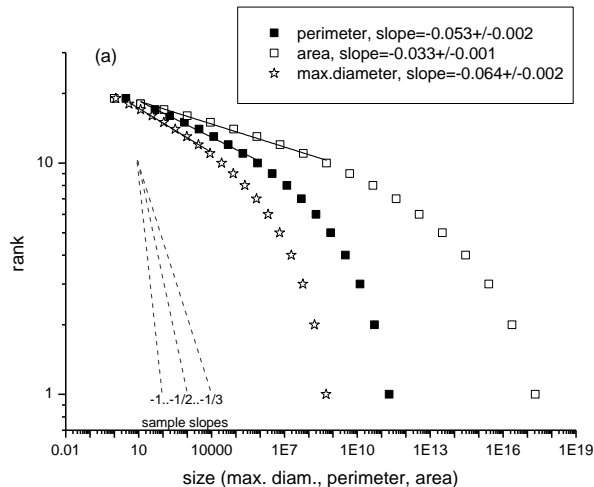


Figure 1: Size-rank diagram for a set of Koch-snowflakes. The data should be fitted with lines for the full size-range, if Korcak- and Haussdorff-fractality would be the same [1].

Remaining work

There is no remaining work in the project.

Related publication

- [1] A. R. Imre and J. Novotný: *Fractals and the Korcak-law: a history and a correction*, European Physical Journal H **41**, 69–91 (2016)

PHASE EQUILIBRIUM; METASTABLE AND SUPERCRITICAL SYSTEMS

Attila R. Imre

Objective

Various processes in energetically relevant fluids were studied, namely the sudden collapse of undercooled or pressurized steam bubbles, the explosive boiling of superheated water and finally some basic adiabatic processes in binary fluid mixtures.

Methods

For sudden steam pocket collapse, WaHa3 code was used. For explosive boiling and adiabatic processes calculations, analytical methods and the ThermoC program were used to calculate stability limits and energy balance.

Results

Modern power technology is facing the need to achieve a good efficiency under partial load. Improving process efficiencies is therefore mandatory, and this means, among others, the optimization of the working fluids. For fine-tuning the working fluids as well as for achieving optimal performance under varying operating conditions, the use of mixed fluids is seriously considered. This means that the processes typical of power plants like adiabatic compressions and expansions, have to be studied for mixtures (see Fig. 1), especially on higher pressure (around and above the critical point) to describe supercritical and high-pressure two-phase adiabats [1].

In a separate project, we investigated steam condensation induced water hammer (CIWH) phenomena. CIWH might happen under certain conditions, when a hot, steam filled pipe is flooded with hot water. Basic map of high probability water hammer regions on a two-dimensional parameter space (L/D vs flooding mass flow rate, where L and D are pipe length and pipe diameter, respectively) were prepared, using WAHA3 code; we are planning to extend this map into the space of other parameters. Such a reliable database would be a great help for future reactor design and construction [2].

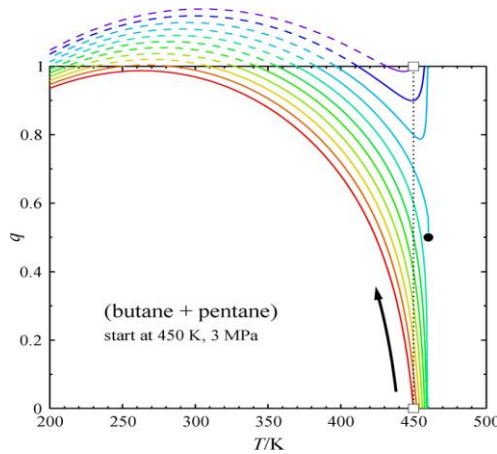


Figure 1: Temperature-vapour ratio diagram for two-phase adiabats in butane-pentane mixtures, with various starting (450 K; 3 MPa) liquid/vapour ratio (red=1...magenta=0; rainbow-encoding) [1]

In working fluids under certain conditions, one might see very fast relaxation processes from metastable state (undercooled steam or superheated liquid) to stable one (equilibrium liquid+vapour). During this processes, relatively high amount of energy will be released in extremely short time range, therefore the energy release can be explosion-like. We tried to give some estimate for the temporal characteristic of adiabatic relaxation processes from metastable to stable states in water/steam under various conditions relevant in nuclear power plants [3].

Remaining work

For working fluid-related research, adiabats for energetically relevant fluids and fluid mixtures should be determined and used to design thermodynamic cycles with higher efficiency. Concerning Condensation-Induced Water Hammer Mapping, we are planning to extend the map to a wider L/D and mass flow rate region, as well as to extend it into a multi-dimensional parameter-space. For explosive processes, more realistic equation of state as well as more realistic models for the dynamics of relaxation processes should be found.

Related publications

- [1] A. R. Imre, S. E. Quinones-Cisneros and U. K. Deiters: *Adiabatic processes in the vapor-liquid two-phase region - 2. Binary mixtures*, Industrial&Engineering Chemistry Research **54**, 6559-6568, (2015)
- [2] I. F. Barna, M. A. Pocsai, A. Guba and A. R. Imre: *Theoretical study of steam condensation induced water hammer phenomena in horizontal pipelines*, Kerntechnik **80**, 420-423 (2015)
- [3] I. Attila: *Kondenzáció és forrás időbeli lefolyásának vizsgálata* (The progress of condensation and explosive boiling), OAH-ABA-38/15-M in Hungarian (2015)

PRELIMINARY NEUTRON ACTIVATION STUDY FOR ESS

Eszter Dian, Zsófia Kókai, Péter Zagyvai, Szabina Török

Objective

The European Spallation Source (ESS) has the goal to be the world's leading neutron source for the study of materials by the second quarter of this century. The generated beam line intensity of the ESS promises higher measurable detector signal; the design of the ESS instruments at a green field site allows for advances in background reduction through the application of advanced modern techniques. Hungary, as one of the partner countries, is taking part in a preliminary study for the selection of potential structural materials to be used in high radiation fields. In this study the effect of remaining activity of neutron activated parts near to the direct beam was examined in terms of radiation background during the lifetime of the facility and for radioactive waste management.

Methods

The focus of the current study is on the potential neutron beam guide materials and the detector materials. The study contains both Monte Carlo simulation and experimental validation. Typical aluminium and borated glass substrates were chosen for neutron beam guides and irradiated at the Budapest Research Reactor (BRR). In this experiment the trace composition of the samples was determined by X-Ray Fluorescent spectroscopy (XRF) and a calculation was carried out to estimate the activity for the expected irradiation based on the XRF measured and also on the nominal composition. The samples were irradiated for 6-12-24 hours in a thermal and a fast vertical neutron channel. HPGe detectors were used to measure the γ -spectra of the irradiated samples. The spectrum analysis was carried out with GSANAL software. The measured γ -activities were compared with calculations made with NAAPro software and further will be compared with MCNP6 simulations.

MCNP6 and GEANT4 calculations were also done for simulation of the particle transport in neutron detectors and the neutron activation of detector filling gases.

Results

The study revealed that there are significant differences in the measured and the nominal trace concentrations of relevant elements in the aluminium substrates. The comparison of the measured and calculated activities showed that the XRF-based trace concentrations usually resulted in $\leq 30\%$ difference but sometimes differed by as much as a factor of three; while the nominal composition did not prove to be reliable to estimate the activity after irradiation (Table 1.).

Table 1: Measured and calculated activity concentrations in aluminium samples

| Isotope | c_A (Bq/cm ³) | | | | | | | | |
|---------|-----------------------------|------------|------------|-------------|------------|------------|-------------|------------|------------|
| | Al sample 1 | | | Al sample 2 | | | Al sample 3 | | |
| | Meas. | Calc.(XRF) | Calc.(Nom) | Meas. | Calc.(XRF) | Calc.(Nom) | Meas. | Calc.(XRF) | Calc.(Nom) |
| Zn-65 | 5.20E+07 | 3.35E+07 | 3.35e+07 | 5.93E+04 | 5.69E+04 | 7.58e+05 | 4.98E+07 | 3.50E+07 | 7.79e+05 |
| Cu-64 | 3.81E+06 | 3.39E+06 | 2.86e+06 | - | 2.46E+04 | 9.03e+04 | 4.02E+06 | 3.37E+06 | 1.37e+05 |
| Ga-72 | 4.38E+04 | 3.40E+04 | 4.19e-01 | 3.15E+04 | 1.66E+04 | 6.39e-03 | - | 3.06E+03 | 9.66e-03 |
| Mn-54 | 4.67E+04 | 7.42E+03 | - | 3.41E+04 | 1.40E+04 | 1.68e+04 | - | 8.74E+03 | 1.76e+04 |
| Fe-59 | 4.59E+04 | 4.13E+04 | - | 4.83E+04 | 4.88E+04 | 5.94e+04 | 4.78E+04 | 4.89E+04 | 9.31e+04 |
| Co-60 | - | - | 3.21e+03 | 8.47E+03 | 1.22E+04 | 2.34e+02 | 1.21E+04 | 3.92E+03 | 1.61e+02 |
| Co-58 | - | - | - | 9.93E+03 | 1.38E+04 | - | - | - | - |
| Cr-51 | - | - | - | 3.95E+06 | 3.72E+06 | 10.00e+06 | 3.09E+06 | 2.03E+06 | 1.89e+05 |

The study proved the importance of the experimental material testing in the selection phase of suitable material in order to avoid the unforeseen operational dose and radioactive waste resulting from neutron activation, and indicated that further collaboration with ESS in the field of material and component testing and detector development is necessary.

Remaining work

Completing present MCNP simulations of the neutron activation of aluminium alloy and borated glass neutron beam guide substrates, and comparison of the upcoming results with the results of the irradiation experiments made for the same samples at BRR.

Related presentations

- [1] E. Dian, F. Gergely, D. Párkányi, P. Zagyvai and Sz. Török: *Neutron activation experiment at BRR*, ESS NMX Workshop, 17 March 2015, Budapest (2015)
- [2] E. Dian, F. Gergely, D. Párkányi, P. Zagyvai and Sz. Török: *Neutron activation experiment at BNC*, Joint ICTP-IAEA Workshop on Nuclear Data, 20-24. April 2015, Trieste (2015)

DEVELOPMENT OF NUCLEAR ANALYTICAL AND IMAGING TECHNIQUES, NUCLEAR DATA MEASUREMENTS AND RELATED TRAINING ACTIVITIES

László Szentmiklósi, Tamás Belgya, Zoltán Kis, Katalin Gmélíng, Boglárka Maróti

Objective

To develop our analytical and imaging capabilities and know-how in PGAA (Prompt Gamma Activation Analysis), PGAI (Prompt Gamma Activation Imaging) / NT (Neutron Tomography) and low-level counting, to accurately determine related nuclear data, and to provide training and education for guest researchers and students.

Methods

(n, γ) measurements, evaluation of data and comparison to literature, computer programming, Monte Carlo modelling, teaching.

Results

The evaluation of the earlier (n, γ) measurements on enriched isotopes of W were completed in collaboration with the Berkeley National Lab. The measured intensities were extended with DICEBOX calculations to make the de-excitation scheme more complete. The results, that are more reliable than others in the literature, and the details of the self-absorption correction were published [1-2]. New data were taken for ^{187}Re isotope. A review paper and a PhD dissertation about the activities within the TANDEM collaboration were published [3, 16]. The slight differences between capture rates measured at Budapest and Garching were identified and accounted for [4]. The capture spectrum of the ^{114}Cd isotope was interpreted with the spectrum unfolding technique [5] whereas contributions were made to the evaluation of ^{77}Se data taken at ILL [6].

In order to generate reliable data for Gen IV reactor design, we measured the prompt fission gamma-rays from $^{239}\text{Pu}(n_{th},\gamma)$ reaction (CHANDA project), in collaboration with Institute for Reference Materials and Measurements (IRMM) Geel and Univ. Hamburg. The 2.4 TB data recorded during the 10 days experiment are still being analysed.

We started to implement digital Compton-suppression with our CAEN N6724 100 MHz digitizer card. This was done in collaboration with a fellow from Eskişehir Osmangazi Üniversitesi, Turkey (Celal Aşıcı), thanks to a CHANDA grant. This might lead to better reduction of the Compton-baseline - that is now in agreement with the *geant4* simulations - and more flexible data analysis options for complex nuclear data measurements.

We managed to fix long-term software instability at the NIPS station and to extend the tomography capabilities of the NORMA station with the transition to 64-bit operation system, device drivers and control software.

We made the proof-of-principle experiment with an upstream-placed graphite scatterer and a pinhole to enhance the spatial resolution and beam homogeneity at the NORMA instrument. An L/D ratio of about 1600 was achieved, compared to the standard value of 233. Following the success of this test, the SUPER-NORMA option will be implemented for the routine use. We published papers about the technical specification of the NORMA facility [7-8] and about the application of the PGAI-NT methodology for nuclear safeguards purposes [9].

At the DÖME low level counting station we worked out a methodology for bulky samples based efficiency and coincidence-correction. We compared the EFFTRAN and ETNA codes for this purpose. The effect of the geometry on the ^{226}Ra equilibrium was tested with horizontal and vertical geometries. During a 9 month measurement campaign, various environmental materials from Angola were measured and the ^{226}Ra , ^{232}Th and ^{40}K activity concentrations were determined [15].

We prepared a book chapter about "Neutron experimental methods in cultural research" to be published by Springer in 2016.

We participated in the domestic and international training of students and scientists:

- 8th Central European Training School on Neutron Scattering: Nuclear Analytical Techniques and Neutron Imaging: lectures and lab exercises
- We hosted undergraduate lab exercises for students from Budapest University of Technology and Economics, ELTE University (5 occasions, altogether about 60 students)
- A newly launched course at ELTE University for geologists: Advanced nuclear analysis methods and their applications in geochemistry research. Lecture slides and lab guides were prepared [10-13].
- Summer training (4 weeks) for a chemist M. Sc. student with PGAA and NAA technique. A continuation as a Master thesis is ongoing.
- Participated in summer training for Saudi students, organized by the Surface Chemistry and Catalysis Dept.
- We prepared 3 training materials (PGAA, NAA, Imaging) and a review paper for the IAEA Compendium on "Research Reactors Utilization for Higher Education Programmes" [14]

Remaining work

The above described international collaborations and development directions are prosperous, thus further experiments and data analysis are foreseen.

Related publications

- A. M. Hurst, N. C. Summers, L. Szentmiklósi, R. B. Firestone, M. S. Basunia, J. E. Escher and B. W. Sleaford: *Determination of the effective sample thickness via radiative capture*, Nucl. Instr. Meth. B **362**, 38–44 (2015)
- A. M. Hurst, R. B. Firestone, L. Szentmiklósi, B. W. Sleaford, M. S. Basunia, T. Belgya, J. E. Escher, M. Krticka, Zs. Révay and N.C. Summers: *Radiative thermal neutron-capture cross sections for the $^{180}\text{W}(n,\gamma)$ reaction and determination of the neutron-separation energy*, Phys. Rev. C **92**, 034615 (2015)
- M. Rossbach, C. Genreith, T. Randriamalala, E. Mauerhofer, Zs. Revay, P. Kudejova, S. Söllradl, T. Belgya, L. Szentmiklosi, R. B. Firestone, A.M. Hurst, L. Bernstein, B. Sleaford and J. E. Escher: *TANDEM: a mutual cooperation effort for transactinide nuclear data evaluation and measurement*, J. Radioanal. Nucl. Chem. **304**, 1359–1363 (2015)
- G. Žerovnik, B. Becker, T. Belgya, C. Genreith, H. Harada, S. Kopecky, V. Radulović, T. Sano, P. Schillebeeckx and A. Trkov: *Systematic effects on cross-section data derived from reaction rates at a cold neutron beam*, Nuclear Instruments and Methods A **799**, 29–36 (2015)
- T. Belgya, R. Massarzyk, L. Szentmiklósi, G. Schramm, R. Schwengner, A.R. Junghans, A. Wagner and E. Grosse: *Combined study of the gamma-ray strength function of ^{114}Cd with (n,γ) and (γ,γ') reactions*, EPJ Web of Conferences, 93 01012 (2015)
- C. Lorenz, R. John, R. Massarczyk, R. Schwengner, A. Blanc, G. de France, M. Jentschel, U. Köster, P. Mutti, G. Simpson, T. Soldner, W. Urban, S. Valenta and T. Belgya: *Neutron-capture experiment on ^{77}Se with EXILL at ILL Grenoble*, EPJ Web of Conferences, 93 01050 (2015)
- Z. Kis, L. Szentmiklósi and T. Belgya: *NIPS-NORMA station – a combined facility for nondestructive element analysis and neutron imaging at the Budapest Neutron Centre*, Nucl. Instr. Meth. A **779**, 116–123 (2015)
- Z. Kis, L. Szentmiklósi, T. Belgya, M. Balaskó, L.Z Horváth and B. Maróti: *Neutron based imaging and element-mapping at the Budapest Neutron Centre*, Physics Procedia **69**, 40–47 (2015)
- L. Szentmiklósi and Z. Kis: *Characterizing nuclear forensic samples within lead containers by neutron-tomography–driven prompt gamma activation imaging (PGAI-NT)*, Anal. Methods **7**, 3157–3163 (2015)

Lecture slides and lab guides

- [1] <http://energia.mta.hu/hu/ELTE-NEMA>
- [2] Z. Kis, L. Szentmiklósi and Zs. Kasztovszky: *Gamma-spektroszkópiai gyakorlat alacsony-háttérű mérőhelyen az ELTE geológus hallgatói számára*, (2014). http://www.kfki.hu/~szentm/DOME_labgyak.pdf
- [3] I. Sziklainé László and D. Párkányi: *Neutronaktivációs analitika jegyzet* (Hungarian + English)
- [4] Z. Kis and L. Szentmiklósi: *Neutronradiográfia jegyzet* (Hungarian + English)
- [5] L. Szentmiklósi, K. Gmélings, Z. Kis, Zs. Kasztovszky, B. Maróti, I. Sziklai-László, D. Párkányi, I. Harsányi and T. Belgya: *Training Activities in Neutron Activation and Imaging Techniques at the Budapest Neutron Centre*

Poster

- [6] J.P. Dembo, P. Völgyesi, Z. Szabó, Z. Kis and Cs. Szabó: *Radioactivity of Angolan Adobe Building Material and Effect of Geology and Climatic Conditions*, Poster presented at the Radon in the Environment 2015, Krakow, May 15 (2015)

PhD. Thesis based on our experiments

- [7] C. Genreith: *Partial Neutron Capture Cross Sections of Actinides using Cold Neutron Prompt Gamma Activation Analysis FZ Jülich - RWTH Aachen University*, ISBN 978-3-95806-036-4 (2015)

PROGRESS AT THE NEUTRON ACTIVATION ANALYSIS LABORATORY

Dénes Párkányi, László Szentmiklósi, Tímea Kocsis, Csaba Katona, Ibolya Sziklai-László

Objective

Application, and development of Neutron Activation Analysis (NAA), and gamma-spectrometry in research, archaeometry and material science. Well- performed service and accurate elementary analysis and radioactivity results.

Method

The maximum time of short irradiation (channel with fast-rabbit system) increased to five minutes; it is safe, and does not require additional material to that usually applied.

Full-energy peak efficiency (with true coincidence correction factors) can be calculated for our HPGe all distance points and cylindrical geometries. Additional efficiency correction factor with MCNP calculation can be used for 'slab' geometry.

We procured and implemented the Kayzero for Windows software for the accurate element-concentration calculation. The lab infrastructure is being modernized with a microbalance and new dosimeters. To improve our radiation safety process, a RadeyeSPRD device was tested and will be purchased for rapid isotope identification.

Results

Material science

As part of an IAEA initiative, the thermal neutron capture cross section for intact bulky molybdenum metal slabs and MoO₃ was successfully calculated, thanks to the neutron shelf shielding calculation processes we implemented in our routine evaluation process.

Trace impurities of titanium dental implants were investigated in a BNC work.

Trace elemental analysis of industrial glasses was carried out additionally to PGAA results.

Biology and environmental science

A publication was completed for the repeating BNC work in the investigation of elemental content of iron-bacteria with NAA.

Archaeometry

Obsidians and ceramic samples were investigated with NAA. The evaluation of results is in process. [2] The possibility of using our higher efficiency HPGe detector (Ortec 55%) for of PGAA off-line counting was investigated; an ancient Ag object was measured with the detector mentioned above.

Quality assurance

During this year another round of Wepal proficiency tests were performed for NAA technique organized by IAEA. Soil and plan samples were analysed. The results show good agreement with the consensus data and show improvement over the years. In the workshop organized in Delft for the participant countries, Hungary got well performed country classification like at the previous event in Vienna, 2013.

Analytical services for BRR

The activity concentrations of characteristic fission and corrosion products in the BRR's primary cooling water and the chemical concentrations of different impurity components in various water systems of the BRR were measured to monitor the water quality. The results are sent every year to the Hungarian Atomic Energy Authority with the fuel-cycle-end report. The activities of irradiated samples and flux monitors were also measured upon internal request.

Related publications

- [1] R. Angelova, V. Groudeva, L. Slavov, M. Iliev, I. Nedkov, I. Sziklai-László and K. Krezhov: *Investigation of iron-containing products from natural and laboratory cultivated Sphaerotilus-Leptothrix bacteria*, Journal of Biological Physics **41**, 367-375 (2015)
- [2] L. Szentmiklósi, D. Párkányi and I. Sziklai-László: *The Budapest Neutron Activation Analysis Laboratory – past, present and future*, poster at MTAA-14, 2015. 08. 23-28, Delft, the Netherlands (2015)
- [3] L. Szentmiklósi, Z. Kis, T. Belgya, Zs. Kasztovszky, D. Párkányi and B. Maróti: *Element analysis and imaging opportunities at the Budapest Neutron Centre (BNC)*, poster at MTAA-14, 2015. 08. 23-28, Delft, the Netherlands (2015)
- [4] Rosta et. al: *Ezüst tárgyak archeometriai vizsgálata roncsolásmentes nukleáris módszerekkel*, BNC Kutatási jelentés (2015)
- [5] Production of ⁹⁹Mo from ^{nat}Mo at Research Reactors: IAEA Inter-laboratory Comparison (Round Robin) working document 2014-2015
- [6] Workshop on Inter-comparison feedback of Proficiency Tests performed in 2015 for NAA and other Analytical Techniques, Report of a Workshop under regional TC projects RAF4022, RAS1018, RER1007 and RLA0037, Working document (2015)

ANALYTICAL APPROACHES TO THE OH RADICAL INDUCED DEGRADATION OF SULFONAMIDE ANTIBIOTICS IN DILUTE AQUEOUS SOLUTIONS

Erzsébet Illés, Erzsébet Takács, László Wojnárovits, Renáta Homlok, Gyuri Sági, Krisztina Kovács, Tamás Csay

Objective

Sulfonamide type antibiotics are regularly detected in surface waters, because of their widespread application. A significant fraction is released to the environment by the wastewater treatment plants. The conventional water purification technologies are not effective enough in their degradation. The purpose of our work was to identify the $\cdot\text{OH}$ induced degradation products of sulfodrugs (sulfacetamide (SCT) and 7 of its derivatives) and to establish the degradation mechanisms.

Methods

For detection of intermediates generated by irradiation pulse radiolysis, experimental setup with kinetic spectrophotometric detection system was applied and for final products's examination gamma radiolysis was used with analysis by UV-Vis and HPLC-MS-MS, ICP-MS techniques. The kinetics of chemical changes was followed by chemical oxygen demand (COD), total organic carbon content (TOC), total nitrogen content (TN) and toxicity measurements.

Results

As pulse radiolysis experiments show, the basic initial reaction is hydroxyl radical addition to the benzene ring, forming cyclohexadienyl radical intermediates. In aerated solutions these radicals transform to peroxy radicals. Among the first formed products aromatic molecules hydroxylated in the benzene rings or in some cases in the heterocyclic rings were observed by LC-MS/MS. Comparison of the COD and TOC results shows gradual oxidation. Simultaneously with hydroxylation, ring opening also takes place. The kinetics of inorganic SO_4^{2-} and NH_4^+ formation are similar to the kinetics of ring degradation (UV spectroscopy). The S atoms of the sulfonamides remain in the solution (ICP-MS measurements) after degradation, whereas some part of the N atoms leaves the solution probably in the form of N_2 (TN measurements). Degradation is accompanied by a high pH drop due to formation of SO_4^{2-} , NO_3^- and smaller organic acids. The degradation goes through many simultaneous and consecutive reactions.

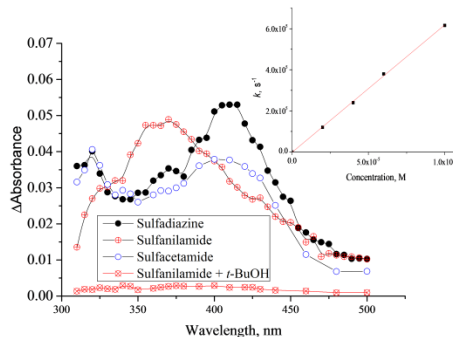


Figure 1: Pulse radiolysis absorption spectra in N_2O saturated $1 \times 10^{-4} \text{ M}$ solutions of sulfadiazine, sulfanilamide without and with $t\text{-BuOH}$) and sulfacetamide (taken $10 \mu\text{s}$ after the pulse). Inset shows the concentration dependence of the pseudo-first-order rate constant of absorbance build up at 420 nm in SCT solution

Remaining work

The research of fenuron, monuron, diuron, amoxicillin, sulfanilamide and its derivatives has been comprehensive, however, some investigations with them, and experiments with other pharmaceuticals or other toxic compounds are still planned.

Related publications

- [1] Gy. Sági, T. Csay, L. Szabó, Gy. Pátzay, E. Csonka, E. Takács and L. Wojnárovits: *Analytical approaches to the OH radical induced degradation of sulfonamide antibiotics in dilute aqueous solutions*, Journal of Pharmaceutical and Biomedical Analysis **106**, 52-60 (2015)
- [2] Gy. Sági, T. Csay, L. Szabó, E. Takács and L. Wojnárovits: *Szulfonamid antibiotikumok OH-gyök indukált lebontásának analitikai megközelítése híg vizes oldatokban*, Autumn Radiochemistry Days 2015, Balatoniszárszó, Hungary, 10.19.2015-10.21.2015. Budapest: MTA Radiokémiai Bizottság, 47-52. (ISBN: 978-963-9970-59-5) (2015)
- [3] R. Homlok: *Relation between chemical structure and degradability in advanced oxidation processes*, PhD thesis (date of defense 28.10.2015) (2015)

SYNTHESIS OF CELLULOSE-BASED SUPERABSORBENT HYDROGELS BY HIGH-ENERGY IRRADIATION IN THE PRESENCE OF CROSSLINKING AGENT

Erzsébet Takács, László Wojnárovits, Tamás Fekete

Objective

The aim of the present work is the optimization of hydrogel properties by systematic modification of synthesis conditions. Hydrogels as three dimensional polymer networks are capable to absorb high amount of water. They have numerous practical applications like diapers, controlled release drug delivery systems. The hydrogels were prepared by γ -irradiation induced crosslinking using high concentration aqueous solutions of four cellulose derivatives (carboxymethylcellulose - CMC, methylcellulose - MC, hydroxyethylcellulose - HEC and hydroxypropylcellulose - HPC) in the presence of N,N'-methylene-bis-acrylamide (MBA) as a crosslinking agent.

Methods

Aqueous solutions of cellulose derivatives were prepared: their concentrations varied from 4 to 40 w/w%. The samples were irradiated in the presence of air with γ -rays of a ^{60}Co source at a dose rate of 9 kGy h⁻¹. The absorbed dose was varied from 0.25 to 200 kGy. The effect of the MBA concentration (between 0.25 to 10 w/w_{polymer}%) was examined using 20 w/w% cellulose derivative solutions at 20 kGy absorbed dose. The gel fraction (GF) was calculated by the equation: GF(%) = $(W_1/W_0)^{*}100$, W_0 and W_1 are the sample weight before and after extraction, respectively. The degree of swelling was calculated as $(W_s - W_d)/W_d$, W_s and W_d are the masses of the swollen and dry samples.

Results

During irradiation of cellulose derivative solutions MBA significantly increased the crosslink density even at very low crosslinker concentrations, leading to a higher gel fraction and a lower degree of swelling (Fig. 1). Moreover, the gelation process required much lower absorbed dose and solute concentration in the presence of MBA. Adding MBA under much milder synthesis conditions improved the water uptake (degree of swelling) without decrease of gel fraction, as compared to the pure derivative gels. The swelling properties of CMC gels showed high sensitivity to the presence of inorganic ions in the solution. The decrease of the water uptake with the ionic strength was much higher for gels with high water uptake. Thus, when proper balance between good swelling properties and high gel content is being established, the environmental conditions of the application, such as the ionic strength, should also be considered.

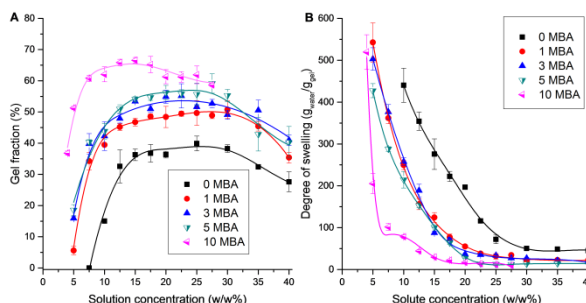


Figure 1: Effect of the CMC concentration on gel fraction (A) and degree of swelling (B) for CMC gels containing 0-10 w/w_{polymer}% MBA (dose: 20 kGy)

Remaining work

The preparation of superabsorbent hydrogels is planned from aqueous solutions of CMC and acrylic acid (AAc) with varying CMC:AAc ratio, by partially replacing the CMC with AAc. PhD thesis is under preparation.

Related publications

- [1] T. Fekete, J. Borsa, E. Takács and L. Wojnárovits: *Synthesis of cellulose-based superabsorbent hydrogels by high-energy irradiation in the presence of crosslinking agent*, Radiation Physics and Chemistry **118**, 114–119 (2016)
- [2] T. Fekete, J. Borsa, E. Takács and L. Wojnárovits: *Synthesis of carboxymethylcellulose/acrylic acid hydrogels with superabsorbent properties by radiation-initiated crosslinking*. Lecture presented at 13th Tihany Symposium on Radiation Chemistry in Balatonalmádi, Hungary, August 29-September 3 (2015)
- [3] T. Fekete, E.Takács, L. Wojnárovits and J. Borsa: *Synthesis of carboxymethylcellulose/acrylic acid hydrogels superabsorbent by ionizing radiation*, Autumn Radiochemistry Days 2015, Balatonszárszó, Hungary, 10.19.2015-10.21. 2015. Budapest: MTA Radiokémiai Bizottság, 53-57. (ISBN: 978-963-9970-59-5) (2015)

ONE ELECTRON REDUCTION OF PENICILLINS IN RELATION TO THE OXIDATIVE STRESS PHENOMENON

László Szabó, Tünde Tóth, Erzsébet Takács, László Wojnárovits

Objective

Redox cycling drugs exert their toxic action by abstracting electrons from redox systems and passing them to molecular oxygen generating $O_2^{\cdot-}$. Our theory suggests a similar mechanism for some bactericidal drugs, which might give a better explanation for the oxidative damage phenomena connected to these molecules. The aim of this work was to study the one-electron reduction mechanism of selected penicillins (amoxicillin, ampicillin, cloxacillin, and their common 6-aminopenicillanic acid sub-structure).

Methods

Pulse radiolysis experiments were carried out using a Tesla Linac LPR-4 accelerator with kinetic spectrophotometric technique. Single pulses of 4-MeV electrons with duration of 800 ns were used. Samples were irradiated in a 1-cm optical path-length cell using continuous-flow technique.

Results

Penicillins behave towards hydrated electron somewhat like a tripeptide in line with their structural similarities. The hydrated electron is accommodated on the carbonyl carbons of these molecules. The forming ketyl radicals are reducing agents that might pass the electron to another acceptor (e.g. O_2). Contrary to peptides, the adduct at the carboxylate group could be stabilized for several μs similarly to benzoic acid. The special electron structure of the thiazolidine ring is obviously behind this effect. It appears to be likely that penicillins accommodate an electron easily and release it to other suitable partner, which might give explanation to the oxidative stress phenomena induced by these therapeutic agents.

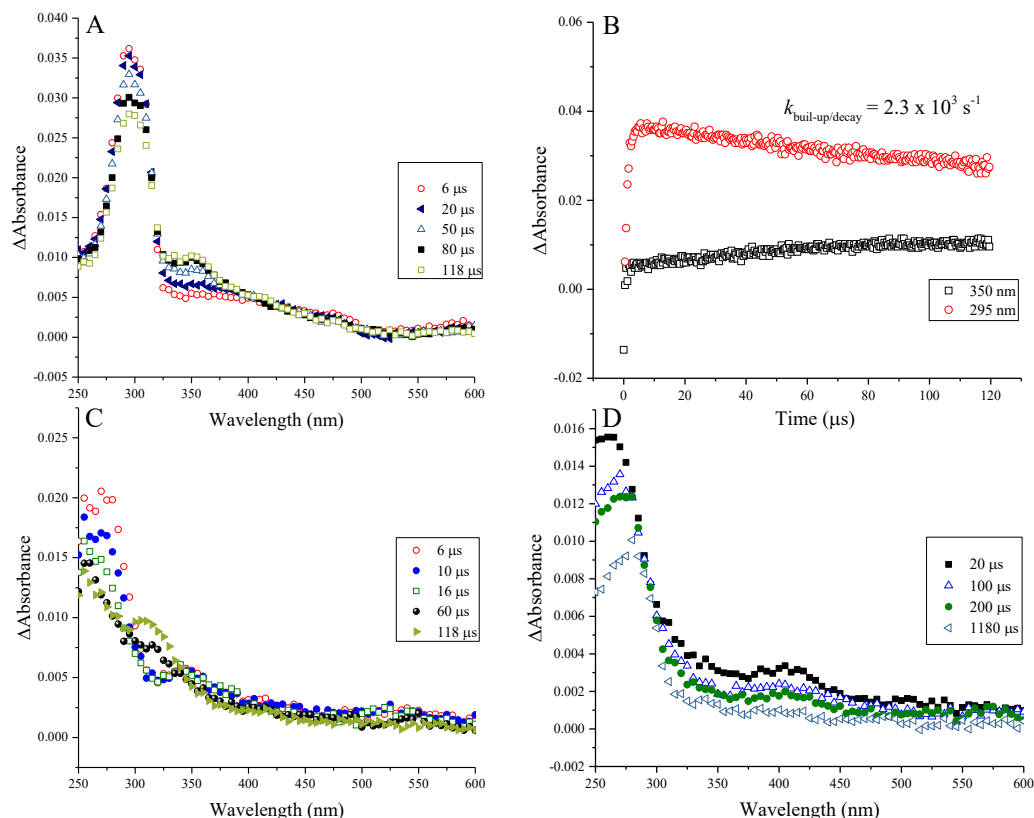


Figure 1: Transient absorption spectra recorded in N_2 -saturated solutions containing 0.5 mol dm^{-3} tert-butanol and $1 \times 10^{-4} \text{ mol dm}^{-3}$ ampicillin (A), cloxacillin (C) and 6-aminopenicillanic acid (D). Kinetic trace recorded at 350 and 295 nm in a solution containing $1 \times 10^{-4} \text{ mol dm}^{-3}$ ampicillin (B).

Remaining work

The radical induced oxidative transformations of penicillins and the change in their hydrophilicity will be studied.

Related publication

- [1] L. Szabó, T. Tóth, E. Takács and L. Wojnárovits: *One electron reduction of penicillins in relation to the oxidative stress phenomenon*, International Journal of Molecular Sciences **16**, 29673 (2015).

Call for CERIC Research
Grants now open
Deadline postponed
March 7th



IX. INTERNATIONAL ACTIVITIES



Central European
Research Infrastructure
Consortium



PARTICIPATION IN THE OECD SCIP III PROJECT

Zoltán Hózer, Emese Slonszki, Katalin Kulacsy,

Objective

The Studsvik Cladding Integrity Project (SCIP) III was launched in 2004 with the participation of MTA EK and Paks NPP. The main objective of our participation is the collection of information on fuel behaviour phenomena in order to apply this knowledge to VVER conditions and review the planned tests.

Methods

The experts of MTA EK attend regularly the meetings of SCIP III and review the obtained results. At the end of each year a summary paper is produced for the Paks NPP on the new results of the project. In 2015 the review focused on two specific items:

- LOCA fragmentation tests.
- Application of mandrel technique for fuel behaviour studies.

Results

The summary report on the 2015 results was produced. The main conclusions were the followings:

- In the framework of the SCIP III project LOCA tests were performed with high burnup fuel rodlets. The main objective of the tests was the determination of threshold values above which strong fuel pellets fragmentation can take place. Furthermore, the fission gas release during LOCA transient was also investigated.
 - Two integral LOCA tests were performed in order to determine the burnup limit for fine fragmentation. The tested fuel rods had 64-65 MWd/kgU and 67-68 MWd/kgU burnup. The results indicated a gradual increase in fine fragmentation between 64 MWd/kgU to 68 MWd/kgU. The strain limit for fuel relocation was 3-4 %.
 - The SCIP III LOCA tests demonstrated significant transient fission gas release at rather low temperature, which increases the internal pressure during the transient. The effect will be further investigated.
- The mandrel technique can be applied for simulation of pellet-cladding interactions. In the current test series slow ramp rate effect and oxygen mitigating effect are investigated. The out-of-pile test results can be compared to ramp test results performed in test reactors. The mandrel technique will be applied in Hungary for the investigation of E110 and E110G alloy, for this reason the learnings from SCIP III experience are very important for MTA EK experts.

Remaining work

The MTA EK experts will review the SCIP III activities by the end of the project.

Related publication

- [1] E. Slonszki: *LOCA fragmentation test in the SCIP III project and the application of mandrel technique*, EK-FRL-2015-962-01/01, in Hungarian (2015)

PARTICIPATION IN THE ESNII PLUS EU PROJECT

Zoltán Hózer, András Keresztúri, Emese Temesvári, Nóra Vér, Szabina Török

Objective

The ESNII Plus project (2013-2017) merges the contribution of 35 European partners in order to support the development of a federate body to ensure efficient EU coordinated research on Reactor Safety for the next generation of nuclear installations.

Methods

The experts of MTA EK participate in several work packages of the ESNII Plus project. The activities in 2015 were focused on MOX fuel and research facilities that are supposed to be applicable for the qualification of ALLEGRO fuel. The main topics of our contributions were the followings:

- Support to facilities development
- Core Safety
- Fuel Safety

Results

MTA EK co-ordinates the work package on "Support to facilities development". The first draft content of deliverables were produced and distributed to project partners. MTA EK directly contributed to the deliverables with the following materials:

- The "GFR Technology Specific Issues" and "GFR Technology European Roadmap" chapters were produced for the Deliverable D3.11 "Identification of functional specifications of the R&D facilities (D3.11)"
- The basic information on a Russian research reactor and on the Halden reactor were collected for the deliverable D3.21 "Qualification and testing infrastructure for irradiation programme"

The ESNII Plus project provided a good opportunity to restart the activities around the fuel properties, first with a State of the Art Report, completed with measurements on fresh and irradiated fast reactor MOX fuels. The new edition is based on measurements on fresh and irradiated fuels, data from literature, and recommendations. The MTA EK contribution to the update of MOX catalogue included extensive review of new publications on the properties of fast reactor MOX fuel and the

checking of related correlations. The chapters "Thermal Expansion" and "Young Modulus" were written by our expert. In WP6, two reactor physics calculation exercises were specified and being solved by the participants. MTA EK was responsible for finalizing the specifications and comparing the results. First, a complicated benchmark of the whole ALLEGRO core was specified and calculated. Large contribution of the user effects - especially for the Doppler feedback - was observed in this case. Secondly, to minimize the user effect, a simple single cell calculation is to be solved. The first results are not too promising because the deviations are of the same order.

Remaining work

The project activities will be continued according to the original plans by 2017.

Related publication

- [1] J.P. Ottaviani, D. Staicu, R. Calabrese, N. Vér, G. Trillon, J. Klousal, A. Fedorov, S. Portier and M. Verwerft: *State of the art with a literature review of MOX fuel properties*, ESNII plus – D7.11 – revision 0 issued on 31/07/, (2015)

PARTICIPATION IN THE SAFEST EU PROJECT

Zoltán Hózer, Imre Nagy, Attila Guba

Objective

The main objective of the EU SAFEST project in 2015 was to specify the severe accident experiments that should be carried out in different facilities in the EU.

Methods

Following the call "Rules of access to SAFEST facilities" released in 2014, several proposals were received. The 1st User Selection Panel Meeting was held in Marseille, 27th March 2015. Concerning the two MTA EK facilities the following proposals arrived:

CODEX:

- Boil-off and air ingress during a spent fuel LOCA, proposed by KIT, Karlsruhe, Germany
- BWR specific test with control blade degradation, proposed by SSM, Stockholm, Sweden

CERES:

- Extension of experimental justification of in-vessel retention strategy for VVER-440 reactors addressing specific aspects of real operational conditions, proposed by Bohunice NPP, Slovak Republic

Results

The user selection panel formulated the following decisions on the proposed tests.

CODEX proposal by KIT:

- The experiment should study the influence of nitrogen on oxidation and degradation of fuel rod claddings in the temperature range of 800 - 1200 °C. The panel recommended to accept this proposal and suggested to invite EDF, PSI, GRS, LEI and IBRAE (consortium which has prepared a proposal with similar experimental conditions in the QUENCH facility at KIT) to join this proposal and define common experimental parameters. Additionally, the panel asked the partners participating in this proposal to consider a possibility of using fuel rods with different cladding materials in this test.

CODEX proposal by SSM:

- Though this proposal is focused on the BWR-specific important phenomena, like influence of control rod blade on bundle degradation and top spray cooling efficiency, the panel recommended to reject this proposal. Scaling down the BWR bundle to the dimensions and geometry of the CODEX facility would result in a more or less 1-dimensional experiment and cannot provide the prototypic conditions for spray cooling and melt relocation. Prototypic distribution of flows and water drop size would be another challenging issue.

CERES proposal by Bohunice NPP:

- The panel recommended to accept this proposal. The experimental realization requires only minor modifications of the CERES facility to increase the sump level. The experiment can be performed in 2016.

Remaining work

Severe accident experiments will be performed on the CODEX and CERES facilities according to the requests of foreign partners. The tests are scheduled for 2016 (CERES) and 2017 (CODEX).

Related publications

- [1] C. Journeau, V. Bouyer, N. Cassiaut-Louis, P. Fouquart, P. Piluso, G. Ducros, S. Gossé, C. Guéneau, A. Quaini, B. Flührer, A. Miassoedov, J. Stuckert, M. Steinbrück, S. Bechta, P. Kudinov, Z. Hózer, A. Guba, D. Manara, D. Bottomley, M. Fischer, G. Langrock, H. Schmidt, M. Kiselova and J. Ždarek: *European Corium Experimental Research Roadmap*, Technical Meeting On Post-Fukushima Research and Development Strategies and Priorities, IAEA, 15-18 December (2015)
- [2] A. Miassoedov, C. Journeau, S. Bechta, Z. Hózer, D. Manara, D. Bottomley, M. Kiselova and G. Langrock: *Severe Accident Facilities for European Safety Targets, The SAFEST Project*, NURETH-16, Chicago, IL, August 30-September 4, 4604-4616 (2015)

RADIATION RESISTANCE OF ITER BOLOMETERS

Levente Tatár, Tamás Fekete

Objective

The ITER tokamak is considered to be the first fusion device to maintain fusion for long periods of time. Maintaining plasma inside the toroidal vacuum vessel (VV) for a long period of time is essential for producing electricity by fusion. However this poses very demanding theoretical and engineering problems which have to be solved. One of the most important problems is plasma stability. An important goal of building the ITER facility is understanding and predicting plasma behaviour, so ITER will be heavily instrumented.

As part of the instrumentation, bolometers will be used in ITER for measuring total irradiated power of the plasma. Their principle is based on the resistance change of a meander-shaped conductive layer of a sensor due to deformation induced by thermal expansion caused by radiation. The bolometer sensor, together with housing, electrical contacts, collimator, etc. is called a bolometer "camera". The installation of a large number of bolometers is planned, as these will be used for tomographic reconstruction of the plasma radiation. Figure 1. presents a bolometer camera and a part of the sensor.

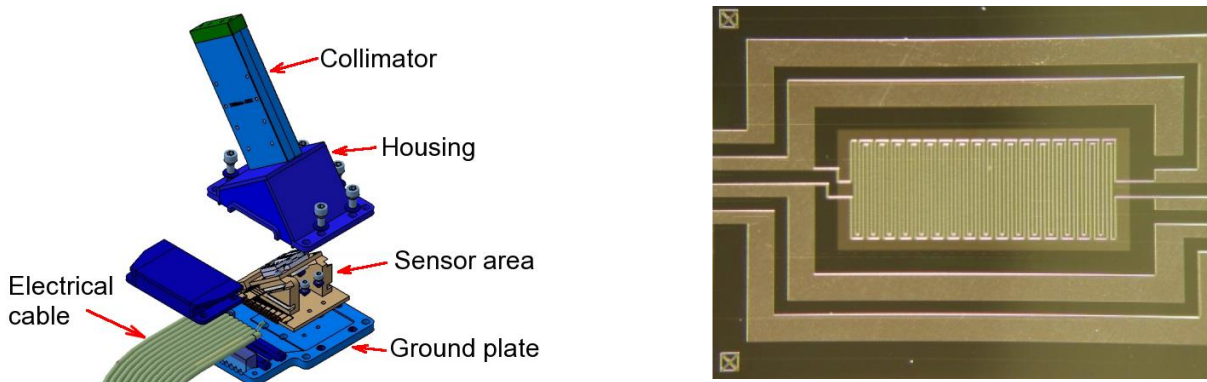


Figure 1: Schematic of a bolometer camera and partial view of the sensor.

Methods

Designing bolometers for ITER is very challenging, since there are many simultaneous requirements to be met. First of all, the delicate sensor has to withstand the harsh radiation environment inside ITER. Furthermore, the space available for bolometer cameras is very limited. An important aspect is that the radiation generates a high amount of heat, which has to be transferred to the VV. The bolometer cameras have to be built for remote handling (RH), since inside the VV high activation is to be expected. Furthermore, every material used inside the VV has to be vacuum compatible; emissions of substances from bolometers are prohibited.

As the ITER consists of several subsystems and there are many connections between these, there are several different requirements for bolometers, written in many different documents. These documents are periodically updated, but they may contain obsolete and/or contradictory requirements. As supporting work for designing bolometer cameras, these documents had to be reviewed, information regarding bolometers extracted, and contradictory and hard to meet requirements outlined.

Results

As a result of this overview, the deliverable D3, entitled "Documented system requirements" has been produced. In this document contradictory and hard to meet requirements are outlined. Some important aspects of our findings are:

- Expected radiative power is given with very large margins.
- Different documents give different values for expected (controlled) VV temperatures.
- Based on the currently available experimental results, the proposed ITER lifetime and the servicing periods, there is a high chance of not meeting the requirements for bolometer sensor lifetime, so it is expected that some bolometer cameras will stop working prematurely.

Remaining work

MTA EK works in a consortium, together with IPP Garching, Fraunhofer Institute and MTA Wigner. The project is organized into Specific Grants (SG). SG01 has been finished, SG02 is ongoing for 3 more years, SG03 has been started and will be finished at the end of the next year. The leader of the consortium is IPP, so we have to solve the individual tasks given by IPP. We have already started the work on the FE model of a camera prototype.

Related publication

- [1] H. Meister et al.: *Overview of the R&D Activities for the ITER Bolometer Diagnostic*, 1st EPS conference on Plasma Diagnostics, 14-17 April 2015, Frascati, Italy (2015)

AGEING OF REACTOR STRUCTURAL MATERIALS - PARTICIPATION IN THE AGE-60 EU PROJECT

Ferenc Gillemot, Márta Horváth, Attila Kovács, Ildikó Szenthe

Objective

The purpose of the AGE-60 project is to collect reactor material ageing information required for long term operation (60 years or longer). The project is financed by the NUGENIA organization. Due to the limited financial support, no new research is planned within the project, only re-evaluation of the existing research and surveillance data is the task, UJV Rez and MTA-EK collecting the WWER data. A small database has been elaborated containing the most important mechanical properties of the as-received and aged (thermally aged and irradiated) reactor pressure vessel (RPV) steels. The final goal is to elaborate new trend curves on radiation and thermal ageing. The trend curves may be used for enhanced evaluation of the safe lifetime of the RPV-s. Parallel with the WWER data use, the West European partners are working with the data of the other European pressurized water reactors' PWR-s.

Methods

Collection of the existing surveillance, extended surveillance, and research knowledge on the ageing the WWER-440, and WWER-1000 steels. The data are input in a simple data base and will be evaluated, and new trend curves will be fit into the database.

Results

Data sheets are elaborated and filled with the existing data. UJV Rez institute organized a "Workshop on Surveillance of WWER Reactors" at October 2015 in Prague. All WWER operating parties were participating, and introduced their results. MTA EK presented four lectures and discussed the differences of the trend curves of the existing WWER-440 units. This trend curves can be separated for three different groups. The differences between the three curve groups will be studied considering the effect of the alloying and polluting elements. Some of the considered trend curves are shown in Figure 1.

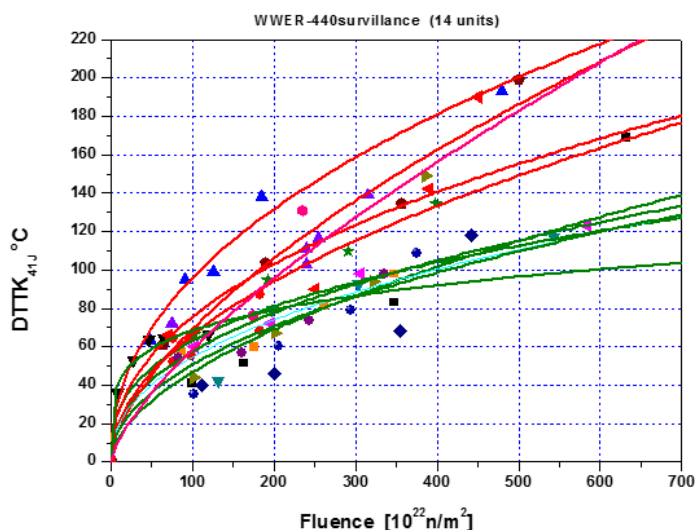


Figure 1: Ageing of WWER-440RPV steels in the function of the fluence

Remaining work

The AGE -60 project started in 2015 and will be finished in 2016. The remaining work is the evaluation of the collected data and elaboration of the project final report.

Related publications

- [1] F. Gillemot, A. Kovács, M. Horváth, I. Szenthe, N. Kresz and F. Oszvald: *Comparison of high fluence irradiation results performed in power and research reactors*, presented on the "Workshop on surveillance of WWER reactors", at October 2015, in Prague (2015)
- [2] F. Gillemot, A. Kovács, M. Horváth, I. Szenthe, N. Kresz, F. Oszvald: *Surveillance Program Extensions for Long Term Operation in WWER-440 reactor*" presented on the "Workshop on surveillance of WWER reactors", at October 2015, in Prague (2015)

DEMO MATERIAL PROPERTIES HANDBOOK

Ferenc Gillemot, Ildikó Szenthe, Attila Kovács

Objective

The next large step in the development of the fusion energy production will be building a model reactor producing electric energy. The name of it will be DEMO (Demonstration Reactor), and the purpose of it is to prove that electric energy can be produced safely and economically using fusion energy. For the purpose of the DEMO research programs are running to develop new materials with the properties required for fusion devices. The designer needs to use the results of these studies. The purpose of the Material Properties Handbook (MPH) is to collect the values of mechanical and physical properties measured in the research programs, evaluate them, and provide them to the designers in user friendly form.

Methods

Results of the material development programs are collected into data templates. Separated templates had been elaborated for the different types of materials: advanced structural steels, functional materials (ceramics, insulation materials, optical materials, mirrors etc.), joints, armor materials. The data in the templates are extended with existing data and literature data. The evaluation of the database is a common task of several institutes. The final product is the MPH which contains the summary of the material properties in a format that can easily be used by the DEMO designers.

Results

During the first year of the programme, MTA EK developed the data templates and started to collect data. The format of the MPH has been elaborated in co-operation of KIT (Karlsruhe Institute of Technology) and MTA EK. The format and the minimum requirements describing the material properties became also a pilot study for the future chapters, and have been widely discussed with the MAT program participants and with the DEMO designers. The first elaborated chapter of the DEMO MPH is the chapter on EUROFER. EUROFER is a low activation ferrit-martensitic steel containing 9% Cr. The chemical composition of it is in Table 1.

Table 1: The chemical composition of Eurofer in wt %

| | C% | S% | P% | Si% | Mn% | Ni% | Cr% | Mo% | W% |
|------------|------|-------|-------|------|-------|-------|------|------------------|----------|
| min | 0.09 | - | - | 0.20 | 0.20 | - | 8.5 | - | 1.00 |
| max | 0.12 | 0.005 | 0.005 | 0.50 | 0.60 | 0.20 | 9.5 | 0.005 | 1.20 |
| | Ta% | V% | Nb% | Cu% | B% | Al% | Co% | N ₂ % | Fe%- |
| min | 0.10 | 0.15 | - | - | - | - | - | 0.015 | Balance |
| max | 0.14 | 0.25 | 0.005 | 0.10 | 0.002 | 0.001 | 0.01 | 0.045 | Balance- |

In case of the EUROFER chapter the following material properties are collected, evaluated and printed in the MPH: information on production technology, Charpy impact energy, magnetic coercive field, chemical composition, creep, density, thermal diffusivity, electrical resistivity, elongation, fracture toughness, thermal expansion, magnetic saturation, Poisson's ratio, remnant magnetization, specific heat, swelling, thermal conductivity, ultimate tensile strengths, Young's modulus, yield strength.

The MPH contains not only the property values of the received materials, but also the aged values. Aged material properties are important for the designers to consider the long term safety of the fusion equipment, and they also are important for the safety authorities to elaborate the operation permissions of the fusion reactors.

The material properties are supplied in tables and diagrams to give quick impression on the ageing processes and on the effects of the environmental conditions (e.g. high temperature).

Parallel with the elaboration of the EUROFER Chapter of the MPH, the preparatory work for the functional materials has been started.

Remaining work

The MAT- program will be continued for several years (the first operation of DEMO fusion reactor is expected around 2040 or later). Every year the new results obtained on materials already included into the relevant chapters of the MPH will be compiled, evaluated and the existing chapter will be corrected or extended using new data.

At the same time the MPH will be extended with new chapters. For 2016, the elaboration of a new chapter containing the properties of the functional materials is planned.

The MPH contains material data owned by the material developing companies and institutes. Some of these data are not public, consequently no publications have been prepared from the DEMO MPH until now.

JOINT HUNGARIAN-KOREAN LABORATORY PROGRAM FOR ADVANCEMENT OF NUCLEAR THERMAL-HYDRAULICS SAFETY

Gábor Baranyai, György Ézsöl, Valér Gottlasz, Attila Guba, Zoltán Hózer, Imre Nagy, Antal Takács, Iván Tóth, István Trosztel

Objective

The objective of the Joint Hungarian-Korean Laboratory (JHKL) is to advance scientific knowledge in two areas important for nuclear power plant safety: the effect of pressure waves on pressure vessel internals and coolant mixing in cold legs and in the pressure vessel downcomer, as well as to increase nuclear safety assessment capabilities via validation of computer codes. As a result of the discussions in the November 2013 workshop, the JHKL activity was extended to the research on the coolability of deformed fuel in a nuclear reactor core.

Methods

The scope of the activity includes performance and evaluation of tests in three test facilities of MTA EK: the PMK, the CODEX-COOL and the plexi model of the downcomer with three connecting cold legs. In addition, available computer codes at MTA EK and KAERI were applied to the test cases with the aim to validate these tools for the given phenomenon.

Results

A third series of pressure wave propagation tests was performed during the last year of the project. In this period a special quick opening valve designed and manufactured by the Korean company Key Valve Technologies Ltd., was used for modelling the break opening in the system. In addition to fast-response pressure transducers, strain gauges also measured the axial and azimuthal stress state of reactor vessel model components at two different locations, producing valuable data for structural analysis. The effect of the break opening time was explored by 3 tests, adjusting the opening time of the quick opening valve over its possible range. It was found that - due to the rather fast opening of the valve in even its slowest mode - the effect of opening time was minimal. ATHLET analysis performed for the tests indicated the importance of modelling the line between the break orifice and the valve, as well as the stem lift of the valve.

In support of the OECD ATLAS Project a pre-test calculation was carried out for the A2-1 station blackout (SBO) test with leakage at the main circulating pump [1]. The calculation indicated much slower event progression than shown by MARS analysis. Post-test calculations were performed by CATHARE and RELAP5 for the A1-1 and A1-2 SBO cases [1]. The analyses pointed out the importance of pressurizer heat losses for the first phase of the transient and that of system heat losses for correctly predicting the timing of maximum core temperatures. The benchmark case A5-1 (modelling a small break in one of the cold legs) was also calculated by both codes. Analysis of participants' results is underway.

As to the issue of coolant mixing in cold leg and downcomer, the new, stereoscopic PIV measurement system was applied to produce high quality three-dimensional velocity profiles. FLUENT calculations performed indicate that maximum and minimum values of measured and calculated velocity component distributions are close to each other in all test cases, but the maximum values of turbulent kinetic energy are always significantly higher in measurements. This could be explained either by the effect of additional turbulent kinetic energy from the branch pipe, where detailed boundary conditions were not measured, or an underestimation of the turbulent kinetic energy in the mixing zone by the turbulence model applied [1].

The research activity on the coolability of deformed fuel focused in 2015 on high temperature tests performed with different bypass configurations and flow rates [1]. The results indicate that in the case of a closed bypass, the bundle was cooled down faster than in the presence of an open bypass. A larger bypass cross section resulted in the increase of cooling down time. The small (2 mm diameter) bypass case hardly differed from the configuration without bypass. The effect of flow rate was also clearly shown, since in case of lower coolant velocity more time was needed to cool down the bundle.

Remaining work

Although the 3-year JHKL activity has come to an end, a continuation project was proposed. Concerning the benchmark activity related to the A5-1 ATLAS test, a benchmark report will be produced discussing the results of all participants.

Related publication

- [1] G. Baranyai, Gy. Ézsöl, V. Gottlasz, Z. Hózer, I. Nagy, A. Takács, I. Tóth, I. Trosztel, Seok Kim, Jongrok Kim, Sang-Ki Moon, Kyoung-Ho Kang, Ki-Yong Choi and Chul-Hwa Song: *Third Year Technical Report*, EK-THL-2015-442-03/M0, (2015)

EUROPEAN JOINT PROGRAMME FOR THE INTEGRATION OF RADIATION PROTECTION RESEARCH - CONCERT

Imre Balásházy, Balázs G. Madas, Árpád Farkas

Objective

The European Atomic Energy Community launched a European Joint Programme titled "Integrating radiation research in the European Union" in 2015, which is a co-fund action based both on European and national supports. Our Research Centre is a member in the consortium as a Programme manager. The objective of this project is to integrate radiation protection research in the European Union during the next five years.

Methods

The final title of the project is "European joint programme for the integration of radiation protection research" with the acronym "CONCERT". Almost all members of the European Union are represented in the consortium. The few ones which are still not represented are invited to join the consortium. The coordinator of the project is the Federal Office for Radiation Protection from Germany. Our Research Centre participates in five work packages out of the seven and is member of the Management Board of the consortium.

The Management Board (coordinator, programme manager nominated by all participant the Member States, plus representatives of four participating platforms) is the principal decision-making body of the consortium on the financial level whose responsibility is to make sure that the project's objectives related to open scientific and integration calls are achieved. This board makes decisions on all budget-related matters.

Thus, we participate in the management, in the elaboration of the main research directions and priorities, in the planning of the usage of related European infrastructures, and in the development of education and training strategies. Each of them runs over the whole period of the project.

Four European platforms active in radiation protection are also members of the consortium: MELODI (Multidisciplinary European Low Dose Initiative), EURADOS (European Radiation Dosimetry Group), NERIS (European Platform on Preparedness for Nuclear and Radiological Emergency Response and Recovery), and ALLIANCE (European Radioecology Alliance). Our Research Centre is member of the first three platforms. A multidisciplinary platform from the medical field is to join the consortium.

Results

The starting date of the 60 month-long project was 1st June 2015. We participated in the kick-off meeting and the Management Board meetings of the project.

We formulated a national research priority with the following title and content: To explore the role of spatial inhomogeneity of radiation burden in cellular, tissue and health effects in case of internal exposure. Risk of cancer related to homogeneous whole body exposure of ionizing radiation is relatively well understood for doses of about 100 mSv. However, current radiation protection does not take into consideration the effect of dose distribution within organs and tissues. Thus, in this dose range, there is an urgent need for the understanding of biophysical effects of internal exposures or inhomogeneous external exposures with accurate dosimetry. Research should be performed with the aim of understanding the local - for example inflammatory - reactions of internal emitters such as hot particles or alpha-particles. Such research needs precise dosimetry determining the relationship between macroscopic exposure and local tissue doses, and experiments as well as numerical modelling at different levels of organisation.

We co-operated in the development of the strategic research agenda, the roadmap and the priorities on low-dose risk research. Two priorities were recommended for the first open scientific call of the project. Topic 1: Improvement of health risk assessment associated with low dose and dose rate radiation. Topic 2: Reducing uncertainties in human and ecosystem radiological risk assessment and management in nuclear emergencies and existing exposure situations, including naturally occurring radioactive materials.

We collaborated in the Access to Infrastructures work package. One of the aims of the CONCERT project is to support the access to state-of-the art research infrastructures. Infrastructure includes so-called large infrastructures such as exposure facilities for animal and plant experiments (both laboratory and field facilities), epidemiological cohorts, biobanks, databases and analytical platforms (including e-infrastructures). One of the deliverables of this activity is a list of recommended infrastructures for radiation protection research in Europe. Our Research Centre is the leader in the subtask: "Incrementing databases".

Remaining work

The work will be continued till the end of the project, which is 2020.

Related publications

- [1] Strategic Research Agenda for CONCERT. http://www.concert-h2020.eu/en/Concert_info/SRA_development
- [2] Access to Infrastructures for CONCERT. http://www.concert-h2020.eu/en/Concert_info/Access_Infrastructures

ACTIVITIES IN THE FP7 EURATOM CHANDA PROJECT

Tamás Belgya, László Szentmiklósi, Boglárka Maróti and Zoltán Kis

Objective

In the FP7 EURATOM “solving CHAllenges in Nuclear DAta” (CHANDA) project the MTA EK’s role is to provide user access to the Prompt Gamma Activation Analysis (PGAA) facility of the Nuclear Analysis and Radiography Department to perform experiments related to nuclear data for GEN IV reactors or radioactive waste transmutation.

Methods

At the PGAA facility we can provide high intensity cold neutron beam for neutron capture reactions, including radiative capture (n, γ), neutron induced fission (n,f), fission gamma ($n,f\gamma$) and particle ($n, \text{particle}$) reactions. We can provide high quality gamma-ray spectrometry and solid state particle track detection, however, the users must provide equipment for fission and multi-detector gamma-ray detection. We can provide full analysis for gamma-ray singles experiments, other analysis must be provided by the user.

Results

In 2015 we had one user group from the DG JRC Institute of Reference Materials and Measurements (IRMM), Geel, Belgium. In fact we had four participants in the group from IRMM (the proposers) and two other interested experimentalist guests from Jülich at the experiment entitled as “First ever correlation measurements of prompt fission γ -rays and fission fragments from the reaction $^{239}\text{Pu}(n_{\text{th}},f)$ ”. The allocated measuring time was 200 hours, practically one 10 days reactor cycle. We started two days before the beam time the setup of the electronics arrived from IRMM to measure the prompt gamma-ray from the ^{239}Pu ($n, f \gamma$) reactions. The detector setup contained a double Frisch-grid fission chamber, three Lanthanum halide gamma-ray (La) detectors, and our HPGe detector (see Figure 1).

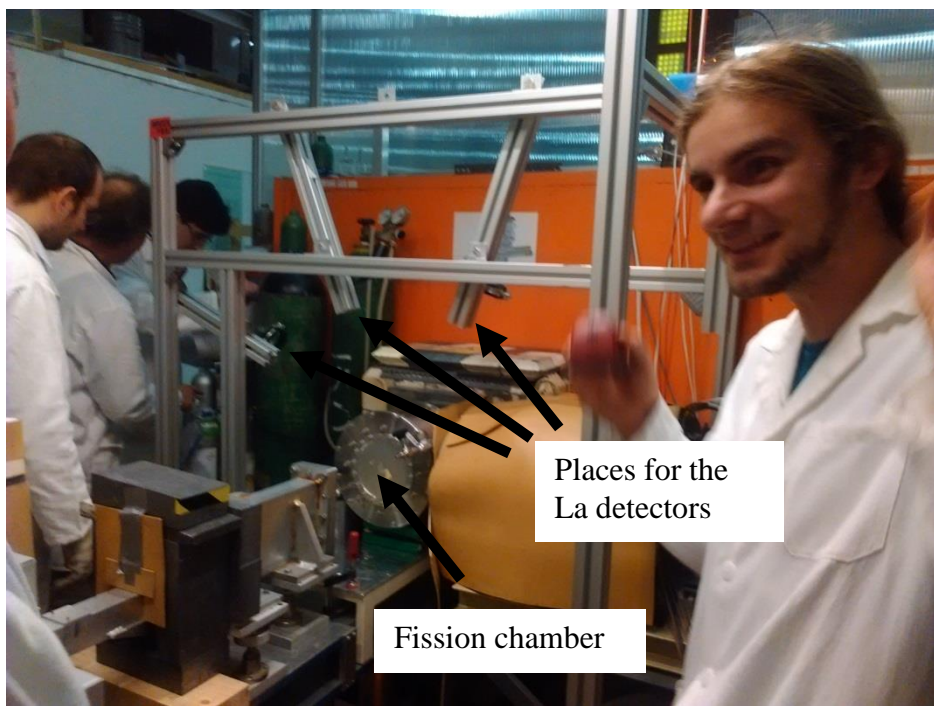
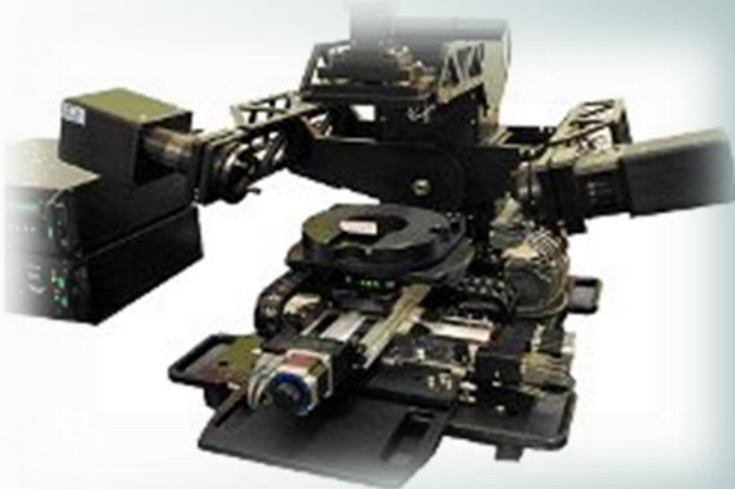


Figure 1: Photo taken during the setup of the experiment (November 2015).

The fission fragment and prompt gamma-ray signals were collected in detector signal trace mode using several fast digitizers. During the ten days sufficient amount of data was collected to provide high quality nuclear data for theoretical and applied purposes. The analysis of the data will be part of the PhD dissertation of Angelique Gatera.

Remaining work

Data analysis is to be performed by the IRMM users and writing an article.



X. RESEARCH RELATED TO THE INSTITUTE OF TECHNICAL PHYSICS AND MATERIAL SCIENCES



nano

Nanocsodák
Mozgásban

Wafer-Scale Integration of Piezoelectric Nanowires

István Endre Lukács, Nguyen Quoc Khanh, R. Erdélyi, Zsófia Baji, Gábor Battistig, János Volk

The EU project PiezoMAT (FP7-ICT-2013-10-611019 High-resolution fingerprint sensing with vertical piezoelectric nanowire matrices (PiezoMAT), <http://www.piezomat.eu/>) proposes new technologies of high-resolution fingerprint sensors based on a matrix of interconnected piezoelectric nanowires (NWs). One of the three targeted chip concepts was realized by the MFA team. Here the integrated free standing vertical NWs are contacted individually at their stock with two metal wires to detect piezoelectricity induced signals between tensed and compressed sides of the NWs upon bending. As it was found by finite element analysis a nearly constant positive/negative stress is built up in the outer/inner side of the NW upon bending it by a lateral loading force directing to its tip (Figs. 1a and b). In contrast, the induced piezoelectric potential has a strong maximum at the bottom of the NW (Fig. 1c). The aim of this sensor concept is to detect this enhanced electrical signal with a pair of metal electrodes contacting the opposite sides of the NWs at their roots. Moreover, with an array of vertically integrated NWs, the distribution of the loading force can also be detected at a very high (>5000 dpi) lateral resolution.

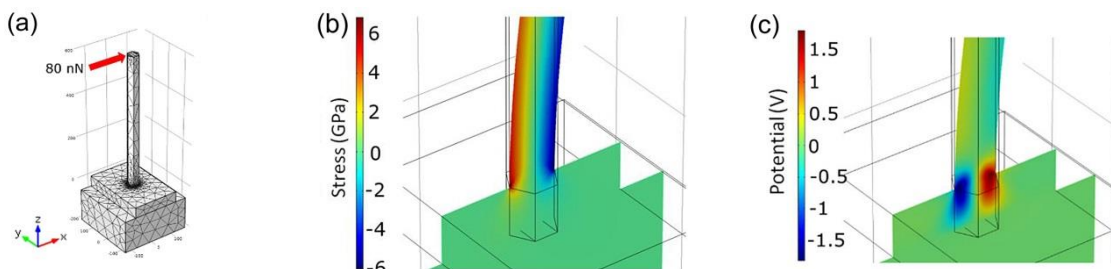


Figure 1: Finite element analysis of NW/seed layer/substrate assembly showing the ideal meshing by triangular elements (a), cross-section of the t_{zz} component of the mechanical stress (b), and the electric potential distribution (c) for the bottom part of the bent NW at a loading force of 80 nN.



Figure 2: Raith 150 electron beam lithography system enabling nanopatterning of full wafers up to 6"-diameter. The system was successfully installed this year in the clean room of MEMS department and is being used in several projects.

contrast to the ones grown on epitaxial ZnO/sapphire substrate (Fig. 3c). High resolution SEM images revealed that the piezocrystals were positioned to the readout contacts with sub-50 nm precision throughout the whole wafer (Fig. 3e).

The optimization of the fabrication procedure was carried out through three stages, at first on small ($10\text{ mm} \times 10\text{ mm}$) sapphire dices, then on 3" sapphire wafer, and at last on 3" Si wafer. The aim of the sapphire wafer is to realize 'ideal' monocrystalline ZnO NWs on epitaxial ZnO seed layer, whereas that of the Si wafer is to demonstrate and test the feasibility of the process on standard Si technology. The optimized process flow consists of more than 25 technological steps, including five electron beam lithography (EBL) alignments. Hence the new Raith 150 EBL system of MFA (Fig. 2), enabling wafer scale processing of sub-20 nm sized patterns, played an essential role in this project. The fabrication process of the wafer had several challenges to be solved, such as the accurate ($<50\text{ nm}$) alignment of the EBL patterns; high quality metal lift-off process after EBL and photolithography; sample charging during EBL; mesa etching of ZnO seed layer; as well as the protection of ZnO mesa island against unwanted etchings.

The processed 3" Si wafer holds several chips (Fig. 3a) each of them having an active sensor array of 8×8 individually contacted NWs in the center (Fig. 3b). Due to the high quality ZnO seed layer deposited at the University of Leipzig (ULEI) the ZnO crystals show an excellent c-axis orientation even on the non-lattice matched SiO_2 covered Si wafer. Nevertheless these NW transducers are polycrystalline (Fig. 3d) in

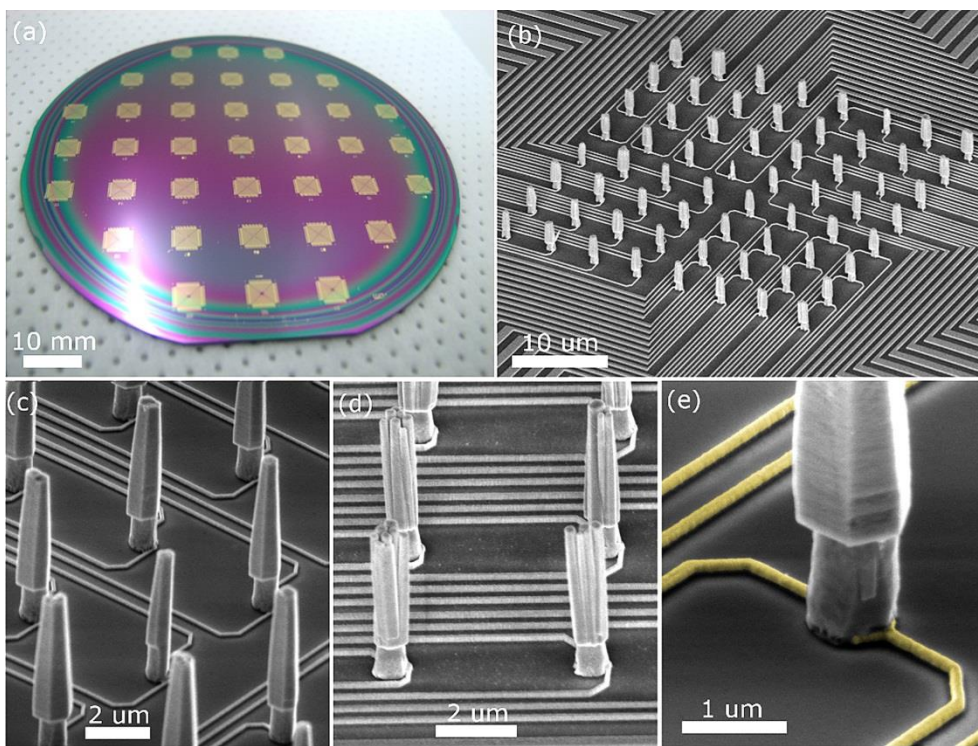


Figure 3: On-chip integrated piezoelectric NWs. (a): Photo of Si wafer with NW chips, (b): SEM image of the 8 × 8 NW array, (c and d, respectively): comparison of contacted ZnO NWs grown on sapphire and Si substrate, (e): high magnification SEM image of the contacted ZnO crystal where the read-out Au electrical lines are colored with yellow.

The electrical connections were verified by current-voltage (I-V) measurements using a probe station and negligible crosstalk was found between the separate circuits. The integrated NW chips are thus ready for the electromechanical characterizations which will

be carried out in two main steps. At first bending experiments will be done on individual ZnO crystals with AFM and SEM micromanipulator tips in a highly controlled way. It will be followed by parallel detection when the whole array is imprinted with a soft stamp mimicking finger-print detection. Beside the targeted goal of PiezoMAT project, the fabricated chips are planned to be used for other purposes as well (e.g. for in-vitro cell monitoring), where very low lateral forces (1–1000 nN), and small movements are to be monitored in high resolution (>5000 dpi).

NANOPARTICLE ASSEMBLIES

Dániel Zámbó, Sz. Pothorszky, E. Gergely-Fülöp, Norbert Nagy, András Deák

One of the core concepts of our work is connected to colloid chemistry, which is essentially the foundation for bottom-up prepared nanostructured, self-assembled systems and processes where nanoscale objects are involved. Our group is engaged in research projects targeting the manipulation and assembly of nanoscale building blocks, with envisaged applications in the field of sensorics (SERS), biomedicine (MRI), energy harvesting (thermoelectrics) and lighting (LEDs). Our activity focuses on both physical and chemical aspects of nanoparticle systems. We rely on state-of-the-art wet chemical synthetic procedure to produce nanoparticles with outstanding uniformity. Physico-chemical and structural characterization of the particles and their structures is also carried out relying on various techniques (TEM, SEM, DLS, various spectroscopy techniques). Computer simulations are also essential part of our activity, boundary and finite element methods are implemented for the simulation of the frequency dependent optical or thermal properties of the nanosystems.

Colloidal template based nanostructures

Interfacial assembly of micron and sub-micron particle has been used to produce high quality mono- and multilayers on various substrates using the Langmuir-Blodgett method that allows the preparation of macroscopic samples. These samples are used by us and several other groups at the institute as well to implement different nanostructuring strategies. In a recent work it was demonstrated that such a structure can enable preparation of plasmonic crystal monolayers. When a monolayer of template particles is partially replicated in a polymer film and uniformly coated with gold, incident angle and wavelength dependent spectral features (absorption bands) arise. The bands are associated with excitation of localized and propagating plasmon modes at the surface, that is, high local electromagnetic fields

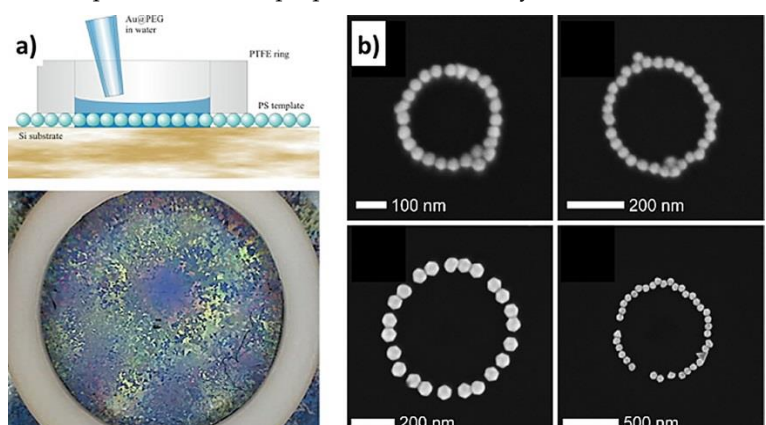


Figure 1 (a): Nanoparticle ‘necklace’ structures preparation by the controlled dewetting of a nanoparticle solution over a template monolayer. (b): Depending on the template diameter, rings with different diameters could be obtained.

are generated in the near-field of these structures. This in turn could be used in sensing and energy harvesting applications to boost the absorption of optically active species, leading to higher sensitivity or improved photon energy conversion efficiency, respectively.

These template monolayers, on the other hand, can also be used as a template to direct the assembly of smaller sized nanoparticles. When a solution of nanoparticles is drop casted over the monolayer and allowed to dry, necklace-like structures can be obtained (Fig. 1). The process relies on the delicate interplay between colloidal and capillary interactions. Additionally, control over the dewetting of such a high pattern-density impregnated structure is also desirable for the successful implementation of such a massively parallel directed assembly of the nanoparticles. Thanks to the plasmonic properties of the assembled nanoparticles, their necklace structure support coupled plasmon modes that can be exploited for the enhancement of the Raman scattering signal of analytes.

Nanoparticle assemblies based on interaction-potential engineering

Assembling nanoparticles into certain structures often results in enhanced or new emerging properties. Assemblies prepared from noble metal nanoparticles can find applications in sensorics, while their hybrid assemblies with luminescent particles (e.g., perovskites) can allow improved light management in absorbing and emitting devices (solar cells, LEDs). Assemblies of magnetic nanoparticles can allow achieving higher contrast in MRI imaging. For the successful preparation of nanoparticle assemblies, extensive knowledge about the (colloidal) particle-particle interaction. This is necessary to identify the factors that allow control over the assembly process. These factors on the other hand, depend on the specific material system (type of nanoparticle, surface coating, desired structure, etc.) and hence require proper engineering of the process from the very beginning. With two recent examples we have shown how implementation of such a holistic approach enables the preparation of compact nanoparticle clusters consisting of hundreds of nanoparticles (Fig. 2), and site-selective directed assembly of single nanoparticles (Fig. 3).

Polyethylene glycol grafted on the nanoparticle surface renders the particles extremely stable against aggregation due to steric repulsion. At increased ionic strength of the medium, however, the polymer chains collapse, that – together with the attractive contribution from the van der Waals interaction – allows to achieve a soft-sphere type interaction with moderate well-depth (Fig. 2a). According to theory, these latter two characteristics are required for the preparation of compact nanoparticle clusters. Dynamic light scattering experiments (Fig. 2b) and electron microscopy images (inset in top panel) confirm the successful preparation of the nanoparticle clusters.

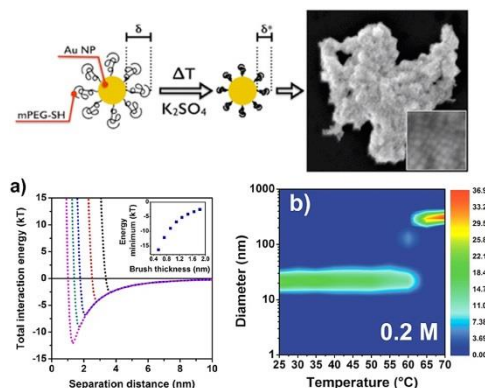


Figure 2: Thermally activated clustering of gold nanoparticles (see main text for details)

When region-selective surface modification of nanoscale object is achieved, it can allow high-precision localization of other small particles, as we have shown recently. By selectively rendering the tips of gold nanorods positively charged while coating the sides of the nanorods with a high molecular weight polymer, tip selective localization of 20 nm gold particles could be achieved (Fig 3a). As the size ratio between a nanorod and the assembled particle is changed, however, the structure changes into a single nanoparticle assembled at the side of nanorods (Fig. 3b). This intriguing finding can be explained by carefully analyzing colloidal interactions involved in the process, and would allow a more rational design of patchy colloids for nanoparticle networks and complex nanoparticle assemblies.

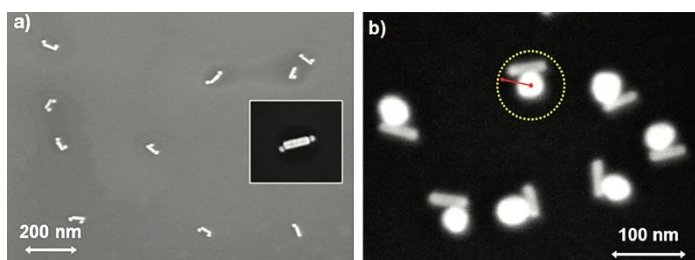


Figure 3 (a): Patchy nanorod (tip: cysteamine; side: polyethylene glycol) assembled with negatively charged 20 nm gold spheres. (b): As the relative size of the sphere increases, side selective assembly prevails.

EXFOLIATION OF LARGE-AREA TRANSITION METAL CHALCOGENIDE SINGLE LAYERS

Gábor Zsolt Magda, J. Pető, Gergely Dobrik, C. Hwang, László Péter Biró, Levente Tapasztó

Layered transition metal chalcogenides (TMCs) display strong intra-layer metal-chalcogenide bonds, and a weak inter-layer bonding between neighboring planes of chalcogenide atoms. The recent interest in studying their two-dimensional (2D) form (consisting of triple to quintuple atomic sheets) is driven by the fact that the properties of atomically thin crystals can drastically differ from their well-characterized bulk counterparts. An eloquent example is the transition in the MoS₂ band structure from indirect to direct band gap as the number of layers is reduced from bulk to a single layer, opening the way towards optoelectronic applications. Furthermore, the family of transition metal chalcogenides is large, covering a broad range of properties from semiconductors (MoS₂, WSe₂) to semimetals (TiS₂, TiSe₂), from topological insulators (Bi₂Te₃, Bi₂Se₃) to correlated materials (NbS₂, NbSe₂). Such large variety of properties holds a huge potential for both fundamental studies and applications, even graphene cannot compete with in spite of the unique versatility of its properties.

The easy access to large TMC single layers is of key importance for exploring their properties, in a similar manner as the facile isolation of large and high-quality graphene flakes enabled the outstanding pace of the graphene research. As several bulk TMC crystals are layered materials, similar to graphite, individual TMC layers can be isolated by mechanical exfoliation ("scotch-tape" technique). Compared to other methods, mechanical exfoliation provides 2D TMC sheets of high structural quality enabling the fundamental study of their pristine properties, and ultimate device performance, similar to graphene, where most of the fundamental discoveries have been achieved on exfoliated samples, owing to their superior structural and electronic quality. The major limitation of the micromechanical exfoliation of various TMC materials is the small yield of single layers and their relatively small lateral size, typically of a few microns, rendering the subsequent investigations and device fabrication more difficult. This lateral size is about an order of magnitude smaller than that of graphene flakes which can routinely be obtained by the same technique. The reason for this probably originates from the unique mechanical strength and ultra-strong adhesion of graphene to SiO₂ that cannot be matched by the otherwise still excellent mechanical properties of TMCs.

We have developed a novel mechanical exfoliation technique that overcomes the limitations of the scotch-tape technique enabling the exfoliation of TMC single layers with lateral size in the range of hundreds of microns. During the mechanical exfoliation process, isolation of single layers is possible because the adhesion of the bottom layer to the substrate becomes stronger than the adhesion to its own bulk crystal. First, thick multilayer flakes had been peeled off from a bulk MoS₂ crystal using a thermal release tape, and these flakes had been placed on the top of the freshly cleaved gold substrates. We used a short ultrasonic treatment in acetone to remove the thick MoS₂ flakes from the gold surface. We found that after a few seconds of sonication several thick flakes have been detached; however, underneath them, the last (bottom) MoS₂ layer remained attached to the gold substrate.

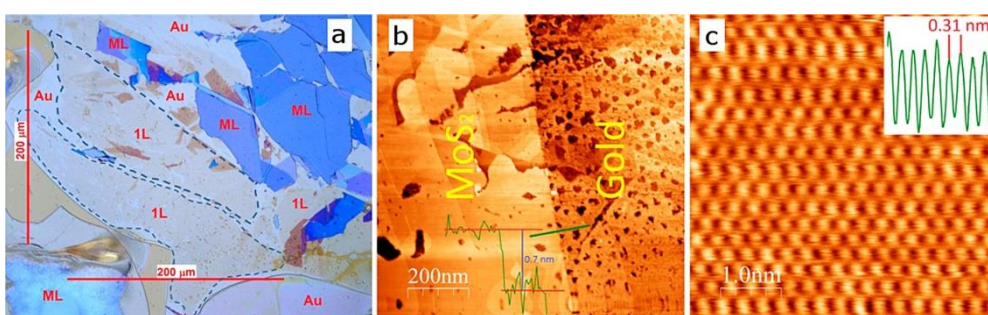


Figure 1 (a): Optical microscopy image of MoS₂ single layer areas (1L, outlined by dotted lines) with several hundreds of microns lateral size exfoliated on gold (Au 111) substrate. (b) STM image of a MoS₂ single layer exfoliated onto a gold substrate. The line cut displayed was taken along the direction marked by the green line across the edge. (c) Atomic resolution STM image of a MoS₂ single layer revealing a hexagonal lattice corresponding to the crystal lattice of the top sulfur atoms.

In optical microscopy images the MoS₂ single layers can be identified as the areas of the faintest color contrast as shown in Fig. 1. The optical images revealed several hundreds of micron large areas covered by thin MoS₂ layers. To confirm that these areas of faintest optical contrast are indeed single layers of MoS₂ we have performed confocal Raman spectroscopy measurements. These measurements were indicating that the several hundreds of microns large areas observed by optical microscopy can be identified as MoS₂ single layers. The exfoliated large flakes on top of the conductive Au substrate enabled us to perform Scanning Tunneling Microscopy (STM) measurements on mechanically exfoliated single layer MoS₂ flakes. The height of the investigated layers relative to the Au substrate was found to be about 0.7 nm from the STM measurements (Fig. 1b), confirming the single layer thickness of the exfoliated flakes. Atomic resolution images could routinely be achieved even under ambient conditions (Fig. 1c). A hexagonal atomic lattice was revealed with a 3.1 Å periodicity, corresponding to the lattice constant of the top layer of sulfur atoms.

We have also investigated whether the exfoliation process is specific to MoS₂ or can be applied more generally to various layered materials. We found that our exfoliation method yielding large-area MoS₂ flakes is not specific to molybdenum disulfide or even sulfides, but works equally well for various layered chalcogenides, including selenides and tellurides. Furthermore, in contrast to the standard scotch-tape method, the exfoliation technique reported here is in principle able to achieve high coverage rates of macroscopic substrates with various TMC single layers.

STRUCTURE AND PROPERTIES OF GRAPHENE ON GOLD NANOPARTICLES

Zoltán Osváth, András Deák, Krisztián Kertész, György Molnár, Gábor Vértesy, Dániel Zámbó, C. Hwang, László Péter Biró

Graphene covered metal nanoparticles constitute a novel type of hybrid materials, which provide a unique platform to study plasmonic effects, surface-enhanced Raman scattering (SERS), and metal-graphene interactions at the nanoscale. Such a hybrid material is fabricated by transferring graphene grown by chemical vapor deposition onto closely spaced gold nanoparticles produced on a silica wafer. The morphology and physical properties of nanoparticle-supported graphene is investigated by atomic force microscopy (AFM), optical reflectance spectroscopy, scanning tunneling microscopy and spectroscopy (STM/STS), and confocal Raman spectroscopy.

Gold nanoparticles were prepared by evaporating a thin gold film of 5 nm onto a 285-nm-SiO₂/Si substrate at room temperature. Subsequent annealing was performed at 400 °C in Ar atmosphere for 30 minutes, which resulted in the formation of Au nanoparticles with heights of 15-20 nm and high surface coverage. We transferred graphene grown by chemical vapour deposition (CVD) onto the prepared gold nanoparticles using thermal release tape. Fig. 1a shows a typical AFM image of the transferred graphene which is considerably rippled. Note, that the lower part of the image is not covered with graphene.

During the transfer with thermal release tape, the initial large area graphene breaks into smaller sheets with dimensions of several micrometers and not all of them remain attached to the nanoparticles. Fig. 1b is a higher magnification image which corresponds to the white square drawn in Fig. 1a. The height profiles corresponding to the line sections 1 and 2 are displayed in Fig. 1c.

In Fig. 1c. Line section no. 1 is measured in the area without graphene, showing a typical gold nanoparticle on the SiO₂ surface, with height of 18 nm. On the graphene-covered side, the line section no. 2 displays the wavy shape of the graphene. The peaks in the height profile correspond to graphene directly supported by nanoparticles, whereas the dip corresponds to graphene bridging two nanoparticles. Comparing the height profiles of line sections 1 and 2, we find that the graphene part bridging the nanoparticles is located more than 10 nm above the SiO₂ substrate, i.e. it is suspended. In fact, this is a general observation for the transferred graphene: it is suspended between gold nanoparticles. We investigated the SERS activity of the graphene/gold nanoparticle sample by confocal Raman spectroscopy performed both before and after annealing. Fig. 2a show typical Raman spectra obtained with 488 nm laser on transferred CVD-grown graphene without annealing. Note that there is no significant difference between graphene peak intensities when measured on SiO₂ and on gold nanoparticles, respectively. In contrast, when using the 633 nm laser we observe an almost tenfold enhancement (Fig. 2b) for the graphene G peak (1585 cm⁻¹), as well as 4-fold enhancement for the 2D peak.

After annealing at 500 °C, these enhancement factors increase to 13 and 22 for the G and the 2D peak, respectively (Fig. 2d). Furthermore, nearly 6-fold peak enhancement is observed with the 488 nm laser also, but only for the 2D peak (Fig. 2c). The higher enhancement at 633 nm laser is due to the fact that this wavelength is closer to the localized surface plasmon resonance of gold nanoparticles (597 nm), where the local electric fields are much more increased compared to the off-resonance at 488 nm.

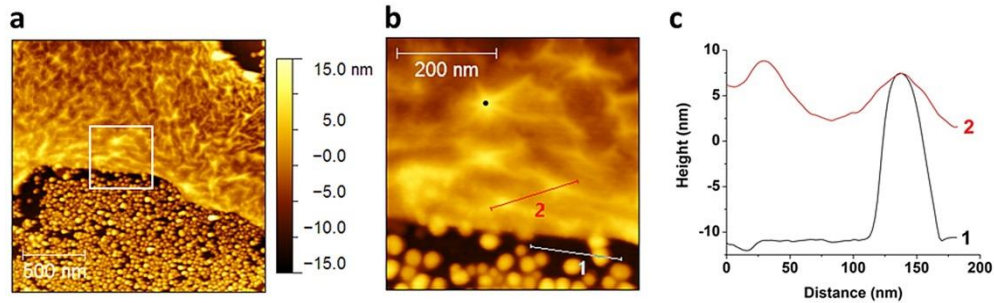


Figure 1: Tapping mode AFM image of graphene transferred onto Au nanoparticles. The area marked by white square in (a) is presented with higher magnification in (b). The black dot in (b) points out star-shaped rippling centred on the top of the underlying nanoparticle. The height profiles representing the sections 1 and 2 are displayed in (c).

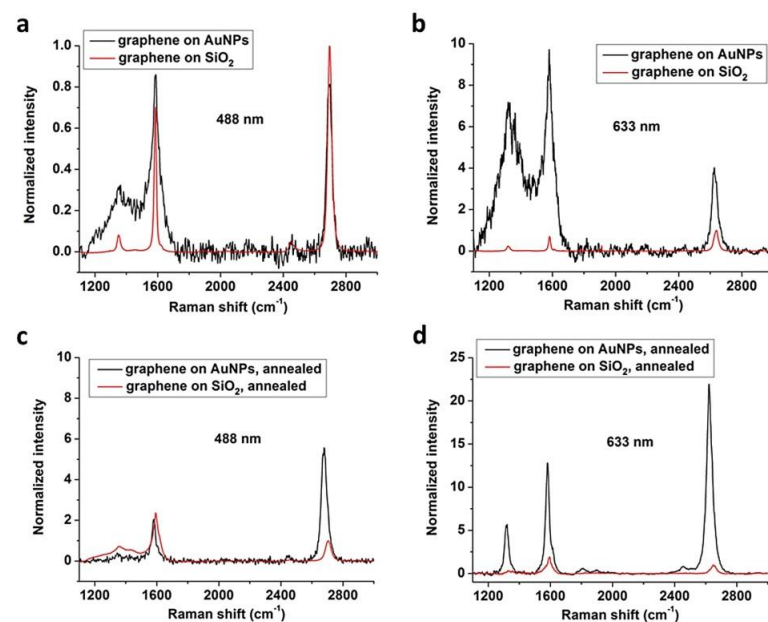


Figure 2: Raman spectra of graphene transferred onto: gold nanoparticles (black line), and SiO₂ substrate (red line). All spectra are averaged over areas of 5×5 μm² and normalized to the 2D peak height measured on SiO₂.

After annealing at 500 °C, these enhancement factors increase to 13 and 22 for the G and the 2D peak, respectively (Fig. 2d). Furthermore, nearly 6-fold peak enhancement is observed with the 488 nm laser also, but only for the 2D peak (Fig. 2c). The higher enhancement at 633 nm laser is due to the fact that this wavelength is closer to the localized surface plasmon resonance of gold nanoparticles (597 nm), where the local electric fields are much more increased compared to the off-resonance at 488 nm.

ELECTRONIC PROPERTIES OF MoS₂ FLAKES GROWN ON GRAPHITE

Antal Adolf Koós, Péter Vancsó, Gábor Zsolt Magda, Zoltán Osváth, Krisztián Kertész, Levente Tapasztó, C. Hwang, László Péter Biró

Hybrids of 2D materials are expected to become building blocks of next generation high performance nanoelectronic devices, like transistors and sensors. In addition to graphene with zero-gap character, other 2D materials, such as MoS₂ with a direct band gap of 1.9 eV, are really interesting. These materials can complement each other in 2D van der Waals heterostructures, offer a tool to engineer wide range of physical properties and open new possibilities for applications. In order to understand the properties of graphene - MoS₂ hybrids, MoS₂ sheets were grown by chemical vapour deposition (CVD) on highly ordered pyrolytic graphite (HOPG). The heterostructures were investigated with Scanning Tunneling Microscopy (STM) and Current Imaging Tunneling Spectroscopy (CITS).

The MoS₂ flakes were triangular (Fig. 1a) and followed the crystallographic orientation of HOPG substrate. The high resolution STM image (Fig. 1b) shows two overlapped periodic structures which form moiré pattern. The smaller 3.16 Å period corresponds to the inter-atomic spacing of S atoms in MoS₂, while the longer 12.5 Å period was caused by the interaction between MoS₂ and HOPG. The 12.5 Å period is nearly 5 times the atomic distance in HOPG, and 4 times in MoS₂, respectively.

The electronic properties of MoS₂ flakes grown on HOPG were investigated using CITS (Fig. 2). In CITS operation the scanning is interrupted in each image pixel, a full I-V curve is recorded and the CITS map displays the tunneling current measured at a selected bias voltage. The measured quasiparticle band gap for single-layer (SL) MoS₂ is around 2 eV, which decreases to 1.75 eV for bi-layer (BL) MoS₂, in good agreement with previous calculations and recent STM studies. The tunneling current of MoS₂ edges is different along the entire edge - irrespectively if the edge is located on HOPG (SL edge) or on MoS₂ (BL edge) - from the current measured on flakes. These changes appear more pronounced at negative voltages. The difference is also clearly visible in the dI/dV spectra (Fig. 2d), where the MoS₂ edges show a metallic behaviour. Our STM measurements have confirmed that the edges of insulating MoS₂ can be viewed as a one-dimensional metallic wire.

STM nanolithography was used to cut MoS₂ nanoribbons suitable for nanoelectronic devices. The most accurate lines were cut when the cutting was started at the edge of the MoS₂ flake and performed in air with 90% relative humidity. With this method we were able to cut less than 20 nm wide MoS₂ nanoribbons for the first time (Fig. 3).

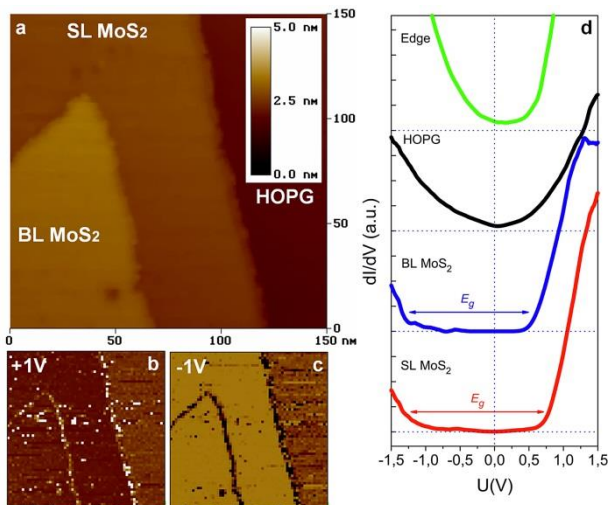


Figure 2: STM image (a), CITS maps (b, c) and dI/dV spectra (d) recorded on SL and BL MoS₂ flakes grown on HOPG.

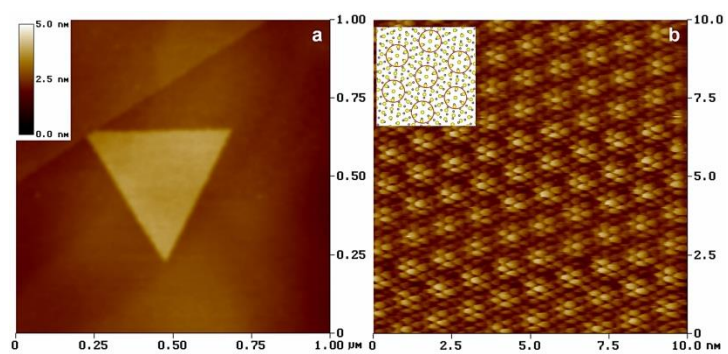


Figure 1: a) STM image of a single layer MoS₂ flake grown on HOPG (200 pA, 1.5 V). b) Atomic resolution STM image of the flake exhibiting moiré type pattern (1 nA, 100 mV). The inset shows a ball and stick model of sulphur (yellow) and carbon (grey) atoms.

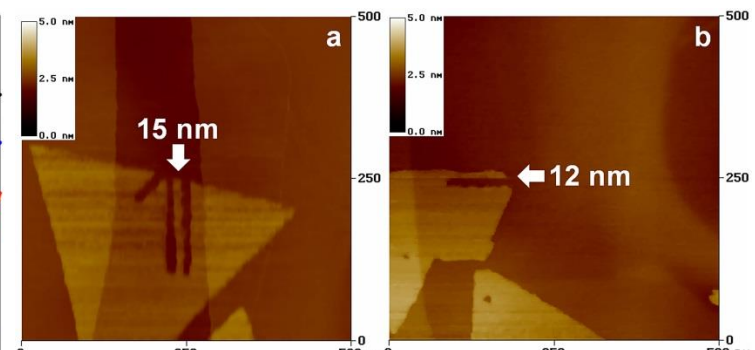


Figure 3: MoS₂ nanoribbons cut by STM nanolithography on HOPG. a) ~15 nm and. b) ~12 nm wide MoS₂ ribbons.

ATOMIC AND ELECTRONIC STRUCTURE OF NATIVE POINT DEFECTS IN MoS₂ SINGLE LAYERS REVEALED BY SCANNING TUNNELING MICROSCOPY

Péter Vancsó, Gábor Zsolt Magda, J. Pető, J.Y. Noh, Yong-Sung Kim, C. Hwang, László Péter Biró, Levente Tapasztó

Transition metal dichalcogenide (TMDC) single layers have recently emerged as strong competitors of graphene in electronic and optoelectronic applications due to their intrinsic direct bandgap. However, atomic resolution TEM and electrical transport measurements indicate the presence of a high concentration of intrinsic structural defects. In this work we revealed the structure of native defects at truly atomic scale by STM investigation of large area exfoliated MoS₂ single layers, and we provide information on their electronic properties by ab-initio calculations, too. Fig. 1 shows typical atomic resolution STM images of 20 nm x 20 nm areas of a MoS₂ single-layer. The basic pattern observed is a hexagonal lattice of 0.31 nm periodicity, corresponding to the atomic lattice of the top sulfur layer of the 2D MoS₂ crystal. Line profiles (inset of Fig. 1b) across the dark triangles reveal that they are centered on a lattice site of the top S layer, except that no S atom is present, indicating their origin from a S vacancy. Since during the STM investigation the introduction of novel point defects has never been observed, we can directly estimate their intrinsic concentration in high quality exfoliated MoS₂ single layers which is in the range of 10¹³-10¹⁴ cm⁻².

Besides the frequently observed triangular defects in STM images (Fig. 2a), defects of circular symmetry (Fig. 2b) have also been observed. To clarify the origin of the point defects we have performed DFT calculations.

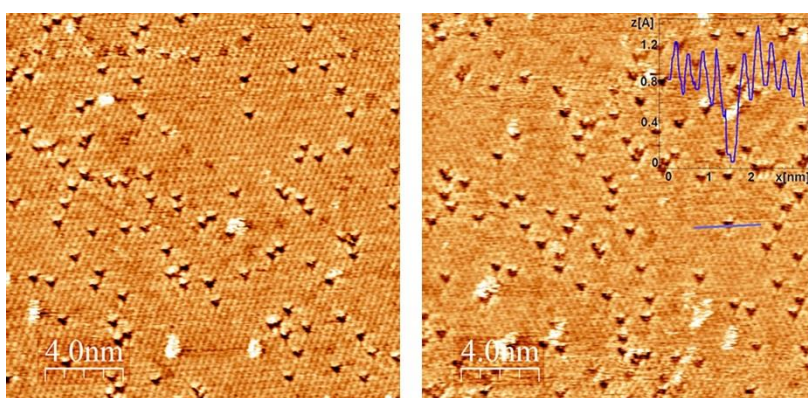
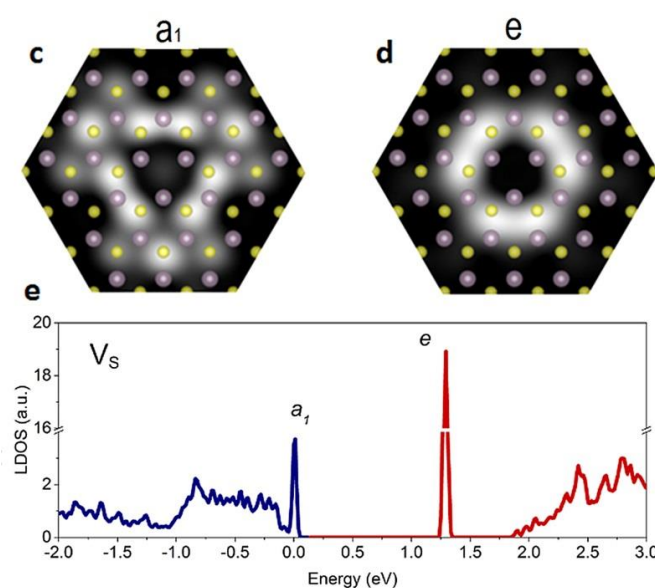
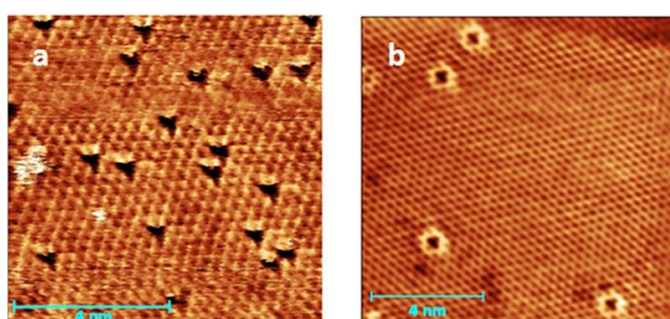


Figure 1: Atomic resolution STM images of native point defects in MoS₂ single layers. A high concentration (10¹³-10¹⁴ cm⁻²) of native point defects (dark triangles) has been revealed by truly atomic resolution STM investigation of mechanically exfoliated MoS₂ single layers on Au (111). The point defects (dark triangles) are centered on an empty site of the hexagonal S atom lattice (see inset).



Our calculations revealed two midgap electronic states (Fig. 2e) localized on the S atom vacancy. The simulated STM images from the calculated local density of states of the neutral a₁ and e states show triangular and circular form (Fig. 2c,d), pointed out that they are distinct STM images of the same structural defect.

By combining STM measurements with theoretical calculations our results provide insight into the electronic structure of the native defects of MoS₂ single layers, which is of key importance for understanding the operation of realistic electronic devices based on 2D crystals of molybdenum disulfide.

Figure 2: (a)-(b) Atomic resolution STM images of single-layer MoS₂ with triangular and circular shaped point defects at different spatial locations of the same flake. (c)-(d) Simulated STM images of the two electronic mid-gap states of a S atom vacancy based on DFT calculations. The sulfur and molybdenum atoms are shown by yellow and purple circles, respectively. (e) Local density-of-states for a neutral sulfur atom vacancy with midgap states.

MODULATION OF PHYSICAL PROPERTIES BY STACKING OF 2D MATERIALS

Gergely Dobrik, Péter Vancsó, Géza I. Márk, Levente Tapasztó, Ph. Lambin, C. Hwang, László Péter Biró

The extraordinary properties of graphene induced a continuously increasing attention focusing more recently on other 2D materials, too, like for example h-BN and the transition metal dichalcogenides. These 2D layers offer the possibility of building new materials, by stacking in a controlled way atomic/molecular thin layers in a layer by layer sequence, leading to novel properties. The vertically stacked heterostructures of 2D materials open a very wide range of possibilities the exploration of which may offer solution from cheap gene sequencing to high temperature superconductivity. As already demonstrated experimentally, the stacking each over the other of the 2D atomic, or molecular crystals gives birth to a full range of very complex phenomena, like Hofstadter's Butterfly, new optical phenomena, charge density waves etc. These may arise from several sources, for example: the lattice mismatch of the adjacent layers; the chemical composition of the individual layers; the orientation of the crystalline lattices of the adjacent layers. Therefore the investigation of the effects of the above parameters may prove to be of paramount importance in understanding the properties of the new material heterostructures systems.

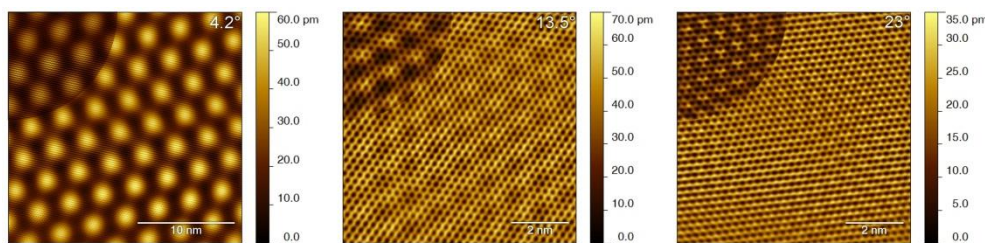


Figure 1: Moiré structures at different angles of rotation (misorientation angles are given in the upper right corners). The rotation angles accurately determined relative to the HOPG substrate. Top left corner inserts; increased contrast.

In this work, we propose as a particularly suitable model system for the understanding of vertically stacked 2D materials the CVD graphene on highly oriented pyrolytic graphite (HOPG). A major advantage of this system is that it allows the separation of chemical composition and lattice mismatch effects from lattice rotation effects. The grain misorientation angles ranging from a few degrees to 30 degrees include the entire range of interest. The moiré type superstructures appearing between the CVD graphene layer and bulk HOPG (Fig. 1) was investigated by scanning tunneling microscopy (STM), scanning tunneling spectroscopy (STS) and Raman spectroscopy.

We found that the different rotation angles caused various effects. At small rotation angles <2° STS measurements show localized states at the Fermi energy (Fig. 2a). When the rotation angle is increased, (between 2° and 7°) the STS measurements reveal an interesting phenomenon, namely secondary Dirac cones are observed in the spectra (Fig. 2b). We found that the energy position of the 2nd Dirac cone is tunable by the rotation angle following linear dependence. This peculiar band structure leads to profound changes in the electronic transport measurement by increased resistivity.

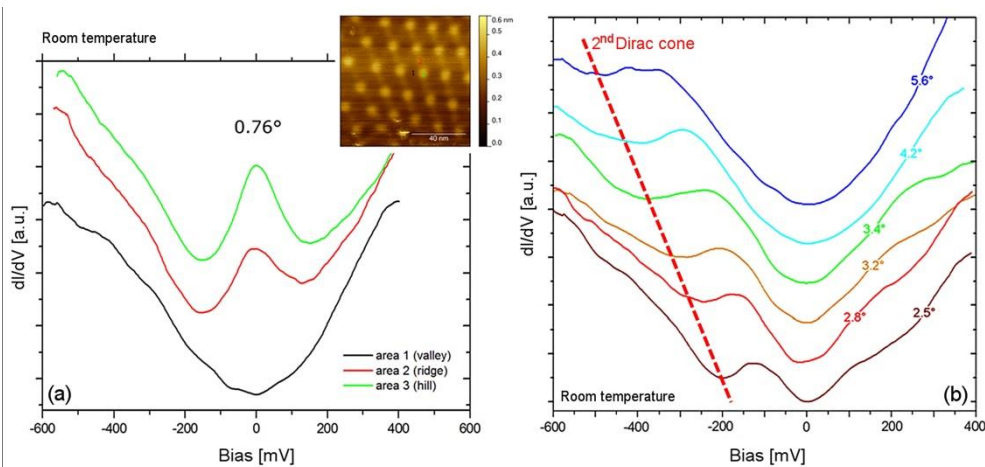


Figure 2: STS spectra at small rotation angles. (a.) Localized states at the Fermi energy. Inset: STM image with the measured points. (b.) Secondary Dirac cone as a function of the angle of rotation.

Further increase of the rotation angle (above 15°) the 2D peak of graphene appears near the graphite's 2D peak in the Raman measurements (Fig. 3). This suggests that the graphene layer is vibrationally decoupled from the substrate. The STS spectra also support the decoupling because no significant changes of the electronic properties have been observed compared with the single layer graphene.

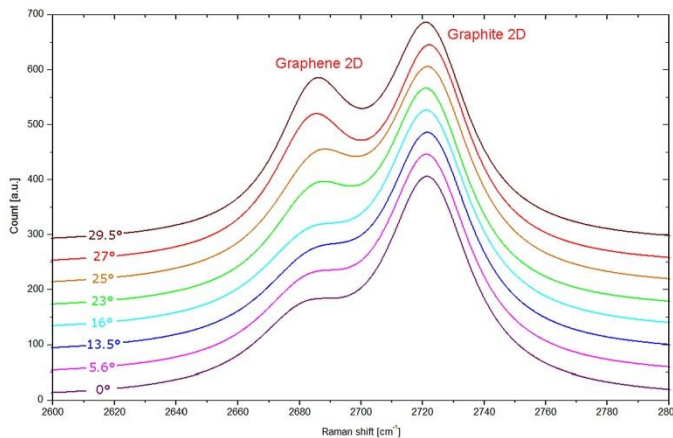


Figure 3: Raman shift of the rotated CVD graphene layer on HOPG. The graphene layer is vibrationally decoupled from the substrate above 15° rotation angle.

VARIABILITY OF STRUCTURAL COLORATION IN BLUE BUTTERFLY WINGS

Krisztián Kertész, Gábor Piszter, Zsolt Bálint, László Péter Biró

Variation exists within all populations of living organisms. This is the basis of natural selection where individuals that differ in phenotypes have different survival and reproduction chances: individuals with the appropriate trait may survive and reproduce more successfully than individuals with other, less suitable attributes, thus the population is able to evolve. The reproductive success can be determined by sexual selection, too, where one gender chooses mate based on phenotypic traits. The conspicuous structural colour on the wings of Blue butterfly males constitutes an important sexual communication channel; therefore it is subjected to strong evolutionary pressure as individuals with the “wrong” colour have a lesser chance to transmit their genes to the offspring.

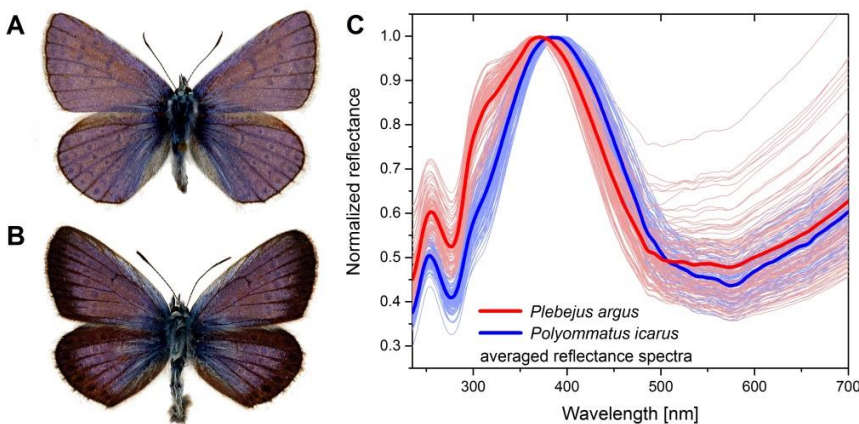


Figure 1: Photograph images of male Blue butterflies: (a) *P. icarus* and (b) *P. argus* specimens are shown. (c) Species-specific reflectance spectra of *P. argus* and *P. icarus*. Note the wavelength difference of the main reflectance peak and the shoulder at 320 nm.

The structural colour of the wings is generated by photonic crystal type nanoarchitecture which is located in the volume of the wing scales. This photonic nanocomposite is constituted of spatially periodic chitin matrix with embedded air holes with the characteristic size range of a few hundred nanometres. This characteristic length of the components’ periodicity and the refractive index contrast between them result in wavelength selective reflection in the blue which is the source of the vivid structural coloration.

Structural colours of butterfly wings are more and more in the focus of attention both from the point of view of physics, and biology. However, studies focusing on the biologic variability of the structural coloration are mostly lacking. Therefore, we investigated this variability of structural coloration in the case of two common Lycaenid species living in Hungary. These species use their blue coloration for conspecific recognition, but display differences in prezygotic strategy as male individuals of *Polyommatus icarus* (Fig. 1a) are patrolling, whilst *Plebejus argus* (Fig. 1b) are lacking in their habitats. From both species 25 male individuals were captured and the colour of all four wings was characterized spectrally, thus providing 100 measurements for each species.

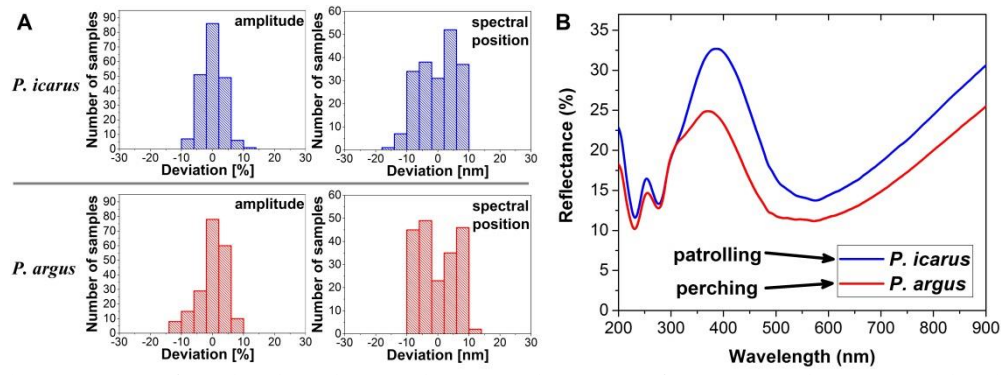


Figure 2: (a) Histograms of amplitude and spectral position deviations of *P. icarus* and *P. argus* males. (b) Averaged reflectance spectra of *P. icarus* and *P. argus* males. Significant difference in the measured intensity can be seen.

The reflectance spectra of the wings were measured using normal incident white light illumination and integrating sphere light collecting. The averaged reflectance spectra of the two species were generated and normalized to the main reflectance peaks in the blue to facilitate comparison. In Fig. 1c the species-specific colour differences of the two species can be observed: there is a small (~15 nm) difference between the wavelength of the maxima in the blue and the averaged spectrum of *P. argus* males has an additional shoulder at 320 nm compared to *P. icarus*.

Based on these averaged spectra the averaged parameters (peak position, amplitude) were determined for both species and the deviation of the two quantities were calculated and histograms were generated (Fig. 2a). For the two investigated species the intensity and wavelength deviations were almost identical which show that the natural variability of the structural colour in the case of species living in the same habitat is very similar due to the colour-based conspecific recognition.

To analyse the intensity of the blue structural colour the 100-100 measured reflectance spectra were averaged by species without normalization and were plotted (Fig. 2b). The two averaged curves reveal the reflected intensity differences: the *P. icarus* males show enhanced reflectivity in the visible wavelength range compared to *P. argus* males resulting in brighter blue colour of the wings. This is in accordance with the naked eye observations and can be a direct consequence of the different prezygotic mating strategies of the two species while it requires different optical properties: the patrolling males of *P. icarus* have to be more conspicuous for an easy recognition by their females, but the perching mating strategy of *P. argus* males lacking in their microhabitats requires less intense blue colour as the females have to identify the males from significantly shorter distances.

MAKYOH TOPOGRAPHY

Ferenc Riesz, János P. Makai

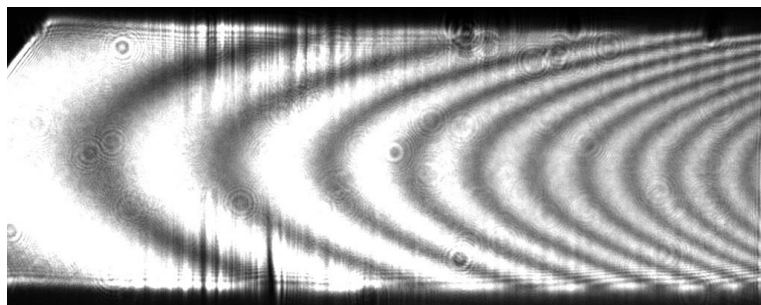


Figure 1: Makyoh-topography image of a SiC/Si heterostructure.

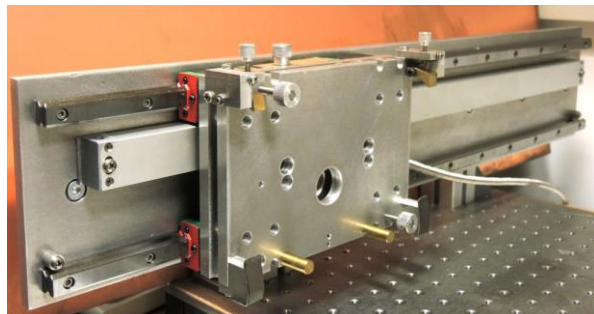


Figure 2: Sample positioning stage for Makyoh characterisation of large-area samples.

In collaboration with IMEM-CNR, Parma, the surface shape and morphology of hot-wall VPE grown SiC/Si heterostructures have been characterized with Makyoh topography in order to study the effects of the addition of methyl trichloro silane. Low amount of sample bow was obtained in an optimized growth process. Fig. 1 shows a characteristic topogram, showing interference fringes related to thickness inhomogeneity and edge slip lines.

Within the project KMR_12-1-2012-0226, in collaboration with Mirrotron, Ltd. and the Wigner Research Centre for Physics, surface flatness of large-area polished Ni(P) coated Al blocks were characterised for neutron guide applications. Fig. 2 shows the purpose-built sample positioning/translation stage.

RADIOECOLOGICAL INVESTIGATION OF BUTTERFLIES

Gábor Piszter, Krisztián Kertész, Zsolt Bálint, Blanka Czitrovszky, Imre Balásházy, Péter Füri,
Péter Szántó, Tamás Pázmándi, László P. Biró

Objective

Wild Lycaenid butterflies captured in regions with radioactive pollution (Chernobyl, Fukushima) exhibited aberrations ranging from modifications of body morphology to alteration of their wing patterns. This suggests the possible use of wild butterflies as monitors of environmental radiation pollution. To check this, experiments were performed to test the effect of both non-radiative environmental conditions, primarily temperature, and of controlled irradiation under laboratory conditions.

Methods

Two series of butterfly breeding experiments were performed: a) on the KFKI campus by researchers of the EK MFA for testing the temperature effects, and b) in the framework of an external contract for the production of pupae to be subjected to controlled irradiation. While track a) yielded more than 100 pupae, track b) failed to produce any pupae. Therefore, 20 pupae from track a) were diverted to track b) for controlled irradiation experiments.

The larvae of track a) immediately after pupation were cooled to 5°C to slow down their biochemical transformation processes. The main investigated parameter was the effect of the length of the cooling period on the morphology and pattern of the butterflies after eclosion. The cooling time ranged from 10 days to 63 days. Following the cooling the pupae were allowed to finish their transformation at room temperature. The 20 pupae diverted to track b) following a 10 day cooling time were divided into 3 groups: a control group (6 pupae), a group irradiated with 100 mGy (7 pupae) and, a group irradiated with 200 mGy (7 pupae) ^{137}Cs gamma irradiation. Then these pupae were allowed to finish their transformation at room temperature.

All eclosed butterflies were evaluated by an expert taxonomist of Lycaenid butterflies, and by UV-VIS spectroscopy. Where the number of individuals allowed this, the data were also evaluated quantitatively.

Results

The spectral evaluation of blue, structural coloration on the dorsal wing side of cooled butterflies (Fig. 1 left panel) clearly shows that the butterflies eclosed from the pupae cooled for more than 10 days sometimes show larger color variations than the uncooled individuals. The magnitude of the color change is of the same order of magnitude as the variability of the color of the uncooled individuals. Similarly, the averaged sum of the alteration of the complex pattern, characteristic for the ventral wing side (Fig. 1 right panel), also shows that for the first 10 days of cooling the alterations are minimal, and after that the magnitude of aberrations increases linearly with cooling time.

In both irradiated groups, two in seven individuals showed alteration of the complex pattern on the ventral wing side, while the other individuals were normal. No spectral alterations exceeding biological variability were observed on the structurally colored blue dorsal side. These findings indicate that the effects of irradiation in this low dose range administered in the pupal stage are probabilistic and much larger experimental groups, as well as larger doses, are needed to rigorously assess the effect(s) of irradiation.

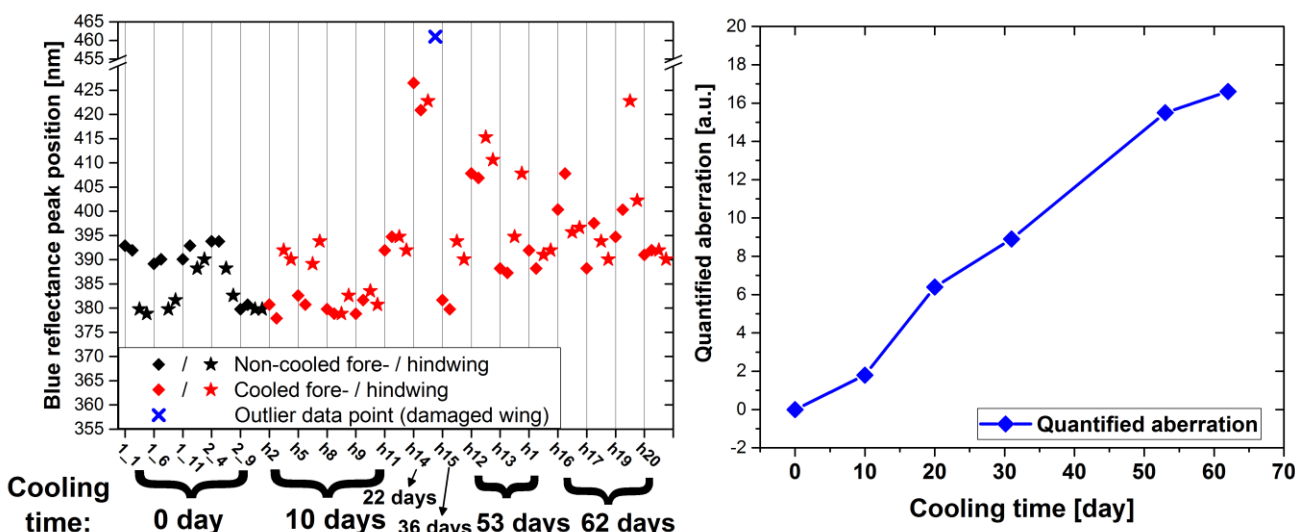


Figure 1: Quantitative evaluation of the effects of prolonged cooling in pupal stage on the structural coloration (left), and on the complex pattern on the ventral side of the wings (right).

As the cooling time increased the number of individuals which did not normally eclose increased dramatically. In certain experimental groups cooled more than 40 days, no normal eclosion took place. This made impossible the quantification of the alterations in these cases. This underlines that the effects of cooling and of irradiation are both of probabilistic type.

NONDESTRUCTIVE INDICATION OF FATIGUE DAMAGE IN FERROMAGNETIC CONSTRUCTION MATERIALS

Gábor Vértesy, Csaba Sándor Daróczi, Antal Gasparics

Magnetic measurements are frequently used for characterization of changes in ferromagnetic materials, because magnetization processes are closely related to their microstructure. The recently developed method (Magnetic Adaptive Testing, MAT) is based on the systematic measurement and evaluation of minor magnetic hysteresis loops. This method was suggested as a highly promising non-destructive alternative of destructive tests for monitoring structural changes in ferromagnetic objects. MAT introduces a large number of magnetic descriptors to diverse variations in non-magnetic properties of ferromagnetic materials, from which those optimally adapted to the just investigated property and material can be picked up.

Many ferromagnetic components are subjected to alternating load in service, which often causes their structural failure as a result of fatigue. Fatigue evaluation and residual lifetime assessment are challenging issues with a high profile in industry. Nearly 90% of industrial component failures take place due to fatigue that occurs without warning. In order to check up health of ferromagnetic construction materials, it is important to timely monitor their fatigue damage, i.e. to detect initiation and propagation of fatigue cracks, and to predict residual lifetime of the constructions.

Fatigue damage was investigated in cyclically loaded low-carbon steel, by the MAT method. A sample made of cold-rolled S235JR steel was chosen for presentation of a typical MAT-measurement of the fatigue damage process. The specimen is ferromagnetic, it is flat, and it can be magnetized for the MAT-measurement by a short solenoid placed over the critical volume, where the fatigue cracks are initiated in the sample. This critical area is the neck, close to the fixed bottom head of the sample. The MAT-measurement of the samples proceeded in such a way, that always after a chosen number of loading cycles a short solenoid containing both the magnetizing and the pick-up coils was placed over the critical part of the sample, a couple of passive soft magnetic yokes was pressed to the sample so, that they and the sample created a closed magnetic circuit, and one family of the minor permeability loops was recorded. Then the yokes were taken away and a next number of loading cycles were applied. Fig. 1 shows the sample with the yokes and with the yoke-holder during the magnetic measurement.

Fig. 2 presents the result of the magnetic measurements. It is seen here, how the properly chosen MAT descriptor changes due to the cyclic loading. The sample was broken after 230 000 cycles. A very significant and fast increase of magnetic parameters close the end of the sample's lifetime is observed.

As a conclusion, satisfactory correlation between nondestructively measured magnetic descriptors and actual lifetime of the fatigued material were found. The method is able to serve as a powerful tool for indication of changes, which occur in structure of the inspected objects during their industrial service lifetime, as long as they are manufactured from ferromagnetic materials.



Figure 1: The critical part of the sample is covered by the magnetizing/sensing solenoid and by a couple of passive soft yokes pressed to the surface of the sample with a plastic spring holder. All are fixed at the bottom in a vice with non-magnetic jaws. The couple of deflection electromagnets can be seen at top of the figure.

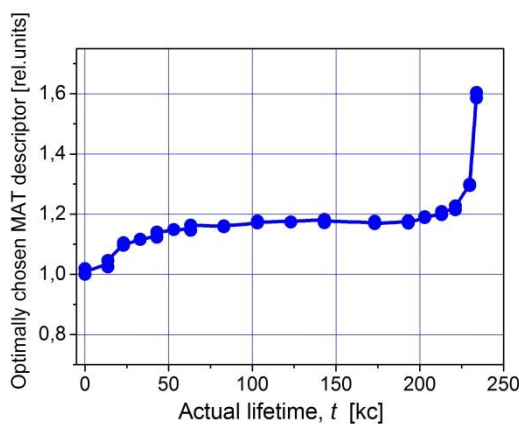


Figure 2: The optimally chosen MAT descriptor as a function of cyclic loading. The fast upward curvature after 200 000 cycles indicates start of the critical crack spreading through the sample.

DETERMINATION OF MIGRATION OF ION-IMPLANTED AR AND ZN IN SILICA BY BACKSCATTERING SPECTROMETRY

István Bányašz, Edit Szilágyi, Endre Kótai, A. Németh, Cs. Major, Miklós Fried, Gábor Battistig

It is well known, that refractive indices of materials important for waveguide fabrication, can be modified by ion implantation. In this work, effect of Ar and Zn ion implantation on silica layers was investigated by Rutherford Backscattering Spectrometry (RBS) and Spectroscopic Ellipsometry (SE). The silica layers that were produced by chemical vapour deposition technique on single crystal silicon wafers were subsequently implanted by Ar and Zn ions.

The refractive indices of the implanted silica layers before and after the annealing at 300 °C and 600 °C were determined by SE.

The migration of the implanted element was studied by real-time RBS up to temperatures of 500 °C.

It was found that the implanted Ar escapes from the sample at 300 °C. Although the refractive indices of the Ar implanted silica layers were increased compared to the as-grown samples, but after annealing this increase in the refractive indices has vanished. In case of the Zn implanted silica layer both the distribution of Zn and the change in the refractive indices were found to be stable. Zn implantation seems to be an ideal choice for producing waveguides.

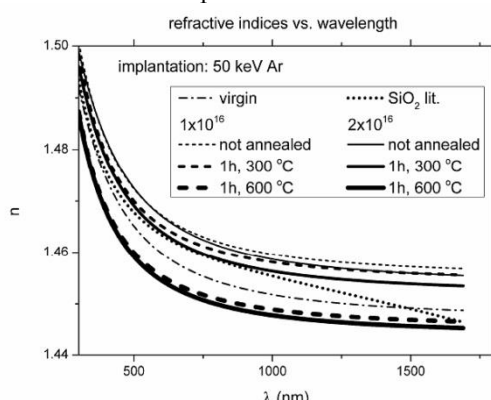


Figure 1: Refractive indices for Ar implanted samples. For comparison, the refractive indices of virgin sample and the thermal SiO_2 (from literature) are also shown.

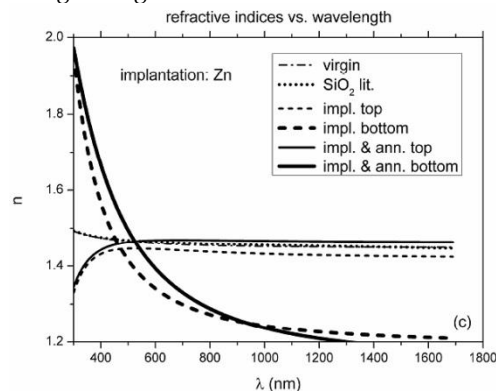


Figure 2: Refractive indices as a function of wavelength for the two sublayers in the Zn implanted sample. For the sake of comparison the refractive indices of the virgin oxide as well as the thermal oxide are also shown.

EFFECT OF HEAT TREATMENTS ON THE PROPERTIES OF HYDROGENATED AMORPHOUS SILICON FOR PV AND PVT APPLICATIONS

Miklós Serényi, Nguyen Quoc Khanh, C. Frigeri

Photovoltaic (PV) solar cells and photovoltaic thermal (PVT) hybrid devices very often employ hydrogenated a-Si (a-Si:H) because of its cost effectiveness and better performance as light absorber. The properties of a-Si:H can be improved by heat treatments that also help to recover the Staebler-Wronski effect. The effects of heat treatments on the properties of hydrogenated a-Si to be used in PV and PVT devices have been investigated. To better study them the annealing was performed at temperatures (350 °C) higher than those (~200-275 °C) usually applied to improve the performance of a-Si:H employed in PV and PVT technologies since those effects were expected to be stronger and more easily detectable. It was found that the heat treatment causes changes in the Si-H bonding configuration with the transformation of the SiH monohydrides to the less stable SiH₂ dihydrides and polysilane chains. The latter polyhydrides, in their turn, cause a strong degradation of the a-Si layer morphology with the formation of surface blisters with size of some microns as well as craters depending on the H content and annealing time.

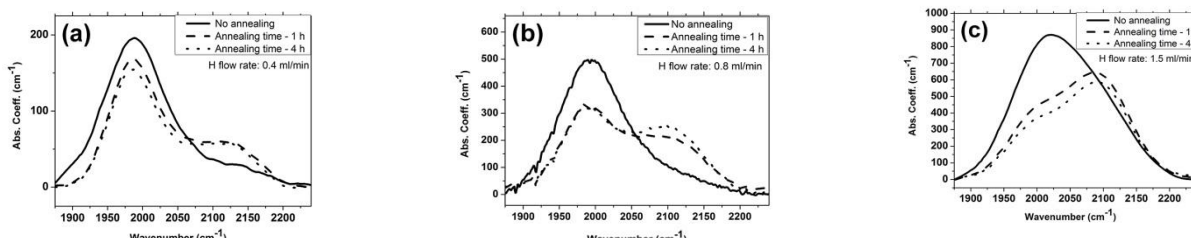


Figure 1: Typical IR absorption spectra in the stretching mode range of the wavenumber for the H content of a) 10.8, b) 14.7, c) 17.6 at%. For each plot the spectra for the unannealed (solid curve), annealed for 1 h (dash curve) and for 4 h (dot curve) are reported.

VERIFICATION OF THE EFFECTIVE MEDIUM APPROXIMATION FOR SURFACE ROUGHNESS BY FINITE ELEMENT METHOD

Bálint Fodor, Péter Kozma, S. Burger, Miklós Fried, Péter Petrik

Finite element simulations were used to calculate optical response of rough surfaces. This way we can generate any surface for the investigation of the simplified optical models of ellipsometry or other characterization method. In agreement with previous investigations on polysilicon samples, we found a correlation between the thickness of the effective medium layer and the RMS roughness. Our method also allows to investigate limits of the effective medium approach in more detail (see Fig. 1, and 2, and Ref. B. Fodor, P. Kozma, S. Burger, M. Fried, P. Petrik, "Effective medium approximation of ellipsometric response from random surface roughness simulated by finite element method", accepted for publication in *Thin Solid Films* in 2016).

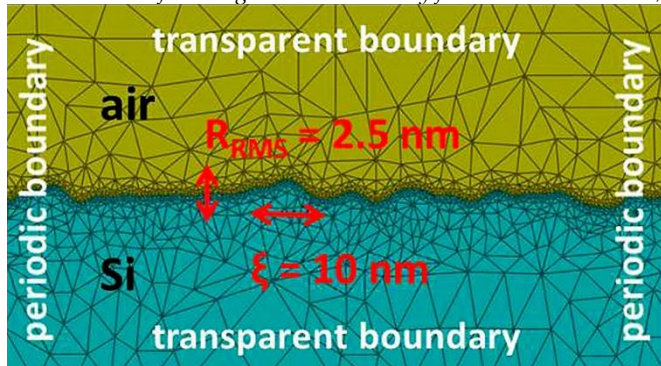


Figure 1: Random surface generated by the JCMWave finite element method.

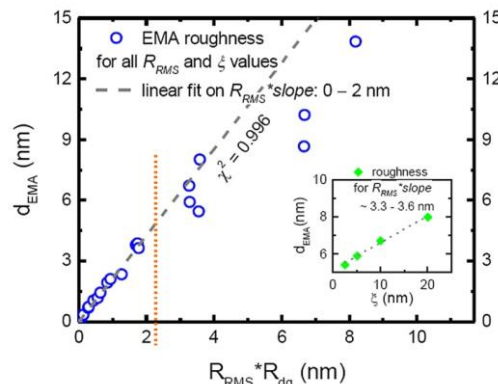


Figure 2: Correlation between the product of RMS roughness and RMS slope ($R_{RMS} \cdot R_{dq}$) and the thickness of the effective medium roughness (d_{EMA}) with linear fit for abscissa values smaller than 2 nm. The inset shows the secondary effect of correlation length (ξ) on d_{EMA} for points which have an $R_{RMS} \cdot R_{dq}$ value of ~ 3.4 nm.

PLASMON-ENHANCED TWO-CHANNEL KRETSCHMANN ELLIPSOMETRY

Judit Nádor, Benjámin Kalas, Eemil Agócs, András Saftics, Péter Kozma, László Kőrösi, Inna Székács, Miklós Fried, Sándor Kurunczi, Róbert Horváth, Péter Petrik

We have developed a flow cell in semi-cylindrical Kretschmann configuration for plasmon-enhanced, internal reflection, multiple-angle of incidence in situ spectroscopic ellipsometry, which can be used to monitor interface processes with a high sensitivity (~40 pg/mm²) and speed (less than 1 s for a full spectrum) in a broad wavelength range (350–1690 nm) (Fig. 1).

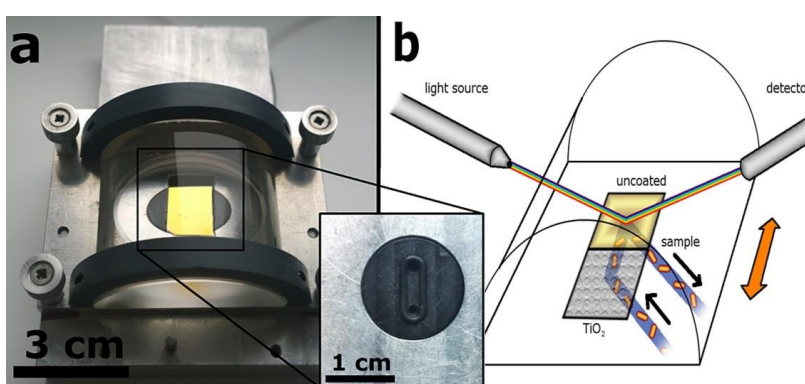


Figure 1(a): Flow cell with a semi-cylindrical lens in the Kretschmann configuration with a gold-covered glass substrate. inset: The 10 μ l flow-cell surrounded by an O-ring. (b): A schematic graph of the measurement geometry.

The cell has a small volume (10 μ l), and it can readily be used with conventional table-top ellipsometers. Configuration with the semi-cylinder allows multi-channel measurements when moving the cell parallel to the axis of the cylinder using a conventional mapping stage.

The device was successfully applied to study protein adsorption, cell adhesion and polyelectrolyte deposition simultaneously on uncoated and titanium nanoparticle-coated gold surfaces.

Related publications

- [1] J. Nádor, B. Kalas, A. Saftics, E. Agócs, P. Kozma, L. Kőrösi, I. Székács, M. Fried, R. Horváth, and P. Petrik: Plasmon-enhanced two-channel in situ Kretschmann ellipsometry of protein adsorption, cellular adhesion and polyelectrolyte deposition on titania nanostructures, *Optics Express* **24**, 4812–4823 (2016)

PROTEIN ADSORPTION, CELL ADHESION AND POLYELECTROLYTE DEPOSITION ON TITANIA NANOPARTICLE COATINGS STUDIED BY TWO-CHANNEL KRETSCHMANN ELLIPSOMETRY

Judit Nádor, Benjámin Kalas, Emil Agócs, András Saftics, Péter Kozma, László Kőrösí, Inna Székács, Miklós Fried, Sándor Kurunczi, Róbert Horváth, Péter Petrik

A flow cell in a semi-cylindrical Kretschmann configuration for performing *in situ* two-channel measurements with a high sensitivity ($\sim 40 \text{ pg/mm}^2$) was developed. A setup was applied allowing to carry out simultaneous measurements on titania nanoparticle (TNP) coated and uncoated gold surfaces, in order to reveal the effects of the coating on protein adsorption, cell adhesion and polyelectrolyte layer deposition. One of the main advantages of this approach is that the measurements on the two different surfaces are performed in the same process, under same conditions (temperature, pH, concentration etc.). Therefore, comparison of the two kind of measurement is more reliable than before, because most of the systematic errors can be ruled out, and concerns about repeatability are minimized.

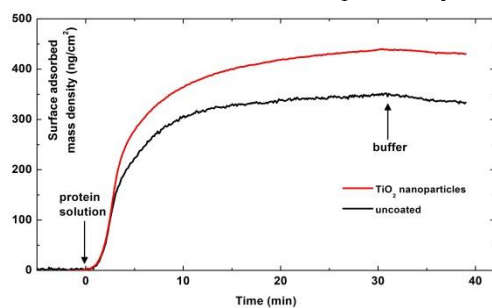


Figure 1: The typical curves of a representative *in situ* ellipsometric measurement of Fgn adsorption on TNP-coated and uncoated surfaces.

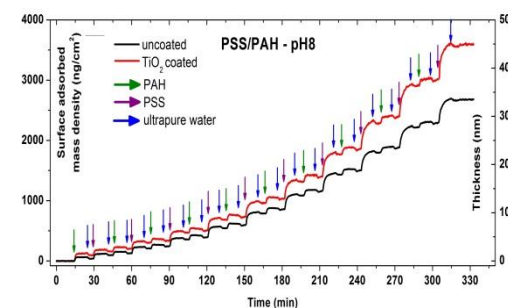


Figure 2: The adsorbed mass density and the thickness of the deposited 10 pairs of PSS/PAH layers at pH 8 on TNP-coated and uncoated gold surfaces

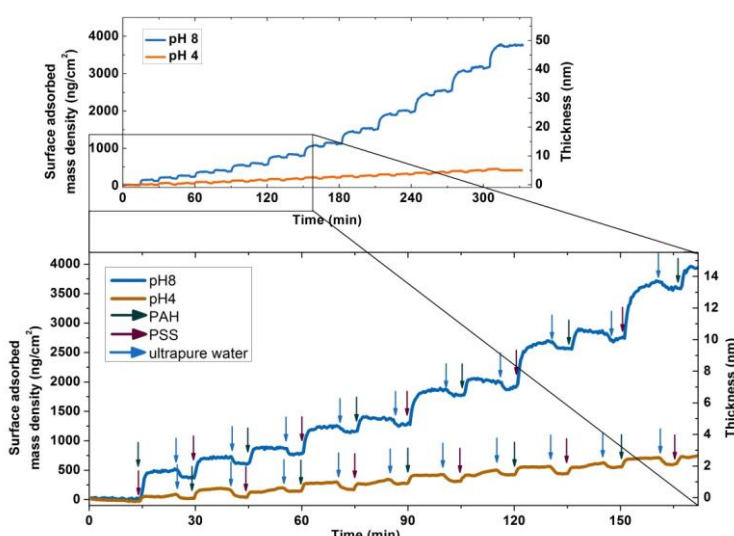
In the protein adsorption experiments a stable and widely used protein, fibrinogen (Fgn) was investigated. Kinetic curves showed that adsorption of proteins was enhanced on TiO_2 -coated surface (Fig. 1), which can be explained by the increased specific surface area due to the TiO_2 nanoparticles.

In the case of preosteoblast cell adhesion no proper ellipsometric model was found in the evaluation, so the ellipsometric measurement proves only that the coating modifies the adhesion of the cells. After the measurement, images were taken with phase-contrast microscope of the residual cells on the surfaces. On the TNP-coated surface significantly more cells were observed, which reveals that the cells adhered stronger to the coated surface.

For the process of polyelectrolyte layer-by-layer adsorption, poly(allylamine hydrochloride) (PAH) and poly(styrene sulfonate) (PSS) was applied as positively and negatively charged polyelectrolyte, respectively. Ten pairs of layers were built and measured in real-time, at pH 8, where both the titania and the gold thin film has negative charges on its surface. The thicknesses of the layers were demonstrated to be increased by the TNP-coating (Fig. 2).

The measurement was also carried out at pH 4, where the surfaces are positively charged. The thickness of the deposited layers was significantly larger at the basic pH than at the acidic pH (Fig. 3). The difference between the thicknesses of the bilayers at the acidic and basic pH can be explained by the strong pH-dependence of the polyelectrolyte layer deposition.

PSS/PAH on TiO_2 nanoparticles



Related publications

- [1] J. Nádor, B. Kalas, A. Saftics, E. Agócs, P. Kozma, L. Kőrösí, I. Székács, M. Fried, R. Horváth, and P. Petrik: *Plasmon-enhanced two-channel *in situ* Kretschmann ellipsometry of protein adsorption, cellular adhesion and polyelectrolyte deposition on titania nanostructures*, Optics Express **24**, 4812–4823 (2016)

Figure 3: The adsorbed mass density and the thickness of the deposited 10 pairs of PSS/PAH layers on TNP coated surface at pH 8 and pH 4.

DEVELOPMENT OF OPTICAL METROLOGY TOOL FOR IN-LINE QUALIFICATION OF THIN FILMS ON LARGE AREA

Cs. Major, György Juhász, Péter Petrik, Miklós Fried



We are involved in 2 EU-projects ("SEA4KET" and the ENIAC-2012-2 "E450DL") to develop "Imaging Optical Inspection Device With A Pinhole Camera". We developed 30, 45-60 and 60-90 cm wide prototypes (Figs 1, and 2).

Figure 1: We successfully installed our mapping device in the clean-room of IISB (Erlangen, Germany). A 300 mm diameter wafer can be seen on the robotic arm (left side).

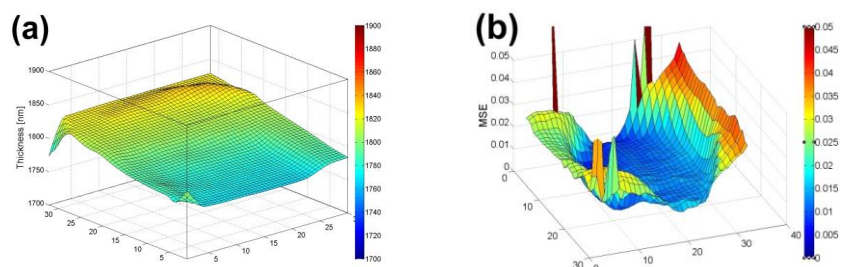


Figure 2: Thickness-map of a nominally 2000 nm thick oxide layer on a 300 mm diameter Si-wafer (a) and the Meanned Squared Error-map showing the edges of the 30 cm diameter wafer (b).

MODELING AND SIMULATION @ MEMS LAB

András Deák, Zoltán Hajnal, Norbert Nagy

Finite Element Modeling (FEM) and multiphysics simulation, as implemented in COMSOL® has been the principal "workhorse" of semiconductor process work-flow of the MEMS laboratory since many years. Several undergraduate and graduate thesis activities, related to deep brain electrodes, 3D (tactile) force sensors, numerous microfluidics devices were designed and optimized relying on insights gained from parametric simulation and models created in MATLAB® and COMSOL.

This year concluded the development of the thermoelectric measurement device for the FP7 UNION project. The device is capable to carry out the complex task of capturing a micron-size composite cluster of nanoparticles from a solution and measuring electric potential drop across it while exposing it to a temperature gradient.

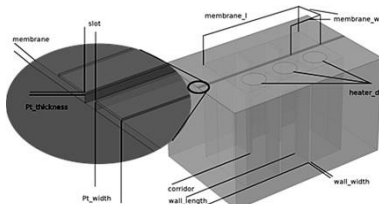


Figure 1: Schematic view of the parameters of the UNION micro-thermoelectric measurement device.

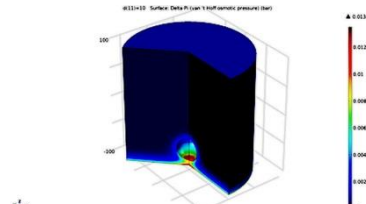


Figure 2: Van't Hoff osmotic pressure arising from electrostatic interactions in the electrolyte near a nanoparticle and potential wall.

Also, as part of OTKA PD-105173 (A. Deák: Nanochemistry for controlled self-organization), the finite element framework has been used to study the elementary physical components of the interaction of surface functionalized (core-shell) nanoparticles in electrolyte with each other and a potential wall. We attained the complete thermodynamical description, changes in the Gibbs free energy depending on characteristic geometrical parameters of the 2D or 3D model systems. An example of the electric potential distribution between two nanoparticles is shown in Fig. 2.

PREPARATION OF COMPACT NANOPARTICLE CLUSTERS FROM POLYETHYLENE GLYCOL-COATED GOLD NANOPARTICLES BY FINE-TUNING COLLOIDAL INTERACTIONS

Dániel Zámbó, György Zoltán Radnócz, András Deák

Control over colloidal interactions might allow the creation of nanoparticle assemblies from individual, nanometric building blocks, giving rise to special optical or optoelectronic properties. These assemblies are excellent candidates for some advanced applications in the field of sensorics, energy harvesting, catalysis, biomedical contrast agents, or even theranostics. Gold nanoparticles are exceptional building blocks for nanoparticle assemblies as they support localized surface plasmon resonances, which is very sensitive to the interparticle distance caused biplasmon coupling. Polyethylene glycol homopolymers are commonly used as a stabilizer agent of gold nanoparticles in various media.

Low-molecular weight polyethylene glycol (PEG) has a lower critical solution temperature well outside the boiling point of water at ambient pressure, but it can be reduced at high ionic strengths. We extend this concept to trigger the clustering of gold nanoparticles through the control of colloidal interactions. At high ionic strengths, low-molecular weight (<2000 Da) mPEG-SH-modified gold nanoparticles (Fig. 1) show clustering with an increase in the solution temperature. The clustering temperature decreases with an increasing ionic strength. The clustering is attributed to the delicate interplay between the high ionic strength and elevated temperature and is interpreted in terms of chain collapse of the surface-grafted PEG molecules.

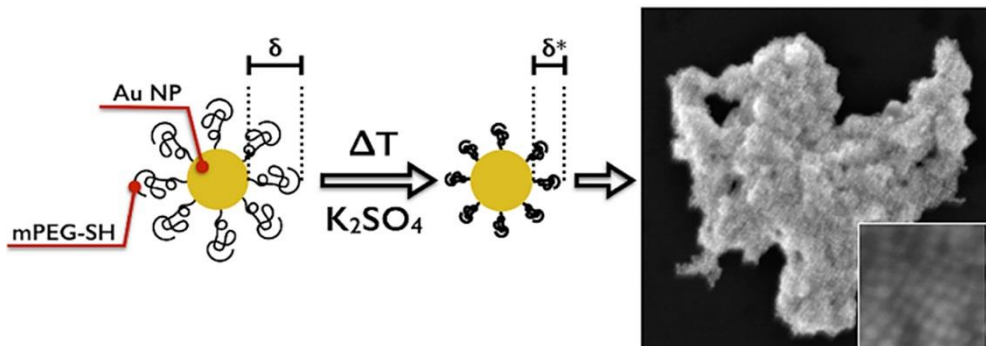


Figure 1: Schematic representation of self-assembly of PEG-covered gold nanoparticles into compact nanoparticle cluster.

The chain collapse results in a change in the steric interaction term, whereas the high ionic strength eliminates the double-layer repulsion between the particles. The observations are backed by nanoparticle interaction model calculations. We found that the intermediate attractive potential on the order of a few kT allows the experimental fabrication of compact nanoparticle clusters in agreement with theoretical predictions.

A new approach for the predesigned, externally triggered clustering of gold nanoparticles was also presented. On the basis of the calculations on the colloidal interaction between the particles and the measurement data, it can be inferred that the experimentally observed clustering of the nanoparticles at high ionic strength and elevated temperature is a result of the chain collapse of the surface-grafted PEG molecules. Threshold temperature of the clustering can be influenced by the ionic strength of the medium. We found that the presence of the PEG shell significantly influences the kinetics of the clustering. The deceleration of particle association can be interpreted in terms of a moderate attractive potential after the chain collapse.

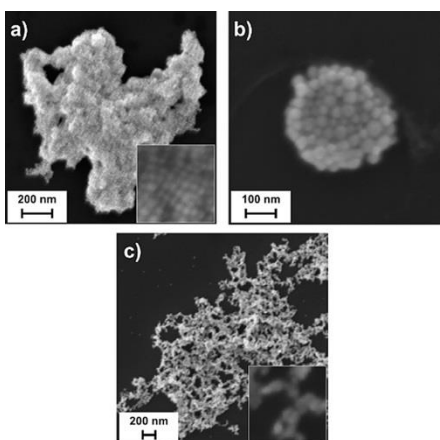


Figure 2: SEM images of compact nanoparticle clusters from PEGylated particles and fractal-like aggregates of citrate stabilized nanoparticles.

The structure of the clusters agrees well with theoretical predictions for such a model system. When the attractive potential between the building blocks is large, the position of two attaching particles gets kinetically trapped and not allowed to reconfigure during the assembly process, resulting in a fractal-like structure. This can be observed for our control sample (Fig. 2), where the elimination of the double-layer forces leads to a rapid aggregation and fractal-like structure. For the PEG-grafted nanoparticles, at moderate interparticle attraction, reconfiguration of the building blocks is allowed; hence, the structure of the cluster becomes more compact. The presented approach allows preparation of complex nanoparticle clusters, where different type of nanoparticles can be incorporated into a single cluster.

INTRODUCING NANOSCALED SURFACE MORPHOLOGY AND PERCOLATION BARRIER NETWORK INTO MESOPOROUS SILICA COATINGS

E. Albert, Péter Basa, András Deák, A. Németh, Zoltán Osváth, György Sáfrán, Zsolt Zolnai, Z. Hórvölgyi, Norbert Nagy

Mesoporous silica thin films were patterned at sub-micron scale utilizing the ion hammering effect in order to combine advantages of mesoporous character and surface morphology, while preserving the interconnected pore system or creating laterally separated porous volumes surrounded by non-permeable compact zones.

Thin coatings of mesoporous silica on Si substrate were prepared by sol-gel method with ordered and disordered pore system using Pluronic PE 10300 and CTAB as molecular templates. Hexagonally ordered Langmuir-Blodgett films of spherical silica particles were transferred on the top of the porous silica coatings and applied as mask against Xe⁺ ion irradiation (Fig. 1). The ion energy was chosen according to Monte-Carlo simulations to achieve structures with high lateral contrast between irradiated and unirradiated, i.e., masked areas.

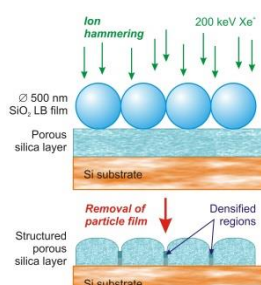
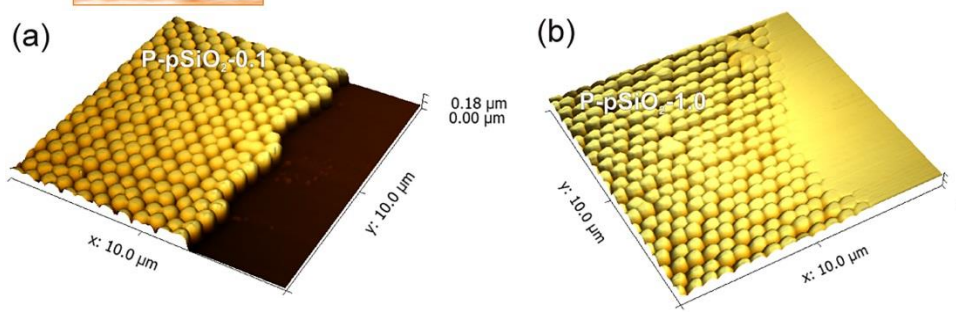


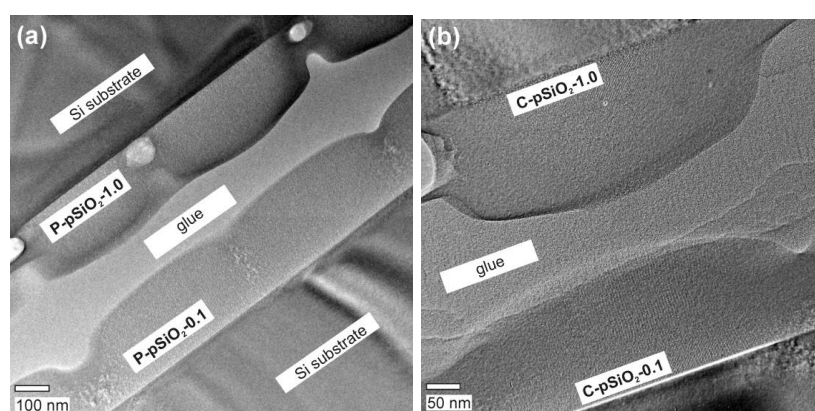
Figure 1: Schematics of the key step of sample preparation: ion irradiation with 200 keV Xe⁺ through an ordered monolayer of silica spheres then removal of the particles.



The aspect ratio of resulted morphology was proved to be high; the created surface structures were very similar irrespectively of the type of template molecules and ion fluences applied (Fig. 2). The densification of both types of porous silica coatings almost reached its maximum already at the lowest fluence. For CTAB-templated coatings the degree of densification was significantly higher than in the Pluronic-templated ones.

Figure 2: AFM images of Pluronic-type silica coatings after ion irradiation with fluences of (a) $0.1 \times 10^{16} \text{ cm}^{-2}$, and (b) $1 \times 10^{16} \text{ cm}^{-2}$, respectively. The measurements were carried out (a) where the edge of the particulate LB mask was located and (b) at the border of irradiated and unirradiated regions of the LB film.

The HRTEM analysis revealed that the pore structure remained intact where the silica spheres were non-transparent for the bombarding ions. For Pluronic-templated silica samples with disordered pore system the pore structure remained interconnected near the Si substrate surface at the lowest fluence. Contrarily, at the highest fluence, the regions surrounding the intact porous columns were fully densified thus forming non-porous border zones (Fig. 3). Therefore, the interconnected or the separated character of the pore system can be tailored by the applied ion fluence, while the created surface morphology is essentially the same in both cases. In case of CTAB-templated coatings with ordered pore structure the results were similar. The densified regions are thicker, while the intact porous volumes are smaller than in the Pluronic-templated case irradiated with the same fluence. Comparing the two different molecular templates the disordered Pluronic-templated pore system proved to be more resistant against Xe-bombardment.



Confocal fluorescent images and ellipsometric porosimetry measurements confirmed that the majority of the porous volume can be preserved as interconnected pore system by the application of low ion fluence. By increasing the fluence value, however, separated porous volumes can be created at the expense of the total pore volume.

Figure 3: HRTEM images of (a) Pluronic-type and (b) CTAB-type coatings irradiated with fluences of $0.1 \times 10^{16} \text{ cm}^{-2}$, and $1.0 \times 10^{16} \text{ cm}^{-2}$.

FINE-TUNING OF GAS SENSITIVITY BY MODIFICATION OF NANO-CRYSTALLINE WO_3 LAYER MORPHOLOGY

Zsófia Baji, Zsolt Zolnai, Máté Takács, Ferenc Bíró, Csaba Dücső

Hexagonal WO_3 layers of different morphologies were deposited on micro-hotplate gas sensors and gas sensitivity for NH_3 was tested. The layers were synthesized by hydrothermal acidic precipitation method using different catalytic chemicals. Thin film sputtered layers were also deposited as reference material. WO_3 suspensions of quasi-equivalent quantity were dropped on the micro-hotplate for all the materials investigated. Additional ultrasonic agitation was introduced to destroy conglomerates of nano-crystals. If Na_2SO_4 or K_2SO_4 catalyst were added to the acidic solution of Na_2WO_4 , ultrasonic treatment proved to be very effective and resulted in uniform sized individual WO_3 nano-rods of 80 nm diameter. Addition of ZnSO_4 catalyst leads to disordered nano-fiber net with typical diameter of 70 nm. Ultrasonic agitation had no effect in case of NaCl catalyst and Zocher methods; thereby the formed WO_3 layers are composed of micrometer size conglomerates of 80-150 nm nano-rods. SO_4^{2-} ions facilitate the formation of long crystallites.

Layers composed of individual nano-rods exhibit 2-5 times higher sensitivity up to 60 ppm NH_3 , while layers of larger conglomerates show linear response in the

10-100 ppm range. The size effect is explained by the comparable sizes of nano-wire width and space charge layer at the solid-gas interface. This effect was also demonstrated by the sputtered thin films of different thicknesses.

NaXWO_3 contamination deteriorates gas sensitivity. No relationship between specific surface and gas sensitivity could be detected.

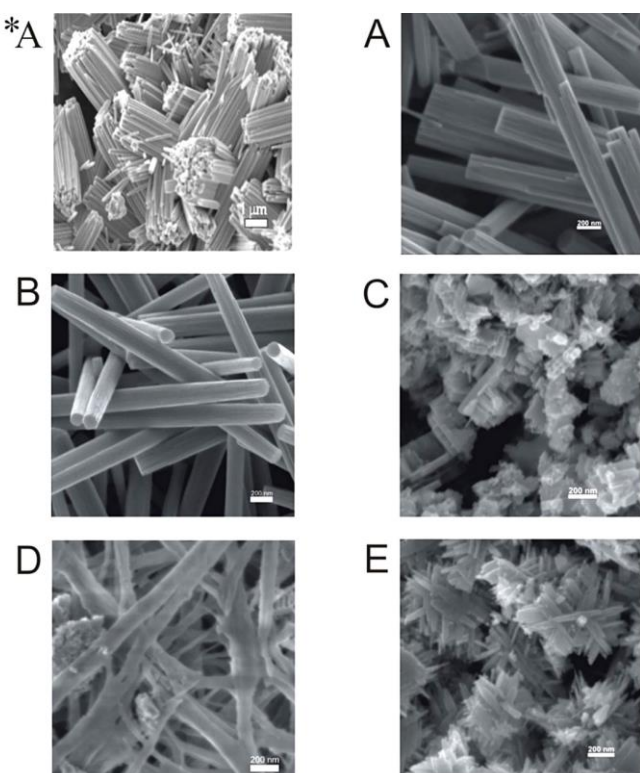


Figure 1: SEM views of hydrothermally synthesised WO_3 layers with different catalysts: (A*): Na_2SO_4 without ultrasonic treatment, (A): Na_2SO_4 with ultrasonic treatment, (B): K_2SO_4 with ultrasonic treatment, (C): NaCl with ultrasonic treatment, (D): ZnSO_4 with ultrasonic treatment, (E): Zocher-method.

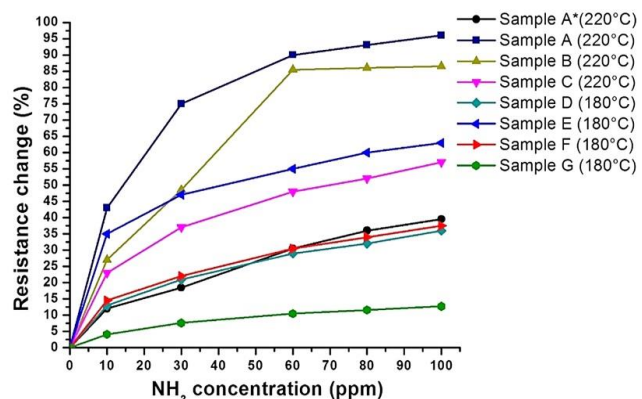


Figure 2: Summary of sensor responses for 0-100 ppm NH_3 in synthetic air.

WAVELENGTH CONVERSION IN GaInAsP/InP NEAR INFRARED SURFACE EMITTING DIODES

Máté Takács, Ferenc Bíró, Gábor Battistig, Zsófia Baji, Zsolt Zolnai, Vilmos Rakovics, Csaba Dűcső

Quality control in food industry and clinical diagnostics requires powerful, versatile and relatively cheap spectrometers. Semiconductor light sources are characterized by small dimensions and low power consumption; therefore they can be suitable components in low price miniature devices. The only disadvantage of their application is that they are temperature sensitive and have a narrow spectrum. Infrared emitting diodes have 50–75 meV spectral bandwidths depending on the growth conditions. Thereby a series of spectrally tailored GaInAsP/InP surface emitting LED chips is required by micro-spectroscopy to cover the NIR (1000–1700 nm) wavelength range completely. Although these chips were developed in our lab and are efficiently applied by our partners, the need for spatially homogeneous, broad-spectrum and bright light sources drove us to develop a monolithic integrated NIR light source.

Present description demonstrates the results of a novel structure and its related technology to form single-chip broad or multi-peak spectrum LEDs. The output spectrum of the LED chip is substantially modified by introducing wavelength converter layers outside of the p-n junction of a normal LED structure. Light emitted from the active region is partly absorbed by the smaller band gap quaternary layers and re-emitted with smaller photon energy (Fig. 1). The emission spectrum and the light intensity can be tailored by the compositions, the thicknesses and number of the absorber layers. As an example, this absorption and re-emission process of the modified LED chips results in substantially broader two-peak emission spectrum (Fig. 2). A special advantage of the novel chip is that the spectral bandwidth of the device does not change with the driving current in the range of 10 mA to 100 mA. Moreover, the temperature dependence is also similar along the whole spectrum. More than 1 mW optical power can be obtained at 100 mA driving current and the corresponding operating voltage is 1.2 V.

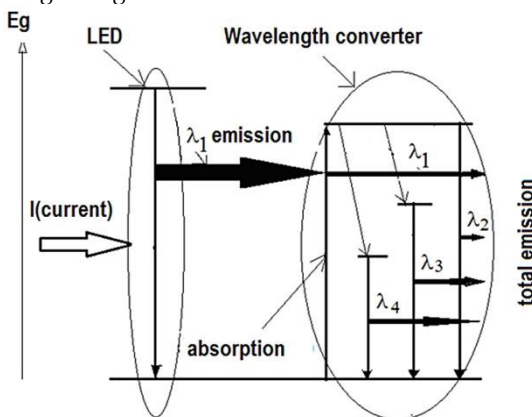


Figure 1: Operation principle of the wide spectrum NIR light source.

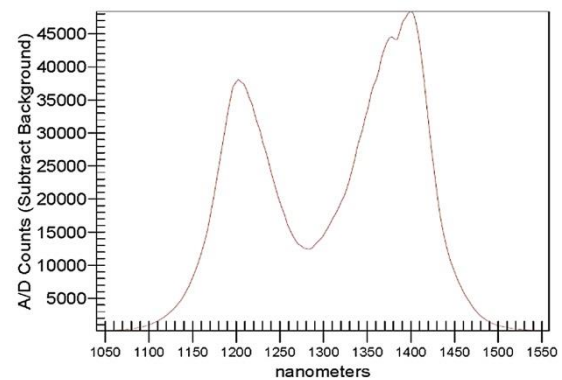


Figure 2: Demonstration of the broad emission spectrum by a two-wavelength single-chip NIR light source. Peak at 1200 nm is from the LED, peak at 1400 nm is from the integrated single absorber layer light converter.

We have obtained even broader spectrum by inserting more additional different composition quaternary GaInAsP layers into the structure. These layers have lower band gap than the active and the first absorption layer. Sandwiching the absorber layer in additional narrow band gap GaInAsP layers the formed potential well enhance the direct recombination of the optically excited charge carriers. The device works similarly to phosphor conversion white LED structure, but it is more compact and stable, because all layers are lattice matched to the substrate. Its optimization is relatively easy if the light emitting layers are substantially thinner than the confining absorption layers. The novel one-chip LED structure provides point-like light source with broader spectra and facilitate the construction of low power miniaturized NIR spectrometers. The multilayer structure enables to form stable light sources of emission spectrum tailored to any dedicated task.

3D FORCE SENSORS FOR MINIMAL INVASIVE SURGERY APPLICATIONS

Péter Fürjes, Csaba Dücső, Péter Földesy

Minimally invasive surgery offers several advantages for the patient and also for the society. The quicker recovery and the smaller trauma are obviously essential for the patient, whereas the reduced hospitalization and recovery time helps the society to spend the medical costs more effectively.

INCITE project is intended to reveal and describe the advantages of the integration and application of various sensing capabilities in Minimal Invasive Surgery (catheter or surgery robot) systems. These subsystems are applicable to extend the functionality of the proposed medical systems to be applied by improving feedback for the operators and surgeons during the intervention. The future aim is to improve the functional characteristics, safety and standards of medical devices (catheters, robotic tools) applicable to minimal invasive cardiac intervention and surgery.

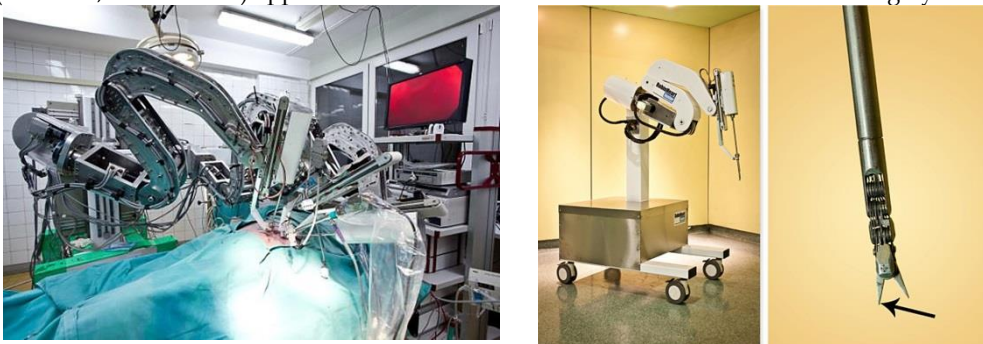


Figure 1: Surgery robots (FRK) and the head where the force sensors will be integrated

In order to improve the safety of the laparoscopic intervention the surgeon must get on-line information about the physical and chemical parameters during operation. The principal parameter required is the force as measured at different locations of the laparoscope head. Built inside the gripper the sensor can measure the strength of which the laparoscope holds the surgical tool. Placed on the tip the sensor can provide information about the hardness and surface roughness of the tissue the laparoscope touches (Fig. 1).

Design and fabrication of the 3D MEMS force sensors

3D force sensors were developed for the further integration in laparoscopic heads of surgery robots. The Si sensors operate with piezoresistive transduction principle by measuring the stress induced signals of the symmetrically arranged four piezoresistors in the deforming membrane. As the chip size has to be reduced to a few mm², the conventional anisotropic alkaline etching technique was replaced by deep reactive ion etching (DRIE) for membrane formation. Besides, DRIE has no practical limitation in membrane geometry and offers the formation of monolith force transfer rod protruding over the chip surface. SOI (silicon on insulator) wafers of appropriate device layer thickness provide the uniformity of membranes and reproducibility of the process.

According to the medical and functional requirements the MEMS sensors will be covered by biocompatible elastic polymer coating. Nevertheless, the elastomer drastically effect on the performance of the device. Therefore, the proposed sensor structures were modeled by coupled finite element simulation to determine the appropriate geometric parameters to meet the functional requirements. Sensors were covered with spherically shaped PDMS (polydimethylsiloxane) polymer and the effect of the elastic coating was also studied in terms of sensitivity and response time.

Four half Wheatstone-bridges were formed on full Si membranes, each composed of two identical resistors and arranged

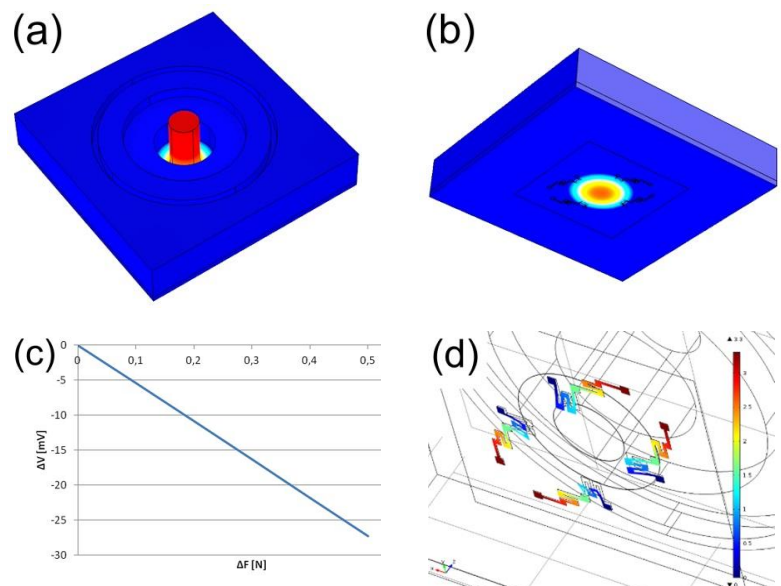


Figure 2: Demonstration of the multiphysical coupled FEM simulation of the piezoresistive 3D force sensors: (a): membrane deformation, (b): stress distribution along the integrated piezoresistors, and (c,d): the (perpendicular) force dependent sensor signal.

such as to represent maximum out-of-balance voltages over mechanical deformation. The geometric design was aided by FEM calculations for any force range to be measured (Fig. 2).

The processed wafer was anodic bonded to boron glass to provide enhanced mechanical stability, cavity underneath the membrane and wire contacts for assembly. Processed chips (Fig. 3a) were mounted on TO8 headers or PCB header (Fig. 3b) for preliminary tests. In order to investigate the effect of the elastic coating, identical chips were covered by PDMS layer (Fig. 3c) and characterized as well.

The standard test includes the measurements of the four out-of-balance voltages over the applied force range in perpendicular directions of loads. (Fig. 4). The sensitivity is heavily affected by the geometry and elasticity of the elastic coverage and this may result in up to 50-90% sensitivity loss.

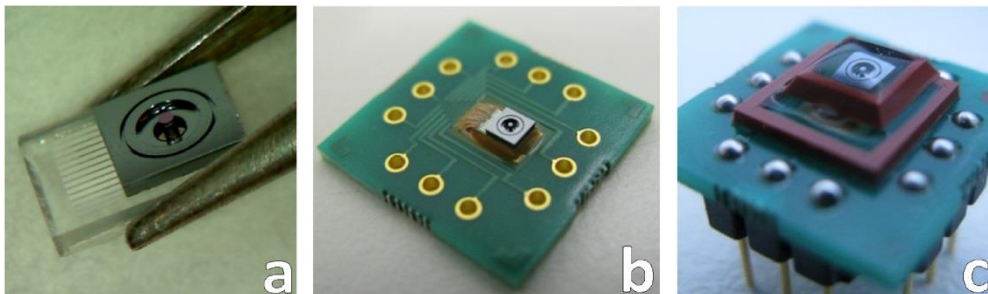


Figure 3: $2 \times 3 \text{ mm}^2$ full membrane force sensor chip (a), bare reference (b), and PDMS coated membrane type chips mounted on a specific PCB header for functional tests (c).

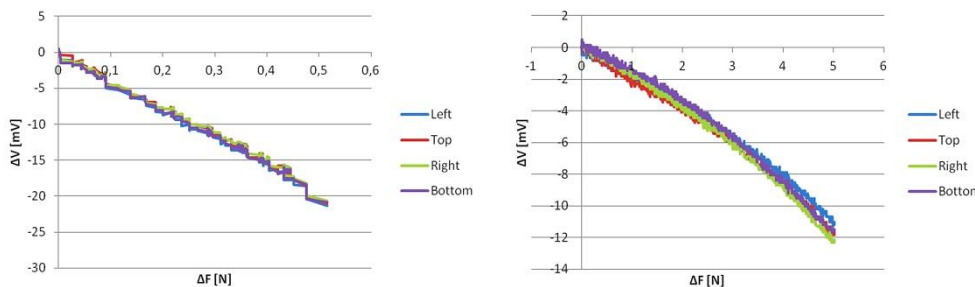


Figure 4: Out-of-balance voltages of the four half Wheatstone-bridges for perpendicular loads. Bare chip (left), PDMS coated (right).

3D INTERPOLATED POTENTIAL FOR MD

Zsolt Zolnai, Péter Földesy

We began development of a novel computational approach, based on multivariate interpolation for a complete and accurate description of three-body interactions in atomic and molecular ensembles. A natural 3-dimensional counterpart of the London dispersion is the so-called Axilrod-Teller-Muto (ATM) potential. For intermediate and large distances, ATM describes the three-body contribution to the energy of interacting particles. When particles (e.g. noble gas atoms) get in the vicinity of each other, quantum-mechanical correlation effects come into domination. Even their approximate (post Hartree-Fock) calculation requires considerable computational resources and time. To make these contributions more available for large ensemble, longer molecular dynamics (MD) simulations, a proper twice differentiable interpolation scheme was developed and implemented, smoothly fitting also the ATM potential at larger distances. First test calculations on many-body systems (4, 5, 6 atom random clusters of He atoms) show, that the total interaction (or cohesive) energy of these can be very closely approximated by the sums of 2 and 3-body contributions. Fig. 1 shows the example of He-4 clusters.

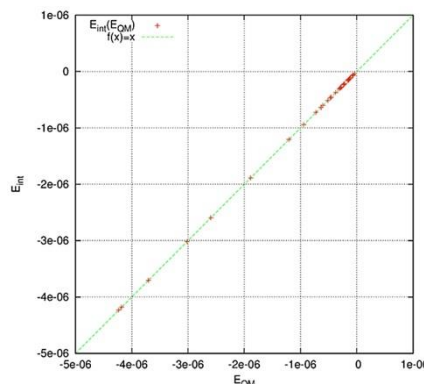


Figure 1: Comparison of the interpolated and "exact" (QM) cohesive energies of random He-4 clusters. The diagonal (green) line means perfect correspondence, which the red points fall indistinguishably close to.

NANOSIZE EFFECT ON THE EVOLUTION OF MAGNETISM ON CURVED SURFACES

Zsolt Zolnai, Péter Földesy, Ferenc Bíró, Csaba Dücső

Similarly to the well-known Moore's law for the number of transistors in an integrated circuit, an analogous tendency was recognized by Mark Kryder for magnetic disk storage density. His prediction shows that the capacity of a 2.5" disk will reach 40 Tbit/in² by 2020. Several developments are now on the way in order to reach, or even to exceed this density.

There are two dilemmas about storage capacity increase. Once, when the magnetic grains are very small, the further reduction leads to the super-paramagnetic effect, where the spontaneous magnetization fluctuation results in data loss. On the other hand, the magnetostatic and exchange interaction between the adjacent grains sets a limit on how "strong" the magnetization should be in a grain without being perturbed by the neighbors.

A possible solution could rely on bit patterned media where the information unit is bound to a nanostructure. In this case the strong exchange coupling within the particle, the shape anisotropy and the isolation of the particles may increase the energy barrier for thermal switching. Such structures are predicted to be eligible to store up to 20-300 Tbit/in². As material properties may differ from bulk when entering the nanoscale regime and this is particularly true for magnetic materials, scientists from all over the world are working to reveal the nanosize effects on magnetism. Our institute EK MFA is also participating in this challenge in cooperation with the ESRF group at the Nuclear Resonance Beamline ID18, the KU Leuven, and the Wigner Research Centre in Budapest.

In this work, an ultrathin iron film was deposited by molecular beam epitaxy (MBE) on a flat silicon substrate as well as on 20 nm and 400 nm diameter silica spheres (Fig. 1), and the effect of morphology such as curvature and interparticle distance, on the evolution of magnetism was studied. The thickness of the iron film was varied in the range where iron shows a nonmagnetic/magnetic transition. To describe the 3D structure, the composition and the magnetic properties of the samples a wide range of analytical tools has been applied such as *in situ* nuclear forward scattering (NFS), X-ray reflectivity (XRR), grazing-incidence small-angle X-ray scattering (GISAXS) and *ex situ* atomic force microscopy (AFM), magnetic force microscopy (MFM), field electron scanning electron microscopy (FESEM), and Rutherford Backscattering Spectrometry with 3D structure evaluation tool (3D-RBS). Based on the detailed characterization, micromagnetic simulations were carried out to model the magnetic moment configurations in the iron cap (Fig. 1).

We concluded that for the two particle diameters largely different evolution of magnetism occurred with increasing the iron thickness. For the 400 nm diameter spheres, the system could be considered as a sum of individual magnetic particles. Here the formed magnetic structure was determined by the topology of the spheres. With increasing the iron thickness, first the upper part of the sphere became magnetic, showing a spiral like (vortex) magnetic pattern on top and out of plane magnetization at the side. For thicker iron layers the out of plane component was gradually eliminated and replaced by a magnetic vortex (Fig. 1b).

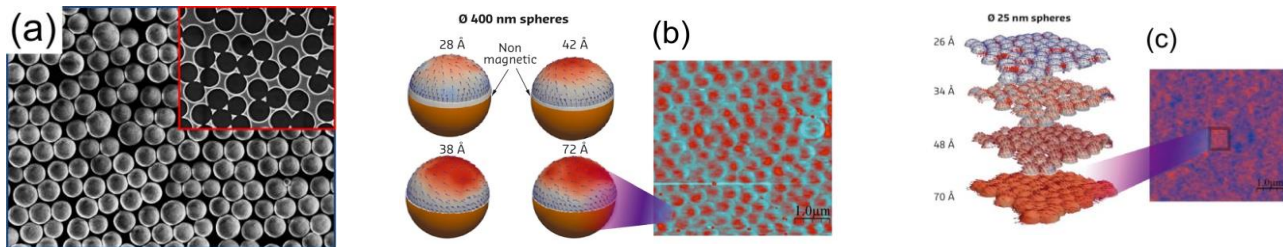


Figure 1: (a): FESEM image of a monolayer of colloidal silica particles (400 nm diameter) deposited on Si substrate with Langmuir-Blodgett technique. A thin iron layer was grown by MBE on top of the spheres. The inset shows the iron pattern on the substrate after the particles were removed. (b, c): Magnetic moment configuration calculated by micromagnetic simulation for thin iron layers with varying thickness deposited on (b) 400 nm and (c) 20 nm diameter silica spheres. The magnetic force microscopy (MFM) images of the thickest iron layer are also shown.

In contrast, for 25 nm diameter particles, iron became magnetic first in the contact region of the spheres and a uniformly distributed, well isolated magnetic structure appeared. With further deposition, the whole layer became magnetic and a topology independent magnetic structure incorporating several particles with in plane magnetization could be observed (Fig. 1c).

MICROFLUIDIC SYSTEM FOR SEPARATION OF CIRCULATING TUMOR CELLS (CTC)

Péter Fürjes, Gábor Battistig, Eszter Holczer, Eszter Leelősy Tóth

Cell sorting could have particular importance in medical diagnostics and therapy – see Clinical Cancer Advances – since it can be applicable to select specific cell types or to remove the background cells from such important and limited volume biological samples as taken from blood or liquid biopsy. Microfluidic Cell Capture Devices (MCCDs) are promising tools for detection, capture and enrichment of the targeted cells since the geometrical dimensions of the cells and the applied channels are in the similar order of magnitude. Due to their small dimensions (with the benefit of high surface to volume ratio), they can offer unusual physical behaviour that is in the macroscopic world.

The specific aim of this project is to design and fabricate microfluidic cell capture devices with special 3D geometry utilizing the advances of combining conventional lithography based rapid prototyping with Proton Beam Lithography (PBW) to improve cell manipulation efficiency. Tilted micropillars were fabricated and applied in order to increase the active surface area, the effective cross-section of the capturing microstructures and to modify the local hydrodynamic behaviour in the sample transport system, in cooperation of the research groups of Prof. A. Guttmann (Univ. of Pannonia) and I. Rajta (ATOMKI).

Computational Fluid Dynamics (CFD) simulations revealed that tilting the pillars not only increases their surface area on which the fluid can interact with the bonded affinity layer but also improves the fluid characteristics of the system. Based on the results of the preliminary FEM calculations special 3D structures were designed and fabricated by multiple tilted proton beam writing method in SU-8 epoxy based negative photoresist and poly-dimethylsiloxane (PDMS) to enhance the cell capturing capability of the proposed microfluidic system. The developed 3D microstructure of the microfabricated cell separation system was imaged by scanning electron microscopy as demonstrated in Fig. 1.

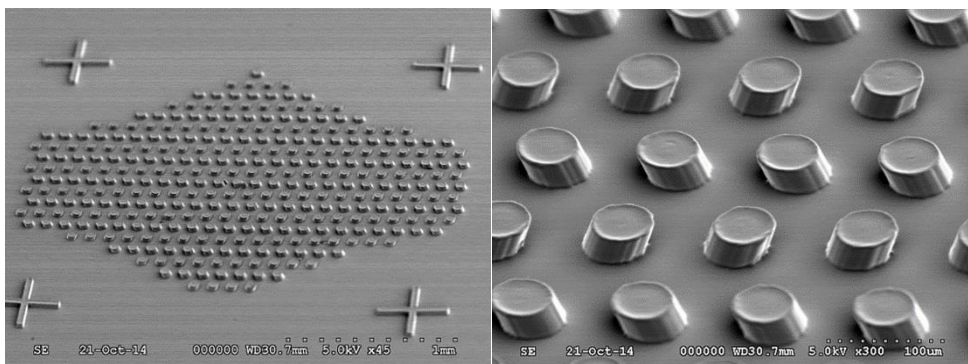


Figure 1: SEM images of doubly tilted micropillars fabricated from liquid PDMS by polymerization with focused proton beam on the top of a cross-linked PDMS layer.

The presented methodology and the applied structural materials are compatible with MEMS/NEMS (micro/nano-electromechanical systems) technology considering the integration requirements for subsystem development. The PBW patterned micropillar array was integrated into the transport microfluidic system manufactured by soft lithography and its performance was characterized by cell injection. The sealed device is presented in Fig. 2.

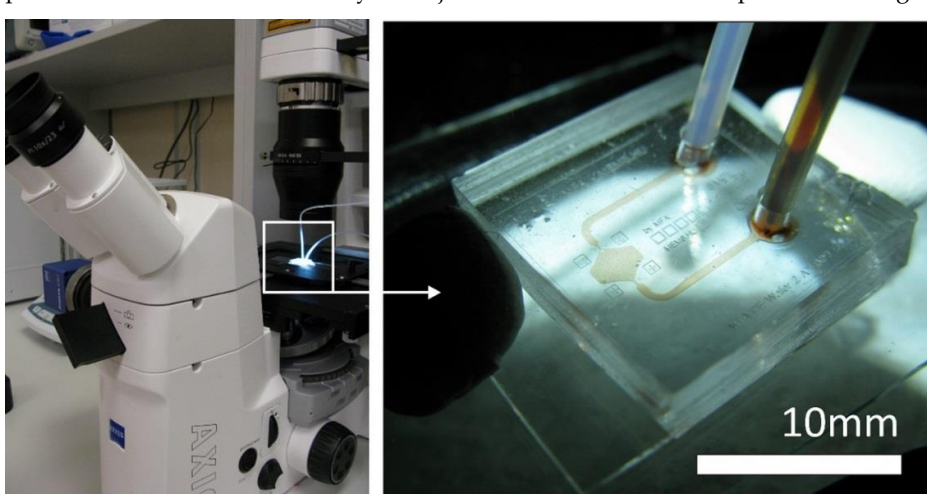


Figure 2: The fabricated cell capturing device sealed by O₂ plasma enhanced bonding of the microfluidic and sorting subsystems was filled by biological test solution containing yeast cell culture.

To validate the FEM modeling of the hydrodynamic processes evolving in the cell capturing chamber, the particle movements were monitored in the fabricated microfluidic system by using fungi cells in typically similar size of red blood cells. The cell trajectories were monitored and followed by microscopic imaging. The experienced deterministic lateral displacement is governed by the asymmetric local hydrodynamic characteristics evolving around the tilted pillars. The particle behaviour corresponds to the FEM modeling results clearly demonstrating the asymmetric pressure and shear force distribution near by the tilted micropillars. These satisfied the expectations that the device is capable for size dependent sorting of injected objects and the microfluidic system is offering advanced cell capturing capability at the functionalized surfaces.

FINITE ELEMENT MODELING (FEM) AND CHARACTERIZATION OF CELL AND MOLECULAR ADVECTION IN CONTINUOUS MICROFLUIDIC SYSTEMS

Péter Földesy, Péter Fürjes, Eszter Leelősy Tóth, Zoltán Hajnal

The aim of the research is the characterization of the fluid-particle interaction in biological samples (blood, environmental samples, etc.) considering cellular and molecular advection and implementation of targeted preparative functions on microscale. Considering the main sample preparation tasks the behaviour of particle- and cell suspensions in the microfluidic systems was analyzed focusing on the separation of the formed elements and particles by size.

Several medical diagnostic tests are based on human blood as sample solution due to its complex and representative marker molecule composition considering pathological issues. Most of these tests require separation of plasma or serum from the whole blood. Recent development of microfabricated Lab-on-a-Chip systems provides outstanding solutions for analytical problems although integration of high performance continuous separation function is challenging. Passive microfluidic inertial plasma separation structures could be promising candidates due to their relatively simple structure and fabrication technology. Zweifach-Fung bifurcation type microscale separation systems utilize viscous lift and shear forces evolving in the low Reynolds regime and developing a cell-depleted layer near the channel walls. This structure could provide excellent plasma purity in single branch, however, in case of cascade separation systems purity is deteriorated subsequently from branch to branch due to the thinning of the cell-depleted layer. In our work the possible recovery of the cell-free layer was studied considering inertial forces evolving in special geometrical singularities.

Characterization of cascade plasma separation structures

Series of different geometric singularities (six types of different expansions) were integrated with bifurcations branching from main stream channel in order to reveal their inertial effects on particle movement and characterized regarding their enhancement of blood plasma separation performance of cascade Zweifach-Fung bifurcations. The evolving flow behavior and particle trajectories were modeled by Computational Fluid Dynamics (CFD) simulation and particle tracing modules of COMSOL Multiphysics and the results were verified experimentally by recording particle trajectories. Microfluidic test structures were fabricated by soft lithography in poly-dimethylsiloxane (PDMS) and fungi cells were injected in to reveal particle movement applying dark field microscopy. The modeled flow fields were compared to the recorded particle trajectories in case of different flow rates (Fig. 1).

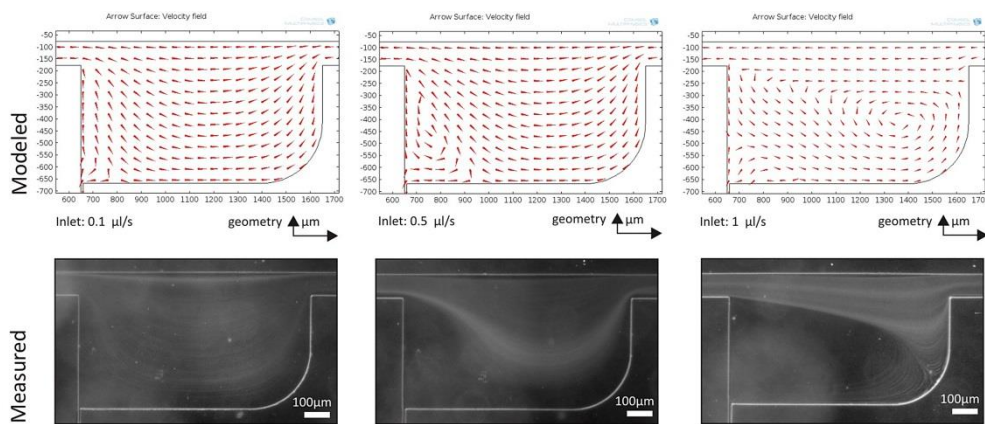


Figure 1: Modeled and experimentally recorded particle trajectories representing the development of depleted layer. The particle distribution and the measured scattered light intensities demonstrate the effect of lateral migration.

The development and recovery of a cell-depleted layer near the channel walls due to lift and shear forces were analyzed considering the applied flow rates and number of singularities. To avoid deterioration of plasma purity due to cell recirculation in evolving vortices but maximize separation efficiency optimal flow rate regime was defined for further experiments. The recovery of the cell-free layer in geometrical singularities was validated and their applicability in enhanced cascade type plasma separation systems was proposed. The effect of the developing cell-depleted layer thickness on the plasma purity was studied to prove the improvement of the separation technique due to the integrated inertial subsystems.

AUTONOMOUS MICROFLUIDIC SAMPLE TRANSPORT SYSTEMS

Péter Fürjes, Eszter Holczer, Eszter Leelősy Tóth

Autonomous capillary micropumps could be substantial brick stones of cheap, simple and self-powered microfluidic systems being capable to manage the sample transport in Lab-on-a-Chip applications. Accordingly the precise control or improvement of the fluid conducting characteristics of these integrable micropumps is in forefront considering their capacity and efficiency. Moreover the management of the achievable flow rate and the transported sample amount could be critical regarding various applications considering the requirements of controlled microreactors or high sensitive diagnostic devices, and the transported amount has to be adjusted by the geometric and surface parameters of the developed passive pump.

Development of self-driven microfluidic systems

To achieve controlled and autonomous sample transport in Polydimethylsiloxane (PDMS, Fig 1) based microfluidic system the surface behaviour of the material was modified, and the efficient transport of patient serum was proved. Since the functionality of the proposed biosensing/Lab-on-a-Chip device is highly affected by the flow conditions during the sample injection, incubation and washing steps, microfluidic chamber system was developed to ensure controlled transport of the sample suspension over the biosensing surface by capillary forces. The microfluidic structure was fabricated by soft lithography technique in PDMS using SU-8 epoxy based photoresist as molding replica. The PDMS was modified to improve its sample transport performance by embedding special PDMS-b-PEO amphiphilic molecules in the matrix.

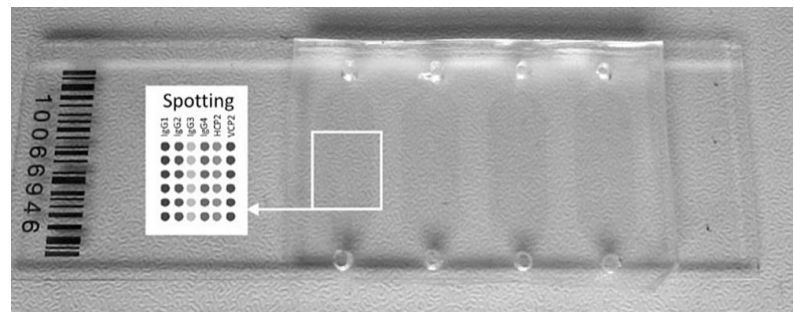


Figure 1: The fabricated PDMS based microfluidic chamber.

Biosensing applications

In cooperation with the ELTE/MTA Immunology Research Group the developed self-driven polymer based microfluidic system was applied for a biosensor to be able to monitor immune cell adhesion and activation on protein microarrays consisting of antigens, antibodies and complexes indicating specific autoimmune diseases. Cells as biosensors were applied for monitoring immune complex composition. When the capillary system was mounted above the slide, first serum samples derived from patients then purified human neutrophil granulocytes were transferred through the capillary system by capillary force. Applying the adequate peptide targets of specific autoantibodies, the adhesion of neutrophil granulocytes on the functionalised surface regions clearly indicated the diseased patient sample. The readout of the assay can be the quantitation of bound fluorescently labeled cells by a microarray scanner as schematically represented in Fig. 2.

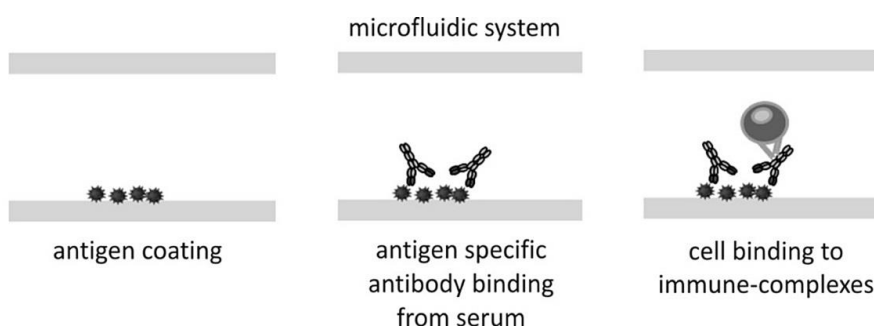


Figure 2: Schematic working principle of the cell-binding biosensor assay for detection antigen specific antibody in the patient serum.

We proved that the capillary driven microfluidic transport system applied for filling the sample chambers of microarrays can significantly improve the effective cell binding and the ease of handling and reproducibility of these assays in diagnostics of disease positive patients.

Complex bioinspired microcapillary systems

The functional behaviour of the capillary structures and the non-specific protein binding on the channel surfaces were also studied to prove the auspicious effect of the surface modification. The geometry and the 3D design of the channels were inspired by the most complex natural microfluidic system, the water-conducting tissue (xylem) of trees and different geometric shapes were developed at the bottom of the channels as stripe and serpent type grooves. The combined effects of different 3D geometries and surface modifications were systematically characterized by flow rate measurements applying ultra fast imaging system for recording fluid movement. The surface modification methods were compared and the advantages of bioinspired capillary systems were also demonstrated.

Bioinspired microfluidic structures as fluidic diodes were also designed and characterized to systematically control the sample flow rate and direction in the microcapillary systems. 3D geometry of the skin of Texas Horned Lizard was adopted and proved for flow direction control in autonomous sample transport systems. Based on the preliminary result autonomous sample transport microfluidic systems were designed and fabricated to be integrated in Point-of-Care Lab-on-a-Chip based diagnostic cartridges in the cooperation with 77 Elektronika Ltd002E.

CELL AND PARTICLE SORTING IN MICROFLUIDIC SYSTEMS

Péter Földesy, Péter Fürjes, Eszter Leelősy Tóth

The aim of the PAMIAQ project in cooperation with Technoorg Linda is the development of a complex analytical system for particle counting and identification by size distribution with integrated sample transport, manipulation and optical detection. Microfluidic systems capable of particle separation by their size utilizing the Dean drive and inertial effects were designed and analyzed. Fluidic chips were fabricated in PDMS by soft lithography and bonded to glass plates. These devices will perform passive separation of the pollutants by their size and the hydrodynamic focusing. The microfluidic devices were characterized with respect to their ability of spatial separation of specific pollutants into sub-channels and focusing of the particles in the field of view of the optical measuring setup maintaining the permeability/capacity of the channels. The size ranges of the targeted pollutants were defined as cells – with diameter under 5 µm, particulates with diameter between 1 and 10 µm and pollen with diameter between 10 and 100 µm.

The channel layout design is based on four physical phenomena. Pinched flow fractionation utilizes the inertia of the particles deflecting their paths in varying degrees based on their size. Inertial and Dean forces divert the smaller particles closer to the channel centre and the larger particles towards the channel walls in curved channels. With hydrodynamic filtering the smaller particles can be separated using a comb-like design and a secondary flow.

The mask layout of the combination of fundamental elements was designed, a manufacturing process and measuring method was defined allowing the optical evaluation of the samples. Fluorescent polystyrene beads (10 and 15 µm diameter) were injected into the flow in order to assist optical evaluation. The trajectories of these beads are well defined using fluorescent microscopy.

The combination of Pinched flow fractionation, Dean and Inertial forces was found to be efficient for size dependent particle separation (Fig 1). The hydrodynamic filtering, however were not feasible on the given size scale and technical conditions.

Hydrodynamic 3D focusing was also studied using finite element modeling. The design for the pinched flow fractionation is considered sufficient for the 3D focusing combining the Dean effect with classical 2D hydrodynamic focusing.

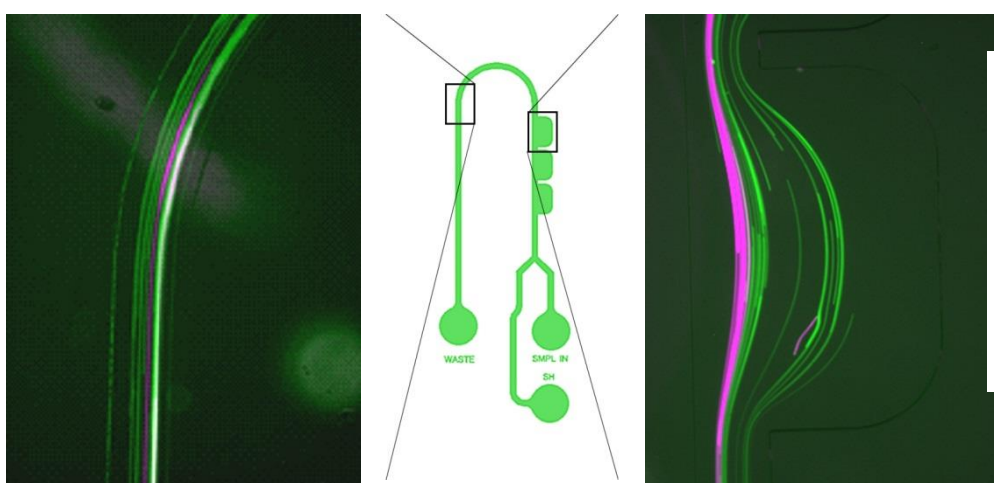


Figure 1: The size dependent separation of the fluorescently labelled particles was proved by recording their trajectories in the different regions of the microfluidic systems (10µm: green, 15µm: violet).

POLYMER MICROECOGS OPTIMIZED FOR IN VIVO PHARMACOLOGICAL INVESTIGATIONS

Zoltán Fekete, Anita Pongrácz

The connectivity between the cortical representations of the visual system through temporary oscillations plays an important role in the pathomechanism of the so-called connectome diseases like schizophrenia or autism. The complexity of the visual cortex makes it difficult to find a reliable electrophysiology technique, which is able to measure the electrical activity of the whole cortical connectome simultaneously. Our goal was to elaborate a chronically implantable polymer based microelectrode grid that is able to monitor large cortical areas in rodents. The feasibility of the subdural electrode system was tested in visual steady-state response experiments, in ketamine induced schizophrenia models and in 4-aminopiridin induced epilepsy models using mature Wistar rats (Fig 1). Our results prove the potential of our microelectrode grid system in future pharmacological research (Fig 2).

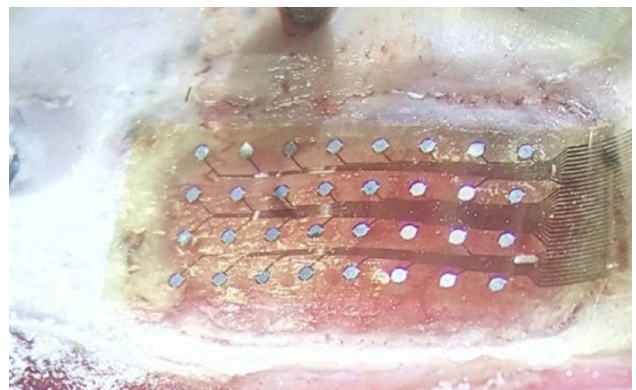
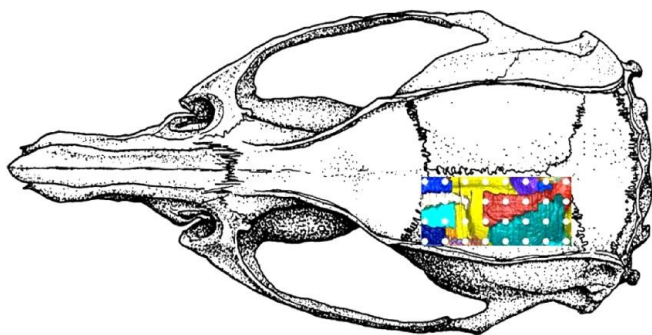


Figure 1: Schematic of rat skull with the implantation sites of the microgrid (left). Our polymer microgrid during surgery (right).

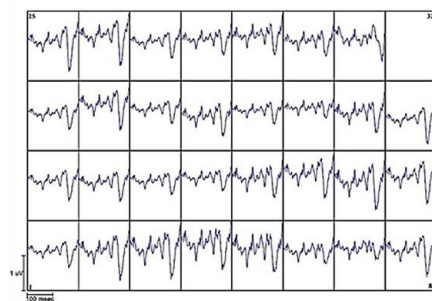
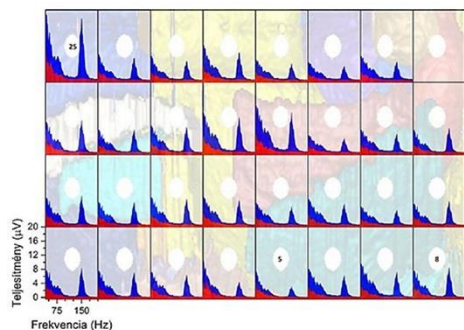


Figure 2: Ketamine induced dissociation state in schizophrenia animal model. Red and blue area represents spectral power density in a control period (10s) and after ketamine injection (10s). Measurements were using a 32-channel microelectrode grid directly placed on the visual cortex. EEG recorded by our microgrid during an epileptic seizure after 4-AP injection.

DOUBLE MARKERS FOR DIRECT CONTACT FORMATION ON ULTRA-LOW DIMENSION OBJECTS

Nguyen Quoc Khanh, István Endre Lukács

For contact formation on very small objects, like TiO₂ nanowires (NWs) with ultra-low dimensions (few nm wide and few tens nm long), determination of the coordinates of the objects in a pre-deposited marker array is a challenge. Thin NWs are hard to see by Scanning Electron Microscopy (SEM), because of weak contrast. Also, the sample becomes contaminated fast at such high SEM magnification.

So far, we carried out very thin metal contact pairs formation with very narrow gap (few tens of nm) to avoid the problem mentioned above. Then Atomic Force Microscope (AFM) has been used to find the adequate NWs, which were accidentally contacted at both ends. Later on, the second metal is to be deposited to make a connection between the leads and the contact pairs. This approach therefore, is very time-consuming due to large number of AFM measurement. Also, the NW's location to the contact is not well controlled. With the new facility (RAITH 150), we have developed a novel technique, where we use a double marker array to enable the contact formation directly on a selected NW.

In our new approach, the thick markers are used to give sufficient contrast of SEM image for alignment at e-beam lithography, while the thinner ones ensure fast determination of the wire coordinates by AFM. The main steps of the procedure are followings:

- Thick marker formation by e-beam lithography and metal deposition. Markers are exposed during alignment procedure, so the thick markers ought not to be located close to the object to be processed
- Thin marker formation with alignment on thick markers
- AFM measurement at thin markers
- Object selection and contact design based on the AFM images
- Contact formation using thick markers

Despite of uncertainties (errors at thick marker alignments, drift in AFM measurements), the results of all NWs of the batch (8 NWs) are acceptable as seen on Fig. 1.

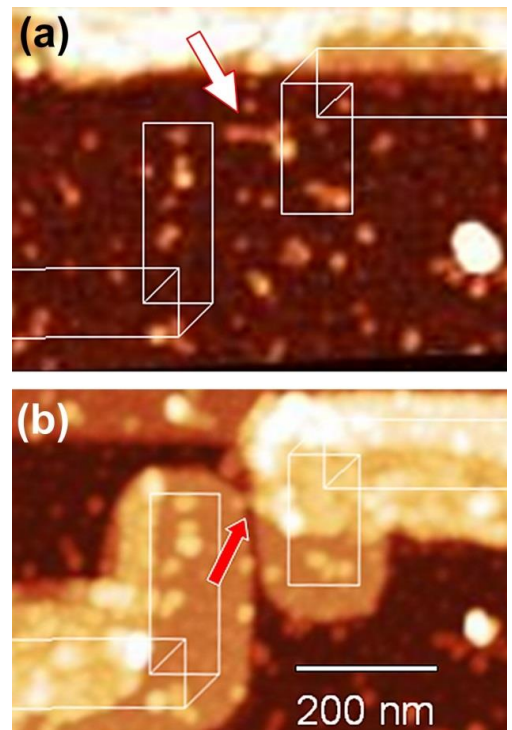


Figure 1: AFM image of the NW to be contacted indicated by the arrow, the contact design is also shown. Part of the thin marker can be seen on the top of the image (a), and a contacted NW with ca. 24 nm gap (b).

SILICON PROBES DESIGNED FOR INFRARED NEURAL STIMULATION

Zoltán Fekete, Anita Pongrácz, Zsófia Bércecs

Infrared neural stimulation (INS) was discovered in 2005, when action potentials were successfully evoked using infrared light. Histology was performed after revealing that there is a radiant exposure range, where action potentials are elicited without damage. In our work, a Michigan-type silicon microprobe for infrared neural stimulation was designed and investigated in terms of technology induced surface roughness and optical transmission. The fabrication of such optrode was realized by deep reactive ion etching and subsequent wet chemical polishing.

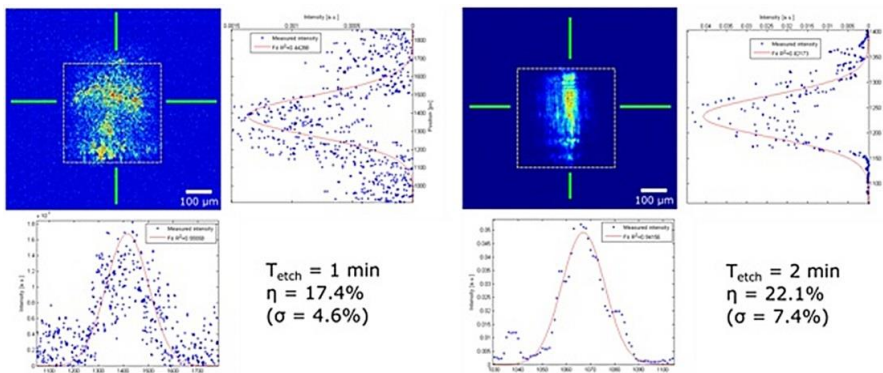


Figure 1: Beam profile of P1 (a-c) and P2 (d-f). Dashed yellow lines represent the contour of the probe shaft, while green lines indicate the X and Y cross-section of represented data on optical power.

The overall efficiency was further boosted by integrated couplers and focusing microlenses etched into the silicon substrate. Due to the proposed fabrication approach, 22.1% in system efficiency was achieved at a wavelength of 1310 nm (Fig 1). We observed that system efficiency does not increase significantly by increasing the time of sidewall polishing; however, the beam shaping effect of the coupling lens is more remarkable, if the tip roughness is reduced down to 8.7 nm RMS value. The spatial distribution of the delivered light can be also controlled through integrated micromirrors at the probe tip, which facilitates lateral out-coupling with a Gaussian beam profile.

IONTOPHORETIC INJECTION MICROSYSTEM DELIVERING PATHWAY TRACER MOLECULES IN THE LIVING TISSUE

Zoltán Fekete, Anita Pongrácz

Exploring the structure and function of the brain's connectome is in one of the major scope of recent neuroscience research. Complementing neuronal recording with pathway tracing is still an indispensable tool to achieve such goals specifically at the microcircuit (single neurons) and mesoscale (neuronal populations) levels of the neural network. However, electrophysiology and neuronal tract tracing are usually applied separately even if combined in the same experiment. In our work, we present the results of *in vivo* local release of a neuronal tracer, biotinylated dextran amine (BDA) in the rat somatosensory cortex using monolithically integrated microfluidic channel of a silicon neural microelectrode (Fig 1). The tracer injection is controlled by iontophoresis using Pt electrodes in the vicinity of the outlet of the microfluidic channel.

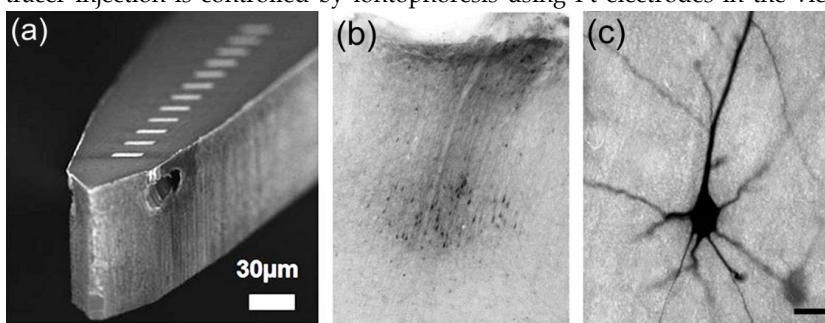


Figure 1: (a): SEM image of a silicon neural electrode with 12 Pt contact sites on the top surface and two buried microfluidic channels. The outlets of the channels are on the sidewalls. Contact closest to the outlet serves as counter electrode during iontophoresis, while the reference electrode is placed in the microfluidic interface connected to the probe. The remaining contacts are applied for electrophysiology. (b): BDA labeled neuronal cell bodies (black dots) are present all along the electrode track and accumulate in the deep layers. Note the lack of a dense tracer deposit and that the labeled neurons are clearly distinguishable. (c): Close view of a both anterogradely and retrogradely labelled neuron.

Using 3-5 μ A, 5-7 s on/off cycle and 15-20 min total injection time the localized injection resulted in clear anterograde and retrograde BDA labeling both within the cortex and in subcortical structures. Anterograde and retrograde labeling revealed the fine details of neuronal processes including dendritic spines and axon terminal-like endings. Injection sites appeared clear lacking any strong diffuse background labelling. Electrophysiological recording performed with the same microdevice immediately after the iontophoresis indicated normal cortical functioning. The results prove that the combination of *in vivo* multichannel neural recording and controlled tracer injection using a single implanted microdevice is feasible, and therefore it can be a powerful tool for studying the connectome of the brain.

IN VITRO STUDIES REVEALING THE IMMUNE RESPONSE OF THE LIVING TISSUE TO NANOSTRUCTURED IMPLANT SURFACES

Zoltán Fekete, Anita Pongrácz, Zsófia Bérce

Our goal is to design and fabricate nanostructured surfaces to reduce the extent of glial cell encapsulation of Central Nervous System implants and to promote neural attachment and regeneration, which improve the biocompatibility and functionality of the interfaces. Recent findings showed that specific glial cells prefer flat surfaces over nanostructured ones with certain geometries, while neural cells proliferate both on nanostructured and flat surfaces (Fig 1).

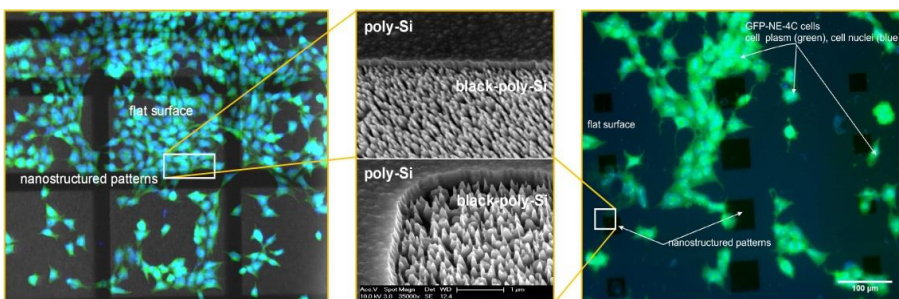
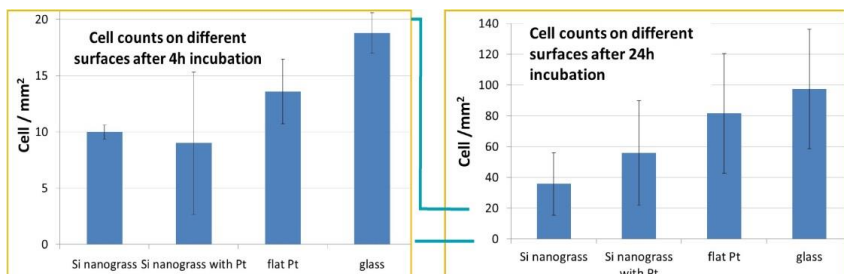


Figure 1: Two channel fluorescent images of GFP-NE-4C cells on nanostructured chips after 24h adhesion (blue channel: DAPI staining - cell nuclei; green channel: green light is emitted by the GFP expressed in the cytoplasm). Black regions are the nanostructured patterns on the samples. Inset images show the transition region, where flat poly-Si regions meet the nanostructured Si grass. Nanostructured surfaces are less preferred by the NE-4C cells compared to flat regions.

Neural progenitor cells were cultured on flat and nanostructured Si and Pt surfaces. Based on the MTT tests, the nanostructured surfaces are non-toxic compared to the glass surfaces. Cell adhesion was hindered by the nanostructured surfaces compared to the flat ones. Analysis of fluorescent microscopy images suggests that the cell number increases on every investigated surface type (Si nanograss, Pt, nano-structured Pt, glass), however, the proliferation is slower on nanostructured regions (Fig 2).

Figure 2: Comparison of cell counts after 4 hr and 24 hr long incubation of NE-4C neural progenitor cells on different surface types (nanostructured Si, nanostructured Pt, flat Pt and glass). Nanostructured regions hinders the adhesion of the stem cells compared to their flat references.



NEW APPROACHES IN THE DEVELOPMENT OF HYPOALLERGENIC IMPLANT MATERIAL IN ORTHOPEDICS: STEPS TO PERSONALISED MEDICINE

Katalin Balázs, Orsolya Tapasztó, Nikolett Oláh, Zsolt Fogarassy, Viktor Varga, D. Delfonse, C. Lohman, J. Lorenzen, M. Ignatiev, Csaba Balázs

The European collaborative project HypOrth (<http://www.hyporth.eu/>) aims to develop hypoallergenic material for endoprostheses, pursuing two major goals: HypOrth intends to improve the understanding and diagnosis of complications associated with an implant, primarily focussing on adverse immune reaction and infection. Based on these insights the project is developing innovative approaches for renewals in orthopaedic arthroplasty with improved biocompatibility.

The project central database allows the compilation of all relevant data and brings together clinical and scientific results. These data are also available to material researchers and developers. For patients with the risk of getting an adverse immune reaction to conventional material composition we developed a new material combination with hypoallergenic and antibacterial properties and a new hypoallergenic endoprosthesis prototype.

The materials used for artificial prosthesis by default are Titanium (TiAl₆V₄, TiAl₆Nb₇ – forged alloy), CoCrMo (forged alloy), ceramics and UHMWPE (Ultra High Molecular Weight PolyEthylene).

The role of Thin Film Physics Department is the development of novel ceramic coatings for existing Mathys implants. The main part of research is confidential.

HOMOGENEOUS TRANSPARENT CONDUCTIVE ZNO:GA BY ALD FOR LARGE LED WAFERS

Zoltán Szabó, Zsófia Baji, István Bárszony, János Volk

Transparent conductive oxides are widely used in photovoltaics, thin film transistors and light emitting devices. The most common TCO material is indium doped tin oxide (ITO), but in the past decades the price of indium has been rapidly increasing. One of the most promising replacements due to its excellent transparency in the visible wavelength range and similar electrical conductivity is highly n-doped zinc oxide. Ga doped ZnO (GZO) has an excellent transparency and low resistivity combined with an electrical stability at elevated temperatures and excellent crystalline properties. Atomic layer deposition (ALD) is a promising candidate to produce high quality GZO layers at relatively low temperatures ($300\text{ }^{\circ}\text{C}$) and at large wafer sizes as well.

We used atomic layer deposition to acquire a series of GZO thin films with varying nominal Ga concentrations. Homogeneity tests were carried out on GZO thin films deposited on a 4" glass wafer. The effect of the annealing and the fabricated devices were investigated on GZO layers deposited on a commercial InGaN/GaN LED-wafer, whereas for electric and electroluminescence measurements fully processed GZO coated LED-chips were used. We also tried a number of different thermal annealing processes to gain a film with properties optimized for LED applications.

To find the optimal concentration, GZO/c-sapphire films with Ga concentrations of 1, 2, 3, 4, 5, and 10 at% were used. According to the Hall measurements, the increasing doping level reduces the specific resistivity of the layers down to $3.3 \times 10^{-4}\text{ }\Omega\text{cm}$ at 3 at% then it increases monotonously with the growing doping concentration. This behavior is governed mainly by the change in free carrier concentration: The doping increases the free carrier concentration up to $1.38 \times 10^{21}\text{ cm}^{-3}$, until reaching an optimal Ga content of 3 at%. In this regime the volume concentration of Ga is close to the free carrier concentration, which indicates a nearly perfect, uncompensated substitutional doping at Zn cation sites (GaZn). In contrast, the electron mobility decreases from 17 to 11 $\text{cm}^2\text{V}^{-1}\text{s}^{-1}$ as the Ga concentration increases from 1 to 10 at%. This can be attributed to the ionized impurity scattering.

The homogeneity of the GZO layers with respect to thickness and conductivity was tested on a 4" diameter glass wafer. As it can be seen in Fig. 1, the wafer scale uniformity of the films was excellent. The relative standard deviation of the average thickness was 2.1 %. As revealed by Eddy current mapping the ALD GZO layer has an average sheet resistance value of $137.1 \pm 2.7\text{ Ohm/sq}$ and a relative uniformity of 2.0 % over the wafer (Fig. 1b). By calculating the specific resistivity map as a production of t and R_{sh} we obtain an excellent uniformity of 0.8 % (Fig. 1c).

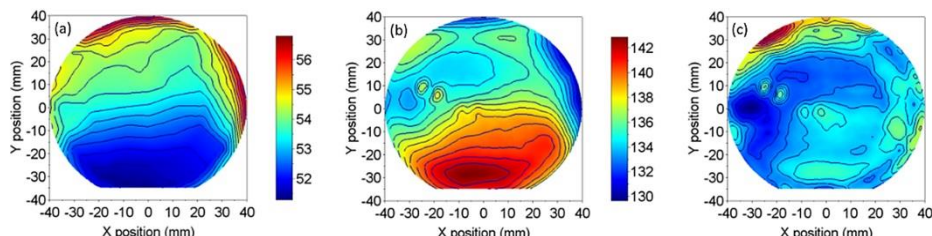


Figure 1: Thickness (a), sheet resistance (b), and the calculated resistivity map (c), recorded on a limited wafer area in a diameter of 80mm.

For LED operation it is also essential to have a high electrical quality TCO/p-GaN interface with ohmic conduction. In order to address this issue, a proper thermal annealing sequence had to be adopted. We carried out a series of post deposition thermal annealing experiments in the range $400\text{--}800\text{ }^{\circ}\text{C}$, i.e. above the deposition temperature of $300\text{ }^{\circ}\text{C}$. Tests by the transmission line method on ALD GZO deposited on commercial InGaN/GaN blue LED wafers were performed. With increasing annealing temperature we found that the I-V curve is gradually improving and becoming fully linear at $700\text{ }^{\circ}\text{C}$. On the other hand the annealing at such a high temperature deteriorated the bulk conductivity of the GZO films. Therefore we introduced an 'interrupted growth by ALD' method i.e. the annealing was performed on a thin ALD grown buffer-layer (of ca. 15 nm). The deposition of the missing thickness followed after that by a second ALD step. This two-step deposition scheme resulted in a slightly improved threshold voltage compared to the as deposited one (2.8 vs. 2.9 V, at $I=20\text{ mA}$), which is even more prominent at higher currents (20-100 mA) (blue vs. black solid line in Fig. 2.). More importantly, the two-step annealing treatment led to a ca. 40-times enhancement in electroluminescence intensity at a driving current of 20 mA (blue vs. black dashed line in Fig. 2.).

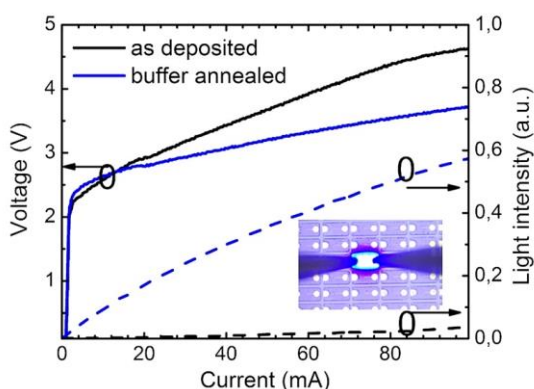


Figure 2: Voltage (left vertical axis) and output electroluminescence intensity (right vertical axis) as a function of driving current recorded on the LEDs for the thin (ca. 45 nm) non-annealed (black) and 2-step deposited annealed GZO TCO (blue), respectively.

As a conclusion, ALD proved to be a promising candidate for the deposition of Ga doped ZnO films for LED applications. The 3% doped GZO films have excellent electrical properties, and an annealing treatment can also optimize the quality of the GZO/p-GaN interface.

CHARACTERIZATION OF BIOCOMPATIBLE CERAMIC TiC/AMORPHOUS C THIN FILMS PREPARED BY DC MAGNETRON SPUTTERING

Nikolett Oláh, Zsolt Fogarassy, Attila Sulyok, János Szívós, Miklós Veres, G. Kaptay, T. Csanádi, Katalin Balázsi

Over the last few years, TiC/a:C nanocomposite protective surface coatings, consisting of hard TiC nanoparticles embedded in a soft amorphous matrix, have attracted a special attention because of their passivation effect on different implant materials (Fig 1). Therefore, our development is focused on the biological application of these thin films [<http://www.hyporth.eu/>].

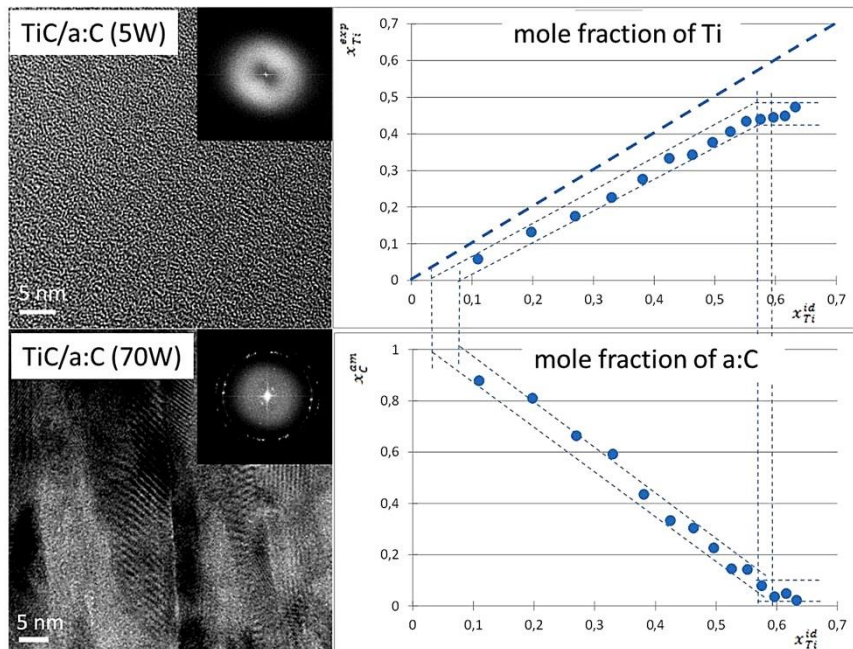


Figure 1: Structure of TiC/a:C films by HRTEM deposited at 5 and 70 W of Ti target power (left) and the measured mole fraction of Ti in the deposited layer (over) and the measured mole fraction of amorphous carbon in the deposited layer (under).

The main goal of our research work is the understanding of deposited TiC/a:C growth mechanism and the determination of TiC crystal formation at different Ti:C ratios. A secondary aim was to investigate the relationship between the exact elemental composition and mechanical and tribological properties of the different films.

TiC/a:C thin films were prepared by DC magnetron sputtering. The detailed preparation steps of the coatings were described in our previous works [N. Oláh, M. Veres, A. Sulyok, et al., J Eur Ceram Soc. 34(14) (2014) 3421-3425], [N. Oláh, Zs. Fogarassy, et al., Ceram. Inter. 41(4) (2014) 5863-5871]. Magnetron sputtering of carbon and titanium were performed simultaneously. The film's composition and morphology were studied in details by High Resolution Transmission Electron Microscopy (HRTEM), X-ray photoelectron spectroscopy (XPS) and Raman spectroscopy. The mechanical characteristics of the TiC/a:C thin films were investigated by nanoindentation technique while the tribological behavior of the films was examined by a ball-on-disk tester (CSM tribometer) moving on circular trajectory at room temperature.

Very good agreement was observed between theoretical calculations and experimental measurements. The thickness of amorphous carbon matrix decreased simultaneously with the increasing Ti content. The amorphous carbon has not gone through to a graphitization process. The highest hardness (H) of ~ 26 GPa and modulus of elasticity (E) of ~ 140 GPa with friction coefficient of 0.268 was observed in case of the film prepared at ~ 40 at% Ti content (by XPS) which consisted of 4-10 nm width TiC columns separated by 2-3 nm thin a:C layers. The H³/E² ratio was 0.9 GPa that predicts high resistance to plastic deformation of the C-Ti nanocomposites beside moderate wear-resistant properties (H/E=0.19).

GRAPHENE-CERAMIC COMPOSITES FOR TRIBOLOGICAL APPLICATION IN AQUEOUS ENVIRONMENTS

Orsolya Tapasztó, Zsolt Fogarassy, Viktor Varga, Csaba Balázsi, J. Dusza, A. Kailer, Katalin Balázsi

Advanced ceramic materials have proved their superior wear resistance as well as mechanical and chemical properties in a wide range of industrial applications. Today there are standard materials for components and tools that are exposed to severe tribological, thermal or corrosive conditions. The main aim of the project is to develop novel, highly efficient tribological systems on the basis of functionalized graphene and ceramic-graphene-nanocomposites and to prove their superior quality and suitability for technical applications e.g., for slide bearings and face seals in aqueous media.

Current research in the field of ceramic nanocomposites shows that it is possible to make ceramic materials with improved mechanical and tribological properties by incorporating graphene into the ceramic microstructure. The electric conductivity of these materials, which is reached already at low graphene contents, offers the possibility to reduce efforts in manufacture and to create new functions that may be utilized in technical applications.

Multilayered graphene (MLG) was prepared by attritor milling technique. 10 hours intensive milling of 1 and 5 micrometer sized graphite powders yielded MLG with 20-30 layers. The large quantity, very cheap and quick preparation process is a main strength of our MLG. Si_3N_4 / graphene nanocomposites prepared by attritor milling and sintered by spark plasma sintering (SPS, partner IMR SAS, Fig. 1a) and hot pressing (HP, partner IMR SAS, Fig. 1b). The Si_3N_4 with 1wt%, 3wt%, 5wt% and 10wt% MLG were produced and their structure was fully examined by our department.

This new approach is very promising, since ceramic microstructures can be designed, that are electrically conductive, possess high toughness and provide improved wear resistance at low friction. Furthermore, electrical conductivity can be utilized for monitoring and electrochemical protection devices.

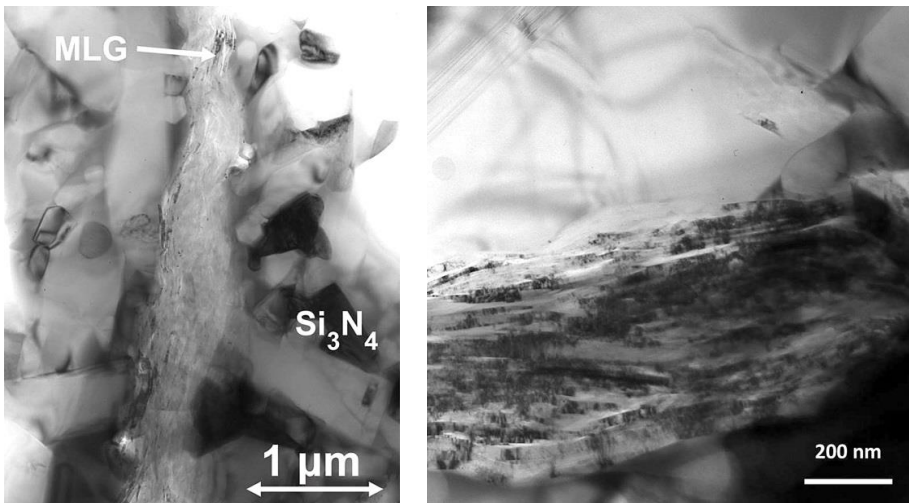


Figure 1: a) Milled and hot pressed Si_3N_4 composite with 10 wt% MLG. Figure 1b) Milled and hot pressed Si_3N_4 composite with 10 wt% MLG.

CHARACTERIZATION OF DEFECT STRUCTURE IN ELECTRODEPOSITED NANOCRYSTALLINE NI FILMS

T. KOLONITS, P. JENEI, B.G. TÓTH, ZSOLT CZIGÁNY, J. GUBICZA, LÁSZLÓ PÉTER, IMRE BAKONYI

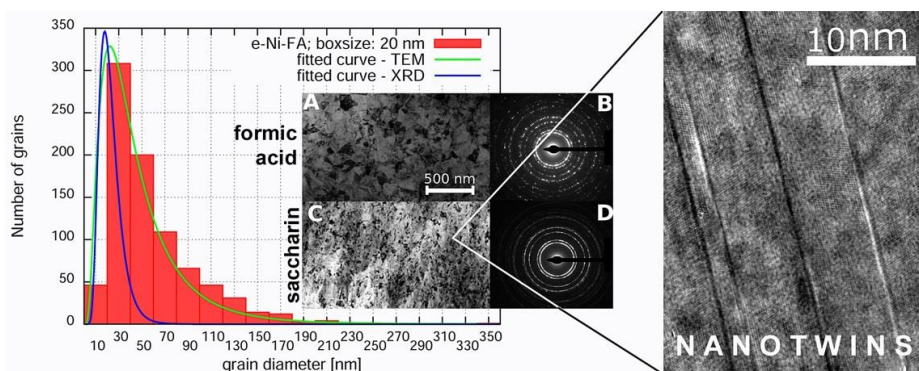


Figure 1: Grain size distribution of nanocrystalline Ni film deposited with formic acid additives determined by TEM and XRD. The grain size refinement is shown in TEM images and electron diffractions. Nanotwins observed in the film deposited with saccharine are illustrated in the HRTEM image.

The effect of organic additives (saccharin and formic acid) on the defect structure in electrodeposited Ni films was investigated by X-ray diffraction (XRD) line profile analysis (eCMWP model) and transmission electron microscopy (TEM) [64]. The main task of the project is to investigate the effect of the additives on the grain structure and defect (dislocation and twin) density which influence the macroscopic properties and application of the layers. The electrodeposited layers were deposited at room temperature at a current density of $j = -43.75 \text{ mA/cm}^2$. The basic electrolyte contained 0.6

mol/ ℓ nickel sulphate ($\text{NiSO}_4 \cdot 7 \text{ H}_2\text{O}$), 0.30 mol/ ℓ sodium sulphate ($\text{Na}_2\text{SO}_4 \cdot 10 \text{ H}_2\text{O}$), 0.25 mol/ ℓ H_3BO_3 és 0.15 mol/ ℓ H_3NO_3 . The 46 mol/ ℓ formic acid or 1 g/ ℓ saccharine was mixed into this bath. In the film deposited without additives, a columnar structure was observed showing similarities to the T-zone of structure zone models. The typical column width was $\sim 120\text{nm}$ and their length was $>3\mu\text{m}$. There was no detectable twinning. Both formic acid and saccharin additives resulted in equiaxed grains with reduced size, as well as increased dislocation and twin fault densities in the nanocrystalline films (Fig. 1). Moreover, the structure became homogeneous and free of texture within the total film thickness due to the additives. Saccharin yielded smaller grain size and larger defect density than formic acid. The inhibiting effect of the additives can be attributed to the surface coverage of the hydrophilic functional groups. The incorporation of $\sim 0.3\text{at}\%$ sulphur was detected only in the films deposited with saccharine which imply different mechanisms for the two additives. In the layers deposited with formic acid no incorporated contamination was detected by EDS. A detailed analysis of the grain size and twin boundary spacing distributions was also carried out with the complementary application of TEM and XRD (Fig. 1). It is important to mark the difference between the grain size - determined by TEM and the crystallite size - determined by XRD. The reason of the difference is the high sensitivity of XRD for the small orientation differences due to different kind of crystal defects. Generally the grain size is approximately 2 times larger than the crystallite size. The defect density distributions determined by TEM and XRD showed similar tendencies. Presumptions of the eCMWP model about the grain size distribution (lognormal) were confirmed by TEM. Twin-boundary spacing follows geometric distribution for large spacing values in accordance with the model used in the XRD line profile analysis. However, for twin-boundary spacing smaller than 5 nm, TEM yields a smaller fraction than that predicted by XRD which discrepancy is due to the presence of numerous nanotwins as evidenced by HRTEM (Fig.1).

MICROSCOPY OF HIGH QUALITY CUBIC SiC GROWN ON Si

M. Bosi, G. Attolini, M. Negri, C. Ferrari, E. Buffagni, C. Friger, M. Calicchio, Béla Pécz, Ferenc Riesz, I. Cora, Zoltán Osváth, L. Jiang, G. Borionetti

Cubic silicon carbide (β -SiC or 3C-SiC) is a wide-bandgap semiconductor with high hardness, high electron mobility, high thermal conductivity, high resistance to chemical attack and it is biocompatible; for these reasons SiC is interesting for potential technological applications, such as power devices and sensors operating in harsh environments. The growth of this polytype is a challenge.

Several samples were grown by varying the deposition temperature and the MTS (monomethylsilane, CH_3SiH_3) content in order to study how these parameters affect the layer quality and the lattice defects. The use of single source precursor (like MTS) increases the growth rate of SiC.

The grown layers were investigated by several techniques including transmission electron microscopy (TEM), Makyooh analysis and Raman spectroscopy. The TEM specimens were prepared by Ar ion milling and then investigated by conventional and high resolution microscopy.

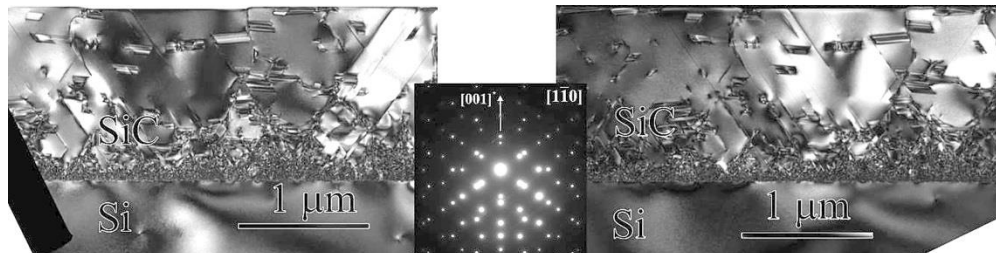


Figure 1: Bright field (left) and dark field (right) images taken on a sample grown with the addition of MTS. Diffraction pattern is inserted to the middle of the above image.

The TEM images in Fig. 1 show the sample grown at 1400 °C with the addition of MTS. The single crystalline SiC layer contains a lot of stacking faults, which give faint streaks in the diffraction pattern. There is a huge density of defects at the SiC/Si interface, which is however, decreased substantially toward the surface.

When we compare a sample grown at the same temperature, however, without the addition of MTS we can observe that the defect density is higher than the previous sample. Beside the well-known stacking faults there were antiphase boundaries inside SiC. The layer is single crystalline as well, but the defect density is not decreased so much like in the former case toward the surface. Low magnification images had shown that the surface of the grown SiC layer is not perfectly flat.

Although in all of the grown SiC layers the defect density is high close to the silicon substrate, we observed that in layers grown with the addition of MTS (both at 1300 °C and at 1400 °C) the defect density is substantially lowered towards the surface region. This observation was supported by the Raman analysis based on the shift of the Raman peaks, as well.

LOW CYCLE THERMOMECHANICAL FATIGUE OF A REACTOR STEEL: MICROSTRUCTURAL INVESTIGATIONS

B. Fekete, Fanni Misják, P. Trampus, György Radnócz

One of the possible damage mechanisms in pressurized water reactors is the low cycle thermomechanical fatigue caused by simultaneous thermal and mechanical loading, during transient operating processes (e.g., at start up and shut down) and accident conditions. The reactor pressure vessel has a key role in the safety of the nuclear power plant operation and possible lifetime extension. It is necessary to ensure the integrity of the reactor pressure vessel during normal and off-normal operating conditions, so the knowledge on low cycle fatigue degradation phenomena is important. In this work we investigated the thermomechanical low cycle fatigue behaviour of the VVER-440 reactor pressure vessel structural materials. Low cycle continuous and interrupted thermomechanical fatigue tests were made on the base metal (15Ch2MFA) of the vessel at parameters corresponding to the exploitation conditions in the reactor. The measurements were carried out at thermo-mechanical fatigue conditions in the range of 150-270 °C using the GEEBLE 3800 mechanical simulator. All fatigue tests were carried out with a symmetric cyclic strain and a triangular waveform at frequency of 0.083 Hz. The longitudinal total strain amplitude level was 0.3 %. The lifetime of the material was determined to be 2376 cycles. Interrupted fatigue tests were carried out to investigate the kinetics of the fatigue softening of the material at different stages of its lifetime.

Transmission electron microscopy measurements made at different stages of fatigue test show that the dislocation concentration after an initial increase starts decreasing (Fig. 1). At about 50 % of the nominal lifetime the structure of grain and cell boundaries changes from strained to relaxed, i.e. the strain field of captured dislocations (Fig. 2a) dynamically disappears. The recovery of dislocation substructure resulted in decrease of dislocation density accompanied with boundary movements, which are well seen in the TEM images (Fig 2b). The reduction of dislocation density can be a result of two simultaneously operating mechanisms: annihilation during movement and entrapment in cell boundaries. Then the micro-deformation process will be continued in the grain boundaries, where micro cracks initiate.

The investigated low cycle fatigue behaviour can provide reference for remaining life assessment and lifetime extension analysis of Nuclear Power Plant components.

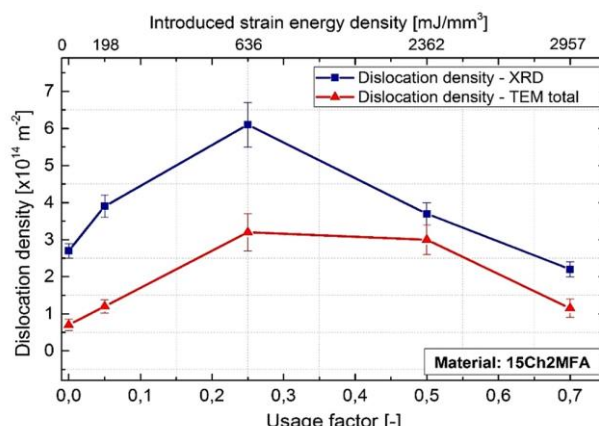


Figure 1: The variation of dislocation density as the function of the lifetime under thermo-mechanical treatment. (The X-ray measurement was performed at the Eötvös University by Bertalan Jóni.)

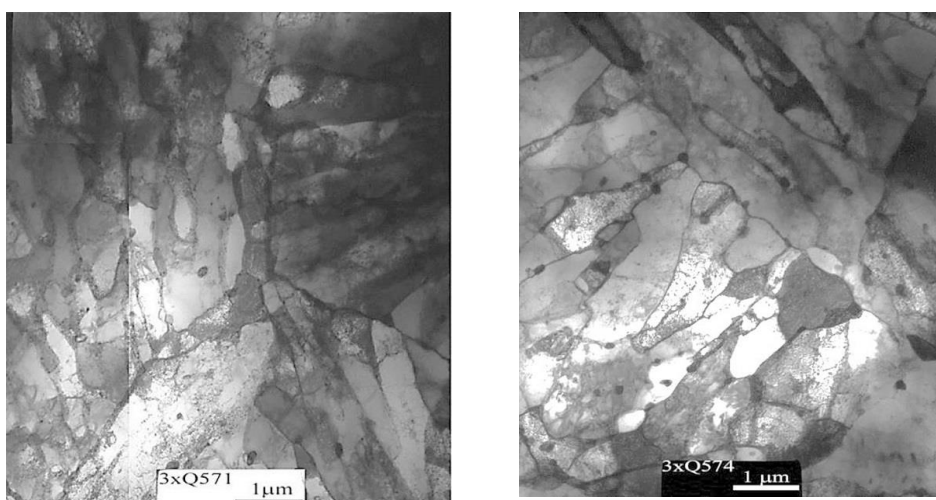


Figure 2: TEM image of the grain/cell structure of 15Ch2MFA steel after thermo-mechanical fatigue for 5% (right) and 50% (left) of lifetime.

CHARACTERIZATION OF THE TOPOGRAPHY OF THE GRAPHENE MOIRÉ SUPERLATTICE ON Au(111) AND Cu(111) SUPPORTS

Péter Süle, M. Szendrő, Gábor Zsolt Magda, C. Hwang, Levente Tapasztó

In the last two years, we reached remarkable results in the theoretical and experimental study of surface morphology of graphene. Graphene moiré superlattices formed on various hexagonal supports (e.g. 111 metal surfaces) exhibit convex (protruded) morphology. In rare cases, suspected to be concave (nanomesh with periodic lattice of depressions) topography may exist (Fig 1). However, the experimental verification of the topography convexity is difficult. The curvature of the surface topography can not be clearly specified by STM due to the bias voltage dependence of the measured convexity (Fig 2). Varying the bias voltage contrast inversion occurs which prevents the unambiguous identification of the surface curvature. Using additional first principles DFT theoretical studies were only able to prove the existence of convex morphology e.g. on Ru(0001). Why is it important to know the precise topographic curvature of the graphene surface? According to our present knowledge and assumptions convex and concave superlattices may exhibit different electronic structure properties such as LDOS or band structure. Moreover, the surface activity, such as the adsorption energy of various molecules and/or the local magnetic property of surface Carbon atoms may depend on the morphology of the superlattice.

The most important results:

- The detailed description of the topography of moiré superlattices using a combined theoretical and STM approach.
- The coexistence of convex and concave superlattices has been explored in the same image which rules out the presence of contrast inversion.
- DFT calculations support the possible coexistence of various superlattices with different curvature due to the tiny energy difference between the various morphologies.

The Au(111) surface reconstructs upon graphene adsorption and exhibits an imprinted topography very similar to that of the moiré superlattice.

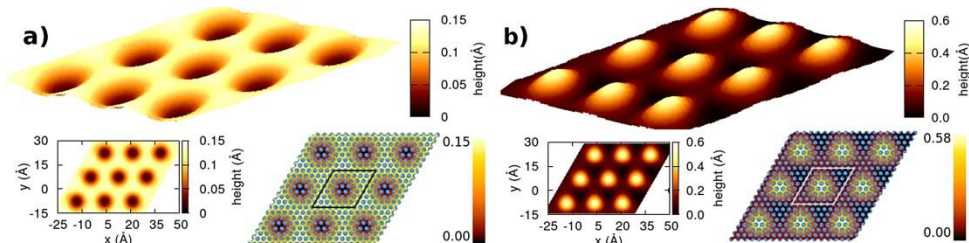


Figure 1: Concave (a) and convex (b) graphene moiré superlattices as computed by molecular dynamics simulations.

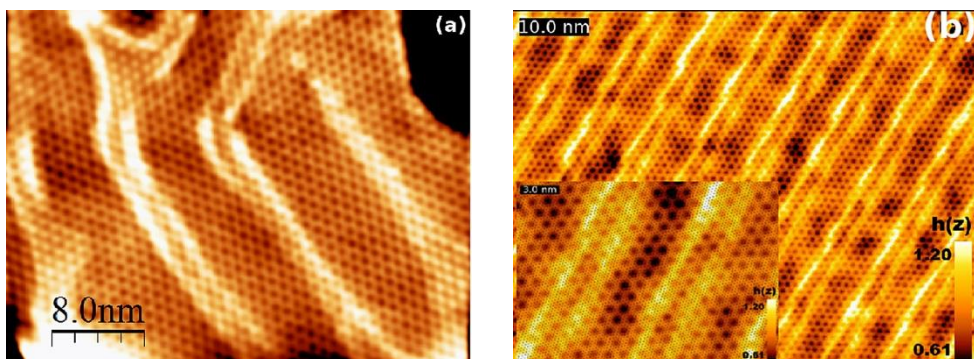


Figure 2: Concave graphene superlattice (nanomesh) on a herringbone reconstructed Au(111) surface. Topographic images as obtained by STM (a) and by molecular dynamics simulations (b).

METAL (Ni) INDUCED CRYSTALLIZATION IN AMORPHOUS Si THIN FILMS

György Zoltán Radnóczti, Erzsébet Dódony, Gábor Battistig, Béla Pécz, I. Stoimenos, N. Frangis, N. Vouroutzis

The formation of various silicide phases was studied to understand the initial stages of Ni induced crystallization of amorphous silicon (a-Si). During the experiments presented here only silicide formation occurred as the Ni supply was practically unlimited in comparison to the a-Si film.

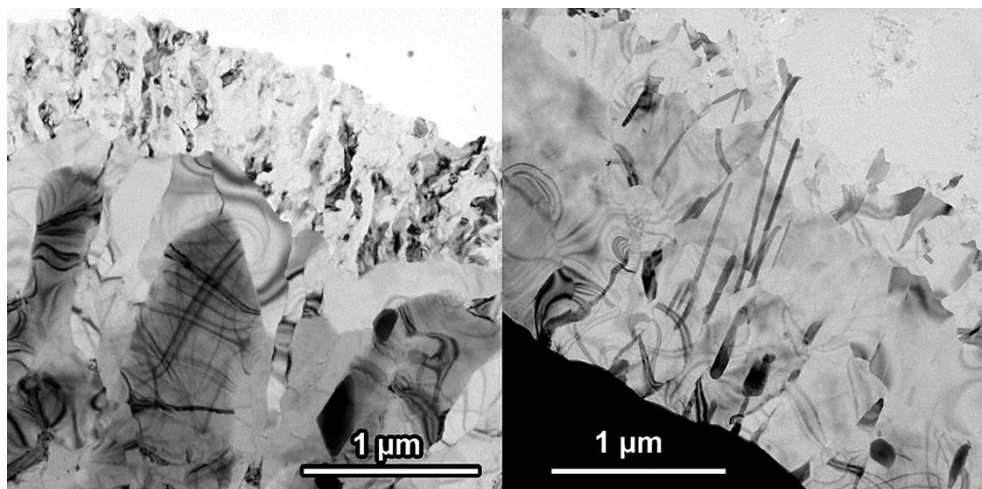


Figure 1: The result of in-situ heat treatment of a Si film with native oxide layer (left) and a Si film cleaned with HF solution (right).

The previously developed model system for in situ experiments was used. The amorphous Si foil on Ni microgrid proved to be a stable and reliable system for the investigation of silicide formation at elevated temperatures; however, some concerns were raised about the native oxide on the surface of the Si film. This thin oxide is believed to hinder the Ni diffusion into the Si film and it is also a relevant difference with respect to the usual MILC structures which contain no oxide film between the Ni and Si. To eliminate this potential diffusion barrier the Si film was transferred to a HF solution before placing it onto the Ni grid. The Ni grids were also cleaned in an etching solution (NH_4OH). In situ experiments were carried out with the new structures. The resulting structure was different from the structures obtained in our earlier experiments. For a comparison see Fig. 1.

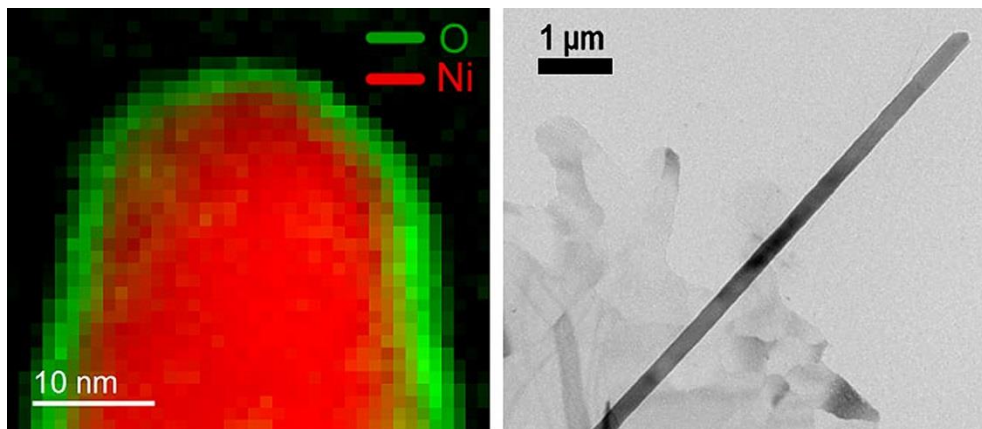


Figure 2: Ni(red) and O(green) elemental maps (left) of a whisker combined into a single image. The map shows a Ni containing whisker with a (silicon) oxide shell. The bright field micrograph of a whisker is shown on the right).

In contrast to previous results whiskers were observed in the new structures (Fig. 2). The whiskers were growing out of the plane of the a-Si film as determined by stereo images recorded with 8° tilt difference. The analysis of the whiskers showed that they consist of Ni_2Si phase and they also have an oxide shell as revealed by analytical measurement carried out by Austrian partners within ESTEEM project.

Related publication

- [1] G. Z. Radnóczti, et al: *Structural characterization of nanostructures grown by Ni metal induced lateral crystallization of amorphous-Si*, Journal of Applied Physics **119**, 065303 (2016)

UNIVERSAL NANOPATTERNING TECHNIQUE USING RF PLASMA ETCHING THROUGH TEMPLATES OF LANGMUIR-BLODGETT FILMS

János Szívós, Miklós Serényi, Sz. Pothorszky, Gábor Vértesy, György Sáfrán

The nanoscale modification of materials has attracted wide research interest recently. At present, mostly, slow and expensive methods are available for the fabrication of ordered nanostructures. Last year a cheap and fast technique was proposed [1] to produce ordered nanopatterns directly or to prepare masks for nanolithography and nanoimprint molds. This technique applies a monolayer of hexagonally self-assembled silica nanospheres (Langmuir-Blodgett (LB) film) as a template and the sample surface is treated by a single UV laser ($\lambda=248$ nm) pulse through the LB film. We could produce nano-patterned Al-oxide layers by this technique successfully. Experiments were carried out in 2015, however, it was found that UV laser patterning is hardly effective in case of metal surfaces: the pattern with a pale contrast in the scanning electron microscope image (Fig. 1) was so shallow that it couldn't be visualized by cross-sectional TEM.

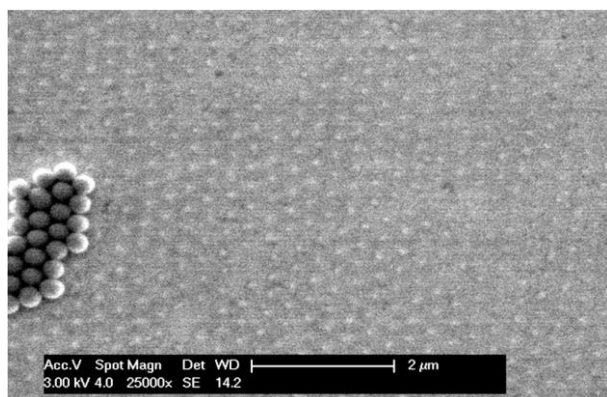


Figure 1: SEM image of the pattern achieved in Pt by UV laser treatment. Some residual nanoballs of the LB film are seen at the left side.

various materials, e.g. oxides, semiconductors and metals.

The LB film-covered sample is placed at the „target” position of the RF sputtering source 40 mm far from the ground plate and is subjected to 1 kV Ar plasma with pressure 2.5 Pa. The nanospheres of the LB film protect the surface and sputtering takes place between the nanospheres. This way the hexagonal pattern of the LB film can be replicated to almost any material’s surface provided that the plasma parameters and etching time are well set. The feature size is determined by the diameter of the nanospheres that, in principle, can be scaled down to about 10 nm.

In order to demonstrate the operability of the technique and the effects of changing the plasma parameters DC magnetron sputtered Pt thin films were nanopatterned. Pt layers are widely utilized e. g. for masking. It is suggested that Pt has a sputtering rate similar to that of FePt and CoPt.

Based on TEM investigations the layer structure of our Pt samples was the following: Si(001) substrate/thermal SiO_x (1140±10nm)/TiO_x buffer (11.3±0.3nm)/35±4nm Pt.

A pattern fabricated with optimum parameters is shown in Fig. 2. In (a) the SEM image shows the patterned Pt layer itself. Hexagonally arranged pattern is shown up, but the domains and stacking faults of the LB film are replicated as well.

The cross-sectional TEM image in Fig. 2 (b) represents part of the SiO_x underlayer, the Pt with the plasma etched pits and the residue of the 100 nm diameter nanospheres of the LB film that protected the layer beneath.

Nanopatterning with RF plasma through an LB film

is a fast and cheap technique that may be suitable, as well, for mass production. Our plans for 2016 are to study, in collaboration with our Japanese colleagues, the magnetic properties of such nanopatterned L1₀ CoPt thin films. That can be an alternative implementation of bit patterned magnetic media.

The reason of the inefficiency is the absorption mechanism of the UV laser in metals: the (quasi-)free electrons are thermalizing the lattice, thus the whole metal surface absorbs the energy nearly despite the presence of the LB film. It is likely that femtosecond pulse length would be required to avoid this effect.

The aim of the PhD work is to find simple, cheap and fast solution for nanoscale patterning of metallic, as well magnetic layers. The latter allows increasing the capacity of FePt or CoPt magnetic recording media by the preparation of ordered nanopatterns thus realizing Bit Patterned Media (BPM).

The LB film is suitable to prepare ordered, self-assembled template at large areas. The goal was to transfer the pattern of the template to a wide range of materials. Experiments with 30 kV ion-implantation have shown that in the case of metals the energy (and flux) of the applied ions (Ar⁺, possibly Xe⁺) is not sufficient. RF plasma etching, however, proved to be very effective that led to a universal technique capable to nanopattern

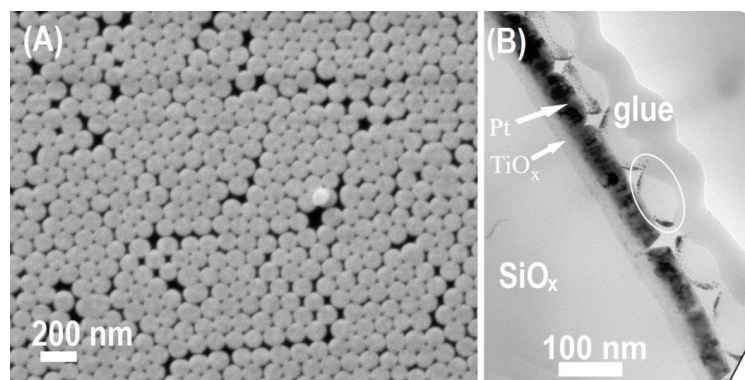


Figure 2: The pattern prepared by our RF plasma etching technique in the Pt layer. Plan view SEM (a) and cross-section TEM (b) images.

Related publication

- [1] J. Szívós, et al: Nanopattern formation in UV laser treated *a*-AlOx and nc-Al/AlOx layers, Vacuum **109**, 200 (2014)

CoPt/TiN THIN FILMS OF ENHANCED PERPENDICULAR COERCIVITY BY N₂ INCORPORATION DURING DEPOSITION

H. An, J. Wang, János Szívós, T. Harumoto, T. Sannomiya, S. Muraishi, György. Sáfrán, Y. Nakamura, J. Shi

The structure formation of CoPt thin films was investigated in collaboration with the Technical University of Tokyo (Department of Metallurgy and Ceramics Science, Tokyo Institute of Technology, Tokyo, Japan). CoPt (and FePt) films are the most promising media for future magnetic data storage. These alloys may transform from fcc to tetragonally distorted L1₀ phase under heat treatment which turns their magnetic easy axis preferably perpendicular to the surface that is crucial for high density data storage. However, with increasing layer thickness, the deviation of the direction of the magnetic easy axis increases, and at the end it returns to horizontal.

The structure and morphology of CoPt films grown by the Japanese colleagues on crystalline TiN buffer layers with and without N₂ incorporation were investigated by TEM. According to the literature, during deposition the incorporating N₂ expands the lattice constant of the alloy. A subsequent heat treatment releases the N₂ which causes a lattice contraction in the plane of the layer. This facilitates the formation of the in plane magnetic easy axis in case of FePt layers, because, in L1₀ phase, the smallest lattice constant is found parallel to the direction of the magnetic easy axis.

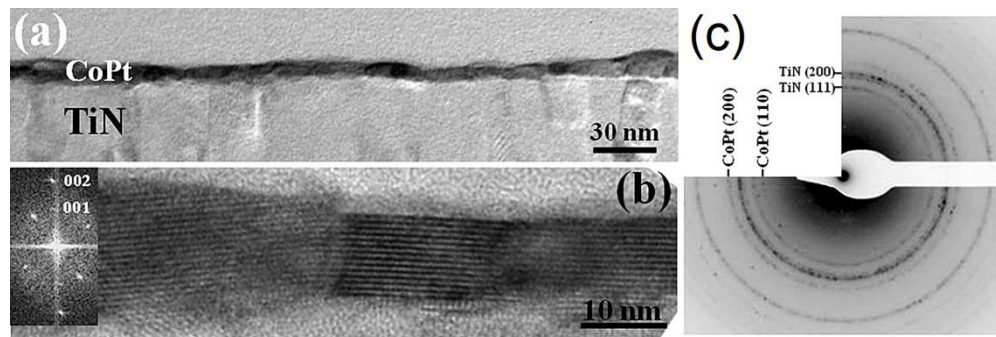


Figure 1: (a) Cross section TEM image of the heat treated CoPt sample. (b) HRTEM showing the superstructure of CoPt. In the FFT inset the L1₀-related reflections are indexed. (c) Plan view SAED pattern of the CoPt/TiN layer.

The Japanese colleagues have found by XRD that also in the case of CoPt the N₂ is built into the lattice and increases the in plane lattice constant. Under annealing, this lattice constant increases up to ~550 °C due to thermal expansion. At 600 °C, however, the built-in N₂ releases, that results in a contraction of the lattice constant. This phenomenon effectively promotes the transformation of CoPt into the L1₀ phase. Magnetic measurements have shown that, in CoPt, the magnetic easy axis is perpendicular to the surface, which is contradictory to the expectations, and to that observed in the case of FePt. The L1₀ phase was identified in the annealed samples by TEM in MFA (Fig. 1a, and b). The layer is polycrystalline with no texture in the layer plane (Fig. 1c).

In one of the several existing CoPt L1₀ phases the lattice constant is – exceptionally – the largest in the direction of the magnetic easy axis. In our samples precisely this L1₀ phase was found as revealed by the intensity distribution of the selected area electron diffraction (SAED) patterns (Fig. 2.). There is no similar phase in FePt. It follows that, in our CoPt, the in plane shrinkage of the lattice results in an easy axis formation perpendicular to the surface, that is favourable in magnetic recording media.

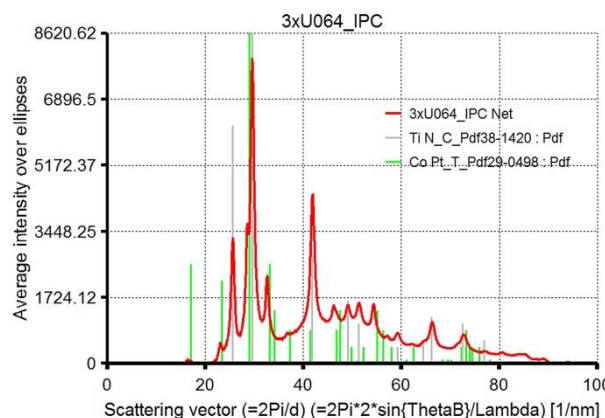


Figure 2: The intensity distribution of the in plane selected area electron diffraction pattern of the heat treated sample. The layer consists of TiN, and the L1₀ CoPt phase.

A DEVICE FOR MICRO-COMBINATORIAL TEM STUDIES

György Sáfrán

Status of technology

The physical chemical and structural properties of the layer systems of cutting edge technology are strongly determined by their composition. The Binary Alloy Phase Diagrams are well explored, however, phases of thin films are hardly studied and may remarkably differ from that of the bulk. The common procedure to reveal the properties of concentration dependent phases is the preparation and investigation of numerous two-component samples, one for each $C_A/C_{B=1-A}$ composition. This costs enormous time of man and machine.

For a study of high number of samples combinatorial methods are recognized i.e. instead of carrying out numerous individual experiments samples of varying composition are prepared in a single process. P. Schultz et al. [Science (1995) 268 (5218) pp.1738-1740] applied two-fold mechanical mask movement and prepared 200x200 micrometer size individual samples in various compositions at a density of 10000 sample /in². K.E. Roskov [J. Comb. Chem. (2008) 10, pp.966-973] prepared for different, fixed composition samples combinatorially, onto individual TEM grids. The above examples are partly efficient solutions because only the preparation of samples is combinatorial. At the Thin Films Physics Dept. of RITP an experimental arrangement [F. Misják et al: Thin Solid Films 516 (2008) pp.3931-3934] was implemented already as micro-combinatorial, since samples of various compositions were both deposited and investigated in a single TEM grid: A shield with a 1mm diameter aperture was fixed above the substrate. Two sources were facing the substrate through the aperture at inclined angles so that the thin film was deposited at two overlapping areas where two-component film of Ag-Cu was grown. The drawback of that method is that the region of changing concentration is very short (100-150 μm), the phases are accumulated and the sample does not contain the entire (0-100%) composition range.

Objectives

The aim was to construct a micro-combinatorial device that eliminates the incompleteness of the above solutions. The preparation and study have to be carried out in a single TEM grid within the whole 0-100% composition range so that the formed binary phases and variants may be well separated.

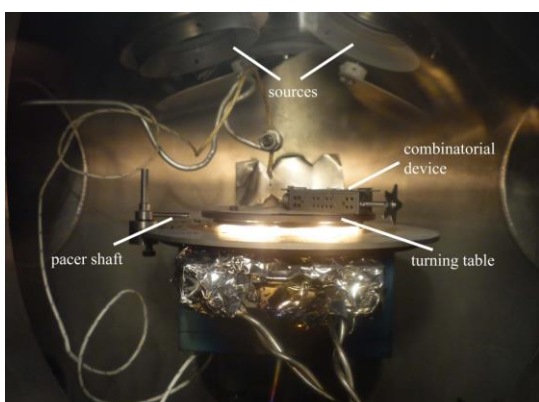


Figure 1: The micro-combinatorial device in operation.

an enhanced areal separation of the formed thin film phases. In addition, the device is suitable for the study of the effects of parameters (residual gas pressure, temperature, etc.) that change with time. The author thanks J. Szívós for contributing to the measurements!

Technical design

The recently patented [Hung. Patent No. P 15 00500 (2015)] micro-combinatorial device (Fig. 1.) incorporates a cover plate with a slit that is moved in fine steps above the TEM grid, meanwhile the fluences of the magnetron sources "A" and "B" are regulated adversely. This new solution provides both micro-combinatorial preparation and investigation, so that the length of the concentration transition increases to 1500 microns.

A TEM grid with a deposited Mn-Al micro-combinatorial sample is shown in Fig. 2a). Fig 2b) represents energy dispersive X-ray spectrometer (EDS) data, that aside from the edges, shows linear concentration distribution. The micro-combinatorial sample prepared as above allows detailed and efficient analysis, because it exhibits the entire 0-100% concentration range in a TEM grid spread along a distance of an order of magnitude longer than earlier. The gradient of a limited concentration range can be adjusted to arbitrarily low values for

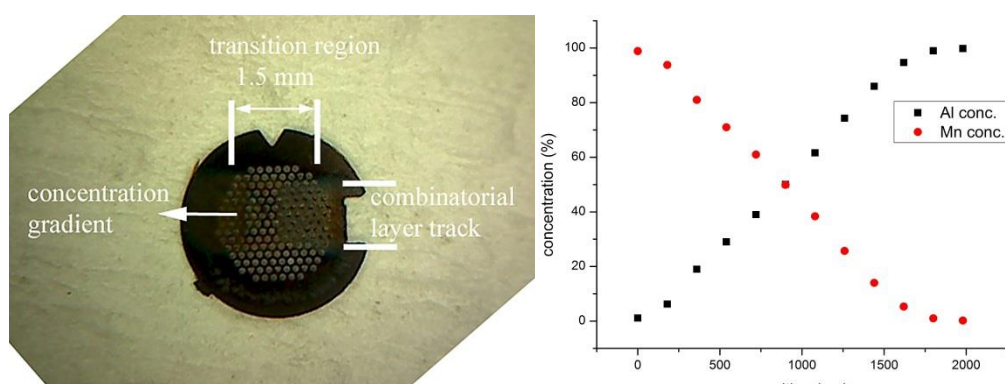


Figure 2: a) TEM grid with a microcombinatorial MnAl sample (1x1.5mm²) that was deposited through a moving slit. b) EDS concentration profile of the sample in 2(a). The transition extends to 1500 μm , and the concentration range is 0-100% for both (Al, Mn) components.

GRAIN BOUNDARY CHARACTERIZATION BASED ON DIFFRACTION DATA

Á.K. Kiss, and János L. Lábár

In materials science and its applications it is important to reveal the correlation between the technique of fabrication and the resulting structure, as well as between the structure and the properties of the materials. This is why the proper characterization of a manufactured material is inevitable. Two newly developed techniques are presented here, which facilitate the investigation of polycrystalline materials with transmission electron microscope (TEM) in terms of grain boundary characterization.

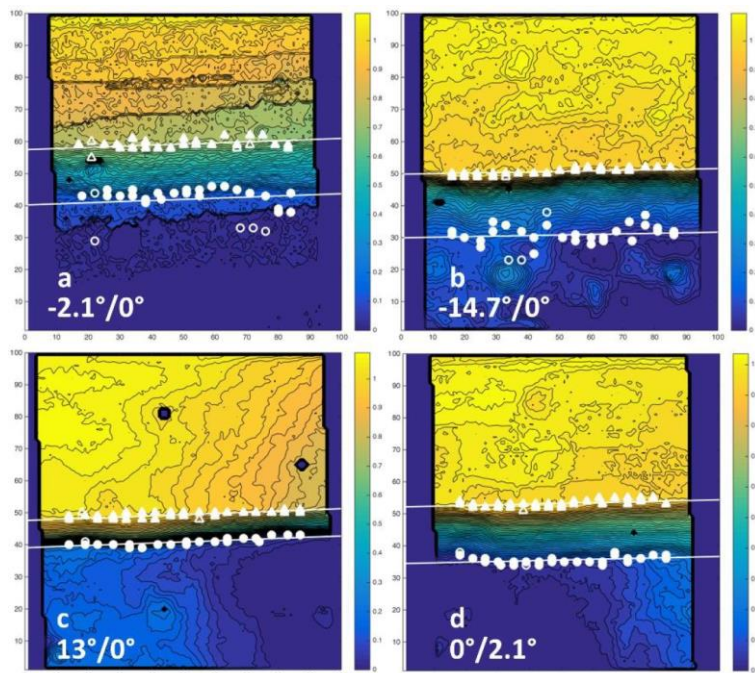


Figure 1: The same part of a GB in silicon thin film is shown here. The diffractions coming from the local neighborhood of the GB were evaluated by NMF at different tilt positions. The extent of the upper grain is identified with the shades of yellow on the contour level representations; the projection of the overlapping area (tilted GB-plane) can be clearly recognised between the marked lines.

misorientation between grains and perhaps the lateral direction of mathematical tool – namely the calculation of the cross-correlation from the area of interest in the sample. The calculation of cross correlation seems to be effective to express the similarity or dissimilarity of two diffraction patterns, thus the correlation coefficients are calculated between the diffraction signal. The correlation coefficients are calculated between

Both methods are based on computer supported measurements, which are capable of displaying either a grain boundary network or dislocations (or both) and additionally determining the orientation of grain boundary (GB) planes (i.e. determining their indices expressed in the coordinate systems of either neighbouring grains). Every step of the method (data acquisition and evaluation) is automated therefore it may serve as a basis of sample-characterization as far as distribution of grain-boundary planes is concerned.

The novelty is that additional information from the sample is obtained in addition to the ones provided by orientation maps. (Orientation mapping was carried out by the ASTAR tool installed on the TEM.)

Two different mathematical algorithms (non-negative matrix factorization, NMF and the calculation of cross correlation) are applied to the same diffraction dataset, which is originally acquired for orientation mapping – without the need of any further measurements. With the help of the first algorithm, the width of the projection of a GB i.e. the overlapping area between the neighbouring grains can be detected and quantified automatically (Fig. 1). This operation predicts the possibility of characterizing TEM samples with respect to the GB-plane distribution, in contrast of those methods, where only the GBs are taken into account [1]. The other is capable of providing qualitative new information which may alter the subsequent diffractions (both through rows and columns) and they are displayed in a grayscale map: it has turned out, that the grains, GBs, overlapping areas and even dislocations can be displayed efficiently with the help of the coefficients (Fig. 2). This technique works with nanometer-resolution and seems to be more efficient than (virtual) bright- and dark field imaging [2].

Related publication

[1] J Á.K. Kiss and J.L. Lábár: Determining Projections of Grain Boundaries from Diffraction Data in Transmission Electron Microscope, *Microscopy and Microanalysis* **22**, 551-564 (2016)

[2] Á.K. Kiss, E.F. Rauch and J.L. Lábár: Highlighting material structure with transmission electron diffraction correlation coefficient maps, *Ultramicroscopy* **163**, 31–37 (2016)

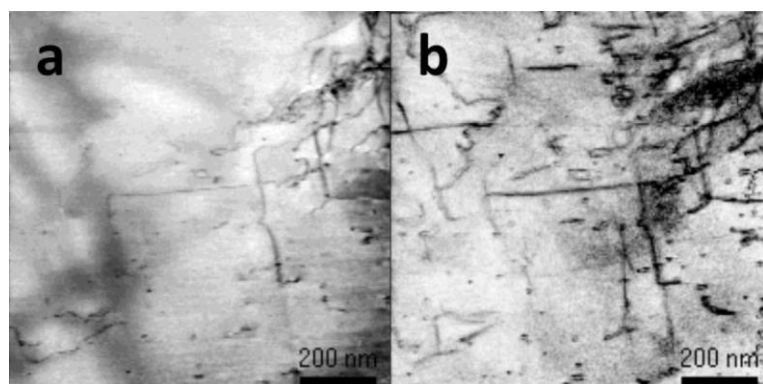


Figure 2: Virtual bright-field image (a) and cross-correlation coefficient map (b) of the same part of a deformed steel sample. The dislocations are displayed more efficiently in the latter case. (Edgar F. Rauch is acknowledged for this figure.)

HYDROGEL FILM FABRICATION FOR BIOSENSING

András Saftics, Sándor Kurunczi, Nguyen Quoc Khanh, Attila Sulyok, Róbert Horváth

Hydrogel interface layers play an important role in the field of biosensors, especially for label-free techniques. The 3D network of carbohydrate hydrogel dextran proved to be advantageous for the enhanced immobilization capacity and for the reduced non-specific binding of the sensor surface. We have been developing tailor-made dextranized surfaces on different substrates.

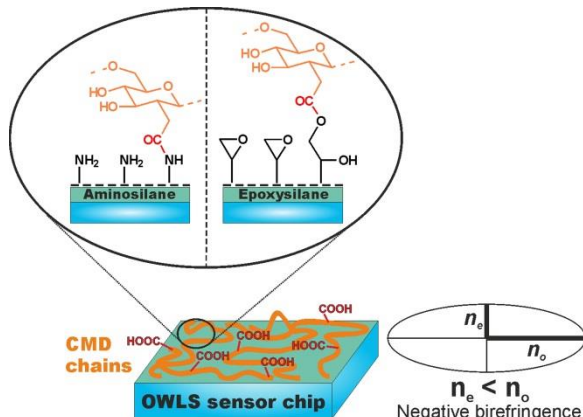


Figure 1: Schematic illustrations of the CMD grafting chemistries and the supposed structure of the CMD chains on the OWLS sensor chip. The negative birefringence of the layer suggested lain down chains on the surface.

Recently we have prepared carboxymethylated dextran (CMD) from native dextran in our lab. Then this CMD (with $M_w = 100$ and 500 kDa) was used for ultrathin surface coatings. Grafting methods based on covalent coupling to aminosilane- and epoxysilane-functionalized surfaces were applied to obtain thin CMD layers. The carboxyl moiety of the CMD was coupled to the aminated surface by EDC-NHS reagents, while CMD coupling through epoxysilane molecules was performed without any additional reagents. The surface layer investigation following the grafting procedures included x-ray photoelectron spectroscopy (XPS), attenuated total reflection infrared spectroscopy (ATR-IR), spectroscopic ellipsometry, atomic force microscopy (AFM) and optical waveguide lightmode spectroscopy (OWLS). The in situ OWLS method was suitable to devise the structure of the interfacial dextran layers by the evaluation of the optogeometrical parameters. Our results suggested an anisotropic layer that can be seen in Fig 1. The developed methodologies allowed to design and fabricate nanometer scale ultrathin CMD layers with well-controlled surface structure, which are very difficult to characterize in aqueous environments using present instrumentation and highly hydrated surface layers.

Related publications

- [1] A. Saftics, S. Kurunczi, Z. Szekrényes, K. Kamarás, N.Q. Khanh A. Sulyok, S. Bösze and R. Horvath: *Fabrication and characterization of ultrathin dextran layers: time dependent nanostructure in aqueous environments revealed by OWLS*, Colloids and Surfaces B: Biointerfaces **146**, 861–870 (2016)

THE DYNAMICS OF LIVING CELL ADHESION ON NANOSTRUCTURED GENETICALLY ENGINEERED MOLECULAR LAYERS REVEALED BY LABEL-FREE OPTICAL BIOSENSORS

B. Kovács, D. Patkó, Inna Székács, N. Orgován, B. Tóth, Ferenc Vonderviszt, Róbert Horváth

Our purpose was to record the kinetics of cancer cell adhesion on layers of genetically engineered protein variants, which are displaying cell adhesive RGD motifs. Wild type protein coatings and synthetic polymer films were used in parallel control experiments. We applied two types of waveguide sensors, optical waveguide light-mode spectroscopy and Epic Benchtop system, to record cell adhesion on the surface. The applied protein is a good target for genetic modifications. We constructed protein variants which can display cell adhesive RGD motif. Specific cell surface receptors (integrins) can recognize and bind these molecules, and trigger cell adhesion.

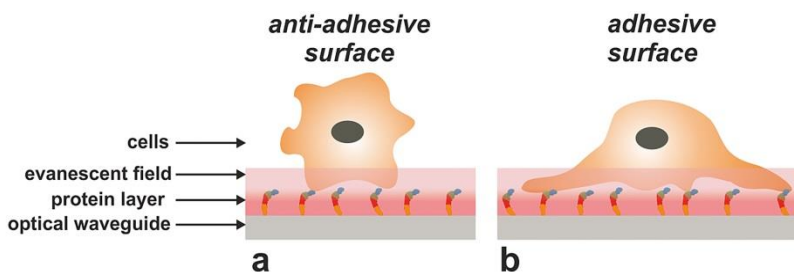


Figure 1: Schematic representation of anti-adhesive and adhesive surface coating induced cell behavior. a: Wild type protein surface coating hinders cell adhesion on the sensor surface. b: RGD displaying protein surface coating induces cell adhesion and spreading

The experimental results confirmed that the PLL-g-PEG polymer coating prevents cell adhesion, while the cells adhered and spread markedly on the RGD grafted PLL-g-PEG polymer layer. On the layer of the wild type protein negligible adhesion could be detected, contrary to the RGD displaying protein variants where significant cell adhesion was observed (Fig. 1). Our work resulted in fine-tuned surface coatings for basic cellular research and biomedical applications. It highlights the possibilities offered by label-free technologies in cell biological research and development.

LABEL-FREE PROFILING OF CELL ADHESION: DETERMINATION OF THE DISSOCIATION CONSTANT FOR NATIVE CELL MEMBRANE ADHESION RECEPTOR-LIGAND INTERACTION

N. Orgován, Beatrix Péter, Szilvia Bősze, Jeremy J. Ramsden, Balázs Szabó, Róbert Horváth

Cellular adhesion is essential to life. Cells usually establish an anchorage with the extracellular matrix or neighboring cells in the tissue using cell adhesion receptors embedded in the cell membrane, such as integrins, cadherins, selectins, syndecans, and the immunoglobulin superfamily of adhesion receptors. Since nowadays many modern drugs intervene at the level of cellular adhesion, there is an ever-increasing demand for techniques that enable the effects of such drugs to be screened in a straightforward and reliable way which moreover produce highly informative (e.g., multiparameter and/or kinetic) data.

Traditional methods for measuring cellular adhesion, including phase-contrast microscopy or mechanical assays, where the adhered cells are subjected to a fluid flow, are cumbersome and hence generally unsuitable for high throughput needed in drug discovery, and kinetic monitoring with high temporal resolution and high signal-to-noise ratio. In contrast, surface-sensitive label-free biosensors are inherently capable of generating good-quality kinetic data. Evanescent field-based label-free optical biosensors including resonant waveguide grating (RWG or Epic) biosensors are considered to be especially straightforward means to monitor cell adhesion, since they can *in situ* detect refractive index changes in the 100–200 nm thick layer closest to the sensor surface, where the anchorage between the cell and its substratum takes place. Moreover, the probing depth of these biosensors can be fine-tuned through waveguide structure design, so dynamic information from various depths can be simultaneously collected using multimode waveguides, potentially permitting the monitoring of changes inside the cell or in its nucleus triggered by surface adhesion.

In this protocol we described how the adhesion kinetics of living cells on a surface coated with integrin ligands can be characterized in detail. We use an optical biosensor, an Epic BenchTop (BT) system to monitor cell adhesion with unprecedented quality in a high-throughput way. The biosensor data recorded at various ligand densities are used to determine the dissociation constant, so the binding between the RGD ligand and its adhesion receptors embedded in their native cell membrane is characterized in a label-free and perturbation-free manner (Fig. 1). Of note, the present protocol is equally applicable for other types of ligands and adhesion receptors and can also be used to measure the effects of drugs interfering with cell adhesion.

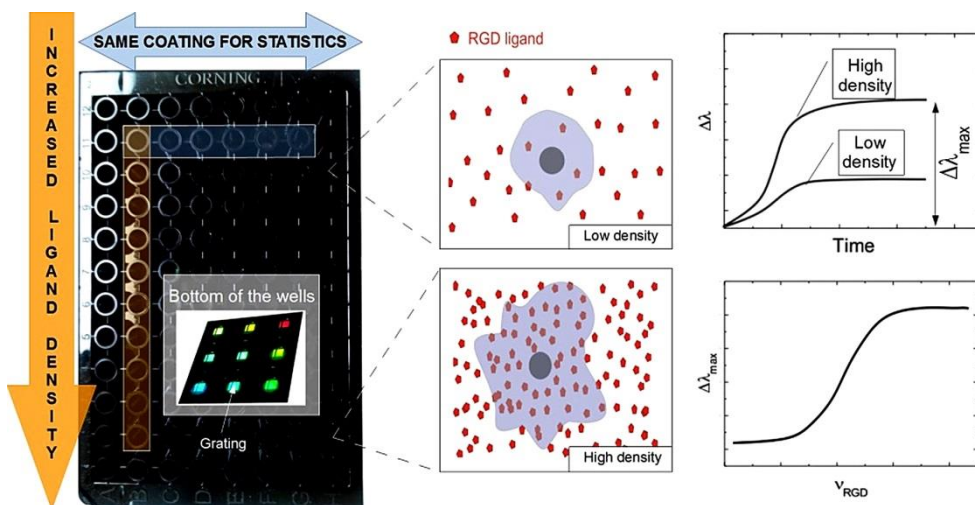


Figure 1: Monitoring the adhesion kinetics of cells with an Epic biosensor on different ligand densities enables the dissociation constant characterizing the interaction of native cell membrane receptors and their ligands to be determined.

Related publications

- [1] Label-Free Biosensor Methods in Drug Discovery, Methods in Pharmacology and Toxicology, Springer (Ed. Ye Fang), 233-252 (2015)

INCUBATOR PROOF MINIATURIZED HOLOMONITOR TO IN SITU MONITOR CANCER CELLS EXPOSED TO GREEN TEA POLYPHENOL AND PREOSTEOBLAST CELLS ADHERING ON NANOSTRUCTURED TITANATE SURFACES: VALIDITY OF THE MEASURED PARAMETERS AND THEIR CORRECTIONS

Beatrix Péter, Judit Nádor, K. Juhász, Á. Dobos, László Kőrösí, Inna Székács, D. Patkó, Róbert Horváth

In 2015 we published two successful applications of holographic microscopy to monitor cancer cell motility, migration, motility speed, and to examine the spreading of preosteoblast cells on a nanostructured titanate coating. The M4 Holomonitor, applied in this study, has a small size, and it is feasible to be put directly into a humidified cell culture incubator. This technique is completely noninvasive and label-free, therefore, nothing disturbs the cells during their movements. A special mechanical stage was also developed in order to position the sample into that range of the optical arrangement where digital autofocus works with high reproducibility and precision. With the help of this novel development, we could perform two successful measurements demonstrating the capabilities of our novel arrangement. In our first study, it is demonstrated that the movement of HeLa cells was temperately reduced after the addition of polyphenol EGCg. This phenomenon could be monitored in a completely noninvasive and label-free manner. With this experiment, we proved that our recently developed sample stage is an excellent tool for observing cell dynamical changes and monitoring the effects of chemical substances on living cells. In another experiment, the Holomonitor M4 was used to study cellular adhesion and spreading on nanostructured titanate coatings. A novel arrangement was developed to measure live cell behavior on spin-coated surfaces. We recorded the adhesion and spreading processes of the cells in real time. From the recorded data, we concluded that the averaged cell thickness and area detected by the instrument saturate after 30 min. These results are clearly contradictive to previous investigations where the preosteoblast adhesion on these nanostructured surfaces was monitored by an optical biosensor. Based on these findings, we concluded that under certain thicknesses, relatively large parts of the cells (parts of the thin lamellipodium) stick into the background surface due to the limited vertical resolution of the optical arrangement (Fig. 1). We determined the time-dependent corrected single-cell contact area and averaged thickness by the assumption that the cell volume is constant during the adhesion process. Our new correction method for estimation of the undetected parts of lamellipodia resulted in more precise evaluations supported by earlier biosensor kinetic data.

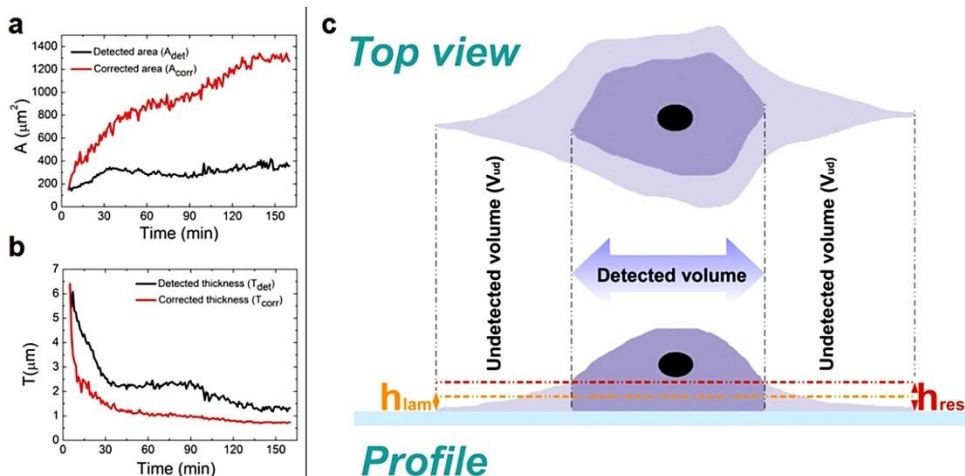


Figure 1: a): The detected and corrected data of the preosteoblast cells, b) the area, and c): the thickness curves. Sometimes the lamellipodia, the very thin parts of the cells, cannot be sensed perfectly by the instrument.

BIOPHYSICAL CHARACTERISTICS OF PROTEINS AND LIVING CELLS EXPOSED TO THE GREEN TEA POLYPHENOL EPIGALLOCATECIN-3-GALLATE (EGCG): REVIEW OF RECENT ADVANCES FROM MOLECULAR MECHANISMS TO NANOMEDICINE AND CLINICAL TRIALS

Beatrix Péter, Szilvia Bősze, Róbert Horváth

Traditionally, tea was drunk to eliminate toxins, to improve blood flow and resistance to diseases, so its habitual consumption has long been associated with health benefits. Among natural compounds and traditional Chinese medicines, the green tea polyphenol epigallocatechin gallate (EGCg) is one of the most studied active substance. Tea catechins, especially (-)-EGCg, have been shown to have various health benefits, for example anti-metastasis, anti-cardiovascular, anti-cancer, anti-inflammatory and antioxidant effects (Fig. 1).

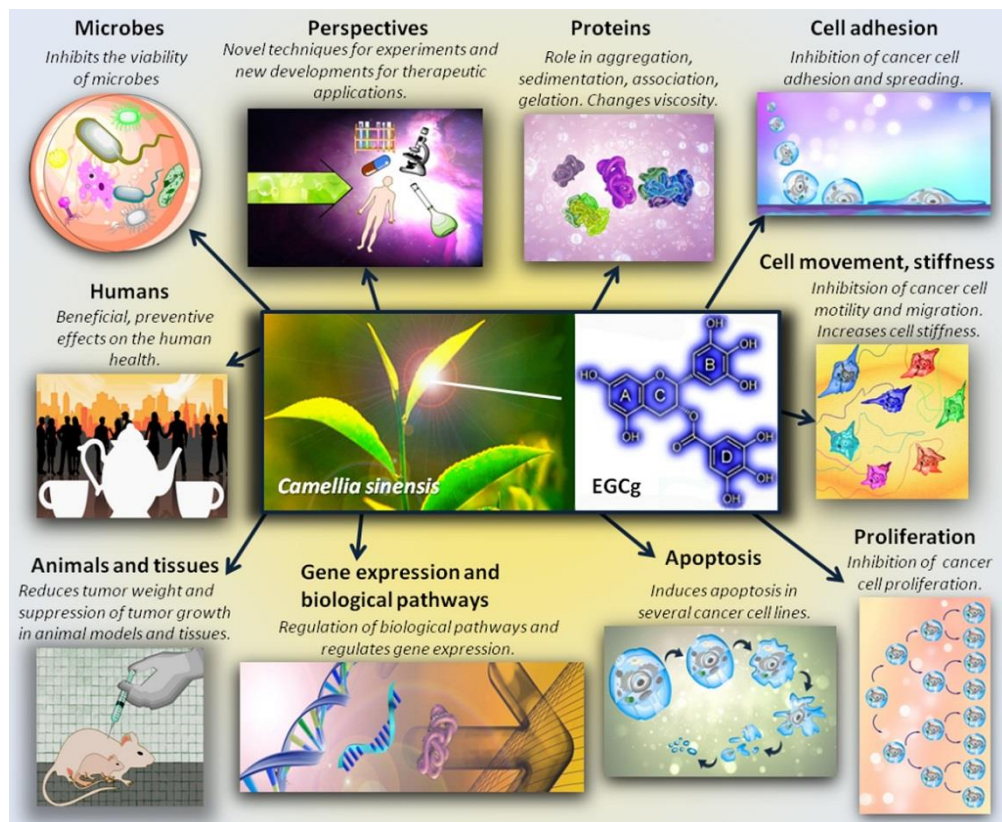


Figure 1: Diversified effects of EGCG.

In 2015 we focused on the molecular scale interactions between proteins and EGCG with special focus on its limited stability and antioxidant properties, the observed biophysical effects of EGCG on various cell lines and cultures. The alteration of cell adhesion, motility, migration, stiffness, apoptosis, proliferation, as well as the different impacts on normal and cancer cells are all summarised in our prospective review article [Beatrix Péter, Szilvia Bősze, Róbert Horváth: Biophysical characteristics of proteins and living cells exposed to the green tea polyphenol epigallocatecin-3-gallate (EGCG): Review of recent advances from molecular mechanisms to nanomedicine and clinical trials]. We also handled the works performed using animal models, microbes and clinical trials. Novel ways to develop its utilization as therapeutic purposes in the future are discussed too, for instance, using nanoparticles and green tea polyphenols together to cure illnesses, and the combination of EGCG and anticancer compounds to intensify their effects. In this review we summarize the experiments and results of the past few years. The limitations of the employed experimental models and the criticisms on the interpretation of the obtained experimental data are summarized as well. We also point out some inaccuracies in the literature.

AUTOMATED SINGLE CELL ISOLATION FROM SUSPENSION WITH COMPUTER VISION

R. Ungai-Salánki, T. Gerecsei, Péter Fürjes, N. Orgován, N. Sándor, Eszter Holczer, Róbert Horváth, Balázs Szabó

Existing single cell isolation robots (Fig 1) can manipulate only surface attached cells seriously limiting the fields of their application for single cell handling. Although naturally adherent cells can be spontaneously immobilized on the surface, the adhesion force needs to be tuned either biochemically or by surface modifications optimized to the cell type. Otherwise the too strongly adhered cells are picked up at an expense of damaging the cell. We developed a computer vision-based robot applying a motorized microscope and micropipette to recognize and gently isolate intact individual cells for subsequent analysis, e.g., DNA/RNA sequencing in 1-2 nanolitres from suspension without immobilizing cells on the surface of the Petri dish [R. Ungai-Salánki, T. Gerecsei, P. Fürjes, N. Orgován, N. Sándor, E. Holczer, R. Horváth, B. Szabó: Automated single cell isolation from suspension with computer vision, accepted for publication in Scientific Reports]. To minimize fluid convection cells were kept in a thin ($\sim 100 \mu\text{m}$) layer of buffer or culture medium covered by oil. It can retrieve rare cells, needs minimal sample preparation, and can be applied for virtually any tissue cell type. Combination of $1 \mu\text{m}$ positioning precision, adaptive cell targeting and below 1 nl liquid handling precision resulted in an unprecedented accuracy and efficiency in robotic single cell isolation. We applied a 3D printer to build miniature multi-well plates into the Petri dish. Single cells were injected either into the wells of a miniature plate with a sorting speed of 3 cells/min or into standard PCR tubes with 2 cells/min. We could isolate labeled cells also from dense cultures containing $\sim 1,000$ times more unlabeled cells by the successive application of the sorting process. We compared the efficiency of our method to that of single cell entrapment in microwells and subsequent sorting with the automated micropipette: the recovery rate of single cells was greatly improved. We expect that image-based automated single cell manipulation will become an everyday technique of molecular cell biology.

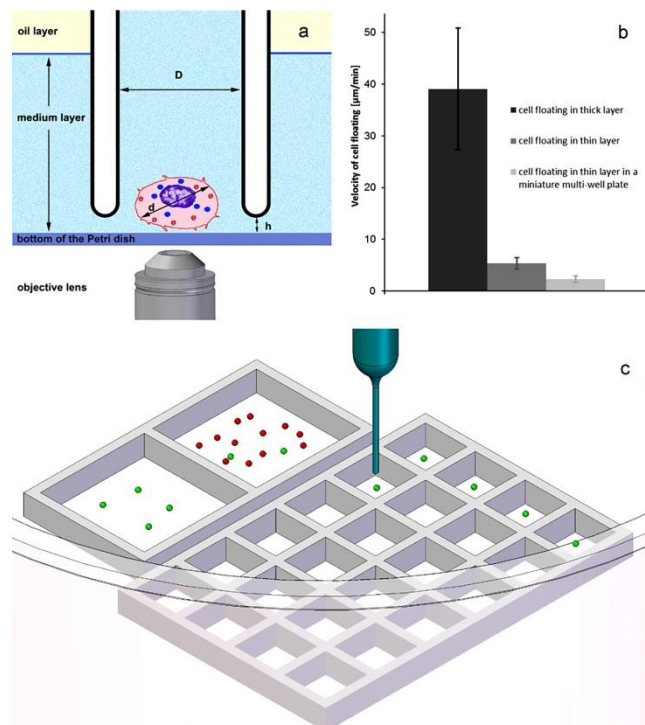


Figure 1: Automated micropipette for single cell isolation from a thin layer of suspension. Panel a shows the concept of cell sorting. Cells are detected by computer vision. Cell suspension confined into a thin $\sim 100 \mu\text{m}$ layer of culture medium or buffer covered with oil to avoid the convection-driven floating of cells. The glass micropipette with an inner diameter of $D = 30 \mu\text{m}$ approaches the surface of the dish to a distance of $h = 5 \mu\text{m}$. Targeted cell is picked up by a slight vacuum connected to the micropipette and controlled by a high speed fluid valve. Inhibitory effect of cell confinement into a thin layer on cell floating is shown in b. Wells of the miniature plate (shown in c) printed into the Petri dish further decreased convection.

MONITORING OF CELLULAR TOXICITY ASSESSMENT OF AGROCHEMICALS BY USING LABEL-FREE OPTICAL BIOSENSOR TECHNIQUE

Inna Székács, D. Patkó, Róbert Horváth, A. Székács

In 2015 we continued our work on the application of digital holographic microscopy to cytotoxicology studies. This technology has been successfully applied by our research group for the first time in the world for in vitro cytotoxicity investigations, and occurs to be a promising tool in reducing animal experimentation in toxicology. Digital laser holographic transmission microscopy is a label-free, non-invasive, non-destructive and non-phototoxic method allowing both qualitative and quantitative high resolution measurements of living cells over time. Thus, it offers a highly sensitive and versatile method to study cell morphology parameters, cellular processes and cell viability, including cytostatic and cytotoxic effects of various xenobiotics of chemical or microbiological origin cells are exposed to. In our study on a widely used agrochemical, the herbicide preparation Roundup, currently being criticized for its potential endocrine disrupting effects and carcinogenicity, we evidenced cytostatic and cytotoxic effects of the preparation at concentrations even 200-fold below agricultural administration levels. Cell morphology parameters, like cell area, thickness and volume, can be very useful when monitoring the effects of different treatments. The toxic effect of Roundup at the concentration 20-fold below agricultural application was seen in 10 minutes, cells take rounded shapes due to cytoskeletal response, and become detached from surfaces they had adhered to (Fig. 1). Consequently a time-dependent decrease in cell area and an increase in maximum thickness of the cells were seen in response to treatment.

The above cytotoxic effects have also been evidenced by our group using the rapid and high throughput optical biosensor technique, Epic BT. The main advantage of this sensor is that it applies parallel multiple optical waveguide sensoric detection (e.g. on 384-well microplates) of given analytes or surface molecular processes using resonant waveguide grating. This allows rapid parallel analysis of many samples. With the Epic BT method we expand our study of Roundup, as well as its active ingredient glyphosate and adjuvant polyethoxylated tallowamine (POEA) on

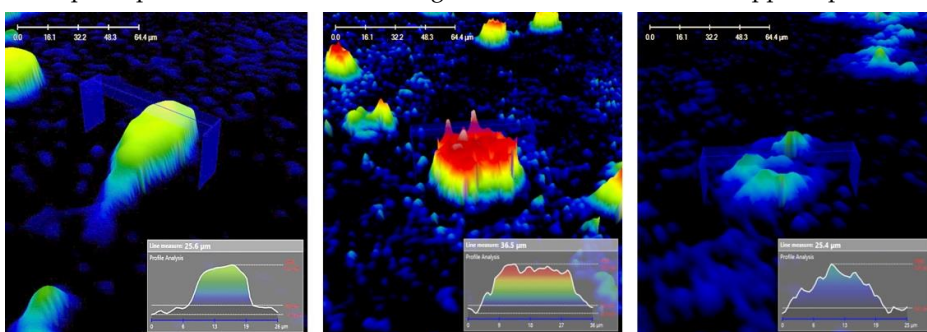


Figure 1: Time-dependent morphological changes of cells exposed to Roundup (0.1%), detected by phase contrast holographic microscopy. Images were captured every five minutes from the beginning of treatment with Roundup (0 min). After a few minutes of treatment the cells become round, then turn uneven and later break apart.

preosteoblastic cell line MC3T3-E1, as glyphosate has been indicated to inhibit bone development in rats.

EURASIAN MTDNA ANALYSIS WITH A NEW ITERATIVE RANK-CORRELATION METHOD

Zoltán Juhász, T. Fehér, E. Németh, H. Pamjav

We have analysed 27-dimensional mtDNA haplogroup distributions of 174 Eurasian, North-African and American populations to describe the haplogroup distributions of populations as composites of certain hypothetic ancient core populations immediately or indirectly determining the migration processes in Eurasia [58]. To identify these core populations, a new iterative algorithm determines the clusters of the 27 studied haplogroups having strong rank-correlations. Combined with our Self Organising Cloud algorithm this allowed us to determine geographically, historically and linguistically interpretable clusters of our dataset having a very specific structure defying classification. Fig. 1 shows the rank correlations, where the distances driving the MDS algorithm

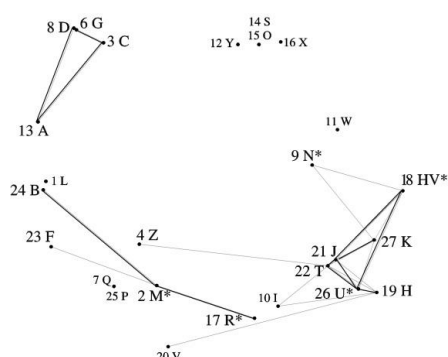


Figure 1: MDS graph of the correlations between 27 MTDNA haplogroups in Eurasia and America. Thin and thick edges indicate correlations over 0.67 and 0.74

were calculated as 1-rank correlation for all pairs of Hg-s. Three disjoint "correlating haplogroup clusters" (CHgC) are clearly identified:

The relatively large number of ancient DNA samples provided an invaluable tool for comparing ancient population movements with the location of living populations. Comparing the ancient data of the Andronovo and the Kurgans areas to recent distributions led us to conclude that current East and Central European populations may consist of a Western substrate arising from the Near Eastern Neolithic stock and a Siberian-Western composite population arising from the Andronovo area. The close relations of recent and ancient haplogroup distributions of these areas also make it probable that Uralic and Altaic languages could have played a significant maternal role in the Andronovo culture, and Uralic-speakers in the Kurgans culture.

DOES KNOWING THE OPPONENT'S STRATEGY GUARANTEE OPTIMAL PLAY?

Attila Szolnoki, M. Perc

Knowing the strategy of an opponent in a competitive environment conveys obvious evolutionary advantages. But information is costly, and being informed may not necessarily offset the additional cost. By using the methods of statistical physics we have studied a spatial social dilemma game in which beside cooperator (C) and defector (D) strategies we also introduced “informed” strategies: the latter are those who invest extra efforts to explore the aim of neighbours and behave accordingly. In particular, IC players refuse to be exploited by defectors, while ID players avoid being punished when encountering other defectors. We suppose that being informed conveys an advantage to ID players compared to D players. The simplest way to ensure this is to still punish defectors if they meet an ID player. (Fig 1)

As a result, we could identify elementary relations between the four competing strategies in the governing food web, which revealed the existence of two three-strategy defensive alliances. We have shown that a direct evolutionary advantage of a strategy within a defensive alliance can be compensated by the other alliance through a faster internal rotation of its strategies. Thus, even though in the food web the informed defectors are superior to unconditional defectors, the alliance whose defense relies on the weaker strategy can still prevail. We have demonstrated that the competition between a direct food-web-based evolutionary advantage and an evolutionary advantage that is rooted in the spatio-temporal dynamics of a defensive alliance gives rise to a re-entrant phase transition. In-between the two stable phases, that form the re-entrant pair, we have also identified a very narrow region of coexistence of both defensive alliances, which emerges as a consequence of a delicate equilibrium of the two competing mechanisms. (Fig 2)

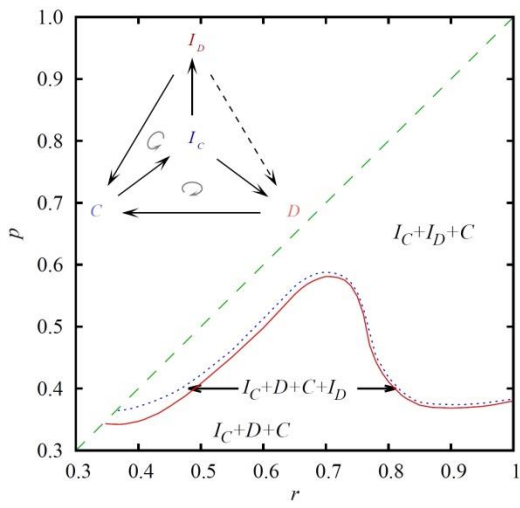


Figure 1: Full r - p phase diagram, as obtained at a specific cost value. Solid red line denotes continuous phase transitions from the very narrow but stable $I_C + D + C + I_D$ phase to the stable $I_C + D + C + I_D$ phase, while the dotted blue line denotes re-entrant continuous phase transitions to the stable $I_C + I_D + C$ phase. Dashed green line is the $p < r$ border.

Inset in the left-up corner shows the direction of invasion between the competing strategies (see arrows)

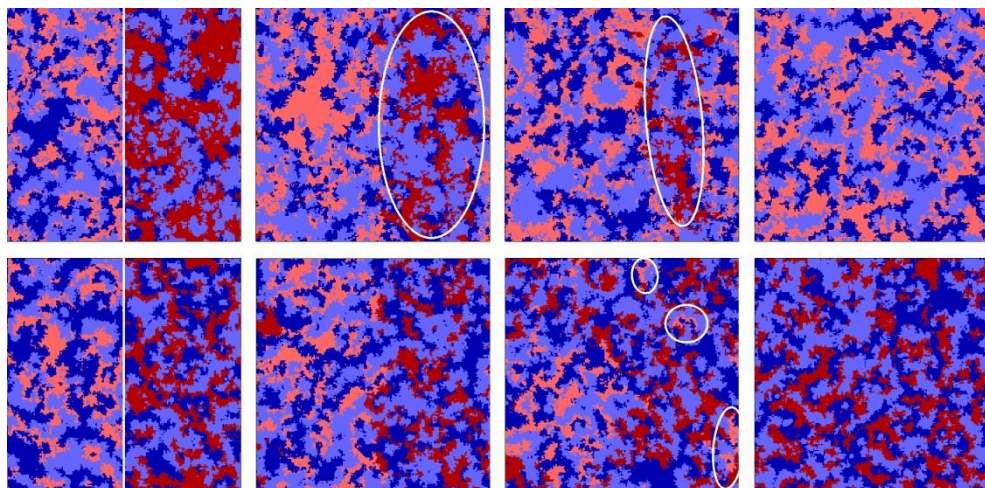


Figure 2: Snapshots of pattern formation, as obtained for $r = 0.65$ (top row) and $r = 0.95$ (bottom row) starting from a prepared initial state. During the relaxation period, each half of the lattice contained the strategies of one triplet only. After the characteristic patterns evolved (leftmost panels), the separating white wall was removed and the two defensive alliances started to compete with each other. In the top row, the $(I_C + D + C)$ triplet (dark blue, light blue, and light red, overall lighter), gradually compresses the $(I_C + I_D + C)$ triplet (dark blue, light blue, and dark red, overall darker). The typical size of the shrinking alliance is encircled with a white ellipse. The snapshots were taken after different iteration steps from left to right. In the bottom row, the $(I_C + I_D + C)$ triplet gradually gets dominant because I_D players are superior to D players. Accordingly, the domains of the $(I_C + D + C)$ triplet (white ellipses) vanish over time.

GRIFFITHS PHASES AND LOCALIZATION IN HIERARCHICAL MODULAR NETWORKS

Géza Ódor, R. Dickman, Gergely Ódor

We have studied variants of hierarchical modular network models suggested by Kaiser and Hilgetag [Front. in Neuroinform., 4 (2010)] to model functional brain connectivity, using extensive simulations and quenched mean-field theory (QMF), focusing on structures with a connection probability that decays exponentially with the level index. Such networks can be embedded in two-dimensional Euclidean space. We explored the dynamic behavior of the contact process (CP) and threshold models on networks of this kind, including hierarchical trees (Fig 1). While in the small-world networks originally proposed to model brain connectivity, the topological heterogeneities are not strong enough to induce deviations from mean-field behavior, we showed that a Griffiths Phase (GP) can emerge under reduced connection probabilities, approaching the percolation threshold (Fig 2). In this case the topological dimension of the networks is finite, and extended regions of bursty, power-law dynamics are observed. Localization in the steady state was shown via QMF. We investigated the effects of link asymmetry and coupling disorder and showed that localization can occur even in highly connected small-world networks in case of link disorder.

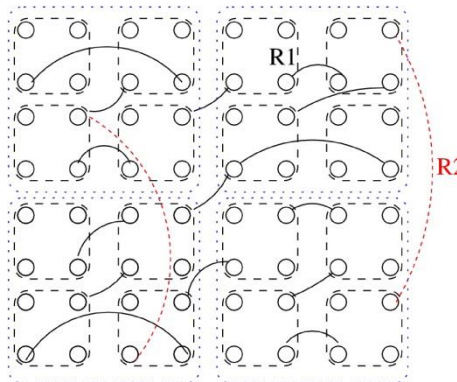


Figure 1: Two lowest levels of the HMN2d hierarchical network construction. Dashed lines frame bottom level nodes, which are fully connected there, dotted lines frame the nodes of the next level. The solid lines denoted R1 are randomly chosen connections among the bottom level modules, ensuring single connectedness of the network, while those denoted R2 provide random connections on the next level. Links can be directed.

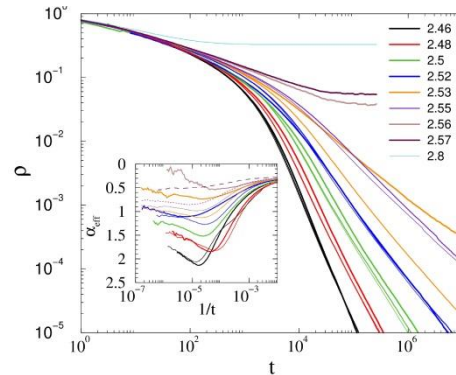


Figure 2: CP on asymmetric HMN2d networks with average node degree $k \sim 4$: decay of activity for activation rates (λ) values as indicated. System sizes: $l_{\max} = 8, 9, 10$ levels (thin, medium, and thick lines, respectively). Size-independent power laws are observed for $2.45 < \lambda < 2.53$. Inset: local slopes of the curves in the main plot. In the GP the effective decay exponent α_{eff} tends to non-universal values, in addition with logarithmic corrections.

ABBREVIATIONS

| | |
|-----------|---|
| 67P/C-G | 67P/Churyumov-Gerasimenko |
| AAc | acrylic acid |
| ALLIANCE | European Radioecology Alliance |
| ÁNER | (Hungarian acronym) Refuelling Neutron Monitoring System |
| APSD | Auto Power Spectral Densities |
| AU | Astronomical Unit |
| BME | Budapest University of Technology and Economics |
| BzOH | benzyl alcohol |
| CMC | carboxymethylcellulose |
| CODEX | Core Degradation Experiment (test facility) |
| CONCERT | European joined programme for the integration of radiation protection research |
| CPSD | Cross Power Spectral Densities |
| CZT | Cadmium-Zinc-Telluride |
| DBA | design basis accidents |
| DIM | Dust Impact Monitor |
| DNBR | Departure of Nucleate Boiling Ratio |
| DRIFTS | Diffuse Reflectance Fourier Transform Infrared Spectroscopy |
| DRM | dry reforming of methane |
| EK | Centre for Energy Research |
| EURADOS | European Radiation Dosimetry Group |
| EVA | extravehicular activity |
| FE | Finite Element(s) |
| FGR | Fission Gas Release |
| FORTRAN | "Formula Translation", imperative programming language, suited to numeric computation |
| FRI | Fuel Reliability Index |
| FSS | First Science Sequence |
| FT-IR | Fourier transform infrared spectroscopy |
| GC | gas chromatography |
| Gen3 | Generation 3 |
| Gen4 | Generation 4 |
| GF | gel fraction |
| GIADA | Grain Impact Analyser and Dust Accumulator |
| GIPSI | GIADA Performance Simulator |
| GS | gamma spectrometry |
| HAEA | Hungarian Atomic Energy Authority |
| HAS | Hungarian Academy of Sciences |
| HEC | hydroxyethylcellulose |
| HPC | hydroxypropylcellulose |
| HR-ICP-MS | High Resolution Inductively Coupled Plasma Mass Spectrometry |
| HRP | Halden Reactor Project |
| HRTEM | high resolution transmission electron microscopy |
| HZP | Hot Zero Power |
| IAEA | International Atomic Energy Agency |
| IBMP | Institute for Biomedical Problems |
| ICP-MS | inductively coupled plasma mass spectrometry |
| ICRP | International Commission on Radiation Protection |
| ISS | International Space Station |
| ITER | International Thermonuclear Experimental Reactor |
| LBLOCA | large break loss of coolant accident |
| LHR | linear heat generation rate |
| LIBS | Laser Induced Breakdown Spectroscopy |
| LOCA | Loss-of-Coolant Accident |
| MC | methylcellulose |
| MCNP | Monte Carlo N-Particle Transport Code |
| MCNP5 | Monte Carlo n-Particle v. 5 |
| MCP | Main Circulating Pump |

| | |
|----------|--|
| MELODI | Multidisciplinary European Low Dose Initiative |
| MOX | Mixed Oxide |
| MPHFtool | general software framework tool for Multi-Physics (MPH) investigations of hot channel calculations |
| MPI | Message-Passage Interface |
| MS | mass spectrometry |
| MTA | HAS, Hungarian Academy of Sciences |
| MTC | Moderator Temperature Coefficient of reactivity |
| N,N' | methylene-bis-acrylamide – MBA |
| NERIS | European Platform on Preparedness for Nuclear and Radiological Emergency Response and Recovery |
| NP | nanoparticle |
| NPP | Nuclear Power Plant |
| OECD NEA | Organisation for Economic Co-operation and Development, Nuclear Energy Agency |
| OM | optical microscopy |
| OMSZ | Hungarian Meteorological Services |
| PAKS NPP | PAKS Nuclear Power Plant |
| PAZAR | (Hungarian acronym), Paks Autonomous Noise Data Acquisition System |
| PAZAR-K | (Hungarian acronym), Evaluation system for measurements acquired by PAZAR |
| PCMI | pellet-cladding mechanical interaction |
| PRISE | primary to secondary leakage |
| PVA | polyvinyl alcohol |
| PWR | Pressurized Water Reactor |
| RH | Remote Handling |
| RING | Release of Iodine and Noble Gases (computer code) |
| RMR | (Hungarian acronym) Reactivity Monitoring System |
| RMS | ROOT Mean Square |
| ROMAP | Rosetta Lander Magnetometer and Plasma Monitor |
| RVR | (Hungarian acronym) Reactor Protection System |
| SCIP | Studsvik Cladding Integrity Project |
| SDL | Separation, Descent and Landing |
| SEM | scanning electron microscopy |
| SESAME | Surface Electrical, Seismic and Acoustic Monitoring Experiments |
| SFAT | Spent Fuel Attribute Tester |
| SG | Specific Grant |
| SG | Steam Generator |
| SITON | Simulation TTool for modelling the Nuclear fuel cycle, a computer code |
| SODAR | Sonic Detection And Ranging |
| SPM | Simple Plasma Monitor |
| SPND | Self Powered Neutron Detector |
| SPR | surface plasmon resonance |
| TEM | Transmission Electron Microscopy |
| TLD | thermoluminescent dosimeter |
| TOF | turn-over frequency |
| TPO | temperature programmed oxidation |
| TPR | Temperature Programmed Reduction |
| TS | Telescope Sipping |
| UAM | Uncertainty Analysis in Modeling |
| UOX | Uranium dioxide |
| UTS | ultimate tensile strength |
| UV-vis | ultraviolet-visible spectroscopy |
| VERONA | Core Monitoring System for VVER type NPPs |
| VV | Vacuum Vessel |
| VVER | Water-Cooled Water-Moderated Energetic Reactor |
| WANO | World Association of Nuclear Operators |
| XPS | X-ray Photoelectron Spectroscopy |
| XRD | X-ray powder diffraction |

IMPRINT

Editors

Ákos Horváth
Katalin Gmélíng
Attila R. Imre

Lectors

Ferenc Szlávik
Jesse L. Weil

Publisher

MTACentre for Energy Research
H-1121, Budapest, Konykoly Thege M. út 29-33.
Hungary

Designe

Katalin Gmélíng
Anikó Jécsai

Pictur credits

Centre for Energy Research,
Hungarian Academy of Sciences

Accessibility

<http://www.energia.mta.hu/>

Contact

Centre for Energy Research, Hungarian Academy of Sciences
Location: KFKI Campus 29-33 Konkoly Thege Miklós street 1121 Budapest, Hungary
Mailing address: 1525 Budapest 114., P.O. Box 49., Hungary
Phone: (+36 1) 395 91 59 **Fax:** (+36 1) 395 92 93
E-mail adresses: info@energia.mta.hu

